STRUCTURE AND FUNCTIONAL DEVELOPMENT OF THE EEL LEPTOCEPHALUS *ARIOSOMA BALEARICUM* (DE LA ROCHE, 1809)

By W. H. HULET

The Marine Biomedical Institute, University of Texas Medical Branch, Galveston, Texas 77550, *U.S.A.*

(*Communicated by N. B. Marshall, F.R.S. – Received* 22 *February* 1977)

[Plates 1–30]

CONTENTS

Eels, elopids, notacanths and other elopomorph fishes spawn in the ocean and the hatchlings spend their larval life as pelagic, planktonic organisms. The larvae are known as leptocephali and their transparent, leaf-like body characteristically bears little resemblance to the respective adult form. Planktonic life in the ocean may last for years before the leptocephalus undergoes a morphological transformation and takes on a recognizable fish-like appearance. A prolonged larval life suggests a delay in structural and functional development and this premise was the basis for the present study. Before this work on morphology, chemical analysis of the whole leptocephalous body indicated an internal salinity and osmolality far and above the known values for marine teleost fishes. For that reason, particular attention was given to the structural maturation of the gills, gut and kidney, all of which are intimately concerned with osmoregulation.

The leptocephalus of the bandtooth conger *Ariosoma balearicum* was chosen for morphological studies because of its abundance in the tropical western Atlantic and because the Bathymyrinae, which includes *Ariosoma*, is a reasonably generalized subfamily of congrid eels. The congrids are primitive and representative of the basic eel plan and, as such, are accorded a rather ancestral position.

In order to grasp the fundamental organization of a leptocephalus it was soon discovered that all parts of the body needed to be examined. One by one, a long list of structural peculiarities came to light, each of which seemed to have a direct relation to the functional adaptation of the leptocephalus for a prolonged oceanic existence. The section describing the chondrocranium is particularly detailed and permits comparison with an examination of the leptocephalous skull in *Anguilla* performed by Norman some fifty years ago. The advantages of current methods for processing tissue and the electron microscope are evident in the micrographs of cell surfaces and intracellular organelles. Gill function in the premetamorphic leptocephalus is limited by structure to a mandibular hemibranch. The four gill arches are present, but the vasculature is undeveloped and gill filaments are absent. The gastrointestinal tract is always devoid of food material and some sections of the intestine do not have a discernible lumen. The size, shape and appearance of the teeth seem unrelated to the source of nutrition. All kidney tubules are aglomerular. In summary, the leptocephalus demonstrates many features of structural and functional immaturity and, until transformed by metamorphosis, appears to be an obligatory inhabitant of the open ocean.

Introduction

The work herein presented was begun with the intention of learning about the structures responsible for the regulation of water and electrolyte metabolism in the leptocephalus. Existing literature on leptocephali is mainly concerned with taxonomic characters useful for species identification, and no information is available on morphology as it relates to the physiology of osmoregulation. The one published work on the leptocephalus that gave substantial attention to anatomical features was a treatise on the chondrocranium by J. R. Norman written some fifty years ago (1926). My studies on the physiology of the leptocephalus (Hulet, Fischer & Rietberg 1972) led to many questions on morphology, and, for that reason, I chose to review the gross and microscopic anatomy of the leptocephalus as it exists before metamorphosing to a recognizable form of the adult. The premetamorphic leptocephalous larva of the congrid eel *Ariosoma balearicum* (De La Roche, 1809) was selected for anatomical studies because of its great abundance in the tropical waters of the Western Atlantic.

This simple inquiry into the general morphology of the leptocephalus brought to light many features of eel larvae that differ remarkably from other groups of teleostean fishes. Although the detailed anatomical work is limited to one species, it seems quite probable that the morphology of other anguilliform leptocephali will be similar, at least in a general sense, to that of *Ariosoma balearicum*.

The 'eel problem'

Eels are hardy fishes, prized as food, mostly marine in habitat, shy by nature and spawn in great secrecy. Adult individuals of anguilliform or true eels look much alike and, at times, cannot be distinguished even at the family level by anyone except an expert. The paucity of easily-recognized morphologic characters has severely handicapped setting forth a clearly defined taxonomic relation among true eels as well as establishing their relation with other groups of living and fossil fishes. Eels are specialized fishes that have adapted to a life of burrowing in sand or remaining secluded in rocky crevices, coral reefs and grass patches. A few have left a bottom environment to become mesopelagic and bathypelagic. Most eels are nocturnal feeders and, except for morays, are rarely seen during the day. In coastal waters, a poison station is about the only way to obtain an acceptable estimate of an eel population. They are the last to succumb, and this observation is but one of many indications of their hardiness. Anguilliform eels spawn in the ocean and most species spend their adult life on the continental shelf. But, as noted above, some species are free-living pelagic fishes, and a few others live in deep water on the continental slope. *Anguilla* is the most widely known of all genera and has a worldwide distribution. Members of this genus inhabit freshwater streams, rivers and lakes; however, despite a long life in freshwater, *Anguilla* is bound to the sea and all species must return to the sea to spawn. The whereabouts of the spawning grounds of the European and American freshwater eel was at one time a major aspect of the 'eel problem'. A lifetime of devotion by the Danish naturalist Johannes Schmidt (1922) led to his discovery that the European freshwater eel spawns in the Sargasso Sea of the western North Atlantic. The evidence indicating that *Anguilla anguilla* (L.) spawns in the Sargasso Sea is most convincing, but it is interesting to note that spawning adults have never been seen, caught or photographed in the open ocean. In any event, the necessity of 'freshwater' eels to migrate seaward is a strong indication of their marine ancestry.

The unique feature of eels that sets them apart from most other fishes is the form of their larval stage. The pelagic egg hatches into a larva that bears no resemblance to the adult except, perhaps, in its manner of swimming. The laterally compressed body is leaf-shaped and transparent. In the full light of a shipboard laboratory only the eyes of a live and swimming individual are visible. The head, tiny in proportion to the rest of the body, accounts for the name leptocephalus. Two hundred years ago these common occupants of plankton tows were classified under the genus *Leptocephalus* Gronovius, 1763. The fact that they were eel larvae was unknown. The diversity in general appearance of leptocephalous larvae is great, in fact, greater than the differences encountered in adult forms. The genus *Leptocephalus*, now an unacceptable name in Zoology, became the nominal genus of more than a hundred species before the relation between leptocephali and eels was discovered (Delage 1886). In the closing decade of the last century Grassi & Calandruccio (1892, 1897) were able to rear leptocephali in the laboratory and to follow their metamorphosis to recognizable forms of the adult. Their discovery that *Leptocephalus brevirostris* Kaup, 1856 is the larva of *Anguilla anguilla* (L.) was the exciting event that started Schmidt on his search for the breeding grounds. The larvae first appear in the Sargasso Sea and drift in the clockwise gyre of the North Atlantic for two and a half to three years before metamorphosis to an eel form. Near European shores the transformation to juvenile eels or elvers equips them physiologically for life in freshwater.

Thanks to the work of a handful of ichthyologists, the confusion and disarray in eel systematics

have yielded to reasonable and recognizable order. True eels are grouped in the Order Anguilliformes and more than a hundred species of leptocephali have been identified with the respective adult species (Castle 1969). But 'the eel problem' is far from solved. Why does an extant group of fishes have such a bizarre larval stage, and what compels *Anguilla* and perhaps other genera to seek a spawning ground in warm water of high salinity and thousands of miles distant? It is generally accepted that beneath the cover of specialization eels are primitive fishes, that have attained a level of anatomical organization commensurate with bony or teleostean fishes. Even on the lowest rung of teleostean organization, tarpon and other elopiform fishes, related to eels by virtue of leptocephalous larval stage, appear to be less divergent descendants of the ancestral stock (Greenwood, Rosen, Weitzman & Myers 1966). Among the anguilloids and other elopomorph fishes that are considered primitive on osteological and other anatomical grounds, the larval stage, when known, is characterized by a leptocephalus. No spiny-finned species has a leptocephalous larva nor does any fish that lays its eggs in freshwater. With the evidence at hand, it seems reasonable to consider the leptocephalous larval stage as characteristic of a natural assemblage of fishes having a common ancestry. The antithesis requires the leptocephalus to be an example of convergent evolution in unrelated groups of fishes. Regrettably, the fossil record has no leptocephalus. This situation is not surprising since a leptocephalus even large enough to be measured in metres has no organized bone and only a few areas of calcification. Fossil organisms lacking calcified structures have been found but such discoveries are rare. Other means must be found to understand why a bizarre and prolonged larval life as a leptocephalus is a successful adaptation in the phylogenetic history of fishes.

Current knowledge of physiology and metabolism in eels has come almost exclusively from experiments on *Anguilla* spp. Furthermore, most of these works have been concerned with the changes in the mature eel that precede migration. The hardiness of eels has figured prominently in their use as biological models in fish physiology. In fact, Homer Smith (1930) used *Anguilla rostrata* (Lesueur, 1817) in experiments that provided the first insight into the physiological mechanism of water and salt metabolism in marine fishes. In contrast to adult eels, leptocephali are exceedingly delicate organisms and except for our earlier work on body composition (Hulet *et al.* 1972) the physiology of structures controlling the internal environment in the leptocephalus remains unknown.

Contributions to the morphology of leptocephalous larvae

The best available work on leptocephalous larval morphology is the study by J. R. Norman (1926) on the chondrocranium in *Anguilla anguilla* (L.). No morphologic study of equal breadth and magnitude has been published since that time on any other eel species or on any other part of the leptocephalous anatomy. Facciolà (1897) discussed the general anatomy of the leptocephalus but his work is without figures and his nomenclature is difficult to understand. Most published works on leptocephali are focused on features that are accepted morphometric characters in the systematics of fishes. Some workers have broadened the approach and have concentrated on morphologic characters that are lost or gained after metamorphosis. In short, the goal has been to identify the true species of any given leptocephalus. Bauchot (1959) studied the chondrocranium and viscera in leptocephali of *Serrivomer beani* Gill and Ryder, 1883 and *Serrivomer brevidentatus* Roule and Bertin, 1929. More recently, Dean (1968) examined the head skeleton in the leptocephalus and juvenile of the ophichthid eel *Ahlia egmontis* (Jordan, 1885).

The external morphology of the egg and developing embryo of *Ariosoma balearicum* (De La Roche, 1809) was described by Spartà (1938). Castle (1964) has summarized the characters essential for the identification of larvae of *Ariosoma balearicum*. Smith (1971) clarified the taxonomic position of *Ariosoma balearicum* in his revision of the family Congridae.

Taxonomic relations of the bandtooth conger Ariosoma balearicum

Although initially selected because of its abundance and availability, *Ariosoma balearicum* proves to be an excellent species to study in order to gain insight into the leptocephalus and the general eel problem. The reasons are several. Regan (1912) divided eels into two lineages on the basis of whether or not the frontal bones were fused. Although specialized in this one feature those eel families with fused frontals are otherwise more conservative or primitive and more representative of the basic eel plan than those with separate frontals. Congrids which have fused frontals are reasonably generalized eels and within the family, *Ariosoma* belongs to the Bathymyrinae which, next to the Congrinae, is perhaps the most generalized subfamily. In the lineage with unfused frontals, *Anguilla* is accorded a rather ancestral position. More knowledge of physiology and biochemistry of metabolism is available for *Anguilla* (especially *Anguilla anguilla*) than for any other eel. Although *Anguilla* and *Ariosoma* differ by more than fused or unfused frontals, their anatomical similarities suggest inquiry into physiological and biochemical differences between congrid and anguillid eels that may explain the divergent habitats chosen for adult life.

Ariosoma balearicum has been known in the tropical western North Atlantic as the bandtooth conger *Ariosoma impressa* (Poey). Differences between members of eastern and western Atlantic populations are unsupported and *A. impressa* has been submerged in favour of *A. balearicum* (Smith, 1971). Böhlke (1949) places *Ariosoma* in the congrid subfamily Bathymyrinae. Böhlke & Chaplin (1969) reported that *A. balearicum* was the commonest congrid eel in their collection of Bahamian fishes. It inhabits shallow coastal waters and is particularly found on the sandy bottom surrounding patch reefs and the sandy soil of turtle grass beds. *Ariosoma balearicum* spawns at sea but no known particular location has been discovered if, indeed, one exists.

Materials and methods

1. *Collection of leptocephali*

Essential to any study of morphology at the cellular level is the need for fresh material. Since leptocephali are inhabitants of the open ocean, the collection, identification and initial laboratory preparation must be carried out aboard ship. Optimum tissue preservation was observed when the leptocephali were alive, transparent, and swimming about in the shipboard aquarium immediately prior to chemical fixation. Death is imminent when the body becomes faintly visible, and dead leptocephali are milky white in appearance (figure 1, plate 1).

The most consistent catches of live leptocephali have been with a two-metre plankton net of intermediate mesh size and fitted with a plastic cannister at the cod end. On many occasions I have used the Isaacs–Kidd midwater trawl (6-ft. and 10-ft. IKMT) and, although the number of leptocephali captured was greater than with the smaller plankton nets, most of the larvae were dead or damaged. Tows were made between 10.00 p.m. and 4.00 a.m. with an estimated gear depth of no more than one hundred metres. The most productive fishing was at depths between 10 and 50 m for periods of 20–30 min. Trawling stations of the research

vessels (*Pillsbury*, *Gerda*, *Columbus Iselin*, and *Gilliss*) pertinent to this work on larval anatomy are given in table 1. In brief, all leptocephali were caught in the open ocean of the western North Atlantic (Straits of Florida eastward to the Puerto Rican Trench and Virgin Island Basin), Caribbean Sea, and Gulf of Mexico.

2. *Preservation*

Because the tissues of the leptocephalus contain a high percentage of water, they are particularly sensitive to the osmotic concentration of fixing and washing solutions. Seawater has been used as the solvent for fixatives used in the preservation of marine invertebrate tissues (Holland & Jespersen 1973), and for the preservation of external structures in marine fishes (Dobbs 1974). The rationale for using seawater as a vehicle for the fixative is to avoid an osmotic gradient between the specimen tissue and the bathing medium. The avoidance of shifts in water due to osmotic differences is a significant factor in maintaining the structural integrity of the fixed tissue. From the earlier work on water and electrolyte composition of whole leptocephalous bodies (Hulet *et al.* 1972), calculation of an approximate osmolality for leptocephalous extracellular fluid gave a value close to one osmole. This approximation of osmotic concentration in the body fluids of leptocephali served as the basis for the preparation of fixing and washing solutions. All aqueous solutions to be in contact with the leptocephalous tissue were prepared so that the final osmotic concentration of each solution was close to 1000 milliosmoles per litre. For convenience aboard ship, molar was preferred to molal in making up solutions. Although seawater can be used as a solvent for glutaraldehyde, osmium and other fixatives, the electrolyte composition of seawater differs considerably from the body fluids of marine vertebrates. Differences are particularly great in the concentrations of sulphate and magnesium. For the adjustment of osmolarity in fixing and washing solutions, I found that the polyelectrolyte solution used in hemodialysis for treating patients with renal failure was a preferable substitute for seawater. The hemodialysis concentrate is readily available from commercial houses and is sold as a 5 molar solution. The polyelectrolyte concentrate used in this study contained the following ingredients in each litre of solution:

Sodium chloride	194.0 g
Sodium acetate ($NaC_2H_3O_2 \cdot 3H_2O$)	167.0 g
Potassium chloride	5.2 g
Calcium chloride ($CaCl_2 \cdot 2H_2O$)	7.7 g
Magnesium chloride ($MgCl_2 \cdot 6H_2O$)	3.6 g
Glucose, anhydrous	70.0 g
Dissolve and add distilled water to make one litre.	

The osmolarity of this concentrated polyelectrolyte solution is approximately 9300 mosmol/l. The high osmolarity greatly facilitates making up the fixing and washing solutions with the desired final osmolarity. For both light and transmission electron microscopy, glutaraldehyde (2.5%) was the primary fixative (Hayat 1970). Tissues were secondarily fixed in osmium tetroxide. The advantage of osmium fixation is that after stabilization of cell structures with aldehydes, cells fixed with osmium have been changed to a structurally-intact but osmotically-inert skeleton (Bone & Denton 1971). Throughout the preservation procedure the final concentration of the fixative in contact with the tissue was 2.5% glutaraldehyde and 1.0% for osmium tetroxide. The osmotic contribution of each of these chemicals to the total osmotic concentration of the fixing solution must be considered in the calculations.

Optimum fixation requires good buffering capacity of the working solutions. Phosphate buffer is unsatisfactory when using full strength seawater (salinity 35‰) or the polyelectrolyte solution as diluents for the fixative. Calcium salts precipitate despite adjustment of the pH to near neutral. The organic buffer *s*-collidine was the final choice of buffer, and it was incorporated into the fixing and washing solutions to give a concentration of 0.2 molar. All procedures for the preparation of leptocephali for sectioning up to the final step of dehydration in 100 % acetone were carried out in the cold (0–4 °C). Precautions and directions relative to washing after fixation, pH, contamination, and many other features peculiar to ultrastructural studies are given by Hayat (1970) and other standard texts on the subject. The significant aspect of this procedure developed for the preservation of leptocephali is the adjustment of all aqueous solutions to approximately one osmole with a solution more in keeping with their body fluid composition than ordinary seawater.

TABLE 1. TRAWLING STATIONS (1969–76) FOR COLLECTION OF LEPTOCEPHALI OF *ARIOSOMA BALEARICUM*

vessel	station	identification number
R/V *Pillsbury*	815	EM364, 365
R/V *Gerda*	1199	EM418, 419, 420
R/V *Pillsbury*	1147	EM429, 430
R/V *Pillsbury*	1378	EM502, 503
R/V *Pillsbury*	1379	EM504, 505, 506, 507
R/V *Pillsbury*	1388	WM(S)-3, 6, 7, 9
R/V *Pillsbury*	1391	WM(A)-1, 2, 4, 5, 8
R/V *Pillsbury*	1398	EM510
R/V *Pillsbury*	1390	EM511, 512, 513, 514, 515
	cruise	
R/V *Columbus Iselin*	7403	chemistry
R/V *Gilliss*	7510	chemistry
R/V *Gilliss*	7604	chemistry

3. *Plastic embedment*

Dissected as well as entire leptocephali which had been fixed, washed and dehydrated were embedded in either the aromatic resin, Araldite, or low viscosity Spurr media (Spurr 1969).

The advantages of a whole mount of an organism such as a leptocephalus are several. All external features, counts, and measurements can be recorded without haste and without worry of postmortem autolysis. Whole mounts of leptocephali (figure 2, plate 1) prepared in the manner described can be kept indefinitely and sectioned at any time. The entire procedure from initial fixation to plastic embedding was carried out aboard ship. In tables 1–6, numbered whole mounts of leptocephali embedded in Araldite are prefixed by the letters WM(A); those embedded in Spurr media bear the prefix WM(S). The prefix EM refers to leptocephali from which portions of the body were cut into small pieces before fixation.

4. *Microscopy*

All sections were cut with a Sorval MT-2 Porter-Blum Ultra-microtome or with the LKB Ultrotome III. Sections for light microscopy were stained with toluidine blue; those for electron microscopy were stained with uranyl acetate followed by lead citrate. Grids were examined and photographed by means of a Philips EM300 transmission electron microscope (Dawes 1971).

White light photographs were taken with a Linhoff camera through a Leitz microscope with built-in illumination and a two-diaphragm Berek condenser. Illumination of unstained specimens was made according to the procedure of Musil & Belleme (1970). A photographic record was kept of the external features of each whole-mounted leptocephalus. Reflections from the surface of the plastic were eliminated by immersing the plastic block containing the larva in a glass pan partially filled with mineral oil. The glass pan was slid into the film slot of an enlarger and the outline of the larva projected on the copying table. In this way prints of each larva were made without the use of photographic film. An alternative method was to project the image of the larva on a large piece of sheet film. The developed negative could later be used for making any number of contact prints. For a photograph of a specific area such as the gall bladder or some other organ, the mineral oil pan was put on the microscope stage and a photograph taken through a low power objective.

5. *Preparation of chondrocranium*

The preparation of the chondrocranium for three-dimensional views by the illustrator posed a serious problem. The cartilaginous skull had to be free of brain, eyes and other soft tissues, but sufficiently intact so that it could be divided for views of the interior. The answer was enzymatic digestion with *Streptomyces griseus* protease (Pronase, Calbiochem, La Jolla, California). Formaldehyde-fixed heads were digested overnight in a solution of 1 % Pronase. An electrically-driven mechanical rotator assured constant and gentle mixing of the digesting solution. After several hours of digestion, the olfactory organs, eyes, brain and fragments of other tissues were easily removed with a small tweezers. For interior views of the neurocranium, the heads were frozen and cut in a cryostat along the desired plane and then placed in the digesting solution. The same procedure worked very well to loosen the small cartilaginous bones of the hyoid and gill arches.

Results

1. *Identifying characters*

(*a*) *Form and appearance*

Premetamorphic leptocephali of *Ariosoma balearicum* are of moderate size in length and body depth (figures 1 and 2) (Facciolà 1897). The largest premetamorphic larva of *Ariosoma balearicum* captured during the six years of plankton towing for this study measured 220 mm s.l. The teeth are prominent and the front pair of each jaw project forward in a nearly horizontal plane (figures 3–5, plate 2). The gut is a long straight tube spanning most of the body length. The dorsal and anal fin are short and confluent with the caudal fin. One or two minute melanophores occur between and near the origin of the fin rays of the median fins. Small expanded melanophores are present on the ventral aspect of the gut tube from the beginning of the esophagus to the region of the gall bladder. Lateral melanophores, small and six to nine in number, occur in tandem at each myoseptum immediately below the midline formed by the notochord. Total myomeres number about 126. This summary agrees with the descriptions given by D'Ancona (1931), Spartà (1938) and Castle (1964).

(*b*) *Measurements and counts*

For terminology, counting, and measuring I followed the definitions and methods given by Smith (1969). Standard length (s.l.) was taken to the closest millimetre by means of a pair of

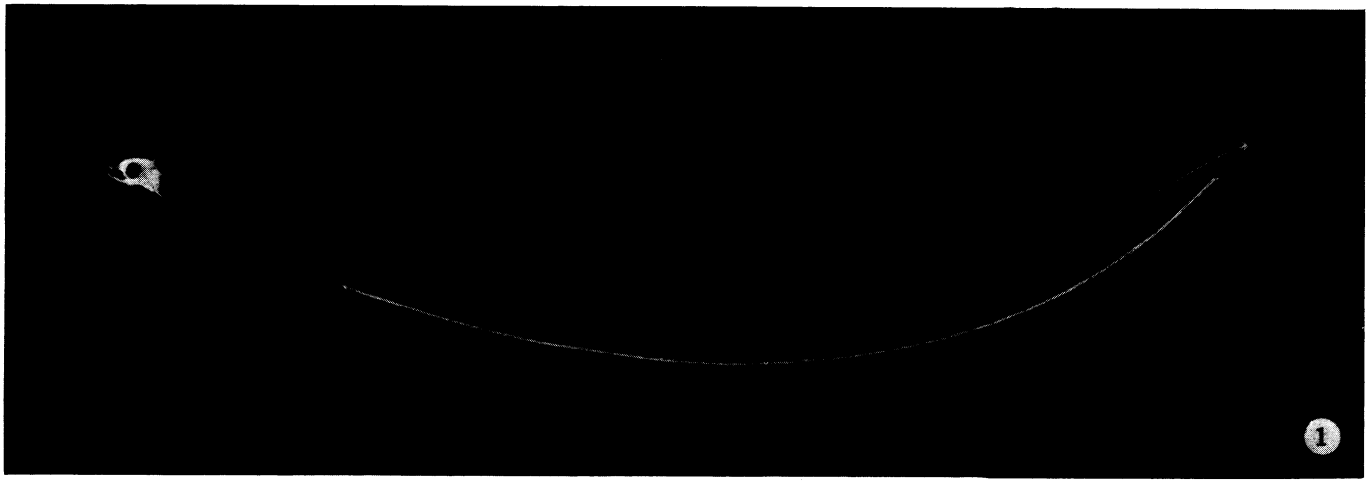

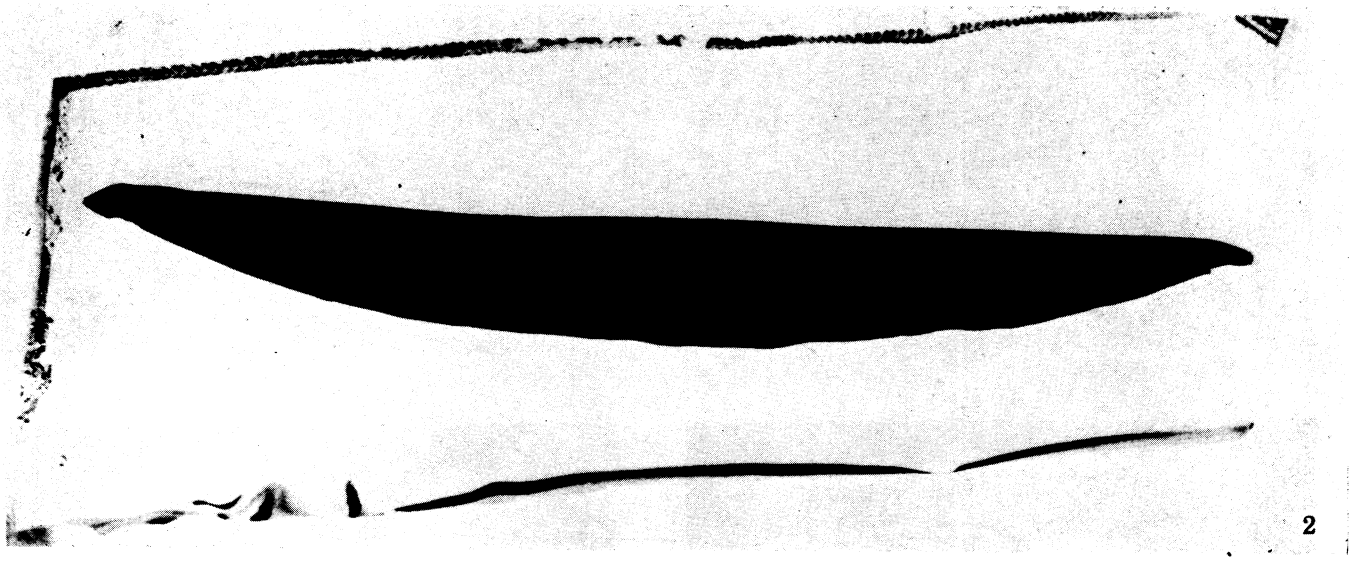

FIGURE 1. Formalin-fixed premetamorphic leptocephalus. All figures are of *Ariosoma balearicum.* (Magn. × 1.35.)

FIGURE 2. Leptocephalus, whole mount. Specimen fixed in glutaraldehyde, post-fixed in osmium tetroxide and embedded in Spurr low-viscosity media. Specimen WM(S)-3, 78 mm s.l.

(*Facing p.* 114)

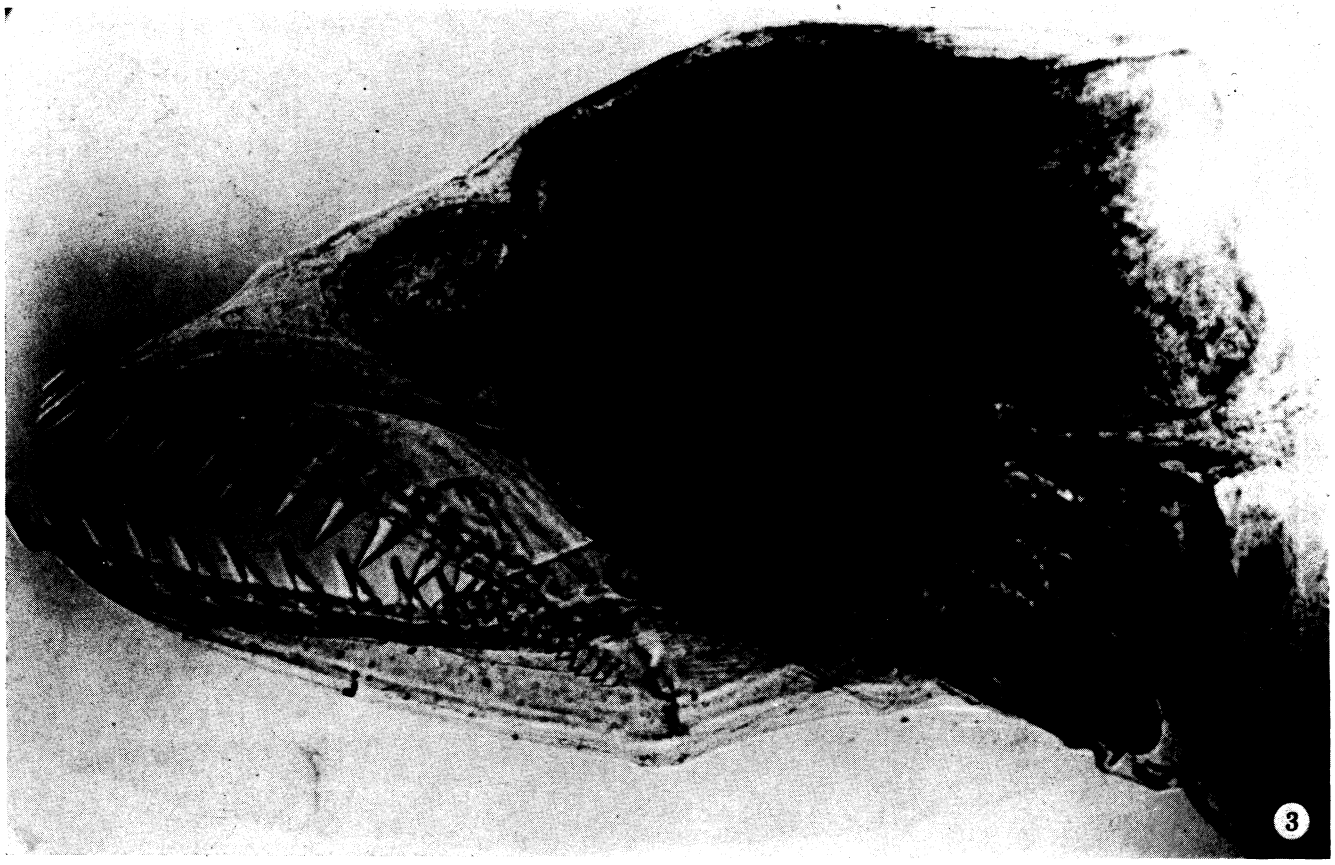

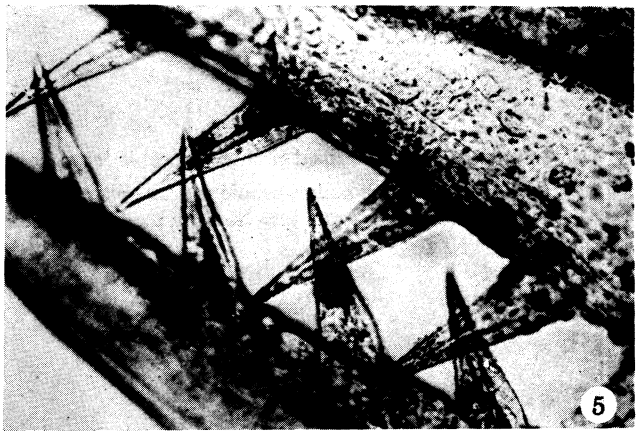

FIGURE 3. Head and anterior body of leptocephalus in glutaraldehyde. The numerous small teeth on the maxilla are well visualized. The esophagus bends sharply downward as it passes over the ventricle. The eye has been blacked out.

FIGURE 4. The left premaxilla and its attached tooth are above the first tooth of the maxilla.

FIGURE 5. Anterior teeth. Note that the teeth are inclined forward.

DESCRIPTION OF PLATE 3

FIGURE 6. Lateral view of the ventral part of the body. Branch of dorsal aorta to liver and stomach. The ventral liver lobe ends slightly posterior to the gall bladder.

FIGURE 7. Two renal arteries in a common sheath enter the posterior end of the kidney.

FIGURE 8. The external opening of the urinary bladder is directly above the anus.

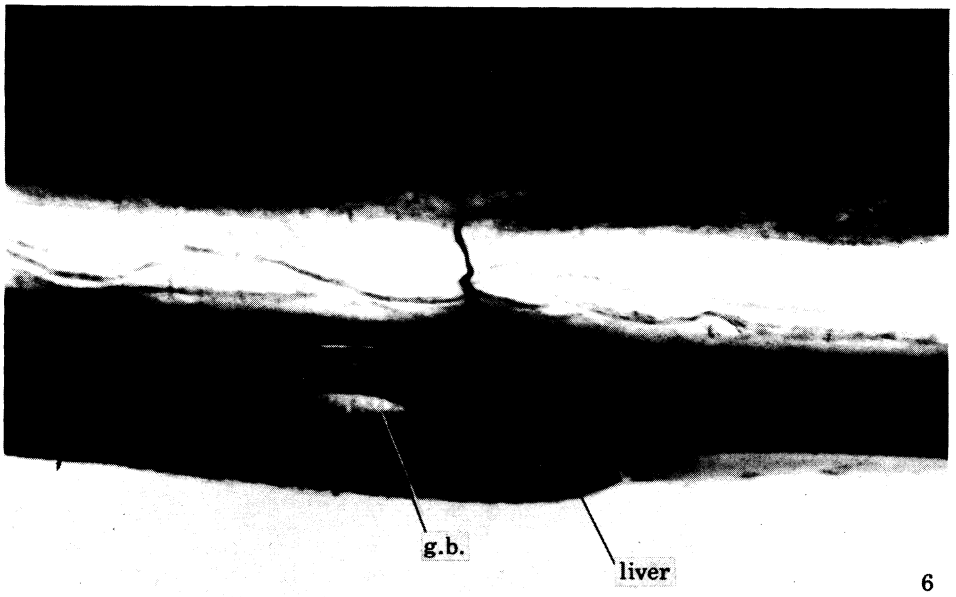

6

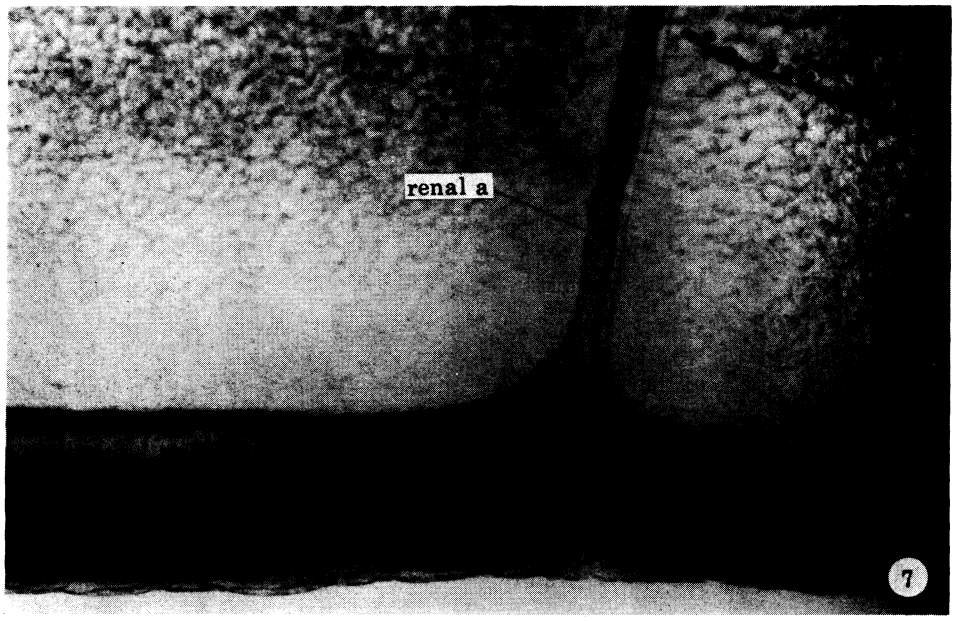

7

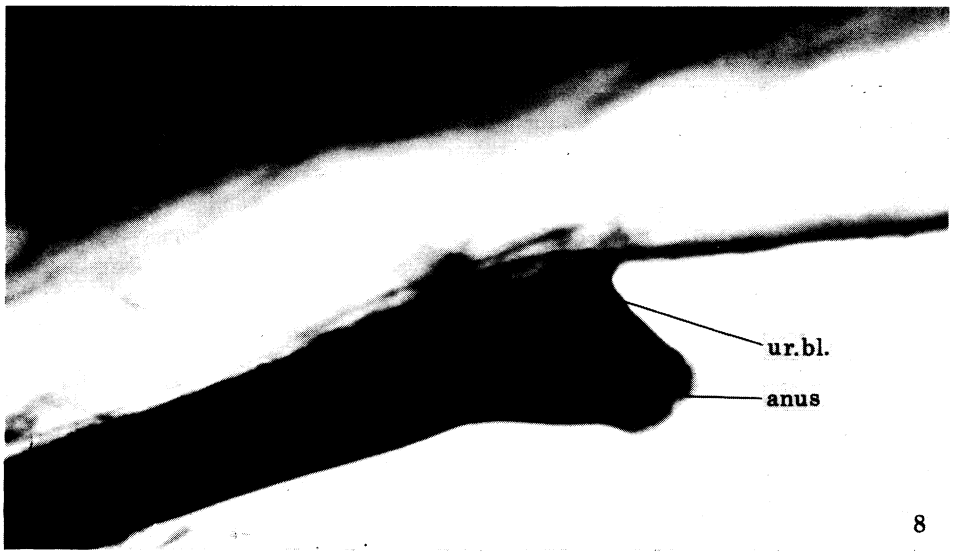

8

FIGURES 6–8. For description see opposite.

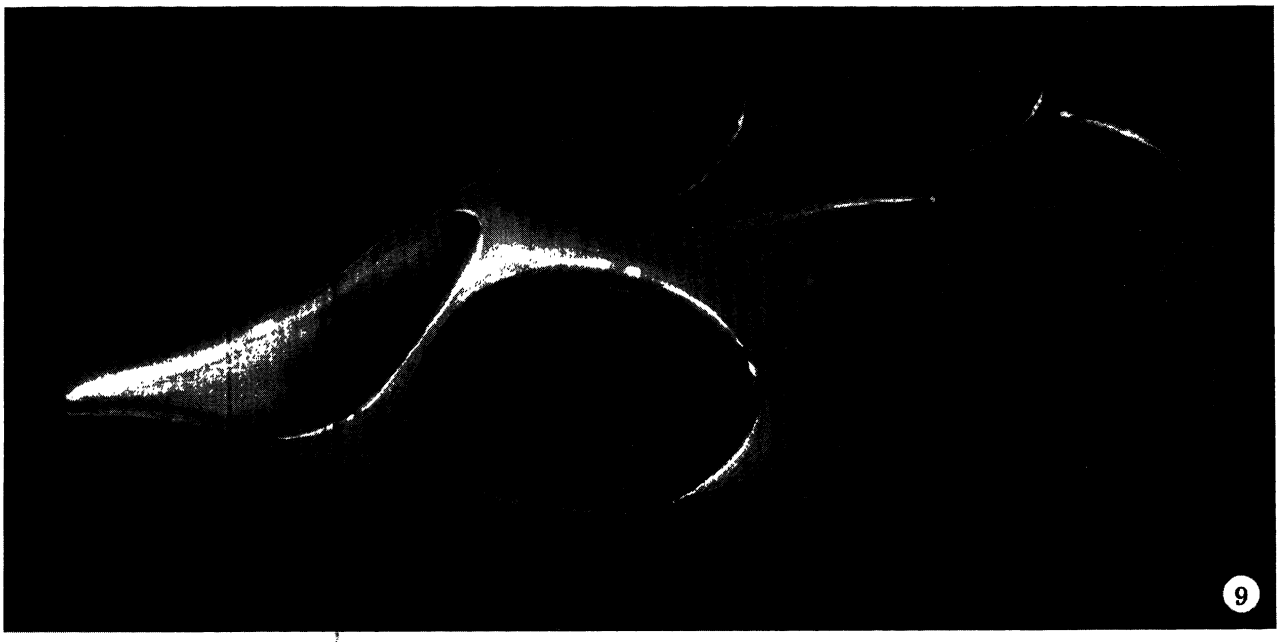

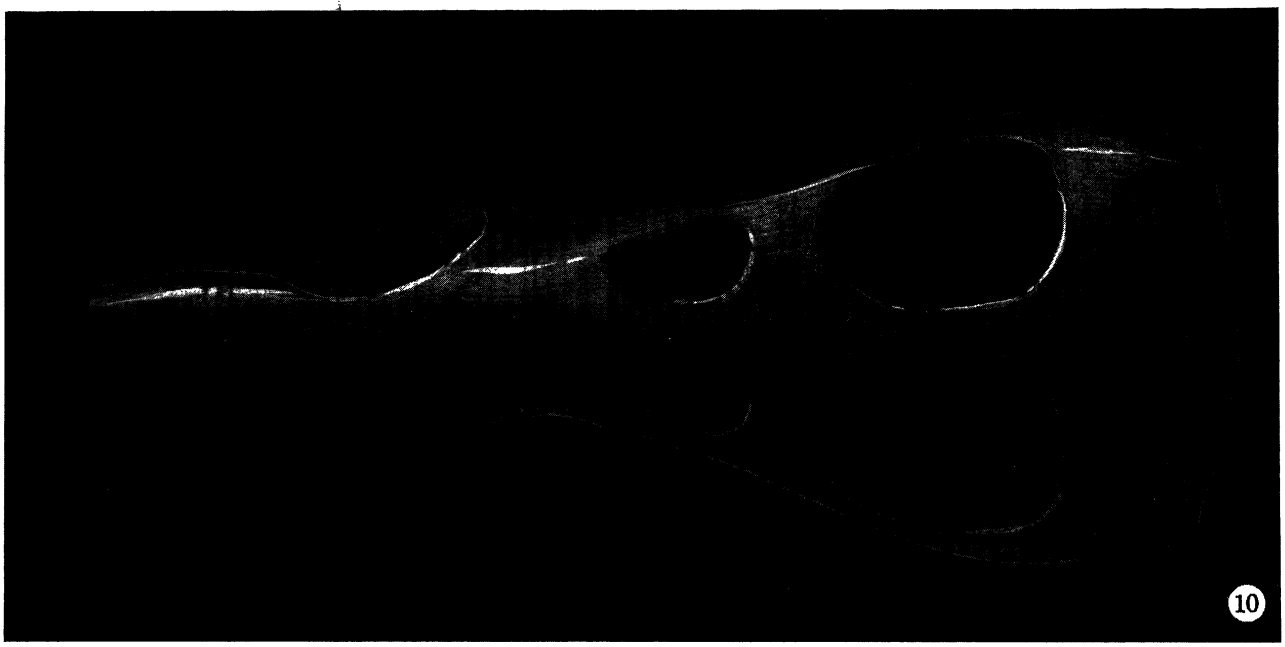

FIGURE 9. Lateral view of the cartilaginous neurocranium. Anteriorly, the ethmoid cartilage gives support and protection to the olfactory organ. Three structures join the anterior cartilaginous neurocranium to the posterior portion: (*a*) a thin midline ribbon of cartilage from the ethmoid to the epiphysial tectum, (*b*) the lateral supraortibal bars, and (*c*) the ventral, midline trabecula communis. Posteriorly, the otic capsule comprises the major portion of the cartilaginous neurocranium. (Magn. × 38.)

FIGURE 10. Viewed from above, the dorsal aspect of the brain receives little protection. The epiphysial tectum and the midline cartilage extending from the ethmoid to the synotic tectum leave four large fontanelles unprotected. (Magn. × 38.)

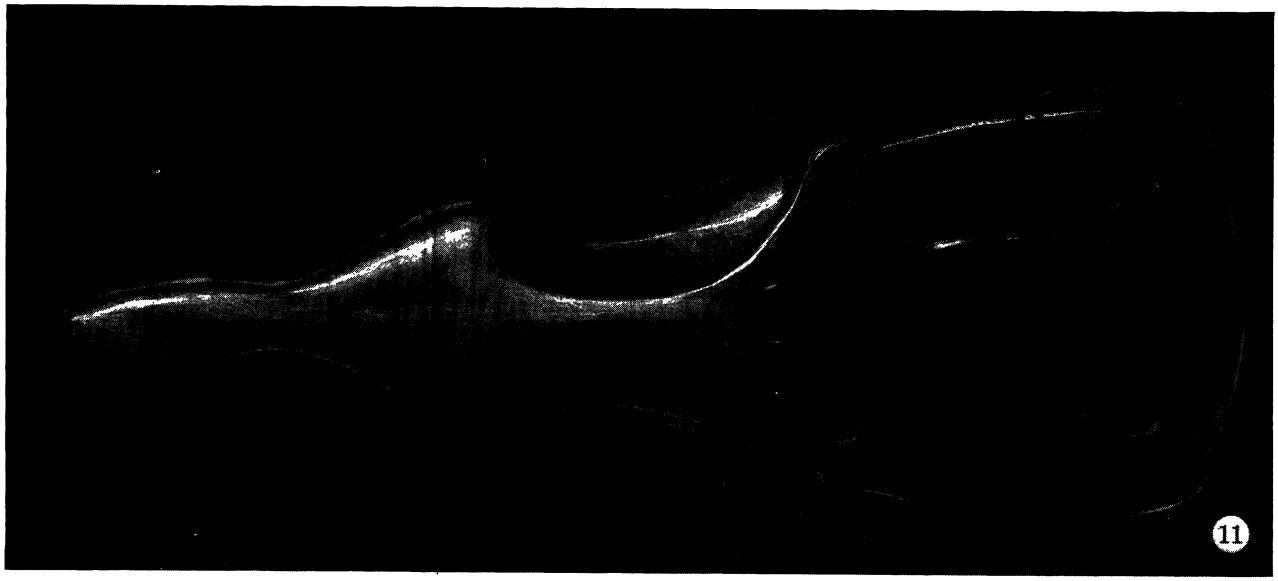

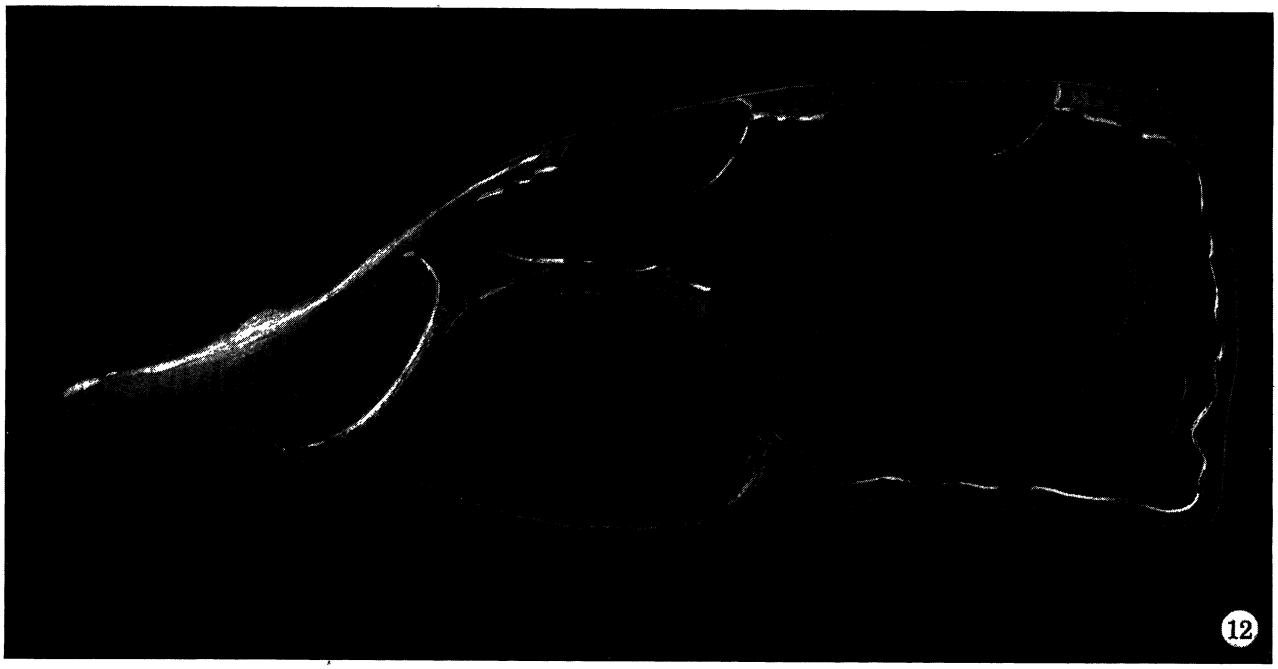

FIGURE 11. Ventral view of the cartilaginous neurocranium. Near the posterior termination of the trabecula communis, two foramina provide entry for the carotid arteries; foramina for the facial nerve (VII) are slightly more posterior and lateral. Posteriorly, the glossopharyngeal (IX) and vagus (X) nerves leave through paired foramina in a groove between the parachordal cartilage and the otic capsule. (Magn. × 38.)

FIGURE 12. Internal view of the auditory region. Posterior to the circular bulge of the cartilaginous otic capsule are additional supports for the posterior and lateral semicircular canals. (Magn. × 38.)

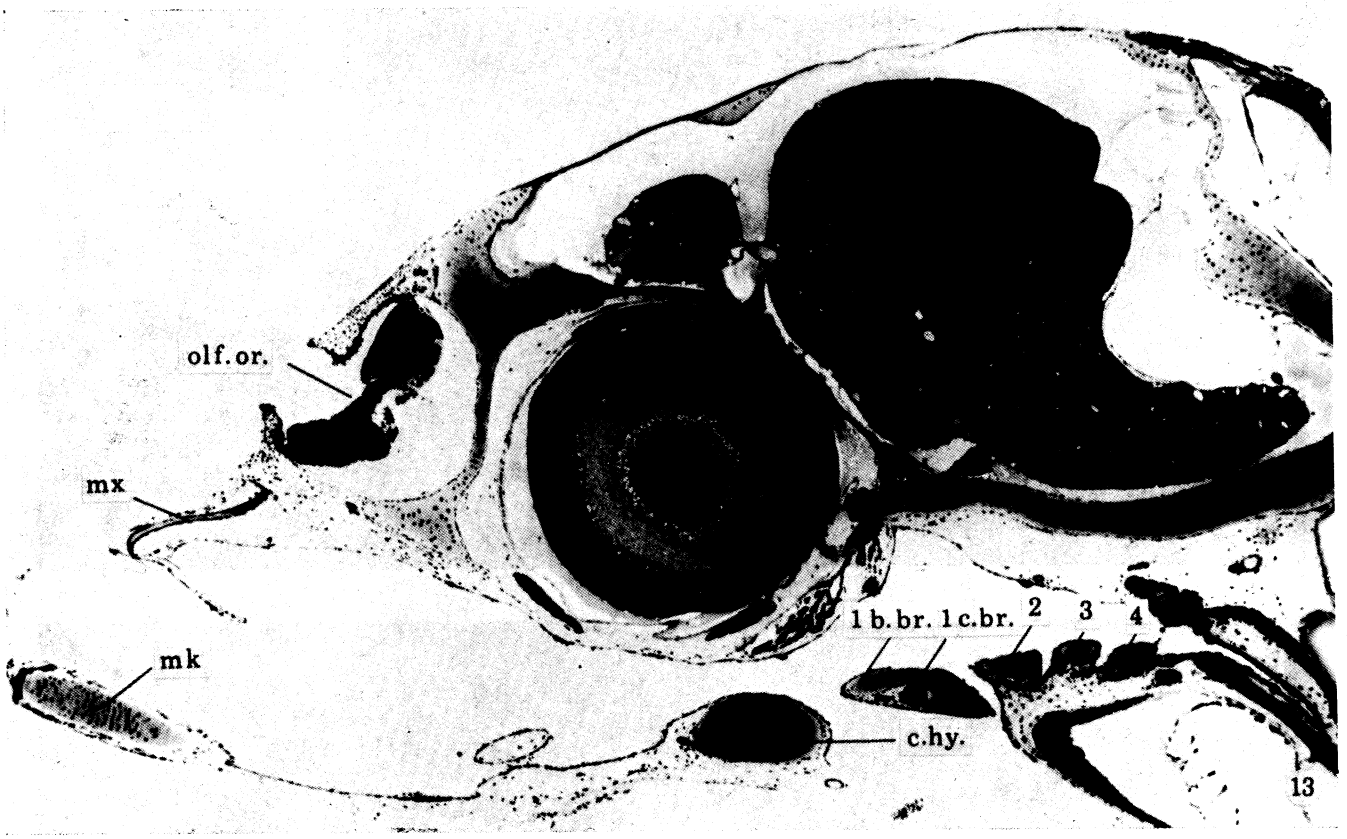

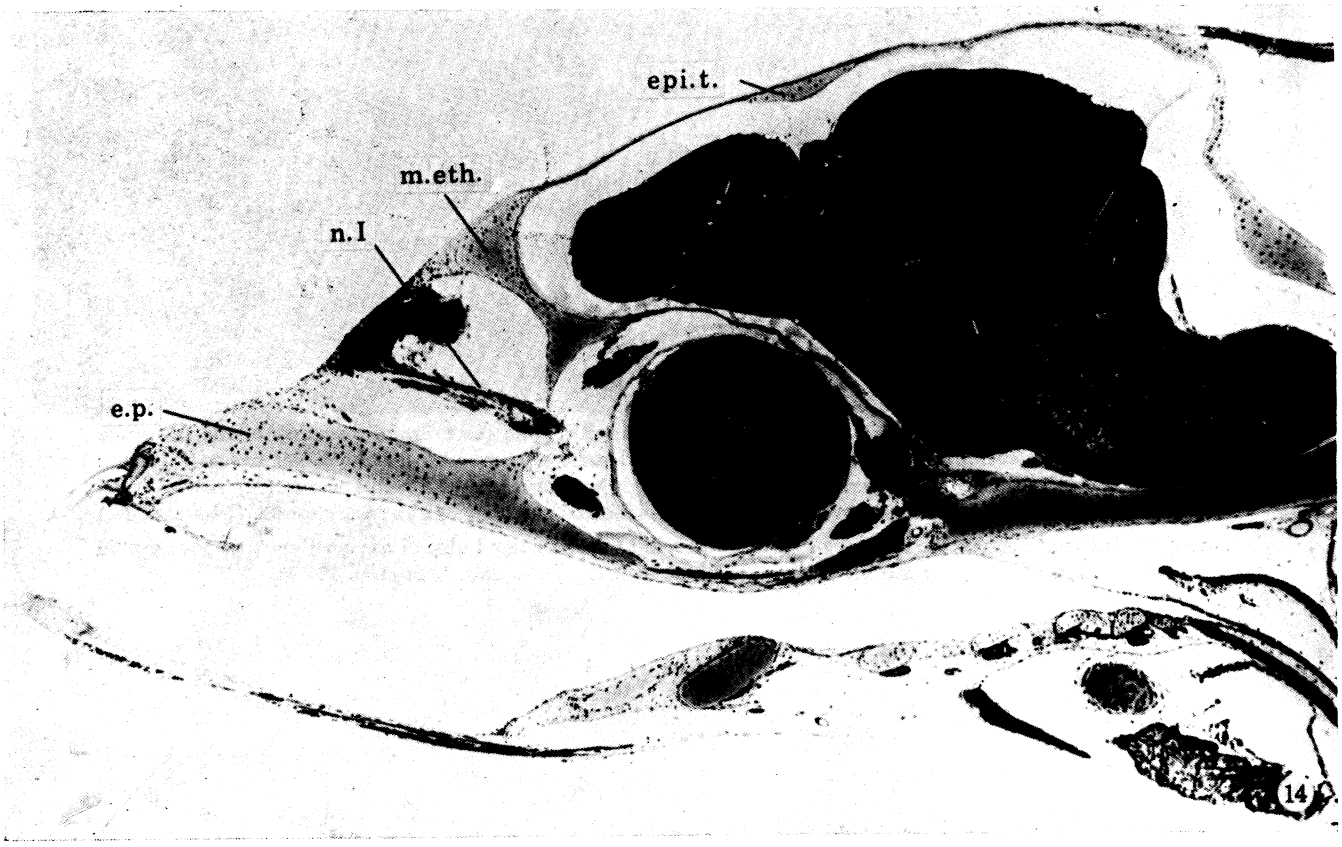

FIGURE 13. Sagittal section of head, left side. Figures 13–22 are from specimen WM(A)-4, 82 mm s.l. (Magn. × 60.)

FIGURE 14. Sagittal section of head, left side, medial to figure 13. (Magn. × 58.)

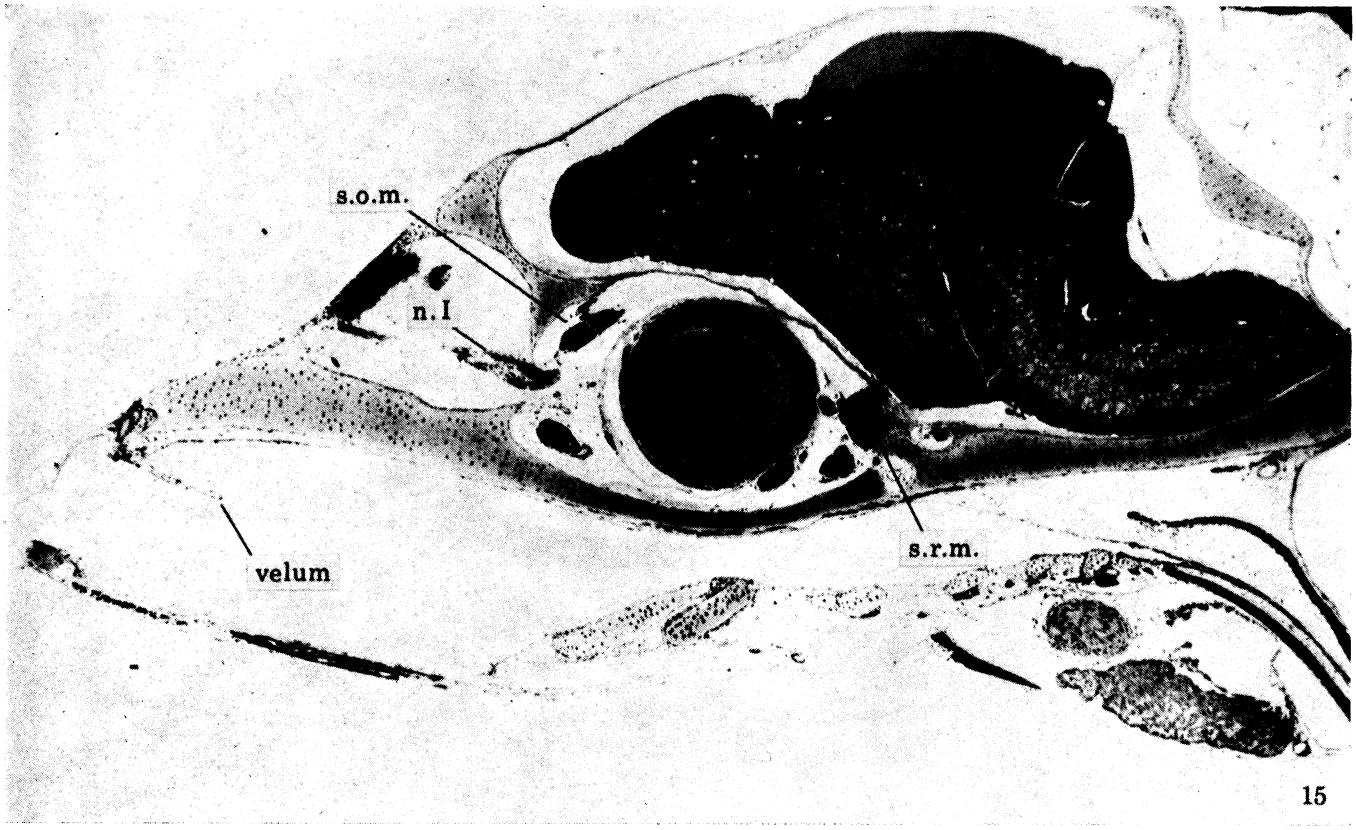

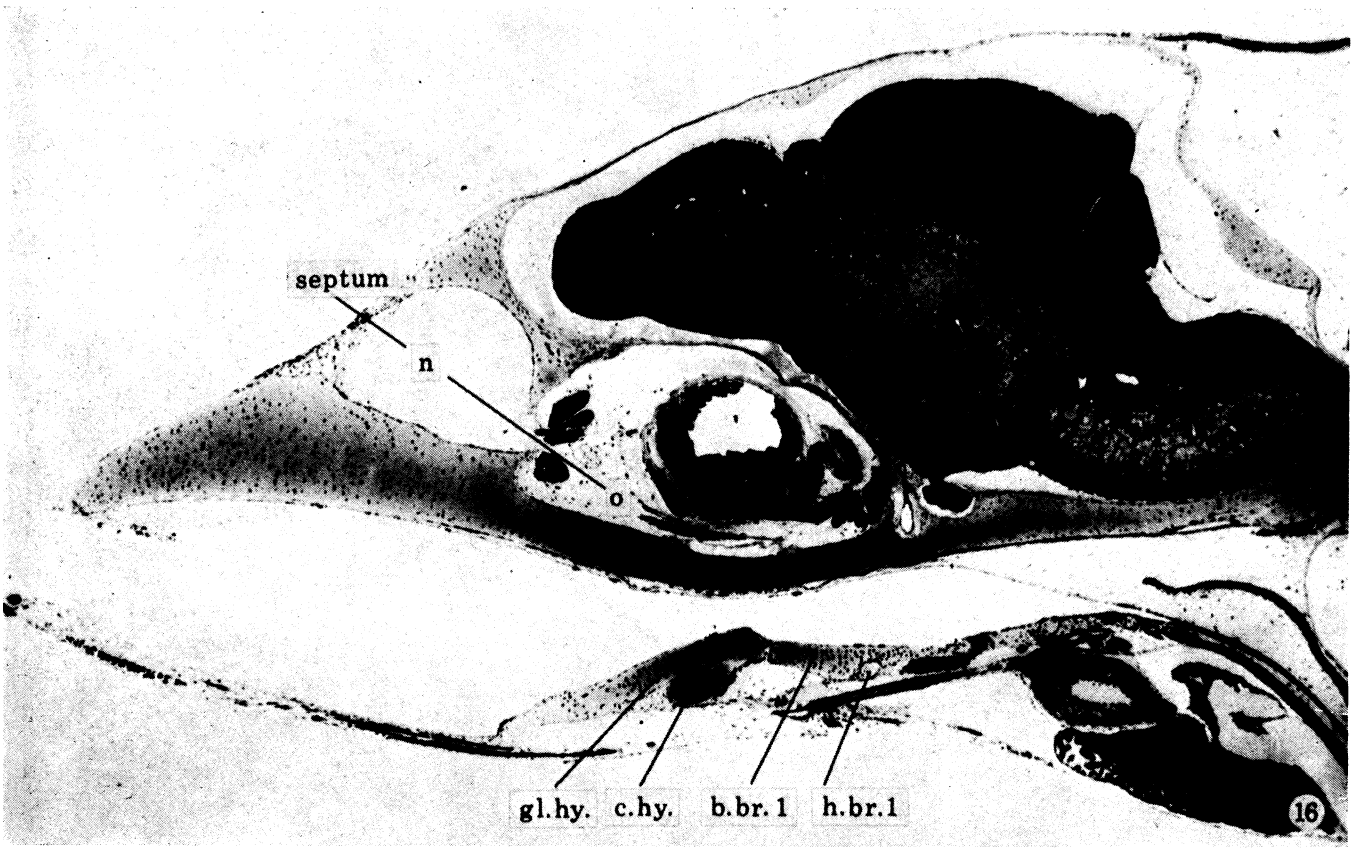

FIGURE 15. Sagittal section of head, left side, medial to figure 14. (Magn. × 57.)

FIGURE 16. Sagittal section of head, left side, medial to figure 15. (Magn. × 57.)

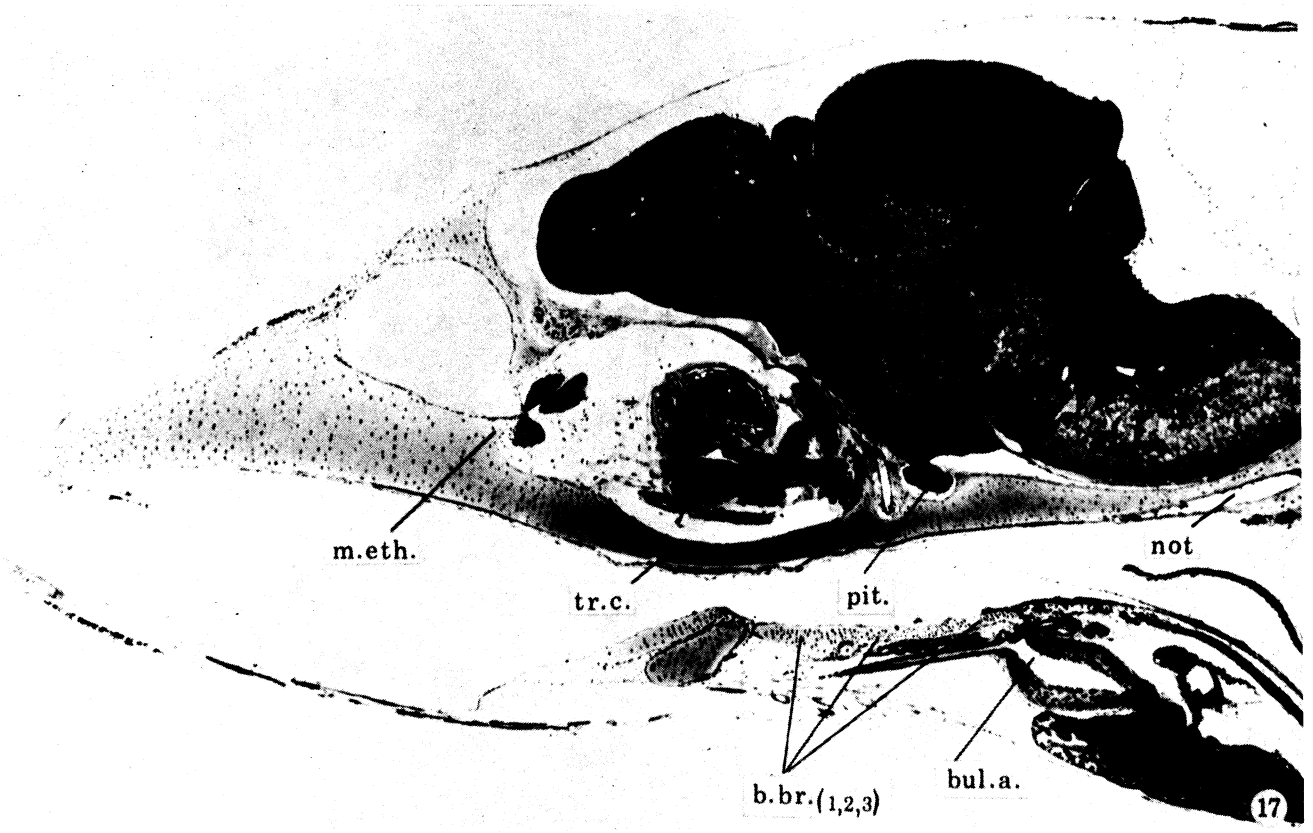

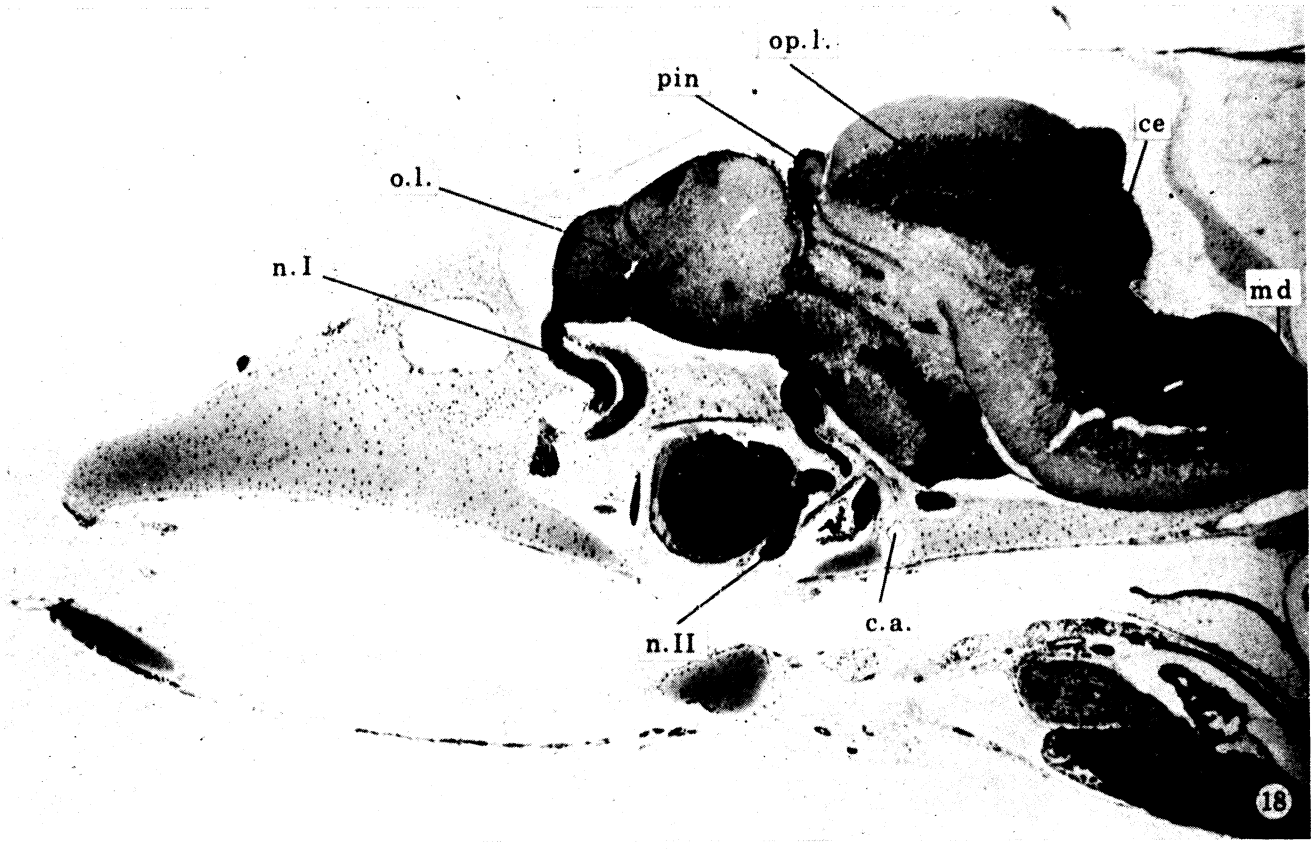

FIGURE 17. Sagittal section of head, midline. (Magn. × 58.)

FIGURE 18. Sagittal section of head slightly to right of midline. (Magn. × 66.)

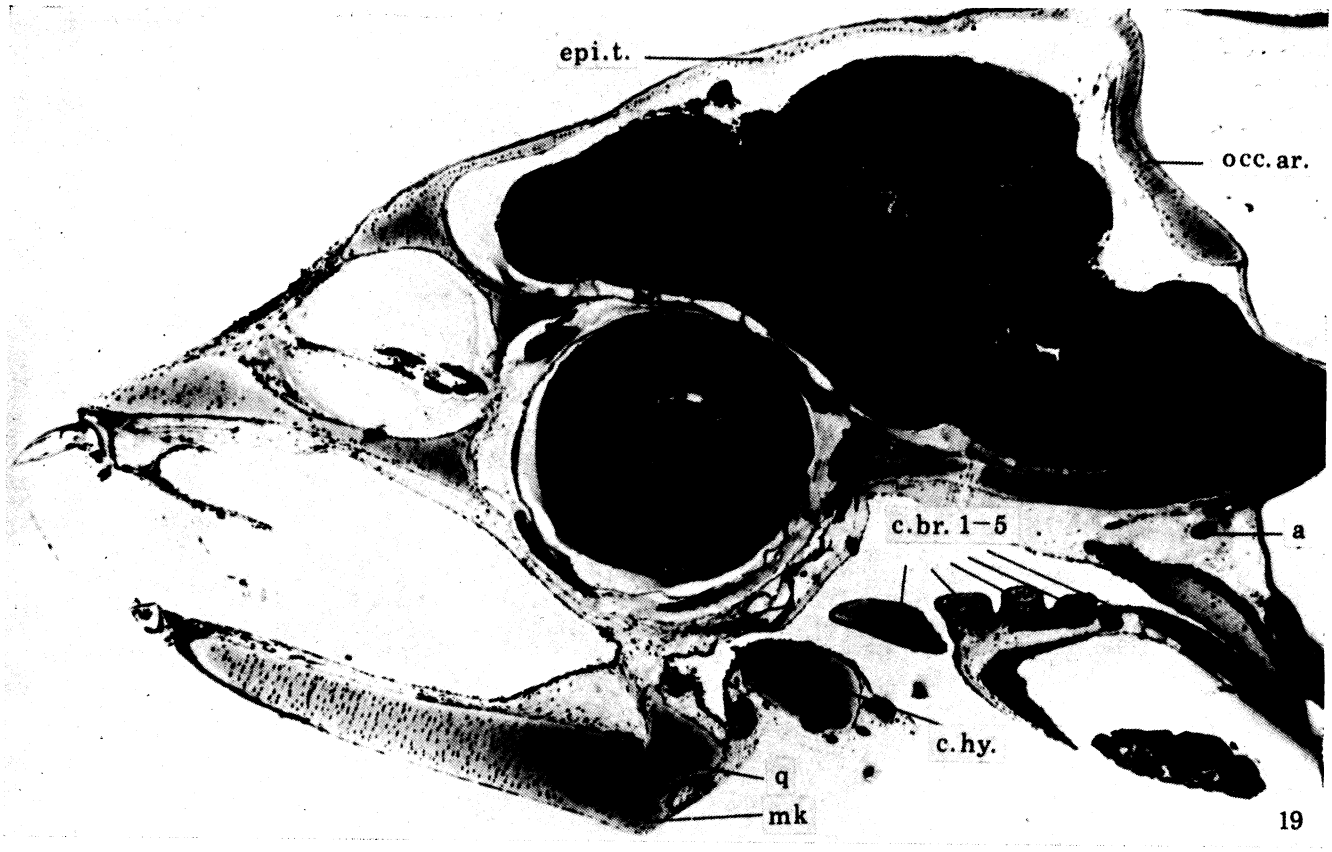

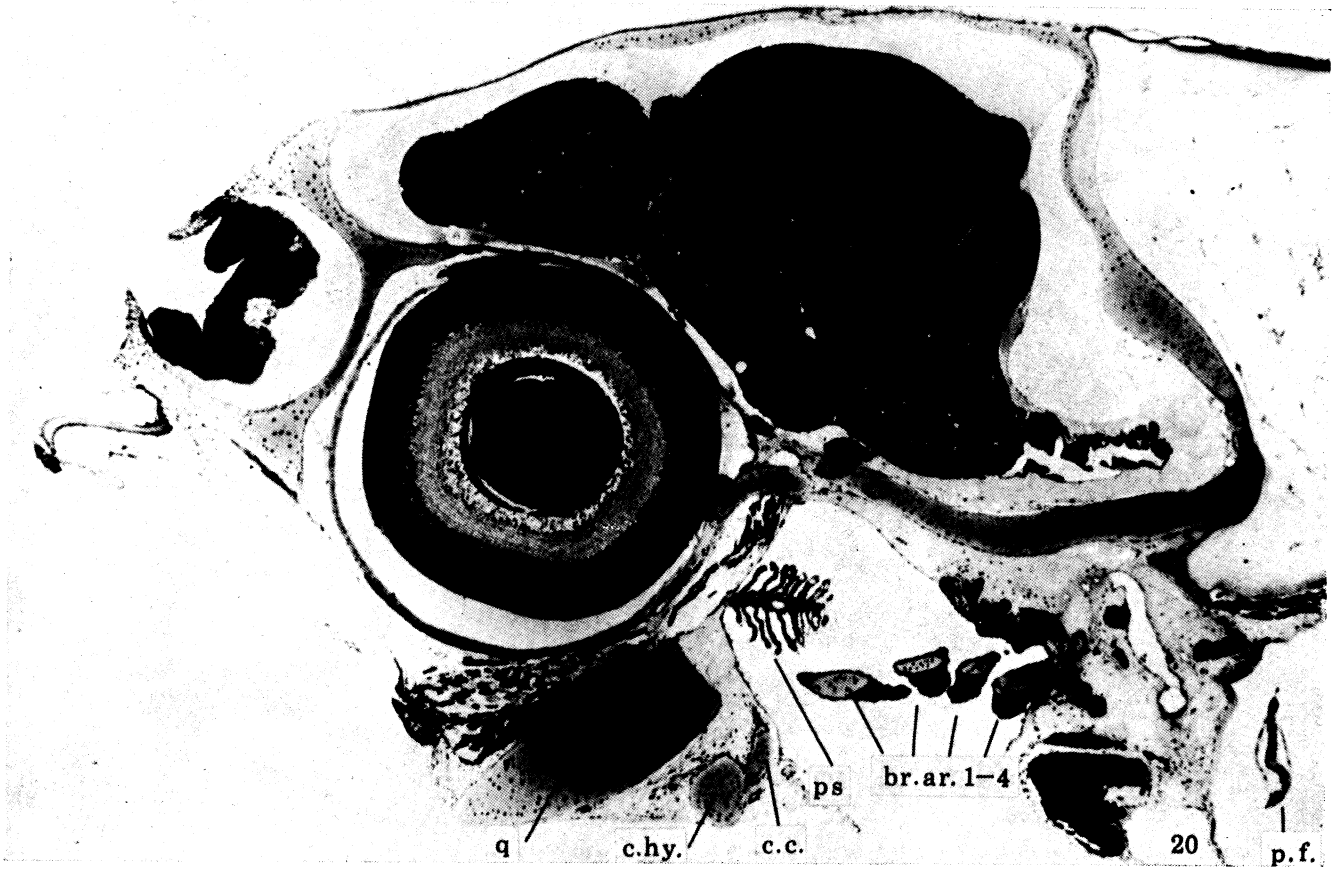

FIGURE 19. Sagittal section of head to the right of figure 18. (Magn. × 58.)

FIGURE 20. Sagittal section of head to the right of figure 19. (Magn. × 63.)

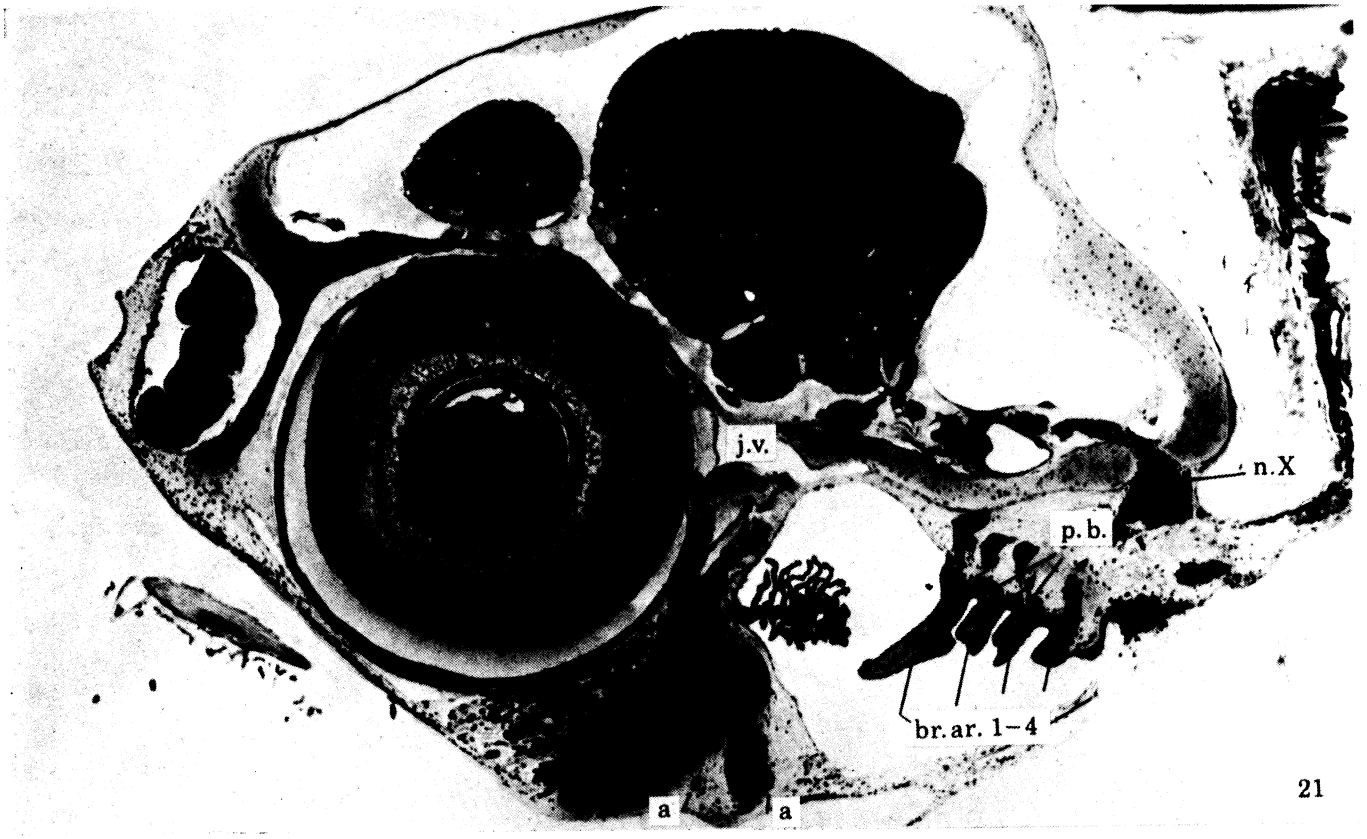

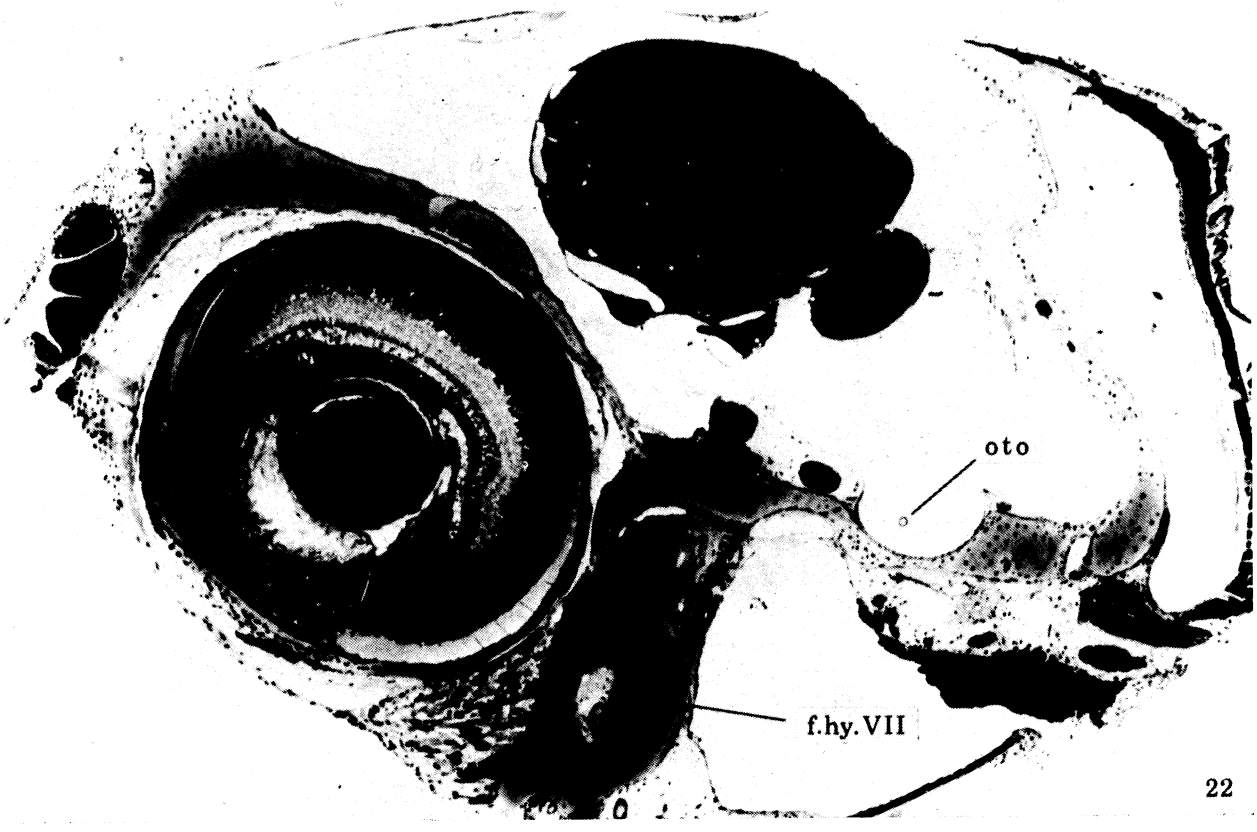

FIGURE 21. Sagittal section of head lateral to figure 20. (Magn. × 63.)

FIGURE 22. Sagittal section of head lateral to figure 21. The mass of tissue in the roof of the pharynx is the thymus. Above is the ganglion of the vagus nerve. (Magn. × 74.)

23

24

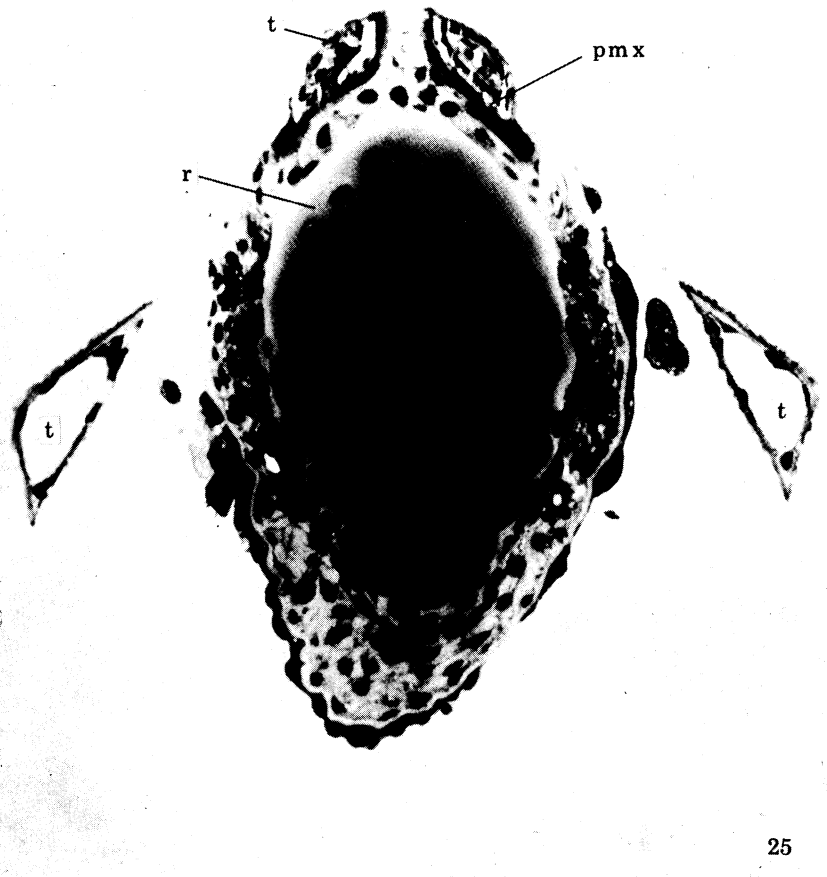

25

FIGURE 23. Tip of lower jaw showing the fusion of Meckel's cartilage. (Magn. × 640.) Figures 23–60 show the head of the leptocephalus in serial transverse sections (specimen EM507, 104 mm s.l.).

FIGURE 24. Fused Meckel's cartilage with dentaries on the lateral margins. (Magn. × 640.)

FIGURE 25. Tip of upper jaw with each premaxilla bearing a single, small tooth. (Magn. × 525.)

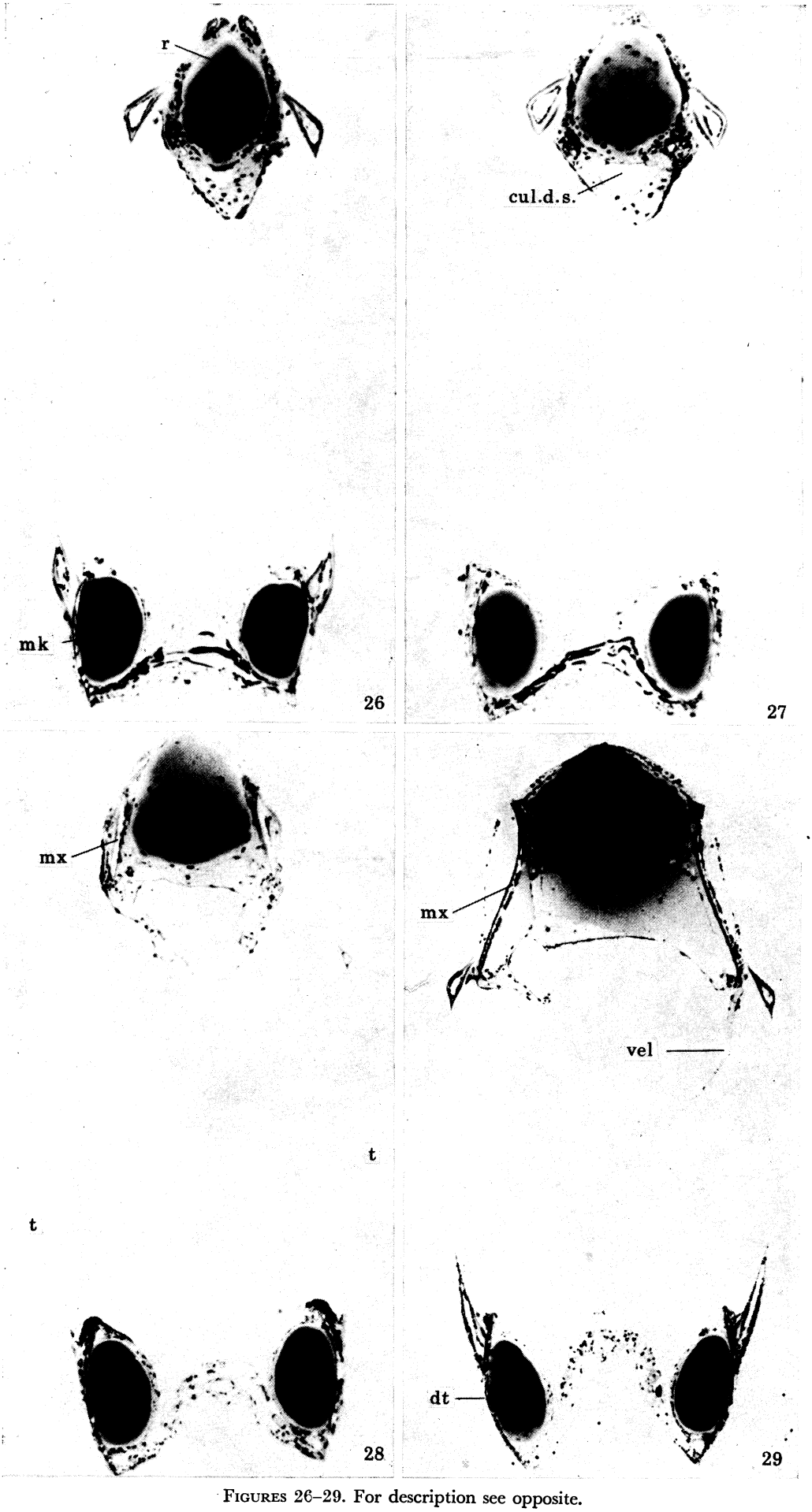

FIGURES 26–29. For description see opposite.

dividers and a ruler (table 2). With living larvae I did not try for greater accuracy because immediate fixation was essential. Precise measurements were made on leptocephali prepared as whole mounts (tables 3 and 4). These data indicate that head growth is slow compared to the growth rate of the axial skeleton. Comparison between the smallest (62 mm s.l.) and the largest (118 mm s.l.) larvae shows an increase in the length of the jaws (mandibular length 1.45 mm against 2.12 mm) and an enlarging eye (diameter, 0.73 mm against 1.00 mm) as part of the overall increase in head length and depth. Maximum head width of 1.10 mm was noted in the larva with the greatest standard length (118 mm s.l.). Measured on the horizontal, the average distance from the tip of the snout to the rostral commissure was 0.5 mm. The pectoral fins are short (0.3–0.4 mm in length) and broader than long (0.5 mm in depth).

TABLE 2. STANDARD LENGTH OF PREMETAMORPHIC LEPTOCEPHALI OF *ARIOSOMA BALEARICUM*, PROCESSED FOR ELECTRON MICROSCOPY

identification number	standard length before fixation	identification number	standard length before fixation
EM364	69	EM511	106
EM365	64	EM512	137
EM418	125	EM513	118
EM419	93	EM514	113
EM420	150	EM515	174
EM429	119	WM(S)-3	78
EM430	114	WM(S)-6	109
EM502	148	WM(S)-7	115
EM503	145	WM(S)-9	118
EM504	93	WM(A)-1	62
EM505	102	WM(A)-2	76
EM506	94	WM(A)-4	82
EM507	104	WM(A)-5	106
EM510	95	WM(A)-8	117

TABLE 3. DECREASE IN STANDARD LENGTH OF LEPTOCEPHALI OF *ARIOSOMA BALEARICUM* DUE TO PROCESSING OF TISSUE

leptocephali identification number	before fixation s.l. mm	embedded in plastic s.l. mm	shrinkage percentage
WM(A)-1	62	55	11.3
WM(A)-2	76	70	7.9
WM(S)-3	78	73	6.4
WM(A)-4	82	76	7.3
WM(A)-5	106	98	7.5
WM(A)-6	109	98	10.1
WM(S)-7	115	108	6.1
WM(A)-8	117	105	10.3
WM(S)-9	118	112	5.1

DESCRIPTION OF PLATE 12

FIGURE 26. Upper and lower jaws. (Magn. × 170.)

FIGURE 27. The velum is closed anteriorly and forms a cul-de-sac. (Magn. × 150.)

FIGURE 28. Maxillae are evident and the cul-de-sac is near to the point of separation. (Magn. × 130.)

FIGURE 29. Lateral folds of velum. Note the dentaries and projecting lower teeth. (Magn. × 130.)

(c) Teeth

All manner of adjective has been used to describe the teeth. Terms such as primary and secondary teeth are misleading rather than explanatory. As shown in figure 3, there is no argument that, relative to the size of the leptocephalus, the teeth are large. It is noteworthy that the tip of each tooth is inclined forward. The paired premaxillae are separate and a small

TABLE 4. MEASUREMENTS OF PLASTIC-EMBEDDED PREMETAMORPHIC LEPTOCEPHALI OF *ARIOSOMA BALEARICUM*

identification number	s.l. mm	preanal length mm	preanal length percentage of s.l.	greatest depth mm	greatest depth percentage of s.l.
WM(A)-1	55	53	96	6.6	12
WM(A)-2	70	68	97	7.0	10
WM(S)-3	73	70	96	7.3	10
WM(A)-4	76	73	97	7.5	10
WM(A)-5	98	96	98	8.7	9
WM(S)-6	98	94	96	9.6	10
WM(S)-7	108	104	96	9.1	8
WM(A)-8	105	101	96	7.7	7
WM(S)-9	112	107	96	9.4	8

TABLE 5. MEASUREMENTS OF PLASTIC-EMBEDDED PREMETAMORPHIC LEPTOCEPHALI OF *ARIOSOMA BALEARICUM*

identification number	length of head† mm	length of head† percentage of s.l.	depth of head‡ mm	snout to anterior eye margin mm
WM(A)-1	2.90	5	1.87	1.15
WM(A)-2	2.96	4	1.75	1.10
WM(S)-3	2.95	4	1.97	1.10
WM(A)-4	3.13	4	2.10	1.16
WM(A)-5	3.60	4	2.20	1.20
WM(S)-6	3.75	4	2.15	1.50
WM(S)-7	3.34	3	2.40	1.23
WM(A)-8	3.50	3	2.05	1.27
WM(S)-9	3.65	3	2.40	1.24

† Tip of snout to pectoral fin.
‡ Vertical measurement at the angle of the jaw.

TABLE 6. MYOMERE COUNTS ON PLASTIC-EMBEDDED PREMETAMORPHIC LEPTOCEPHALI OF *ARIOSOMA BALEARICUM*

identification number	total myomeres	preanal myomeres
WM(A)-1	122	114
WM(A)-2	124	117
WM(S)-3	122	114
WM(A)-4	120	112
WM(A)-5	126	117
WM(S)-6	122	112
WM(S)-7	124	115
WM(A)-8	125	117
WM(S)-9	129	120

tooth projects from each bone (figure 4). From the paired maxillae and dentaries a tooth emerges from the most anterior aspect of each bone. A tooth growing from the tip of these developing bones is in a plane continuous with the long axis of the jaw. Each jaw has 40 to 50 teeth. Each maxilla or dentary has 6–8 anterior teeth of the type shown in figure 5. These are followed by an almost equal number of intermediate size. The small teeth are blade-shaped, 7–10 in number (figure 3). The teeth on the posterior half of each jaw are difficult to count without the risk of damaging the specimen.

(d) Gut and blood vessels

To define the gut as a simple straight tube is an obvious oversimplification used only for taxonomic purposes. However, the gut tube in *A. balearicum* is smooth and free of bulges and indentations described in some other species. From its origin, the esophagus passes over the heart, curves sharply downward and terminates at the beginning of the stomach a few myomeres posterior to the gall bladder (figures 3 and 6). Two branches of the dorsal aorta enter the gut tube over the length of the esophagus (table 7). Close to myomere 21 a third branch of the dorsal aorta passes in front of the gall bladder (figure 6, plate 3) and enters the gut tube. This artery and one or both of the preceding vessels probably enter the ventral lobe of the liver which commences about myomere 10 and lies beneath the esophagus. This lobe ends a short distance behind the gall bladder. In a larva of 78 mm s.l. the horizontal dimension of the gall bladder was 0.47 mm. The fluid in the gall bladder is clear because there are no circulating erythrocytes at this stage and, consequently, no bile pigments for excretion. About 6–8 branches from the dorsal aorta enter the gut tube along the course of the intestine. These arteries are not large and it is worthwhile to remember that the cross-sectional diameter of the entire digestive tract is only 0.3 to 0.5 mm. Near myomere 62 a pair of vessels from the dorsal aorta join in a common sheath and enter the caudal end of the kidney (figure 7, plate 3). The anal papilla and urinary bladder are far posterior and open to the exterior several myomeres from the caudal fin (figure 8, plate 3).

TABLE 7. POSITION OF MAJOR BRANCHES OF DORSAL AORTA IN NINE PLASTIC-EMBEDDED LEPTOCEPHALI OF *ARIOSOMA BALEARICUM*

area supplied	myomere	variations
esophageal 1	8–12	first esophageal vessel usually at myomere 8; a third esophageal present in two larvae
esophageal 2	12–16	
hepatogastric	19–22	myomere 21 most frequent
intestinal 1	23–27	Four larvae with 5, 6, 8 and 9 intestinal vessels, respectively
intestinal 2	26–32	
intestinal 3	31–36	
intestinal 4	36–42	
intestinal 5	42–46	
intestinal 6	44–51	
intestinal 7	50–59	
kidney 1,2	58–66	paired renal arteries; arteries remain separate but have a common sheath midway between the dorsal aorta and kidney; renal arteries usually enter the kidney at myomere 62
caudal	112–120	continuation of dorsal area into the postanal region was arbitrarily designated as caudal artery in the larva.

2. *Chondrocranium*

(*a*) *Neurocranium*

The description of the head skeleton is based on premetamorphic larvae ranging in standard length (s.l.) from 62 to 174 mm. The sagittal sections of the neurocranium are from a leptocephalus of 82 mm s.l. (WM(A)-4 in table 2). The transverse sections are from a leptocephalus 104 mm s.l. (EM507 in table 2) in which the head was fixed and embedded separately from the rest of the body. Serial sections of nine other larval heads were reviewed in preparing the description. Leptocephali of *Ariosoma balearicum* between 80 and 120 mm s.l. represent a fairly uniform stage of premetamorphic development. This stage is comparable to stage III of premetamorphic larval development in *Anguilla anguilla* (Norman 1926; Jespersen 1942). Sources for the terminology of bones and their relations were Goodrich (1930), Gosline (1971), Greenwood *et al.* (1966), Robins (1971), Robins & Robins (1971), Harrington (1955), Peyer (1968), Orton (1963) and Romer (1962). The key to abbreviations used for the figures is given at the end of the paper.

Cranial cartilages serve two purposes. They protect the brain from injury and provide surfaces for attachment of other skeletal parts. The olfactory, optic and otic organs are partially protected by the lateral walls while the cartilage of the floor and roof support and protect the brain. In the vertebrate embryo the cranial floor develops first and begins with two pairs of cartilaginous rods (Kerr 1919). The anterior pair of trabeculae extend forward beneath the orbits, fuse together to form a single trabecula communis, and terminate in the rostrum as an ethmoid plate. The basal plate or posterior floor of the cranium originates from a pair of parachordal cartilages, one on each side of the notochord. The posterior wall develops from chondrification of an occipital arch and protects the medulla and emerging spinal cord. The cartilaginous nasal, orbital and otic capsules collectively form the lateral walls of the neurocranium. Blood vessels and cranial nerves pass in and out of the cranial vault in the fissures between the growing cartilages. The anterior trabeculae fuse directly with the posterior parachordals through an interpolated pair of polar cartilages. The embryonic neurocranium grows rapidly and partial fusion of adjacent cartilages is already present in larval fishes only a few millimeters in length. The roof is the last region to develop maximal chondral protection. In bony fishes, the brain has

---

Description of plate 13

Figure 30. Transverse section through the midportion of the ethmoid region. (Magn. × 120.)

Figure 31. Incurrent opening of the nasal sac. The mesethmoid is thin to accommodate the olfactory organs. (Magn. × 100.)

Figure 32. The olfactory organs are separated by a thin internasal septum (i. sep.). (Magn. × 75.)

Figure 33. The ectethmoids extend up and back to join the upper bar of the mesethmoid. (Magn. × 75).

Description of plate 14

Figure 34. The posterior aspect of the ethmoid complex. (Magn. × 100.)

Figure 35. The ethmoid cartilages form the anterior neurocranium. (Magn. × 70.)

Figure 36. The ceratohyals begin at the level of the articulation of Meckel's cartilage with the quadrate. (Magn. × 70.)

Figure 37. The parasphenoid lies beneath the trabecula communis. The olfactory tracts are near the union with the olfactory lobes. (Magn. × 70.)

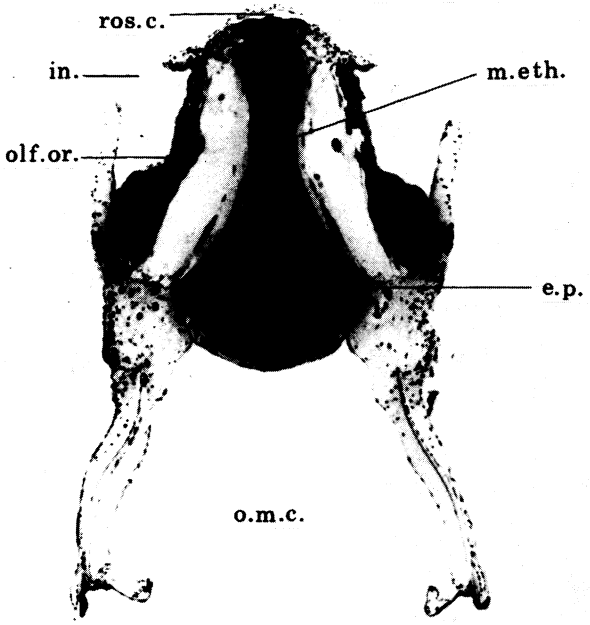

30

31

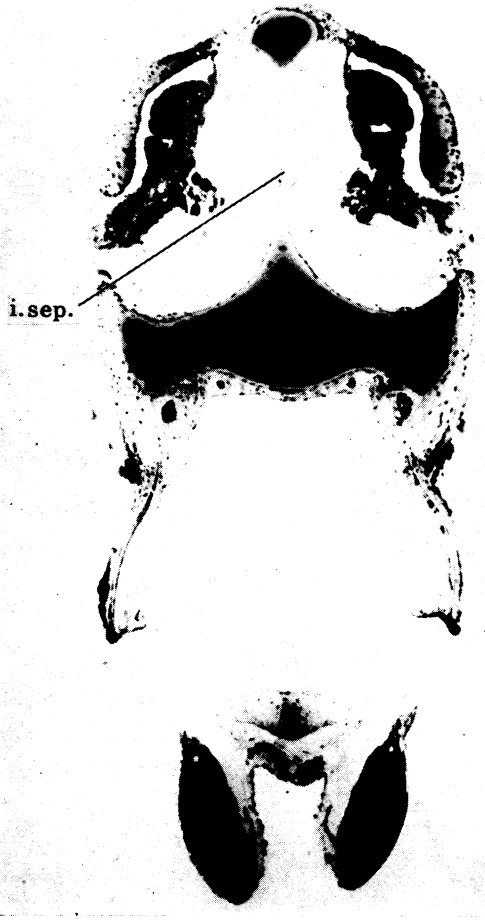

32

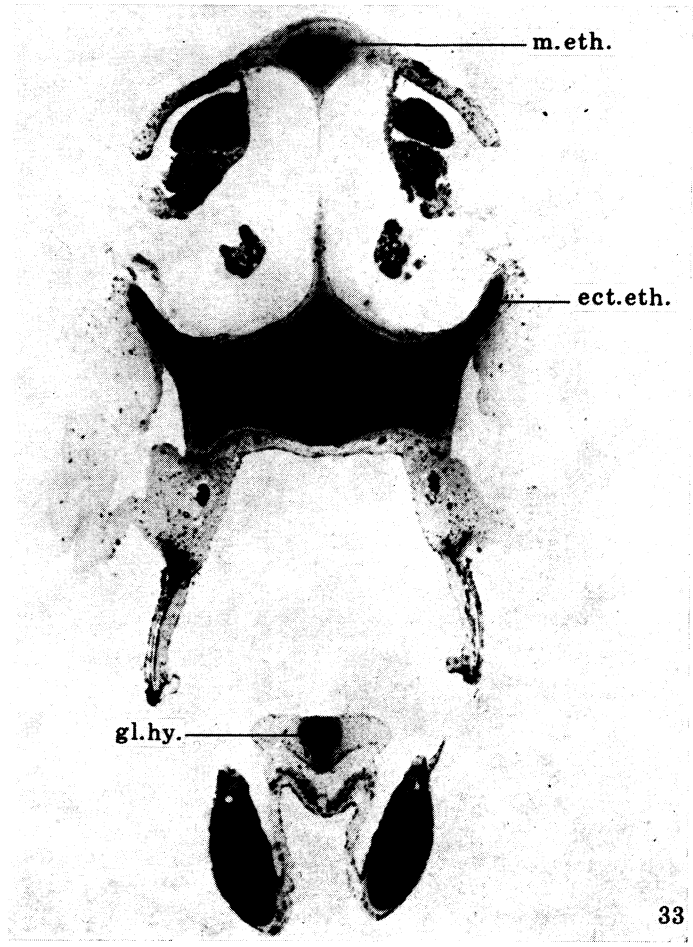

33

FIGURES 30–33. For description see opposite.

(*Facing p.* 118)

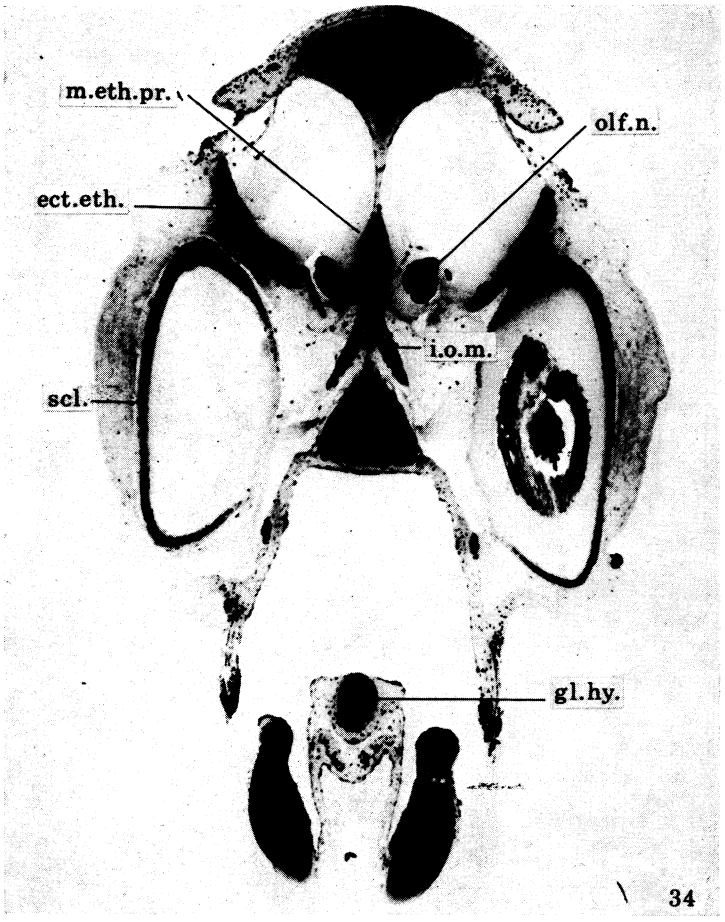

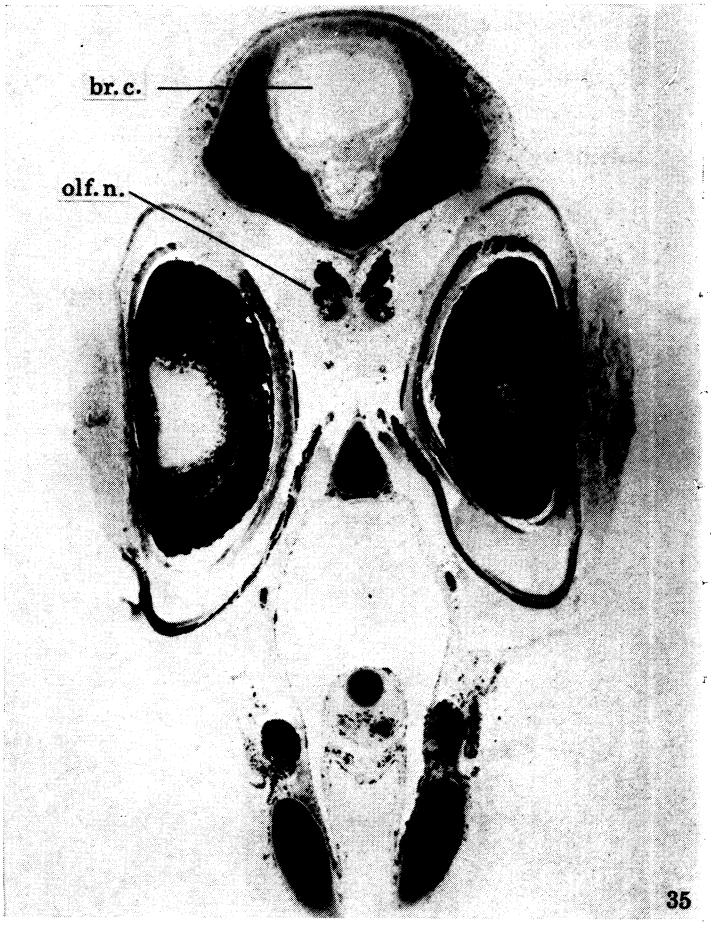

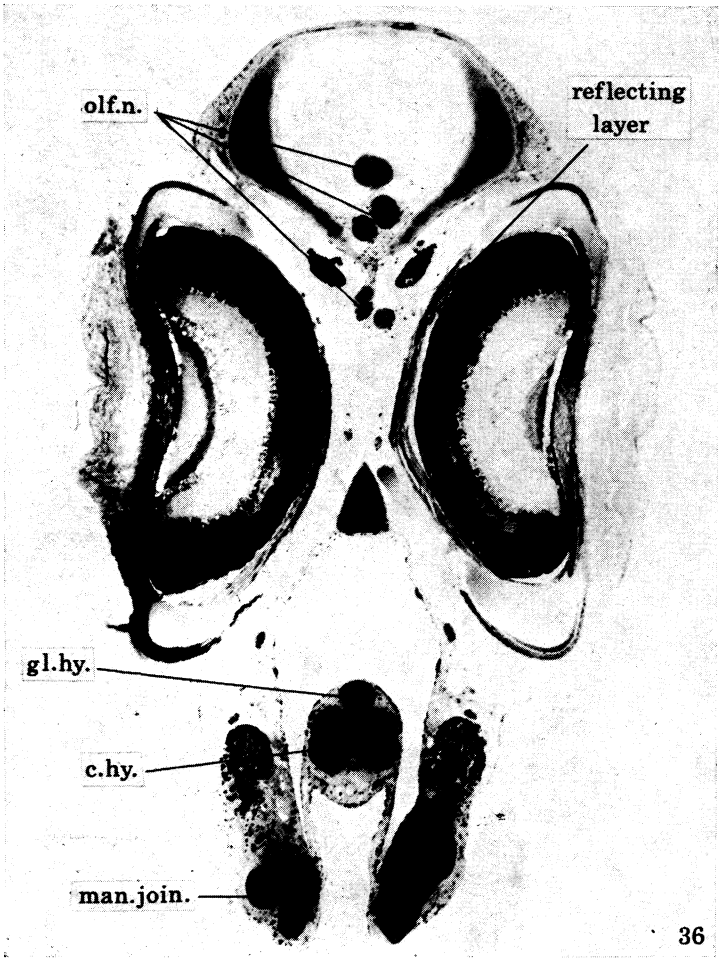

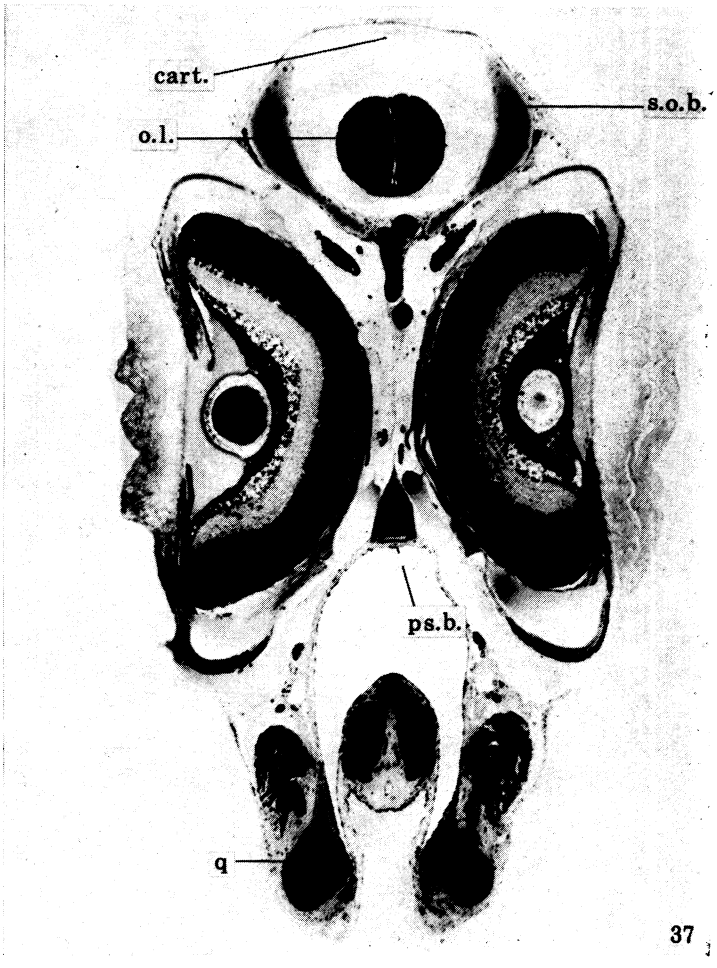

FIGURES 34–37. For description see p. 118.

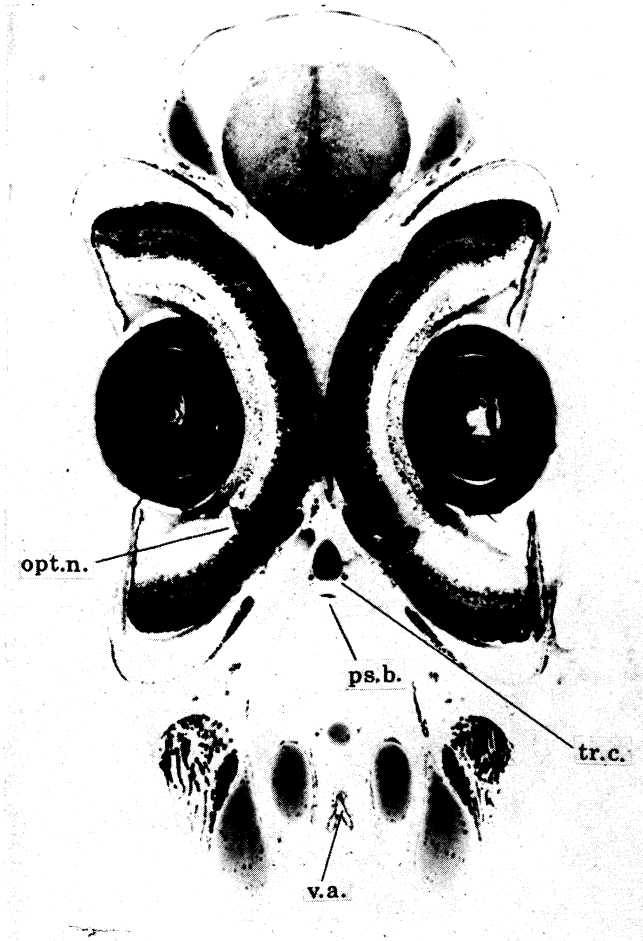

38

39

40

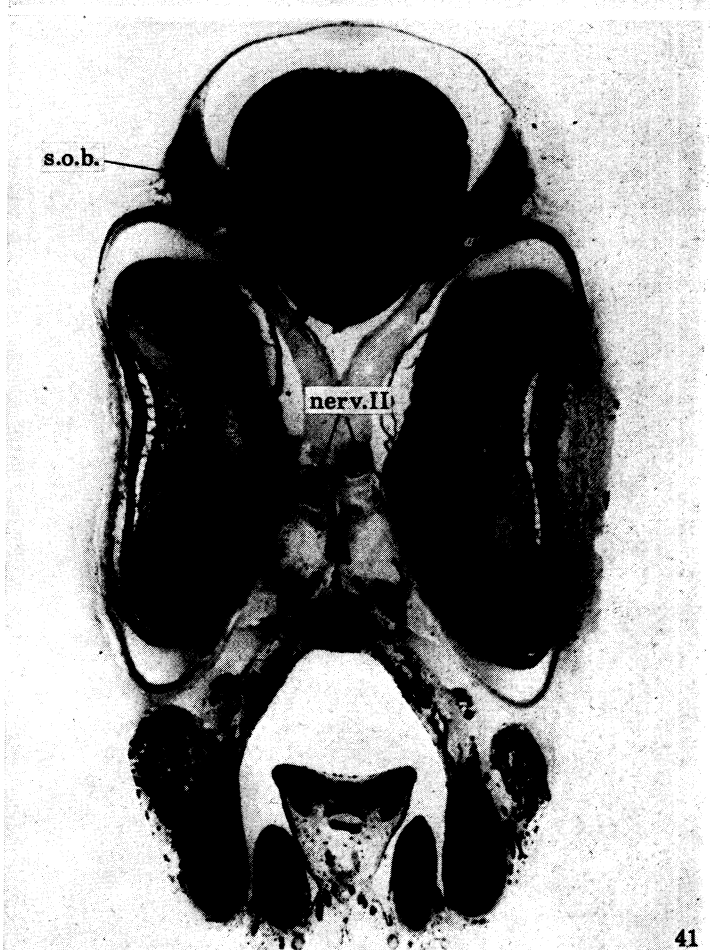

41

FIGURES 38–41. For description see p. 119.

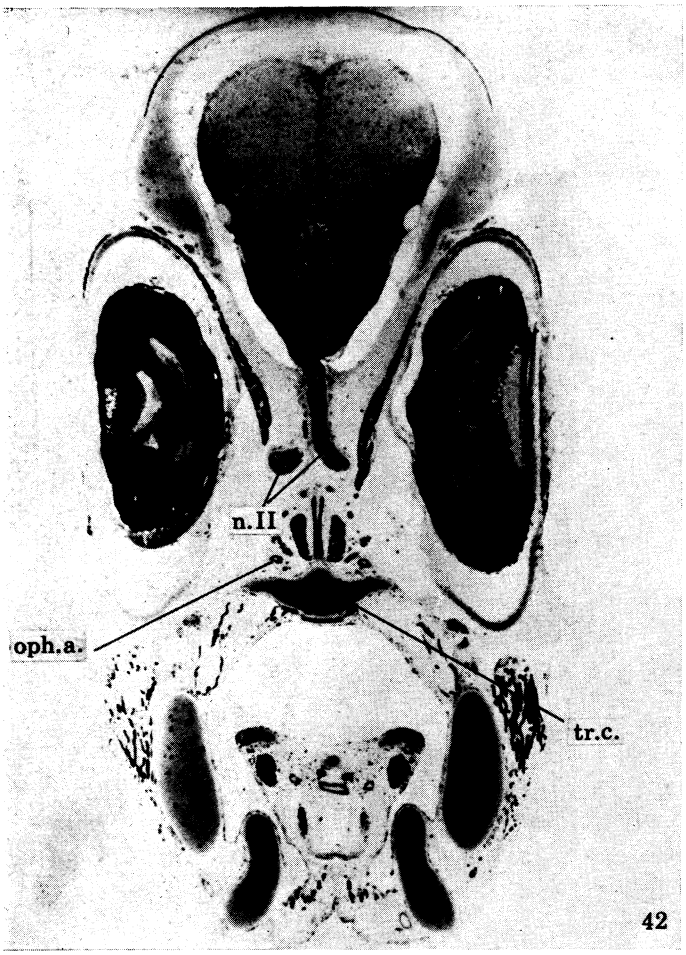

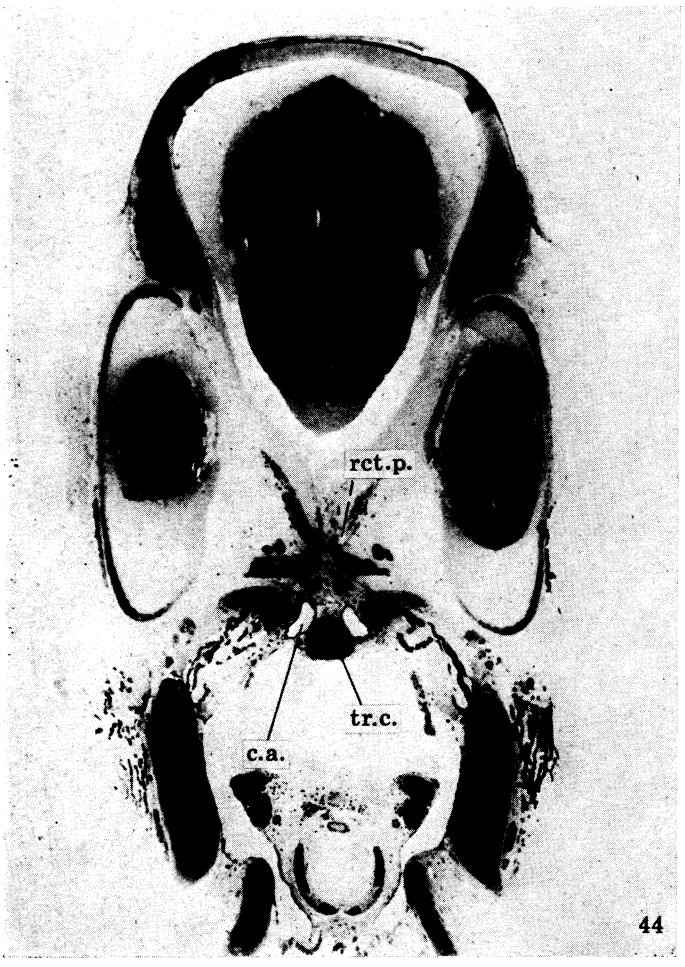

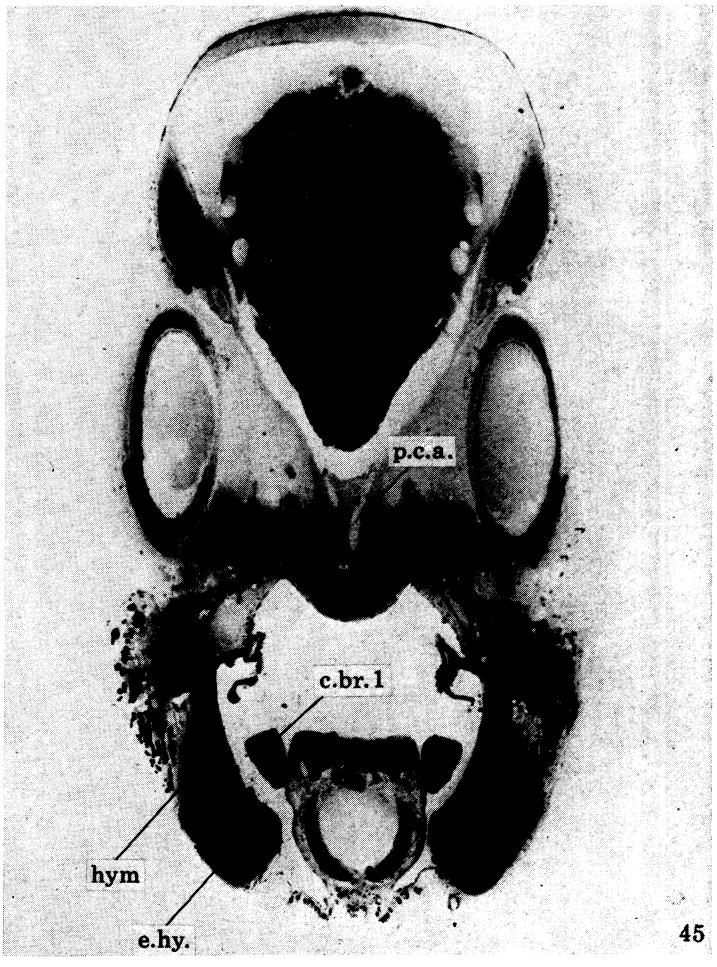

FIGURES 42–45. For description see opposite.

little protection from cartilage and must await dermal ossification for closure of large fontanelles. Growth of the auditory capsule and occipital arch over the head partially protects the hindbrain. Laterally, a supraorbital bar bridges the gap between the nasal sac and otic capsule in the form of a lateral strut and thereby strengthens the walls of the neurocranium. In some fishes a transverse strip of cartilage connects the supraorbital bars over the pineal. This transverse epiphysial tectum separates a large anterior and posterior fontanelle.

In the leptocephalus, the ethmoid is a solid wedge-shaped block of cartilage containing the rostrum, ethmoid plate and mesethmoid (figures 17 and 30). A large depression on either side of the mesethmoid houses the olfactory organs. Posteriorly the ethmoid block is continuous with the trabecula communis (figure 17, plate 8). In the larvae examined, the trabecula communis is always a midline rod of cartilage and its origin from paired cartilages is not apparent (figure 38, plate 15). The olfactory organs occupy such a large excavation in the mesethmoid that the vertical cartilaginous separation is short and diminishes quickly to a connective tissue septum (figures 30–32, plate 13). The most dorsal element of the mesethmoid continues posteriorly and upward. From the ventral aspect of the mesethmoid a lateral process termed the ectethmoid extends dorsally on both sides (figures 33 and 34, plates 13 and 14). The dorsal mesethmoid bar and ectethmoids unite with the paired supraorbital cartilages and together encircle the forebrain as a cartilaginous cup (figures 13 and 35, plates 6 and 14). The vertical septum between the olfactory organs projects posteriorly as the interorbital septum. A midline projection of the mesethmoid penetrates this septum for a short distance and provides attachment for the oblique eye muscles (figures 16 and 34, plates 7 and 14).

Each orbit contains an independent sclerotic cartilage (figure 34) to which the eye muscles insert. The interorbital septum is attached dorsally to fibrous tissue that joins the inferior borders of the paired supraorbital cartilages. The supraorbitals form the anterior lateral walls of the brain case. A flat longitudinal bar of cartilage lies between the two supraorbital cartilages and unites posteriorly with the epiphysial tectum (figures 10, 14 and 40, plates 4, 6 and 15). The inferior border of the interorbital septum attaches to the fused trabeculae which form the median trabecula communis. The trabecula courses posteriorly between the orbits. Near the posterior margins of the orbit the cartilage becomes broader but maintains a median ridge.

Description of plate 15

Figure 38. The optic nerves are seen entering the orbits. (Magn. × 70.)

Figure 39. All the retinal layers of the vertebrate eye occur in the leptocepalus. The reflecting layer is external to the retinal pigment. (Magn. × 70.)

Figure 40. Beginning of the gill arches. (Magn. × 70.)

Figure 41. Connective tissues from the cartilaginous supraorbital bars and the trabecula communis form the interorbital septum. (Magn. × 70.)

Description of plate 16

Figure 42. Below the optic chiasma the trabecula communis widens and gives attachment sites for the rectus eye muscles. (Magn. × 70.)

Figure 43. The first pair of ceratobranchials are shown in cross section. The efferent pseudobranchial arteries will join the lateral aortae and form the carotid arteries. (Magn. × 70.)

Figure 44. The carotid arteries enter the neurocranium through separate foramina. (Magn. × 70.)

Figure 45. The second pair of hypobranchials are in close contact with the long basibranchial. The epihyal is interposed between the ceratohyal and hyomandibular. (Magn. × 70.)

The rectus eye muscles attach to the posterior and terminal prominence of this ridge (figures 42–44, plate 16). At this point two foramina on either side of the median bar of cartilage give passage to the carotid arteries (figure 44). The midsagittal section through the head shows the uninterrupted posterior course of the ethmoid plate, trabecula communis, and fused parachordals (figure 17). The large embryonic basicranial fenestra is not present and the passage for the carotid arteries consists of two distinct foramina (figure 11, plate 5). The carotid arteries remain separate and do not fuse within the cranium to form a common trunk. Continuing posteriorly, the basal plate broadens and forms a depression for the hypophysis (figure 47, plate 17). At some point anterior to the hypophysis the trabeculae have fused with the anterior part of the parachordal cartilages.

The bulk of the brain is retro-orbital and lies between the two auditory capsules. Except for the weak areas in the roof, the entire brain is protected by cartilage from the optic lobes to the exit of the spinal cord. Behind the eye the supraorbitals broaden to become the postorbital lateral walls of the neurocranium (figures 9 and 46, plates 4 and 17). The postorbitals meet the parachordals ventrally to form the prootic cartilage. This junction of the lateral wall and cranial floor is sharply angular and the ventral surface of the prootic cartilage is grooved for articulation with the hyomandibular (figure 49, plate 17). Above the prootic and within the cranial cavity are the Gasserian and geniculate ganglia of the V and VII cranial nerves, respectively. The postorbitals fuse posteriorly with the auditory capsules. The lateral bulges of the auditory capsule roughly outline the position of the semi-circular canals (figures 54 and 55, plate 19). The medial aspect of the membranous labyrinth is adjacent to the brain and is not enclosed by cartilage. The boundaries of the large auditory capsule are confluent with the cartilaginous occipital arch posteriorly and the parachordals ventrally (figure 12, plate 5). Over the roof of the brain both capsules meet in a synotic tectum (figure 56, plate 19). The posterior fontanelle of the cranial roof is divided by a narrow band of cartilage that extends posteriorly from the epiphysial tectum to the anterior border of the synotic tectum (figure 10, plate 4). The notochord begins midway between the anterior and posterior limits of the parachordals and supplies the strongest structural union between the head and axial skeleton (figure 17).

(b) Brain and cranial nerves

The development of the nose and eyes suggests that these two organs have an essential and important role in the survival of a leptocephalus. On lateral projection the large olfactory lobes reach as far forward as the underlying oblique eye muscles originating from the prominence on the mesethmoid (figure 17). The cortex and remainder of the telencephalon merge into the diencephalon above the optic chiasma. Between the cerebrum and optic lobes the pineal or epiphysial evagination sits under a cartilaginous tectum. From this position the forebrain extends downward and terminates ventrally with the neurohypophysis of the pituitary gland (figures 17 and 47). Most of the brain cortex resides in the large optic lobes of the midbrain. Behind the optic lobes a small cerebellum begins the hindbrain. Because the pronounced embryonic cephalic flexure persists during larvalization, the communicating channel between the third and fourth ventricle is long and somewhat tortuous. The prominent dorsal aspect of the medulla oblongata is a characteristic of an acousticolaterialis system (figure 17).

The *olfactory* tracts (figure 18, plate 8) are large and leave the olfactory lobe from its most anterior aspect (figure 18). The tracts pass abruptly down, back, and forward to complete an S-shaped curve. Each nerve enters its respective nasal or olfactory capsule by passing between

the superior and inferior oblique eye muscles and through the ectethmoid. Histologically the organization of the olfactory organ is well-advanced in comparison with other organs. The *optic* nerve (II) equals the olfactory in structural development (figures 38 and 39, plate 15). A preliminary examination of the retina points to a nocturnal eye in the leptocephalus. Tangential sections of the retina show a uniformity of receptor elements consistent with one type of receptor cell. Their small size suggests rods rather than cones. The heavily pigmented retina is covered by an outer crystalline reflecting layer (figure 36, plate 14). These crystals lie between cytoplasmic bridges and, similar to guanine, they sublime in an electron beam. The spherical lens is centrally located and no part of the retina appears aphakic. The optic nerve perforates the orbit on the inferior medial aspect (figure 38). Within the interorbital septum the two nerves travel posteriorly up and over the rectus eye muscles (figure 41, plate 15). Partial decussation occurs as the nerves turn sharply upward and enter the ventral brain surface (figure 42, plate 16). The *oculomotor* (III), *trochlear* (IV) and *abducens* (VI) nerves innervate the ocular muscles. From the ventral brain surface they pass through the interorbital septum to their respective muscle groups. The rectus eye muscles originate together on the posterior prominence of the trabecula communis. None penetrates the basicranial foramina and no myodome is present. The Gasserian ganglion of the *trigeminal* (V) and geniculate ganglion of the *facial* (VII) lie side by side within the neurocranium above the hyomandibular articulation with the prootic. The Gasserian ganglion is located lateral to the geniculate ganglion (figure 49, plate 17). The lateralis ganglion and associated profundus nerve are separate from the main trigeminal. The large facial foramina perforate the floor of the neurocranium and each contains the hyomandibular branch of the facial and the jugular vein (figure 49). The *auditory* labyrinth (VIII) was previously described, but it may be added that the macula of the sacculus is histologically the most prominent. Between the parachordals and the lateral walls of the neurocranium two separate and paired foramina contain the *glossopharyngeal* (IX) and *vagus* (X) nerves. The jugular ganglion of the vagus is prominent because of the large ganglion cells lying outside the braincase (figures 22 and 57, plates 10 and 19). The peripheral fibres of the vagus travel caudally in two large nerves on the dorsal surface of the esophagus.

(c) Mandibular arch

Two large Meckel's cartilages give form and substance to the lower jaw (figure 58, plate 20). They fuse anteriorly in the midline and, posteriorly, they articulate with the quadrates figures 19, 23, 24 and 36, plates 9, 11 and 14). The posterior portion of Meckel's cartilage later ossifies to become the articular bone. The quadrate is smooth, free of projections, and merges imperceptibly with the hyomandibular (figures 19–22, plate 10). The quadrate and Meckel's cartilage are homologous with the respective upper and lower jaws of ancestral fishes, but in teleost fishes the functional significance of these elements has changed significantly. The jaws have moved backward to encroach upon and incorporate elements of the hyoid arch. Dermal bones have taken over the formation of the anterior two-thirds of the jaw. The quadrate and hyomandibular function as the suspensorium for both upper and lower jaws (hyostylic) in eels and other teleostean fishes.

(d) Hyoid arch

As the name implies, exact homology of the hyomandibular with elements of the hyoid arch is uncertain. The long dorsal surface of the hyomandibular is firmly attached to the lateral

cranial floor beneath the otic capsule (figures 49–52, plates 17 and 18). Medial to the upper part of the hyomandibular, the jugular vein leaves the neurocranium and goes posteriorly along the inner surface of the hyomandibular (figures 49–51). The hyomandibular branch of the facial nerve passes laterally through a foramen in the hyomandibular cartilage (figure 49). A large foramen in the lower part of the hyomandibular contains the afferent branches of the pseudobranchial circulation (figure 46, plate 17).

The unpaired, median glossohyal lies in the anterior floor of the branchial chamber (figures 17 and 36). Two large ceratohyals flank the posterior part of the glossohyal and attach to the hyomandibular through an intermediary cartilage (figures 20, 36 and 45, plate 9). This connecting cartilage is not small and I have called it an epihyal rather than an interhyal or accessory cartilage. No hypohyals are present. There is no evidence of a cartilaginous structure that is a precursor of the urohyal.

(e) Gill arches

Four complete arches are recognized (figure 59). Paired hypobranchials and ceratobranchials are present in arches 1, 2 and 3 (figures 17–21, plates 8 and 9). The fourth hypobranchial is missing and this arch begins ventrally with the ceratobranchial. A fifth pair of ceratobranchials lie closely opposed to the fourth pair but do not form a fifth arch. Dorsally, the four ceratobranchials complete their respective arch by attachment to the irregularly shaped epibranchials in the roof of the branchial chamber. A pair of infrapharyngobranchial cartilages on each side complete the cartilaginous elements of the gill arches. The median basibranchial elements consist of two cartilages (figure 17). The long anterior cartilage lies between the first, second and third hypobranchials. The small more posterior cartilage is the fourth basibranchial. The large anterior cartilage is quite separate from the glossohyal and probably contains the elements of the first three basibranchials.

(f) Dermal ossification

Membranous bone arises *de novo* from the calcification of connective tissue between the epidermis and underlying cartilaginous skeleton. Several such bones develop early and are prominent structures in the premetamorphic leptocephalus. The upper jaw has a large maxilla

---

Description of plate 17

Figure 46. The afferent pseudobranchial arteries pierce the hyomandibulars. (Magn. × 70.)

Figure 47. The pituitary rests in a depression in the cartilaginous cranial floor. (Magn. × 70.)

Figure 48. The afferent pseudobranchial vessels are derived from the first and second aortic arches. (Magn. × 70.)

Figure 49. The jugular vein leaves the neurocranium through the facial foramen. The ventrolateral aspect of the branchial chamber opens to the exterior. (Magn. × 70.)

Description of plate 18

Figure 50. The heart consists of a single atrium and ventricle. The bulbus arteriosus is above the ventricle. (Magn. × 60.)

Figure 51. The large auditory capsule is cartilaginous on the external surface. The inner surface is membranous. (Magn. × 60.)

Figure 52. The branchial arches are devoid of gill filaments. (Magn. × 60.)

Figure 53. Ossification of the opercle is evident. The atrium is above the ventricle. (Magn. × 60.)

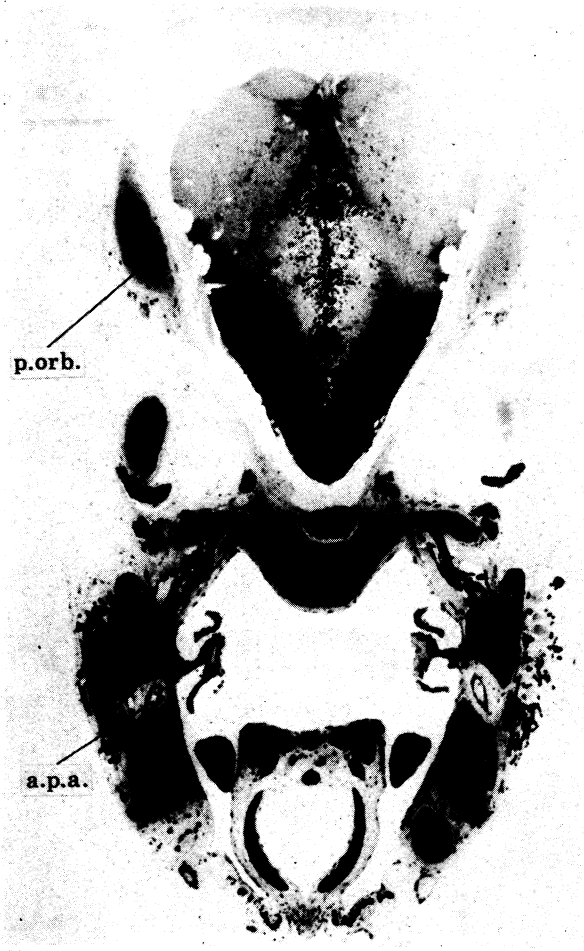

46

47

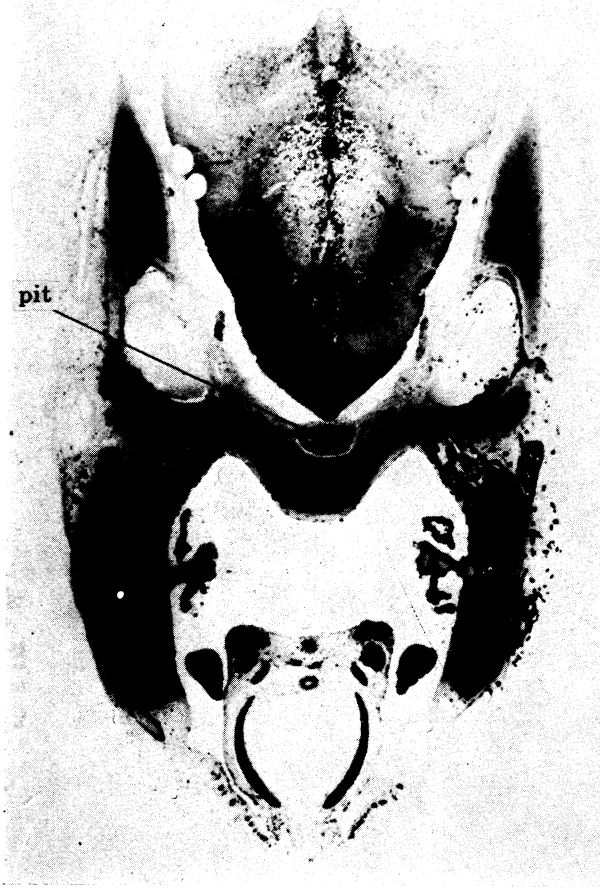

48

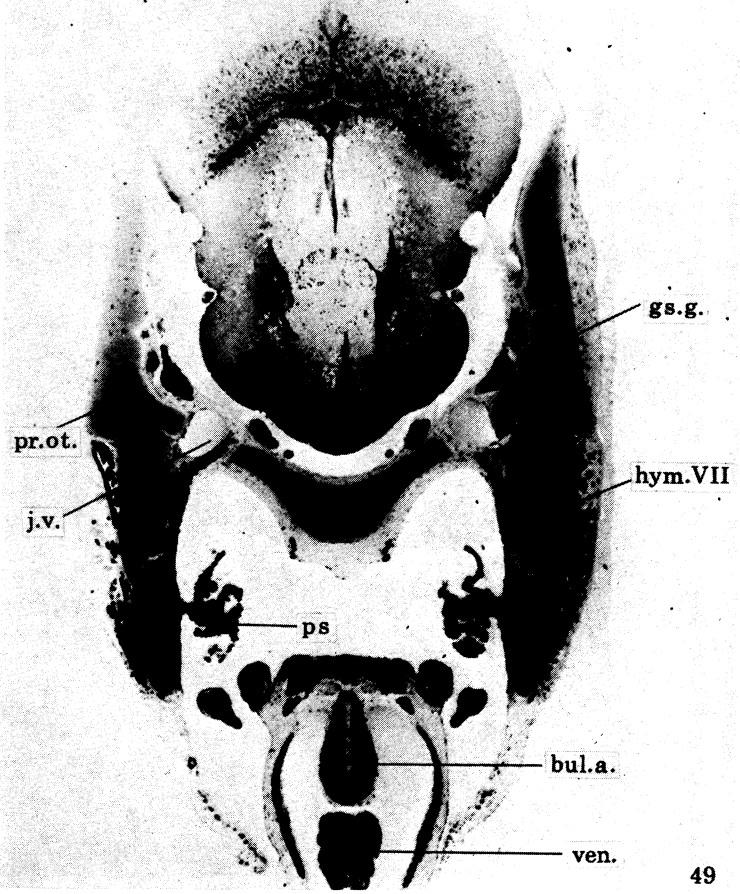

49

FIGURES 46–49. For description see opposite.

(*Facing p.* 122)

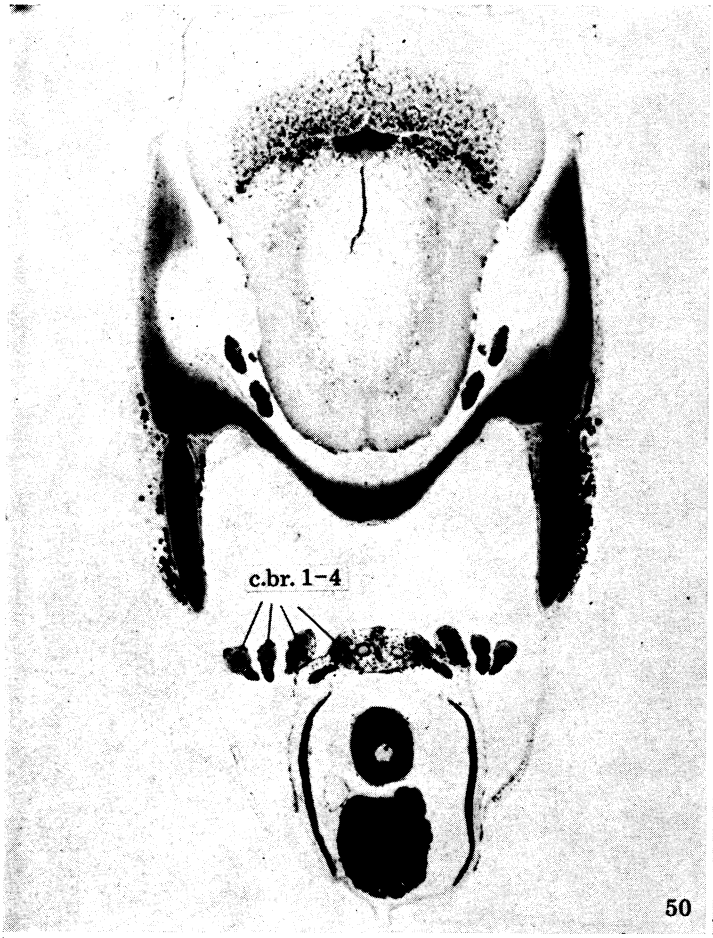

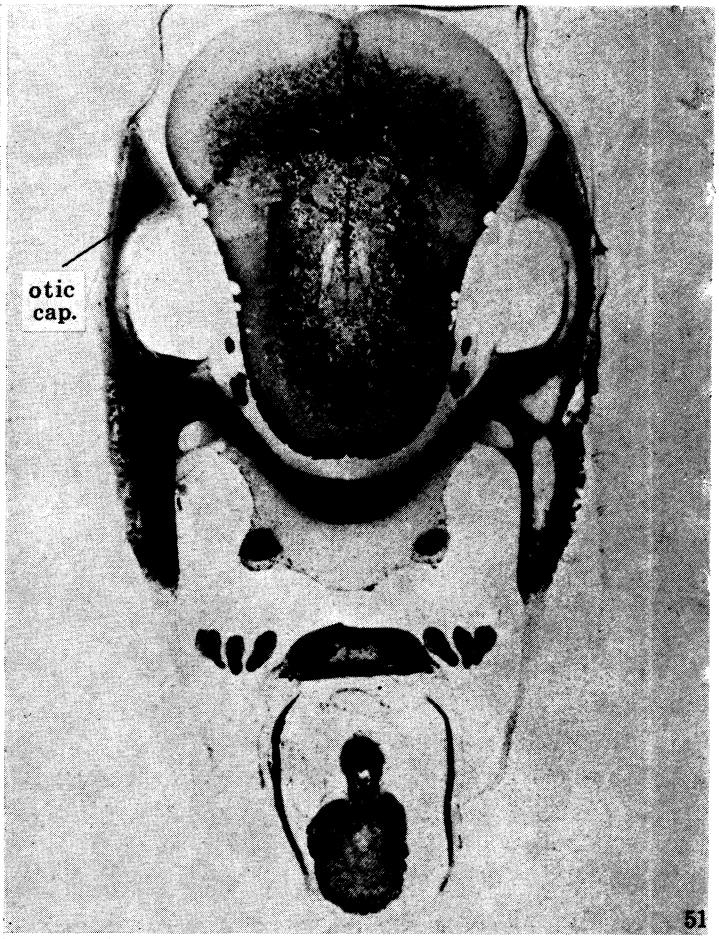

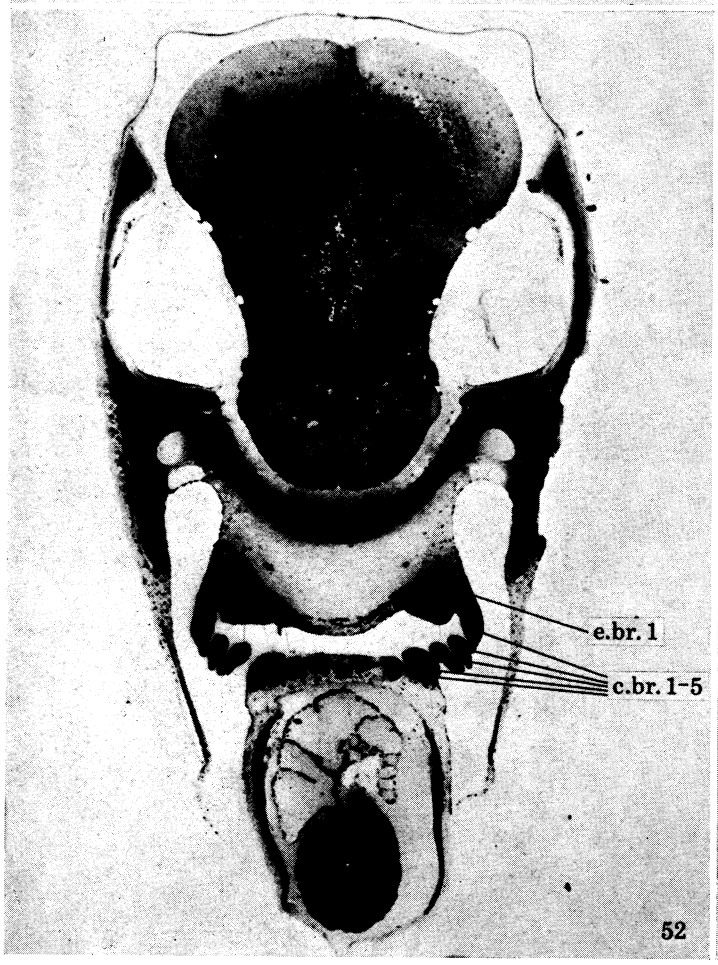

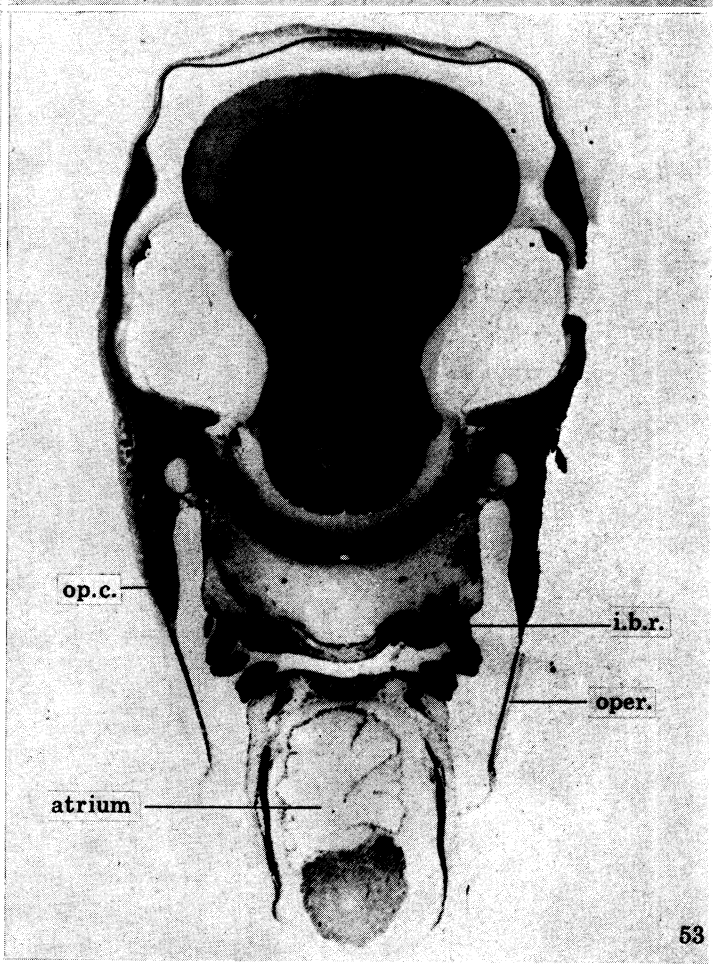

FIGURES 50–53. For description see p. 122.

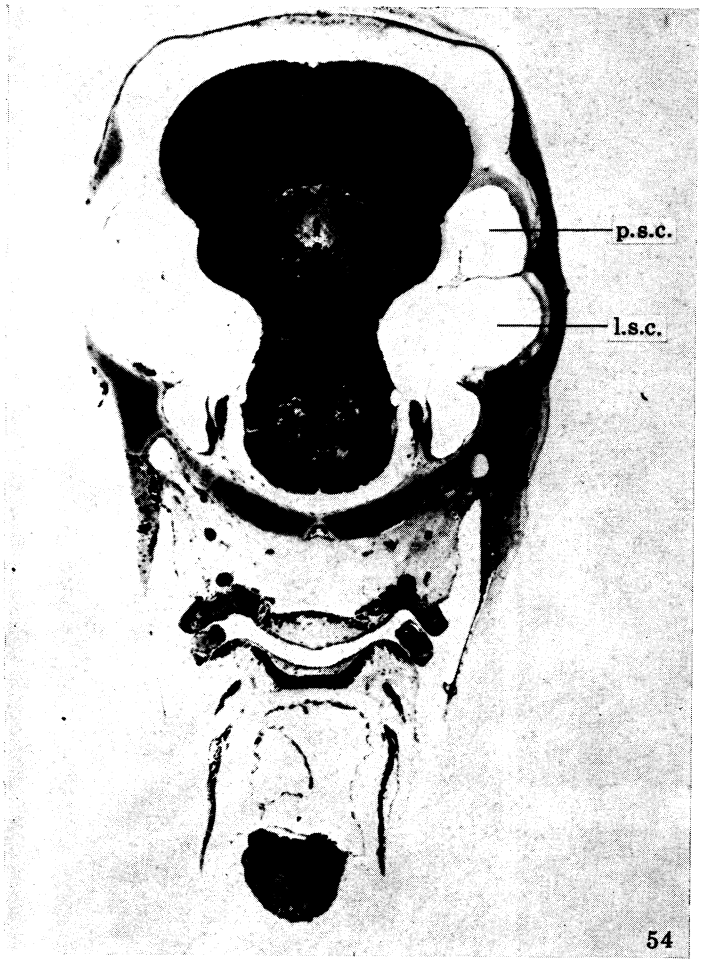

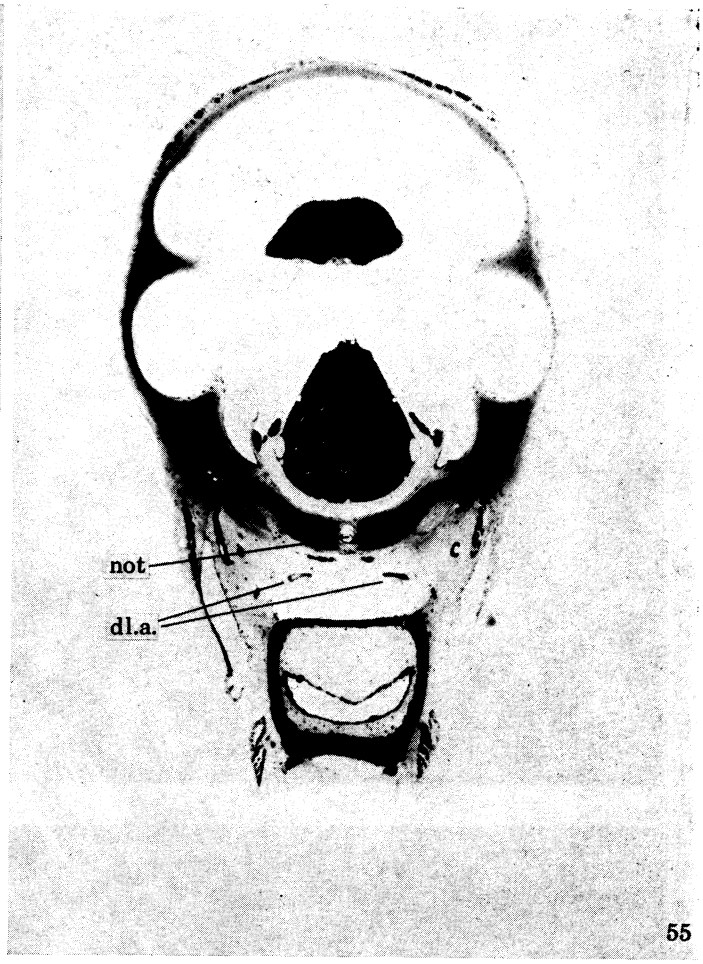

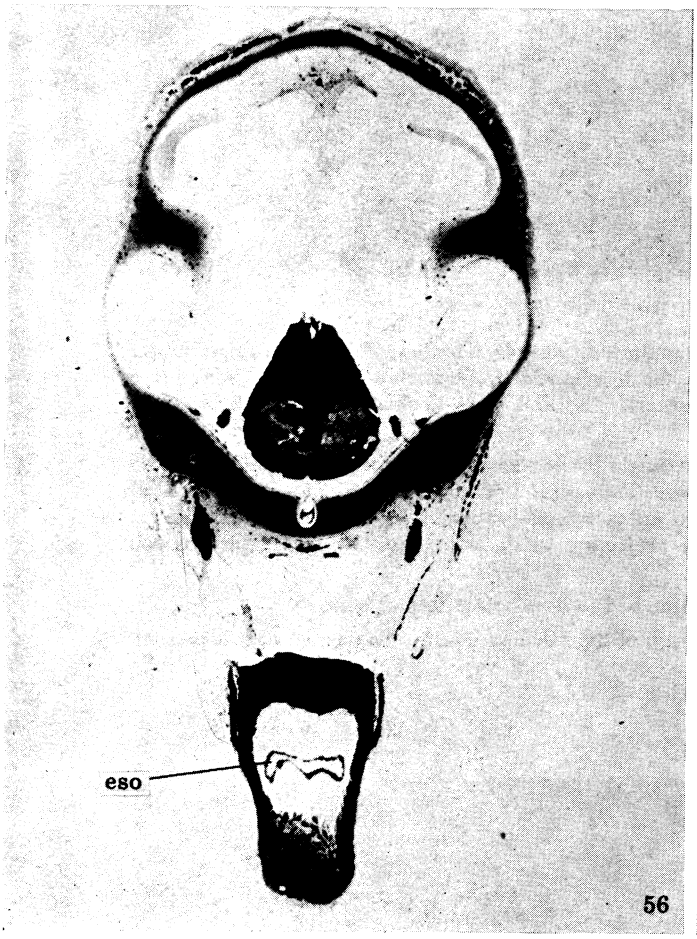

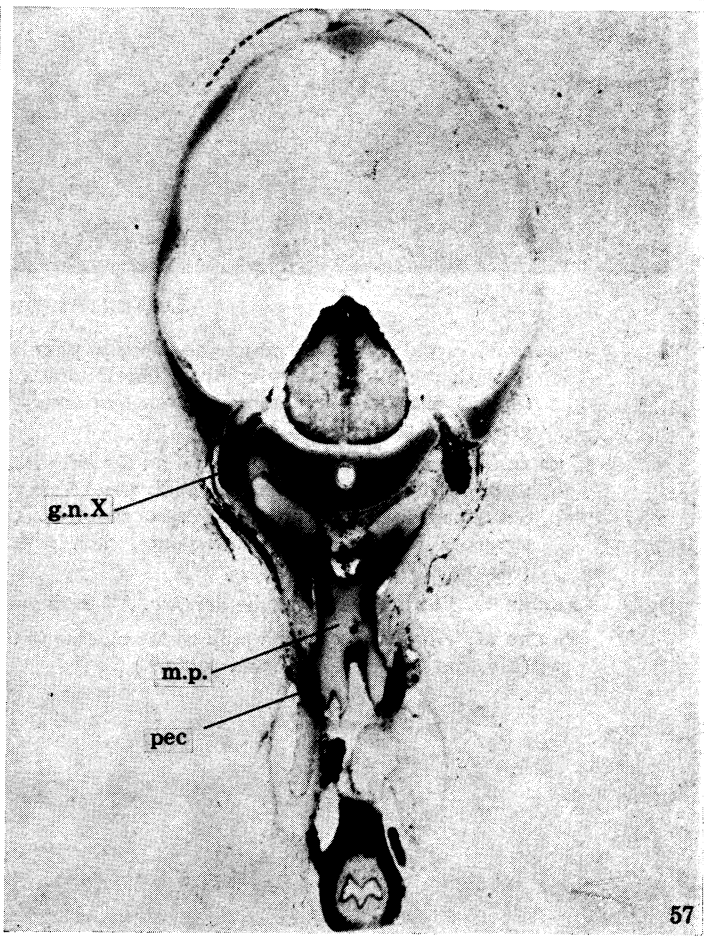

FIGURES 54–57. For description see p. 123.

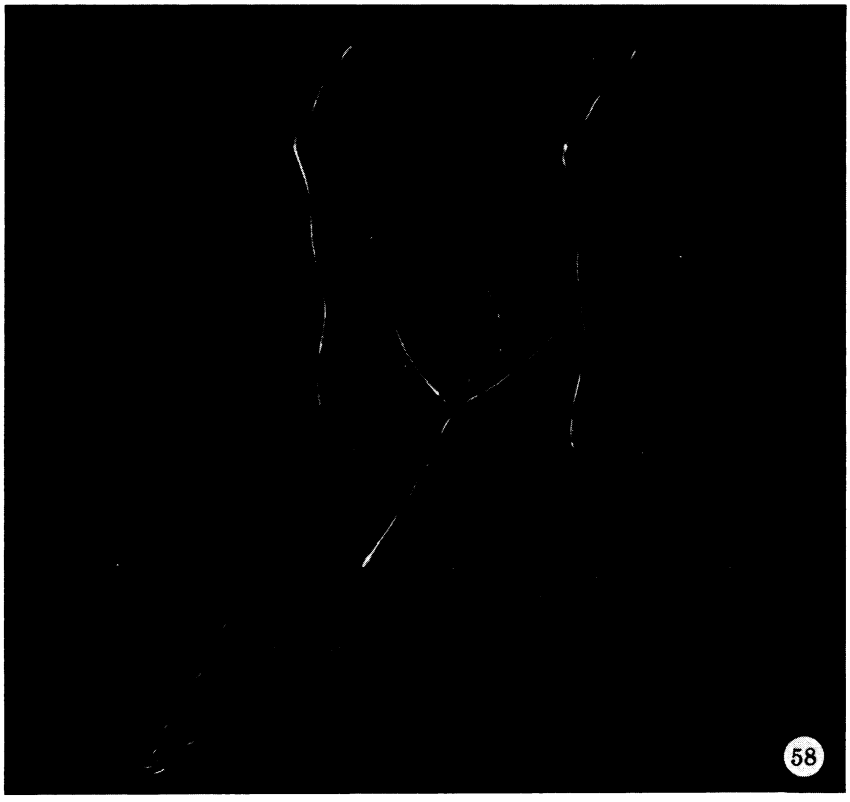

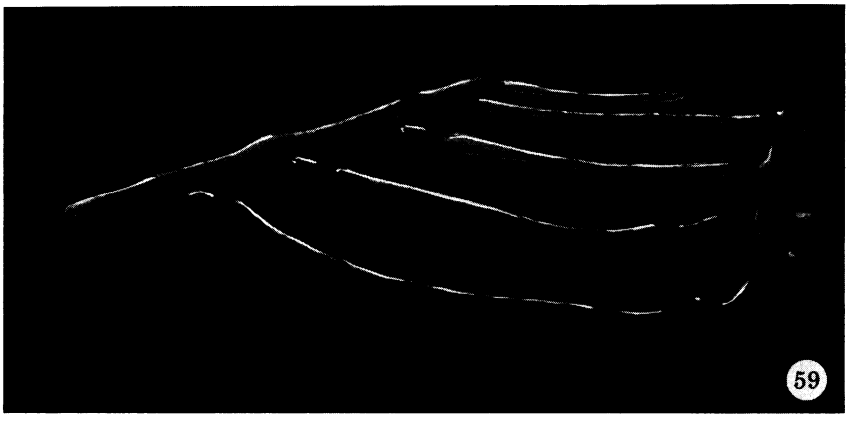

Description of plate 20

Figure 58. Hyoid arch. The ceratohyals arise just posterior to the long glossohyal and attach to the hyomandibular through the intermediary epihyal. The foramina in the hyomandibular branch of the facial (VII) nerve (upper) and the afferent pseudobranchial artery (lower). The first basibranchial is directly behind the glossohyal. (Magn. × 27.)

Figure 59. Cartilages of the gill arches on the left side. A single basibranchial serves for the attachment of the three hypobranchials. Hypobranchials 4 and 5 are absent. Four ceratobranchials attach to four epibranchials positioned dorsally in the pharyngeal chamber. Two infrapharyngobranchials complete the cartilaginous elements. Two minute osseous plates, each with a projecting tooth, represent the upper pharyngeal. (Magn. × 37.)

Figure 60. Tooth attached to the dentary. All teeth are attached to developing dermal bone.

Figure 61. Tip of a tooth. The pulp cavity reaches to the tip of the calcified matrix. No enamel coat is present. (Electron micrograph; magn. × 8300.)

which reaches from the snout to the angle of the jaw on each side (figures 13 and 29, plates 6 and 12). Except for a pair of minute teeth projecting from the premaxillae, the maxillae and dentaries bear all the teeth of the jaws (figures 25–30, plates 11–13). Paired premaxillae bearing teeth have been a consistent observation in the larvae of *Ariosoma balearicum* and they are not part of the rostral cartilage (Berry 1964). Developing upper and lower pharyngeals are also evident from tooth-bearing membranous bones of the gill arches. The neurocranium has three dermal bones. Thin sheets of calcifying tissue over the roof are the developing frontals and parietals. The frontals will fuse at some later stage in development but in premetamorphic larvae they are distinctly separate. The parasphenoid is a ribbon of bone beneath the entire length of the trabecula communis (figure 37). The ossifying opercle is proximate to the opercular cartilage (figure 53, plate 18).

(*g*) *Dentition*

Histologically the teeth all emerge from an attachment to developing dermal bone (figure 60, plate 20). A part of the tooth base is confluent with the dermal bone of origin. The outer layer of the tooth does not have the structural organization of enamel and birefringence is not evident when the tooth is illuminated by polarized light. The outer dentine is densely calcified; however, the pulp cavity reaches out to the tip of each tooth (figure 61, plate 20).

3. *Gills and gill filaments*

(*a*) *Mandibular hemibranch*

The branchial arches are undeveloped and do not bear gill filaments. The only functional gill is a paired mandibular hemibranch. Each gill filament and its lamellae hang freely in the branchial chamber and have the appearance of a miniature pine cone. In histological sections, the base of the gill filament rests on the medial aspect of the hyomandibular cartilage (figures 20 and 46). A supporting cartilaginous rod runs the length of the filament. The internal walls of the lamellae are lined by endothelium which rests on a clearly outlined basement membrane (figures 62 and 63, plate 21). The epithelium covering the external surface of the lamellae has an unusual filamentous appearance (Choi 1963). At high magnification these filaments appear to be rather uniform projections from the outer leaflet of the plasma membrane (figure 64, plate 21). Epithelial cells with marked infolding of the cell membrane occur at random and may represent chloride cells (figure 65, plate 21). The inside of each secondary lamella is converted into an intricate pattern of passages by the pillar cells (figure 63). Although the gill described has been called a pseudobranch, I believe it is more appropriate to refer to it as a mandibular hemibranch (Nelson 1966; Newstead 1967). A spiracular gill slit is not present nor is there a definitive gill slit. Instead, the ventrolateral margin of the entire gill chamber opens to the outside (figure 49).

Description of plate 19

Figure 54. Posterior portion of the branchial chamber. (Magn. × 60.)

Figure 55. The esophagus has thick muscular layer composed of striated muscle fibres. (Magn. × 60.)

Figure 56. The synotic tectum covers the posterior portion of the brain. (Magn. × 60.)

Figure 57. The jugular ganglion contains the afferent nerve cells of the vagus. Note the distinct outline of the anterior portion of the mucous pouch. (Magn. × 60.)

(*b*) *Pseudobranchial vessels*

The mandibular hemibranch is the only source of blood that has been oxygenated by a gill capillary network. Two vessels from the ventral aorta pass beneath each ceratohyal to the lateral aspect of the hyomandibular. They penetrate the hyomandibular and emerge medially as the afferent pseudobranchial artery (figure 46). From the hemibranch the efferent artery joins the dorsal lateral aorta as the efferent pseudobranchial artery. The two vessels anastomose and pass through the basicranial foramen as the carotid artery (figures 43 and 44). The ophthalmic artery branches off the carotid a short distance from its entry to the neurocranium. The circulation of the brain and visceral arches will be covered in more detail below, but it is noteworthy that the eye has almost direct access to the most oxygenated blood of the circulation (figure 67).

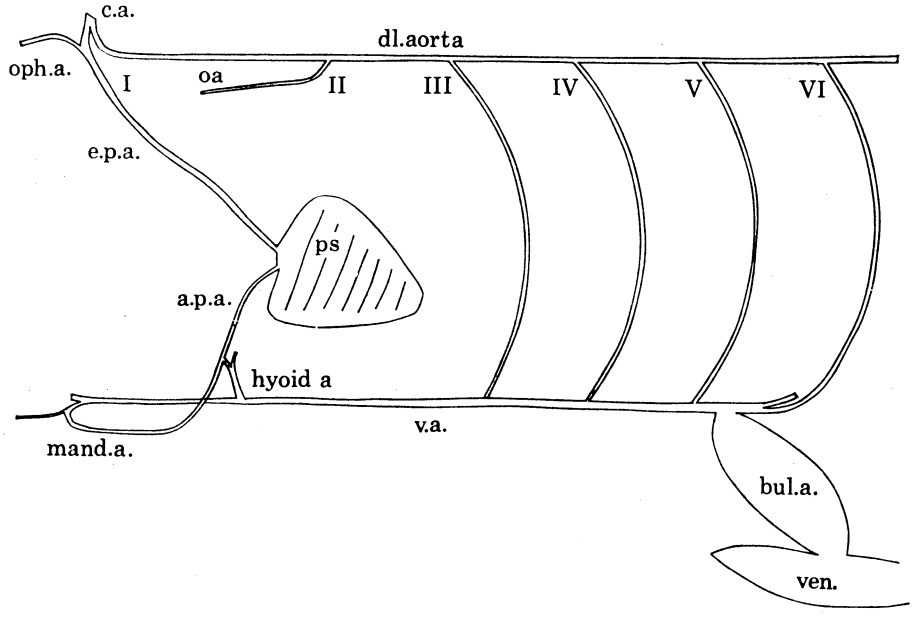

FIGURE 67. Diagram of the branchial circulation in the premetamorphic leptocephalus; left-side view completed. Roman numerals indicate the embryonic arterial arches.

4. *Circulation*

(*a*) *Blood cells and plasma*

The blood of a premetamorphic leptocephalus is colourless. No erythrocytes or other cells with iron-containing pigment are present. The few circulating cells found in the lumina of

---

DESCRIPTION OF PLATE 21

FIGURE 62. The only gill in the leptocephalus is a paired mandibular hemibranch attached to the hyomandibular.

FIGURE 63. Portion of a gill lamella from the mandibular hemibranch. A clearly defined basement membrane separates the endothelial and epithelial cell layers. (Electron micrograph; magn. × 9000.)

FIGURE 64. On the left, the external surface of the gill epithelium contains numerous fine projections which are in direct contact with sea water passing through the gill chamber. (Electron micrograph; magn. × 14100.)

FIGURE 65. Some of the gill epithelial cells contain abundant mitochondria and smooth membranes. They resemble 'chloride' cells. (Electron micrograph; magn. × 8300.)

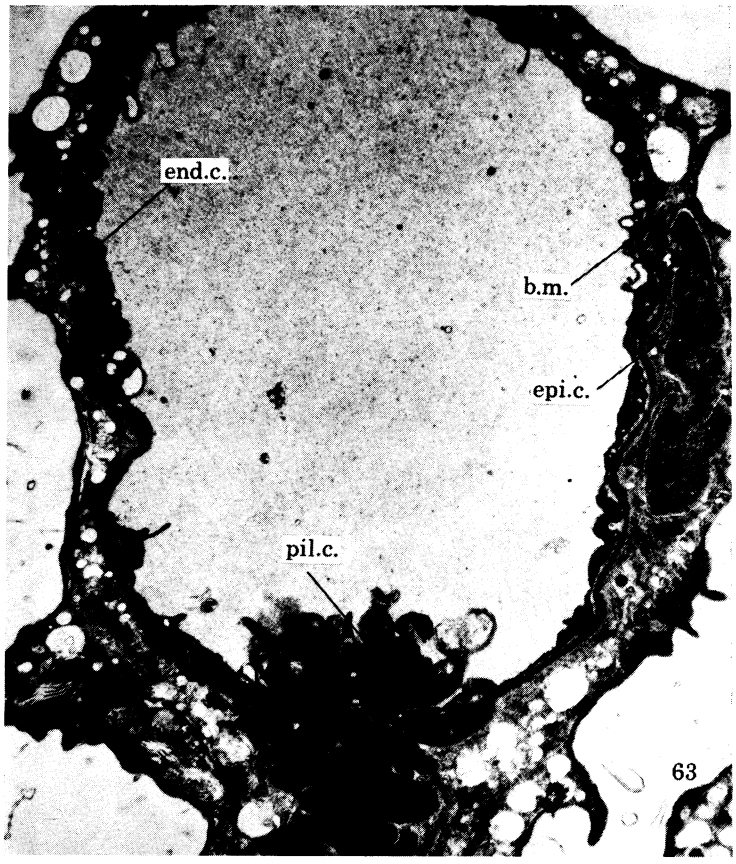

FIGURES 62–65. For description see opposite.

(*Facing p.* 124)

66

FIGURE 66. The upper pharyngeal bone is beginning to ossify. In the branchial arches, only one vessel (efferent artery) is patent along the course of the ceratobranchial.

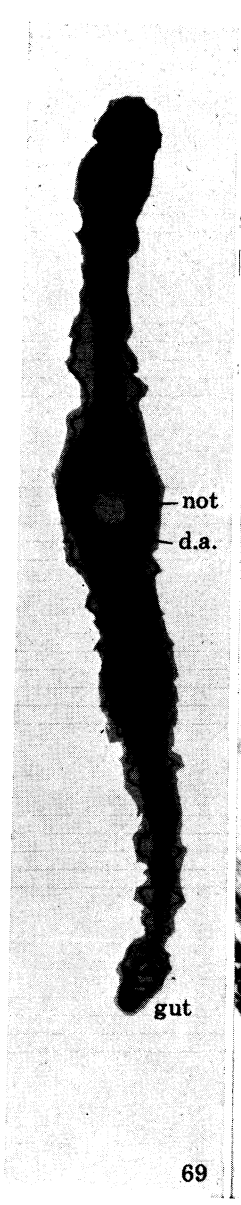

69

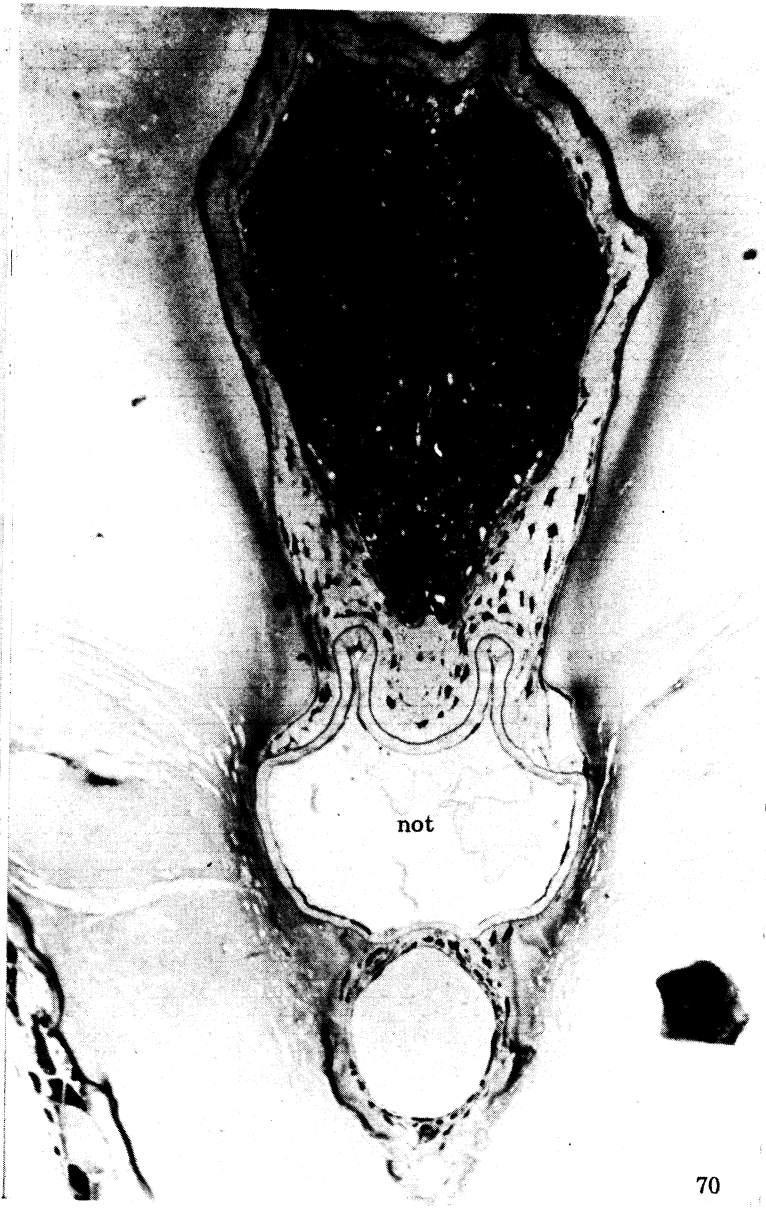

70

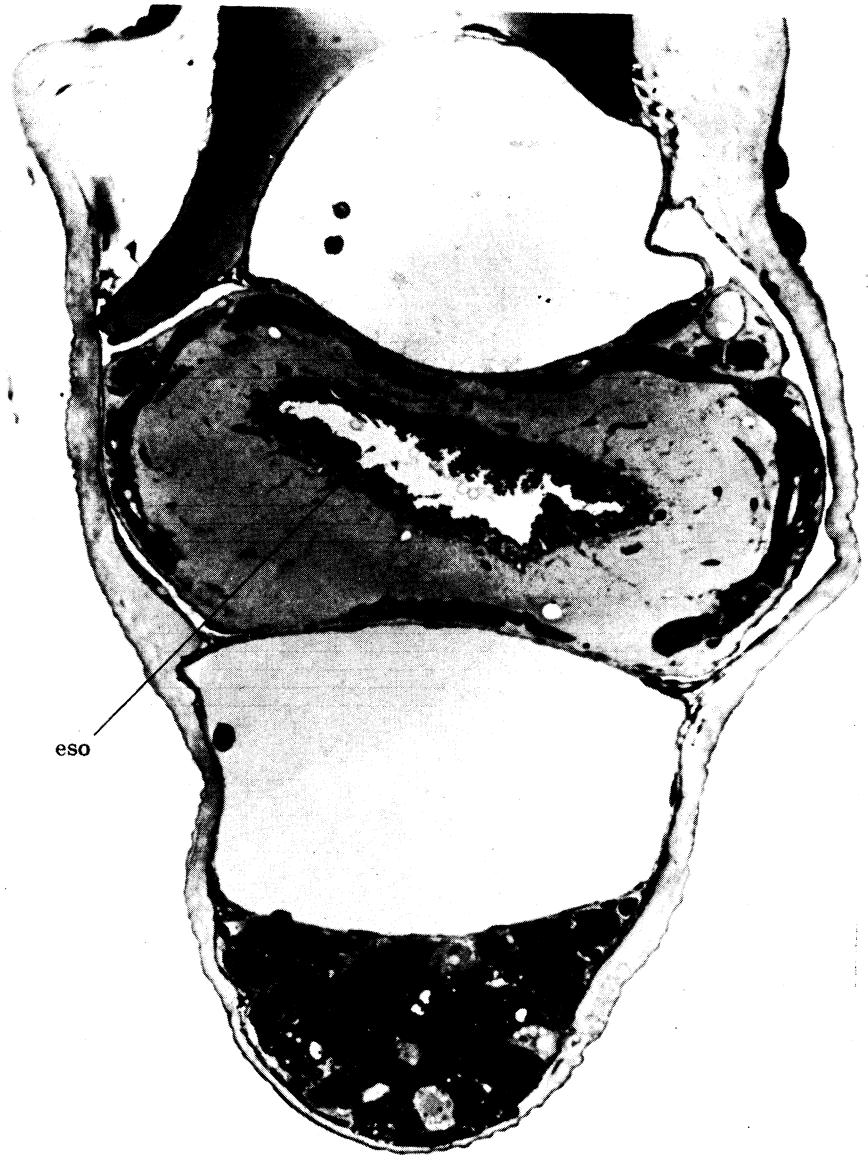

71

FIGURE 69. A cross section through the whole body of a leptocephalus at the level of the esophagus and ventral lobe of the liver. Note the distance between the dorsal aorta and the viscera of the gut. (Magn. × 40.)

FIGURE 70. The notochord is between the spinal cord and dorsal aorta. Acellular mucus material surrounds the three structures.

FIGURE 71. A single post-cardinal vein lies above the esophagus. The large hepatic vein is beneath the esophagus.

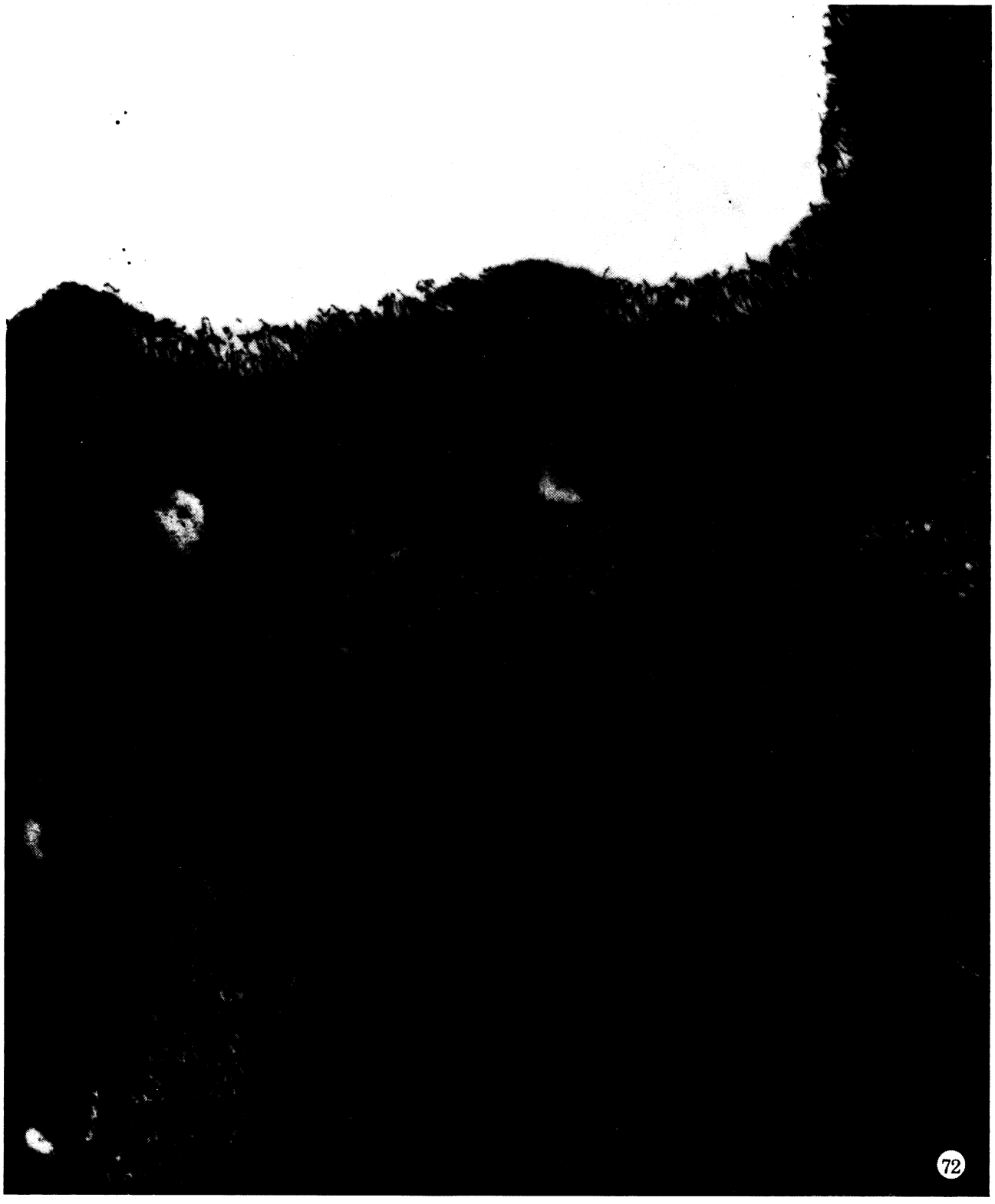

FIGURE 72. The skin is extremely fragile and only a few cell layers in thickness. The epithelial cells in contact with seawater are basically flat with numerous ridges. The outer surface of these cells is covered with fine filamentous projections. (Electron micrograph; magn. × 43780.)

arteries and veins are either white cells or macrophages. Hemopoiesis is not evident. The spleen is absent at this stage and the kidney has no blood-forming tissue. One area does stand out. In the roof of the branchial chamber and behind the arches there is a large collection of cells beneath the pharyngeal epithelium. This mass of cells is in the expected location of the thymus. Arteries have an elastic membrane which helps to identify these vessels, but it is not possible to distinguish between a moderate-sized vein and a lymphatic vessel with the light microscope. Whether or not the leptocephalus even has a lymphatic vascular system has not been answered.

(*b*) *Heart*

The pericardial chamber containing the heart is directly beneath the branchial chamber and anterior portion of the esophagus (figure 17). The atrium (figure 53) receives venous blood from the sinus venosus and communicates with the more ventrally placed muscular ventricle. The bulbus arteriosus has at least one set of valves between its lumen and the ventricular chamber. The bulbus arteriosus (figure 49) is composed of fibroelastic tissue and not cardiac muscle. The ventral aorta arises from the anterodorsal or distal end of the bulb. The course of blood through the heart is unidirectional and the valves between chambers are positioned to prevent regurgitation.

(*c*) *Ventral and dorsal aorta*

The midsagittal section of figure 17 shows a continuous lumen between the bulbus arteriosus and ventral aorta. The ventral aorta remains a single vessel until it reaches the oromandibular cavity. At that point it bifurcates into the mandibular arteries (figure 38). A paired hyoid and branchial arteries one, two and three are given off between the bulb and bifurcation. Posteriorly, the ventral aorta gives off the fourth branchial and continues as a single vessel for only a short distance. It bifurcates beneath the fourth basibranchial. The relation between visceral and aortic arches, gills and gill clefts followed in the discussion is as follows:

visceral arch	aortic arch	gill	cleft
mandibular	I	hemibranch	spiracular
hyoid	II	hemibranch	1
branchial 1	III	holobranch	2
branchial 2	IV	holobranch	3
branchial 3	V	holobranch	4
branchial 4	VI	holobranch	5

None of the branchial arches has gill filaments and only one vessel is patent in cross sections of the arch (figure 66, plate 22). In the developed arch the anatomical sequence in cross section is cartilage, efferent artery and afferent artery. In the leptocephalus the embryonic or primitive condition prevails (Satchell 1971). Blood from the ventral aorta flows through efferent vessels directly into the dorsal aortae (figure 55, plate 19). The afferent vessels which later in development will be the channels for blood from the ventral aorta are represented at this stage by whorls of proliferating cells (figure 66). In other words, the primitive condition in the branchial circulation favours the efferent vessels. In the roof of the branchial chamber the branchial arteries leave their proximity to the ceratobranchials, pass over the epibranchials and enter the respective right or left dorsolateral aorta. Posterior to the entry of the branchial vessels,

the lateral aortae run separately beneath the neurocranium (figure 55). Beneath the notochord they merge and extend caudally as the dorsal aorta. Apart from small branches going to adjacent segmental structures, the dorsal aorta usually gives off twelve large branches to the ventral viscera before terminating in the caudal artery (table 7). With the gall bladder as a reference point, three arteries are anterior and seven are posterior excluding the last two which are the renal arteries (figure 68).

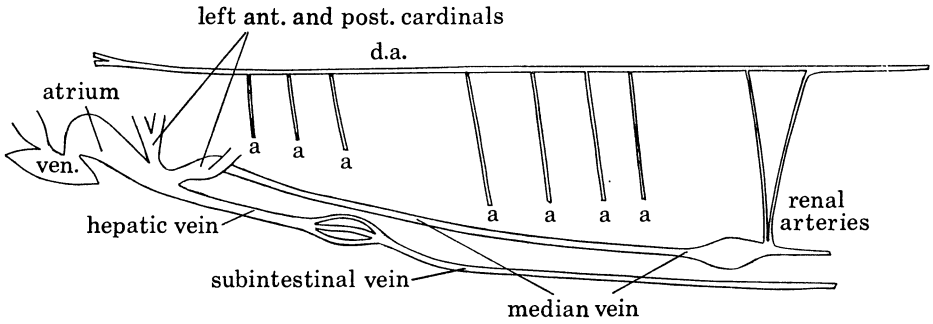

FIGURE 68. Diagram showing the main branches of the dorsal aorta and the venous return circulation with the left-side view completed.

Anterior to the anastomoses with the branchial arteries the two dorsolateral trunks of the aorta project forward beneath the neurocranial floor. Before entering the basicranial foramina each trunk gives off the orbital artery which subsequently enters the neurocranium through a separate foramen. Within the basicranial foramen the aortic trunk receives the efferent pseudobranchial artery and enters the neurocranium as the carotid (figure 44). Inside the neurocranium the first branch from the carotid is the ophthalmic artery which supplies the choroid of the retina. In some specimens it is difficult to determine whether the ophthalmic branch comes slightly before or after the union of the efferent pseudobranchial with the lateral aorta. It appears that the latter of the two possibilities is the more common anatomical event. The second carotid branch is the optic artery. The carotid terminates in anterior and posterior cerebral vessels (figure 45).

The orbital artery corresponds to the second aortic arch of the hyoid bar. The efferent pseudobranchial artery is particularly large in the leptocephalus and is homologous with the dorsal portion of the first aortic arch. The numerous epibranchial and hypobranchial vessels of the adult teleost have not developed. The afferent vessels to the manidibular hemibranch are the most difficult to follow. Two branches from the ventral aorta follow the ceratohyal to the hyomandibular where they join to form an afferent pseudobranchial artery (figures 21, 22 and 46). These vessels can be considered as ventral branches of the first (mandibular) and second (hyoid) aortic arches.

(d) Venous circulation

The jugular vein drains the anterior two-thirds of the neurocranium (figure 49). Although large, this vein is thin like all the others. The jugular leaves the neurocranium through the facial foramen and courses posteriorly along the medial surface of the hyomandibular. This vein is often called the vena capitis lateralis and its course beneath the neurocranium is different in different groups of fishes. For comparison, it is worthwhile to note that the vena capitis lateralis is outside the hyomandibular in the elasmobranchs. The posterior neurocranium is drained by

the posterior cerebrals which accompany the vagus out the jugular foramen and join the two jugular veins (figure 57). The jugular vein and smaller veins of the pharynx and lower jaw join to form the anterior cardinal vein. The right and left anterior cardinals drain into the sinus venosus by way of a larger channel, the duct of Cuvier. Ordinarily the anterior cardinals join the respective right or left posterior cardinal to form a common venous trunk, the duct of Cuvier. In the leptocephalus the posterior cardinals arise from paired veins that drain the musculature and a single median vein that receives blood from the kidney. As it courses anteriorly, the latter vessel, which contains the pronephric ducts (figure 78, plate 27), lies dorsal to the gut tube (figure 71, plate 23). Near the sinus venosus this median posterior cardinal divides, unites with the paired skeletal veins, and joins with the paired anterior cardinal veins to form two venous trunks which enter the sinus venosus. Posteriorly, the dorsal aorta terminates as the caudal artery. The caudal vein drains the caudal fin area and returns cephalad as a median vein. In the leptocephalus the caudal vein joins the single median vein that passes through the kidney to become part of a vascular sinus. A subintestinal vein drains the posterior gut tube and anteriorly in the liver divides into numerous small vessels. Small hepatic veins unite forming one large hepatic vein which empties into the sinus venosus.

5. *Body skeleton*

(*a*) *Notochord*

From a beginning between the parachordals of the neurocranium (figure 17), the notochord spans the length of the body and terminates above the hypural cartilages in the caudal fin. The entire notochord is divided into a series of disks by vertical septa from the fibroelastic sheath. There are usually two divisions per myomere, but they increase to four or five near the caudal fin. As shown in figure 70, plate 23, the internal structure is scarcely more than fluid. No centra are forming nor is there any sign of calcification.

(*b*) *Pectoral girdle*

Between the posterior occiput and the esophagus are the paired scapulo-coracoid cartilages (figure 57). In the upper part of the cartilage, sagittal sections show a nerve within a foramen. Two additional foramina penetrate the lower part of the cartilage. The actinosts of the pectoral fin have not separated. Instead, a thin sheet of cartilage one layer of cells in thickness spreads out from the scapulocoracoid.

(*c*) *Musculature*

The epaxial and hypaxial limbs of each myomere form the characteristic W-shape of teleost muscle (figure 1). All muscles are transparent and presumably free of iron-containing myoglobin. It should be pointed out that gross inspection of the body is deceiving in regard to the musculature. Only in cross section is it apparent that the muscles are thin and that most of the body is occupied by a mucinous jelly (figure 69, plate 23).

(*d*) *Caudal fin*

Axonosts of the anal fin begin one to two myomeres behind the anus. The dorsal fin originates only slightly more anterior than the anal fin. The caudal fin has two prominent hypurals. Each hypural supports three fin rays. Although outwardly the caudal fin is continuous with the dorsal and anal fins, the structure of the fin ray support reveals a basic homocercal caudal

fin. At this stage in development the spinal cord and notochord are straight and the upper hypural cartilage proceeds directly caudad from the end of the notochord.

(*e*) *Mucinous pouch*

The two sides of the body are held some distance apart by thick, clear, sticky mucus (Gabe 1971). Qualitative tests of this material for protein and polysaccharides are positive. This acellular, mucinous material envelops the spinal cord and notochord from head to tail (figure 69). Ventrally, it abuts on the dorsal aspect of the esophagus, intestine and kidney. The mucous material is not free to disperse in tissues. It is enclosed by an uninterrupted covering of flat epithelial cells. The sharpness of the boundaries of this collection of mucus is remarkable (figure 57). It is generally accepted that the dermatomes and myotomes originate from the embryonic mesodermal somites. The primordial mesodermal bar on each side of the notochord becomes segmented into fluid-filled cavities with walls of mesodermal cells. These cavities are of brief duration. The lateral walls separate, proliferate and become the dermatomes and myotomes. The medial walls termed sclerotomes, are the mesodermal cells that will form the vertebrae and associated connective tissues. Ventral cells in the mesodermal somite are precursors of the nephric tubules. The ventro-lateral part of the mesodermal fold will extend ventrally and form the visceral and parietal surfaces of the coelomic cavity (Waddington 1956). In the leptocephalus, the dermis is formed and the somatic myomeres are the most obvious of all tissues. The missing or undeveloped elements are those tissues derived from the sclerotome (Romer 1962). The epithelium enclosing the mucinous pouch is possibly some part of the medial epithelium of the primitive mesodermal somite which has yet to develop into definitive structures.

6. *Skin*

Except for the head region and a few specialized areas the leptocephalus is covered by an epithelium no more than two to three cell layers in thickness (Bolognani-Fantin & Bolognani 1964). A thin, two-layered epidermis is characteristic of a growing embryo (Raffin 1967). The thin epidermis rests on a basement membrane beneath which is a sparsely cellular dermis (figure 72, plate 24). The outer layer of the epidermis consists of squamous epithelial cells and between these very flat cells and the basement membrane is an inner layer of cells somewhat oval in shape. The configuration of surface ridges of the outermost layer of epidermal cells gives each cell the appearance of a solitary fingerprint (Jones, Holliday & Dunn 1966). The epidermis is loosely attached to the dermis and is easily traumatized. The skin on the sides of the body is particularly susceptible to injury. Despite careful handling of each specimen, the epidermis was, more often than not, damaged, detached and lost during the preparation of tissue sections. In contrast to the structure of most of the skin surface, the epidermis of the median fin folds near the developing dorsal and anal fins is many layers thick. Epithelial hyperplasia is also evident around the base of the teeth. Goblet cells, mucus glands and other secretory epidermal structures are not present at this stage in development.

On the midline of the mesethmoid cartilage anterior to the nasal sacs are two open pores in the skin (figures 3 and 30). Beneath the skin and in the tunnel connecting these two pores is a hillock of cuboidal to columnar epithelial cells. Lateral to each open pore a dermal tunnel continues for a short distance. The epithelial cells extend into this tunnel. The gross morphology

and light microscope sections suggest that this rostral commissure is part of the lateralis system and that the epithelial cells in the pit are collectively a neuromast (Allis 1903).

7. *Gastro-intestinal tract*

(*a*) *Pharynx and esophagus*

The thin epidermis covering the jaws continues into the oromandibular cavity and pharynx. In several regions the epithelium makes a transition to tall columnar cells with multiple cytoplasmic extensions. High magnification of these extensions shows numerous extremely fine filaments projecting from the plasma membrane. These filamentous projections are clearly demonstrated in the gill epithelium (figure 64). These rather odd-looking cells, though not particularly odd for larval organisms, serve as the lining epithelium of the cul-de-sac beneath the rostrum (figure 27), the inside surface of the covering over the olfactory epithelium, the lateral recesses of the mouth and pharynx, and the first portion of the esophagus. These cells are not ciliated nor do they appear to be secretory; however, the multiple projections must increase the surface area significantly. Taste buds are separate structures and are scattered over the pharynx. The aforementioned cul-de-sac on the roof of the mouth enlarges posteriorly and separates in the midline into two longitudinal folds which hang vertically on the inside of the jaws (figures 15 and 27 to 29). The outside surface of this velum is more in keeping with the appearance of undamaged skin over the jaws and cranium. The esophageal epithelium remains the same throughout its course to the stomach. The striated muscle of the esophageal wall terminates near the hepatogastric region and is replaced by smooth muscle. Two large trunks of the vagus travel posteriorly along the dorsolateral aspect of the esophagus. The diverticulum for the swim bladder is not developed.

(*b*) *Stomach, liver and pancreas*

The stomach is small and the mucosa consists of several folds of tall columnar epithelium (figure 75, plate 25). Glands and secretory cells are absent and there is no indication of pyloric caeca. Since the liver develops from a ventral endodermal diverticulum and the gall bladder originates from the first outpouching, it is not unexpected to find a well-formed gall bladder in conjunction with a large ventral hepatic lobe. The bulb of the gall bladder is on the right and displaces the esophagus to the left (figure 73, plate 25). The ventral lobe of the liver has a hepatic duct which joins with the cystic duct to enter the pyloric region of the gut as the choledochal or common bile duct. In figure 74, plate 25, the tissue around the stomach and duct system shows marked cellular proliferation. Serial sections of the gut are consistent with the presence of two and possibly three pancreatic lobes. Since the pancreas arises from an endodermal diverticulum, the secretory acini have a connection with the intestine. Two features of the leptocephalous pancreas deserve comment. First, pancreatic tissue occurs from the stomach to the end of the intestine and the strip of pancreatic tissue of the dorsal surface of the gut tube is accompanied by a long thin segment of liver tissue. Secondly, the pancreatic cells contain large amounts of rough endoplasmic reticulum, but the secretory granules have not been extruded from the cytoplasm. These granules must be considered as an accumulation of enzymatic material (figure 77).

(*c*) *Intestine and intestinal contents*

Posterior to the stomach the intestinal mucosa becomes markedly infolded and a lumen becomes difficult to find. The surface of the mucosal cells has a brush border composed of microvilli which is characteristic of intestinal epithelium. The anal mucosa has a similar appearance but there is no question of organization. It is the midgut that appears disorganized. In many areas the mucosa is in the form of many short segments of proliferating intestinal epithelium (figure 76). No real lumen can be found in this part of the intestine. It is noteworthy that not one section of the esophagus, stomach or intestine has shown any remnant of ingested material. The apparently imperforate midgut and the absence of intestinal contents must be given careful consideration in any discussion on the source of nutrition in the leptocephalus (Manfredi-Romanini 1964; Luppa 1966).

8. *Kidney*

The leptocephalous kidney has peculiarities of structure not described in any other vertebrate. The principal or opisthonephric kidney is a collection of aglomerular tubules located in the midline between the mesodermal mucus-filled cavity and the intestine (figure 79, plate 28). The kidney begins about myomere 30 and ends one or two myomeres posterior to the entrance of the renal arteries (figure 7). At approximately myomere 62 the renal arteries enter the caudad portion of the kidney and empty into a vascular sinus lined with tubules. The caudal vein joins this sinus from the posterior. There are no glomeruli. The nephric tubular cells are large and the cytoplasm is filled with mitochondria wrapped in many layers of endoplasmic reticulum. Motile cilia are present on the luminal border (figures 80 and 81, plate 28). The pronephros consists of two tubules that begin as blind ducts at a point caudad to the stomach. They extend posteriorly along the ventrolateral border of the large median vein that leads from the opisthonephric kidney to the sinus venosus (figure 78, plate 27). Although the two pronephric tubules appear to lie within the lumen of the vein, they are separated from the vascular contents by a layer of endothelial cells. Within the substance of the kidney the pronephric tubules anastomose with the terminal portions of the opisthonephric ducts; descend out of the kidney substance as archinephric ducts (figure 76); and posterior to the entrance of the renal arteries, they unite to form a single nephric duct (figure 82, plate 29). This median duct is lined with cuboidal epithelium and lies dorsal to the intestine. Before terminating at the anal papilla it expands into a small vesicle. The external opening of the urinary bladder or urogenital sinus is immediately above the anal opening (figure 83, plate 30).

Description of plate 25

Figure 73. The gall bladder is on the right side and displaces the esophagus to the left.

Figure 74. The hepatogastric region in all premetamorphic leptocephali is very cellular. Beneath the stomach the ventral lobe of the liver is near to termination. The biliary duct has received the cystic duct anteriorly. Islands of pancreatic acinar cells begin posterior to the gall bladder. A coelomic cavity for the viscera is evident. An endodermal outpouching for the swim bladder has not been identified.

Figure 75. The stomach is small and with few folds. The gastric epithelium consists of tall columnar cells resting on a basement membrane.

Figure 76. Posterior to the hepatogastric region the intestinal epithelium is unorganized and a definite lumen is not present.

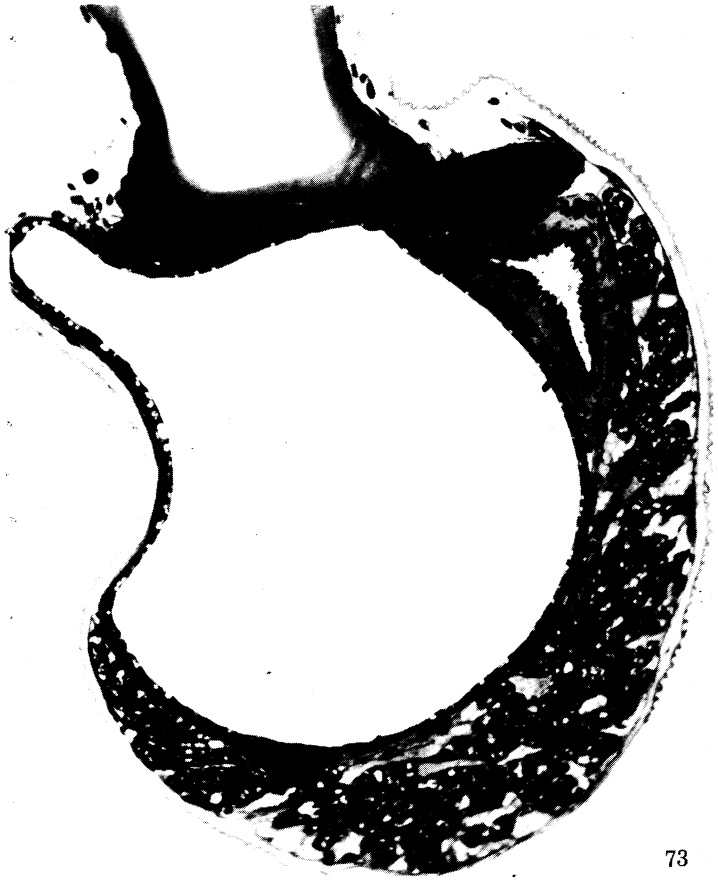

73

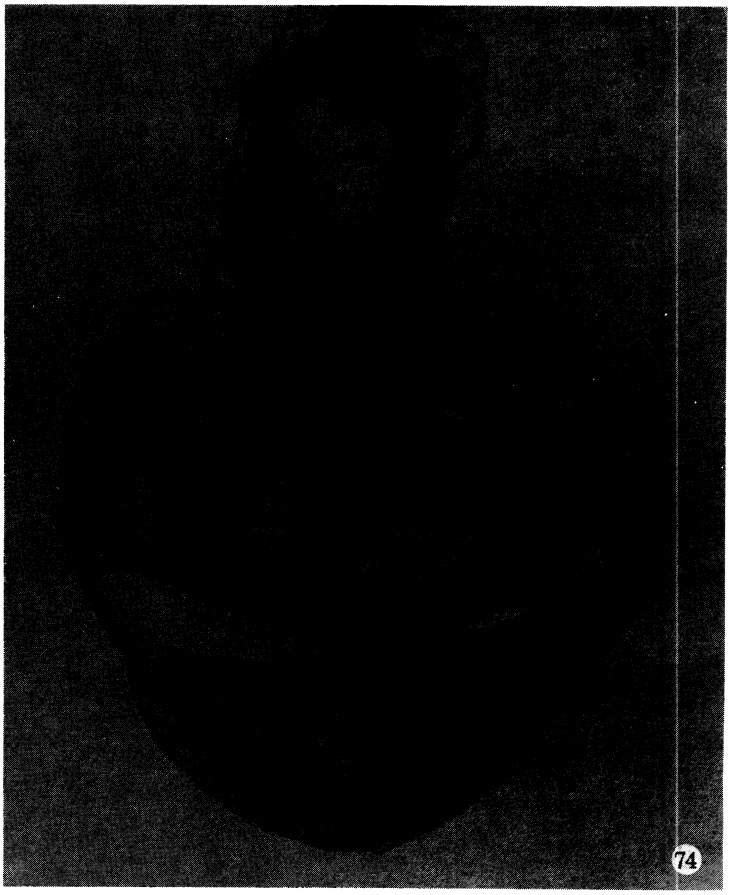

74

75

76

FIGURES 73–76. For description see opposite.

(*Facing p.* 130)

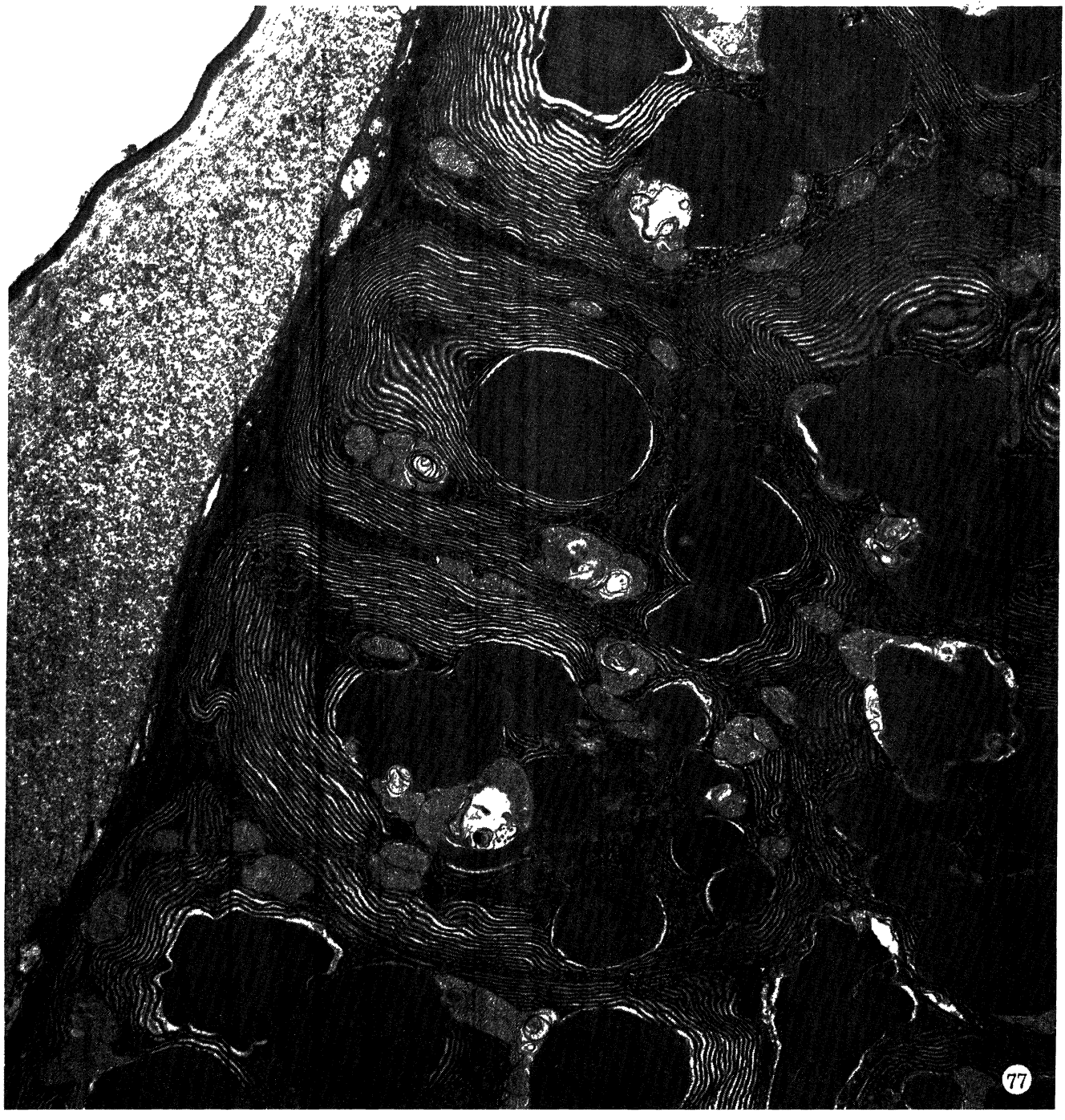

FIGURE 77. Pancreatic acinar cells. The rough endoplasmic reticulum and mitochondria are typical, but the extremely large secretory granules are unusual. (Electron micrograph; magn. × 6700.)

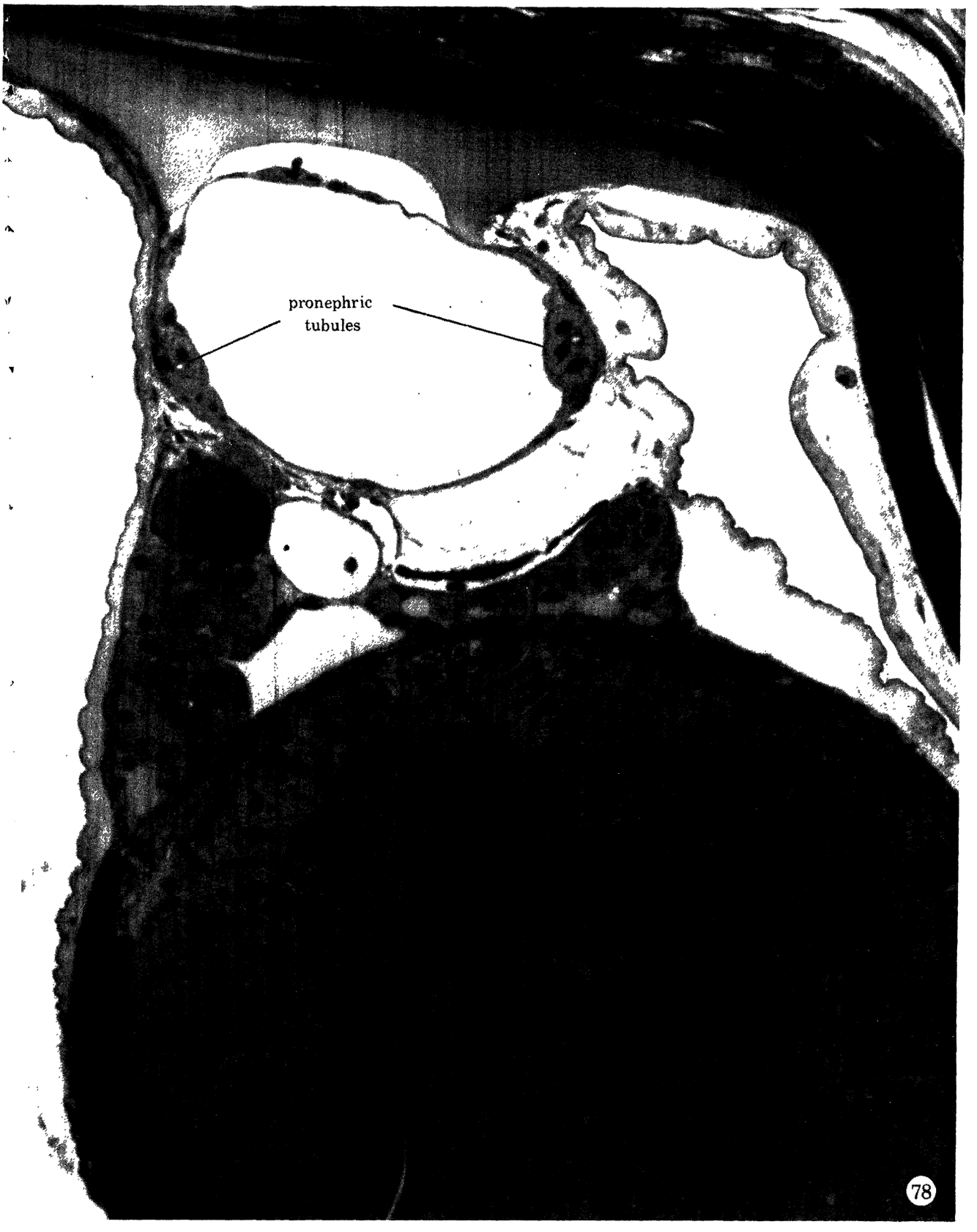

FIGURE 78. The two aglomerular pronephric tubules begin posterior to the hepatogastric region. They are separated from the lumen of the vascular channel by a layer of endothelial cells. As archinephric ducts they drain the aglomerular opisthonephric tubules.

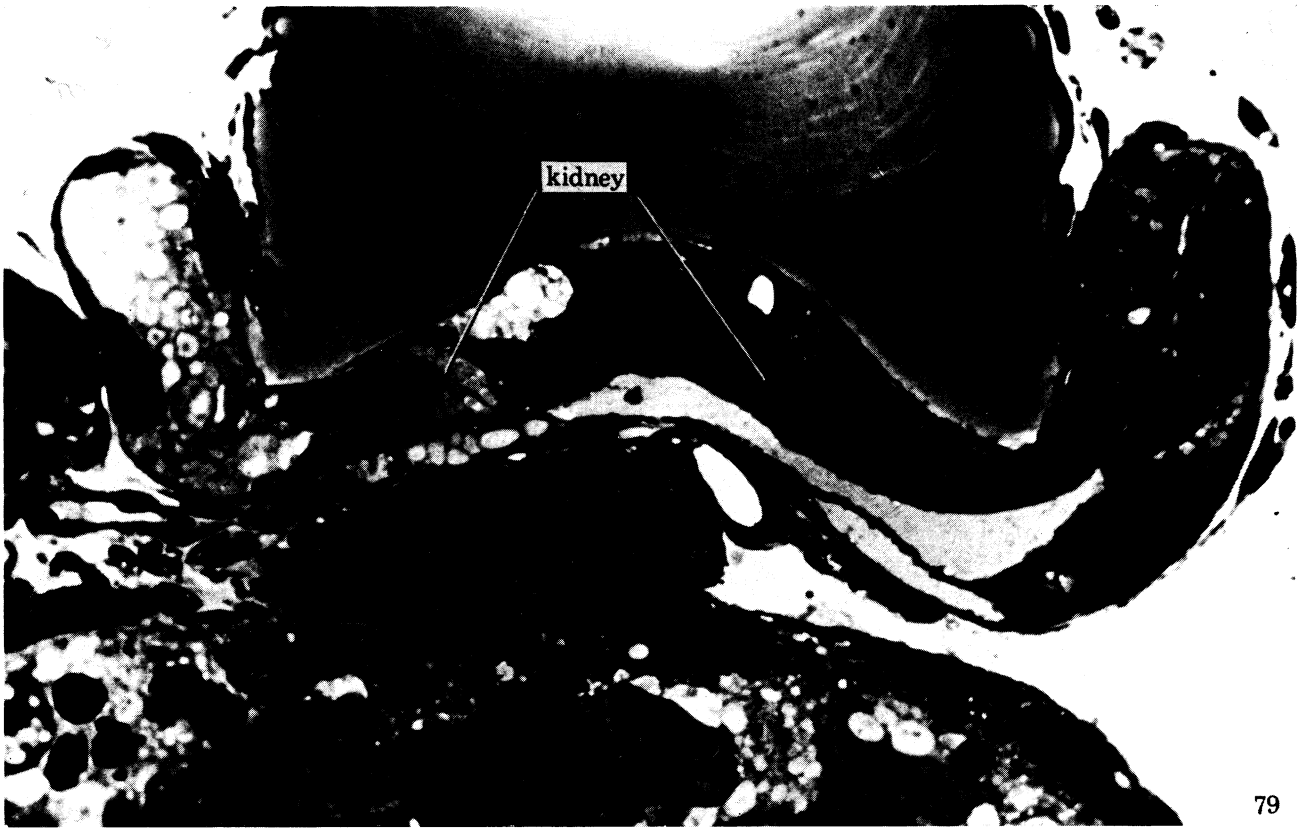

FIGURE 79. The renal parenchyma is a solitary structure and it is not separated into the right and left organs. Renal tubules surround a midline vascular sinus.

FIGURE 80. A renal tubule shown in cross section. The mitochondria are large and are surrounded by cell membranes. (Electron micrograph; magn. × 10980.)

FIGURE 81. Lumen of a renal tubule. The cilia show the familiar '9+2' organization of microtubules. (Electron micrograph; magn. × 50400.)

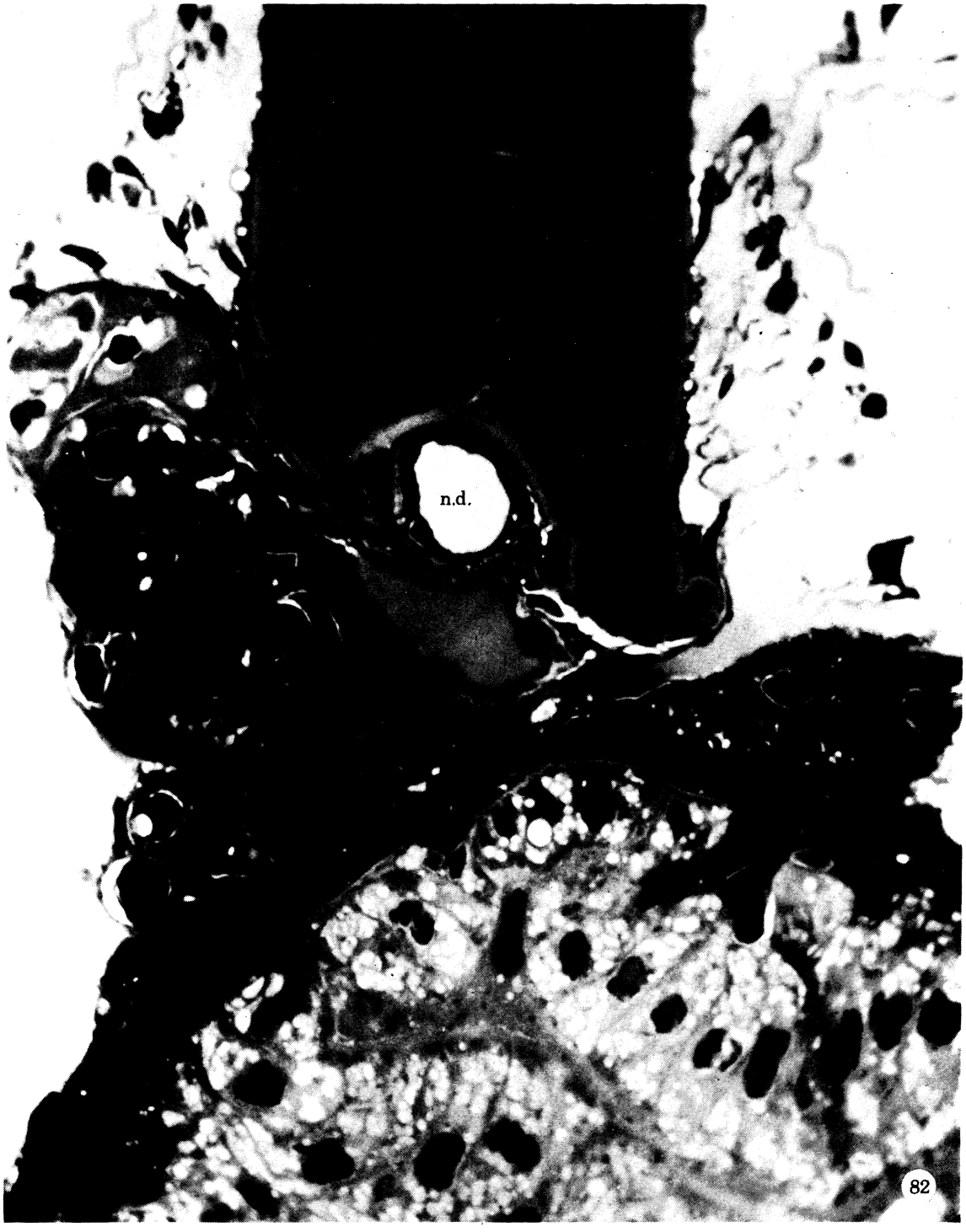

FIGURE 82. A single nephric duct leads from the kidney to the exterior.

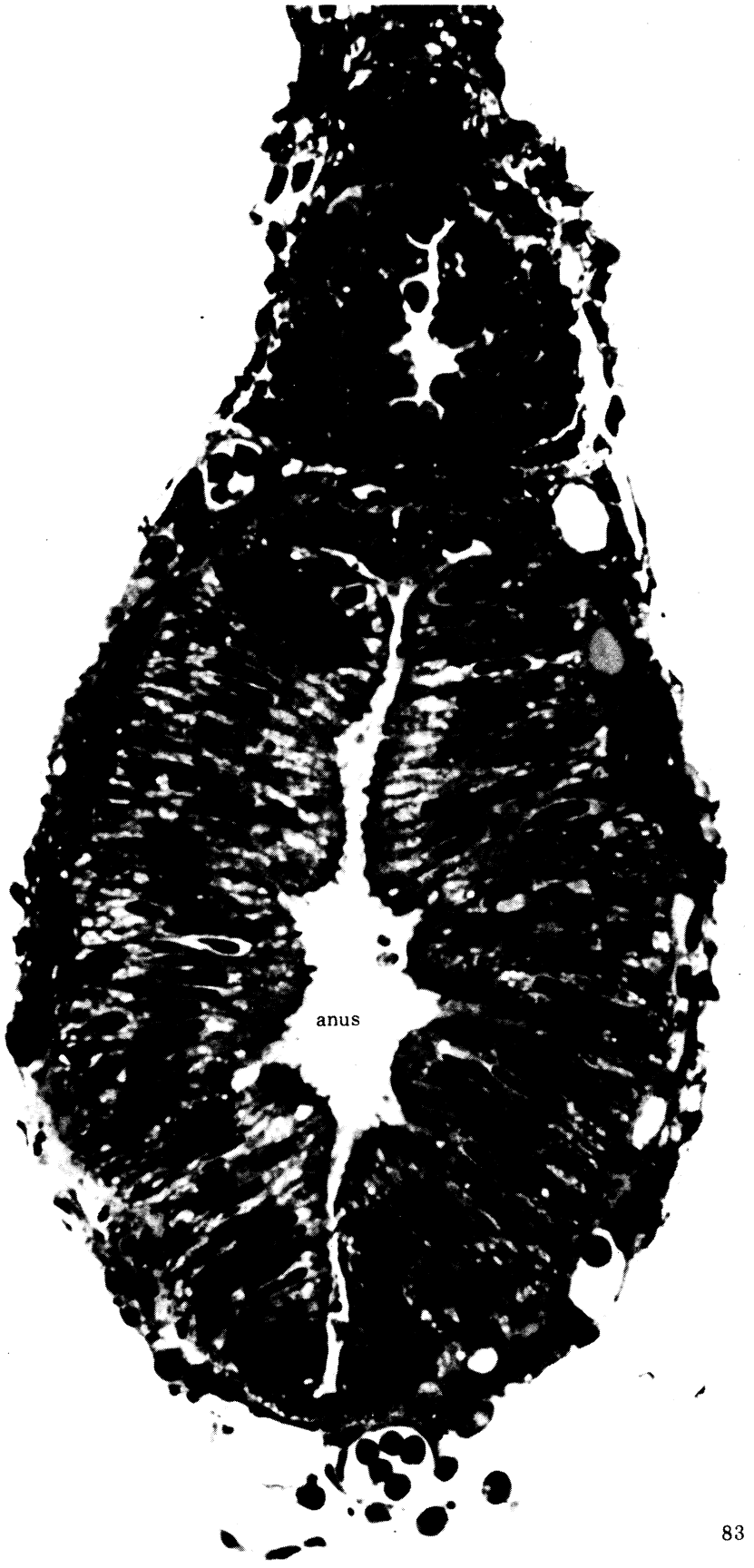

FIGURE 83. Above the anus is the opening of the urinary bladder.

9. *Endocrine glands*

The leptocephalus probably has most of the endocrine glands found in vertebrates, but I was obliged to leave this aspect of morphology to a future study. However, two glands required no search. The first of these is the pituitary (figure 48). In fact, this gland served as the centre of the axes for the transverse and sagittal sections. The pituitary has both a well-formed and cellular adenohypophysis and neurohypophysis. The thyroid gland is easily recognized in the median sagittal section (figure 17). Thyroid follicles can be seen beneath the long cartilage of the second and third basibranchials. They lack any appreciable amount of thyroid colloid.

Discussion

The development of a leptocephalous larval stage together with the stable salinity and warmth of the open tropical seas may have been inseparable factors in the present-day survival of eels and related fishes. Fishes which today begin their early life as pelagic leptocephali are known from the fossil record (Nybelin 1961) to have lived before the fragmentation of the supercontinents in the Cretaceous. Had the leptocephalus developed as an adaptation to the limitations of the continental coastline of the early Mesozoic, limitations set not only by geography but also by the declining shallow water marine life (Valentine & Moores 1970), the breaking up of the continents may have been instrumental in prolonging even further the limbo imposed by the near embryonic existence of a leptocephalus. It takes little effort to suspect that continental drift and the widening of the Atlantic Ocean are reasons for the long migration of *Anguilla* to a spawning site in the Sargasso Sea. The morphologic features described in this study of *Ariosoma balearicum* find the leptocephalus to have unique characters not known in other fishes. This distinctiveness goes beyond the peculiar head and thin, transparent body and centres on features that relate to delayed tissue maturation and functional development. In contrast to delayed development of the gills, gut and kidneys, the eyes and olfactory organs stand out as highly developed sensory structures of seemingly great functional importance.

A larval life as a leptocephalus was a compelling argument given by Greenwood *et al.* (1966) for constructing the superorder Elopomorpha. This assemblage of fishes included the elopids, albulids, true eels, gulper eels, halosaurs and notacanths. Collectively they shared a pholidophorid-like holostean ancestor and stand on the lowest rung of the teleostean level of organization. If elopiform and notacanthiform leptocephali share the many physiologic and morphologic pecularities of anguilliform leptocephali, then such evidence would suggest an evolutionary parallelism rather than the convergent development of larval imagery in unrelated groups of fishes. In this study of *Ariosoma balearicum* I have described a commonly found anguilliform leptocephalus. I have stressed those features which appear to be significant in the life of a leptocephalus and which should be rewarding in future comparison with other eel species and with leptocephali of elopiform and notacantiform fishes.

'Pelagic eel larvae are more in ionic equilibrium with seawater than other marine fishes with the exception of Myxini, a class of primitive agnathans.' Thus concludes a companion work on the electrolyte composition of eel leptocephali (Hulet *et al.* 1972). Chemical analysis of 43 leptocephali gave a mean sodium concentration of 329 mmol/kg of wet tissue. Chloride was also high, 292 mmol/kg. In terms of osmotic concentration, it was calculated that the osmolality of tissue water in the leptocephalus must exceed several hundred milliosmoles per

kilogram. In a first attempt to substantiate this conclusion, live leptocephali were collected at sea, frozen and later thawed in the laboratory. A small drop of tissue fluid was expressed from the body of each of 26 premetamorphic leptocephali. Osmolality was calculated from the melting point of the frozen droplet. Values ranged from 468 to 1175 mosmol/kg of water and the mean was 730. The leptocephali were identified only to the ordinal level and all were less than 100 mm s.l. During a recent cruise of the R/V *James M. Gillis* (8–28 April 1976) we collected a number of premetamorphic leptocephali of *Ariosoma balearicum*. Samples of intravascular fluid from live leptocephali were collected by cardiac and aortic puncture. Determination of the osmolality of the fluid sample was performed immediately by means of a vapour pressure osmometer (Wescor, Inc., Logan, Utah, U.S.A.). Again, values were consistently greater than 700 mosmol/kg of water. Except for the hagfishes, values of this magnitude and due principally to electrolyte content have never been reported in fishes. The data on electrolyte composition and these preliminary observations on osmotic concentration support the hypothesis that leptocephali, particularly larval eels, do not maintain a stable osmotic gradient between their body fluids and the external environment. We are reminded of Krogh's statement (1939) that stability of fluid composition and concentration is determined by structural and functional maturation.

If, and it seems certain from chemical analysis, leptocephali are slow to develop the capability of maintaining constancy of composition and concentration of electrolytes in their internal environment, what anatomical factors contribute to this instability? The skin is the main protection against the extraction of water and the incursion of sea salts (Keys 1931). The skin of an adult anguillid eel is practically impervious to water and electrolyte exchange; the same can be said for the skin of most adult fishes. A leptocephalus immersed in undiluted glycerol will shrink to a fraction of its normal size in a few minutes. Volume is quickly restored by transferring the shrunken leptocephalus to dilute seawater. In addition to the susceptibility of the leptocephalous skin to osmotic gradients, the epithelium of the oromandibular and branchial regions is a single layer of flat to columnar epithelial cells and cannot be considered as a significant barrier to the movement of water. Apart from any exchange that may occur between the skin and outside seawater, marine teleostean fishes swallow and absorb seawater, and the composition of the internal aqueous environment ultimately depends on the balance between absorptive and excretory organs (Smith 1930). The gastrointestinal tract absorbs water, sodium chloride and other monovalent ions of seawater, and, in fishes, much of the calcium and magnesium sulphate is absorbed. Gills excrete excess salt back into the seawater; the divalent ions are handled by the kidney.

A rather long and tedious search for the leptocephalous gills and kidneys brought surprising results, but, in retrospect, the findings might well have been anticipated, particularly when the working hypothesis suggests delay in the physiologic maturation of organs concerned with osmoregulation. To begin with, the branchial arches have no gill filaments. All premetamorphic leptocephali of *Ariosoma balearicum*, large and small, have only a mandibular hemibranch. This paired gill structure, often called a pseudobranch, is functional in the leptocephalus and for that reason it is appropriate to call it a hemibranch. The burden of secreting sodium chloride and other absorbed monovalent ions falls on the mandibular hemibranch. Quite possibly the high internal salinity of leptocephali reflects an imbalance between the inward diffusion of sodium chloride and the capacity of the gill epithelium to excrete salt against a concentration gradient.

In all vertebrates excess divalent ions such as magnesium, calcium, sulphate and phosphate are excreted by the kidney. Excretion of these ions in most fishes is a function of glomerular filtration and tubular secretion. Aglomerular fishes such as the goosefish and seahorse excrete these ions solely by active tubular transport (Edwards 1928). In the chemical analysis of leptocephali the concentration of magnesium was almost equal to seawater in the smallest larvae and decreased to a significantly lower concentration in the largest larvae. Phosphate remained constant. Sulphate was not measured in the earlier work on chemical analysis (Hulet *et al.* 1972), but at a later date, sulphate concentration was measured in three leptocephali of *Ariosoma balearicum*; values were 7.9, 8.8 and 10.9 mmol of sulphate per kilogram of wet tissue. Hagfish serum (*Myxine glutinosa*, serum sulphate 6.7 mmol/l reported by Robertson 1954) is the only vertebrate extracellular fluid with a high sulphate content. The sulphate measurements in *A. balearicum* included both intracellular and extracellular fluid compartments and cannot be compared directly with serum values for *Myxine glutinosa*. However, accepting that extracellular fluid volume is high in leptocephali and that intracellular sulphate is approximately 10–15 mmol/l of cell water, then, an average concentration of 9 mmol/l of total body water would be partitioned in such a manner that leptocephalus serum would have about the same sulphate concentration as in the hagfishes. These results on divalent ions suggested an imbalance between the rate of absorption from the skin, pharynx and gut and the renal excretion of excess quantities above the amounts used in tissue building. The high content of divalent ions was attributed to slow maturation of renal function in the leptocephalus. As with the gills, the structure of the leptocephalous kidney was quite unexpected. The renal arteries terminated, not in glomeruli crowded by hemopoietic tissue, but in an arteriovenous lake containing ciliated aglomerular tubules. Whether or not the adult of *Ariosoma balearicum* has glomeruli is not known, but the kidney sections of *Anguilla rostrata* given to me by the late Homer W. Smith have many glomeruli and my own sections of *Gymnothorax funebris* can be described as typical for a marine teleost. The aglomerular kidney of the leptocephalus is indicative of delayed tissue maturation and it can explain the sustained body content of divalent ions far above expected values. The kidneys of several other species of anguilloid leptocephali were examined following discovery of the aglomerular state of *Ariosoma balearicum* and they too were aglomerular. In summary, it appears certain that the aglomerular pronephric and opisthonephric tubules of premetamorphic leptocephali are unable to maintain an internal environment with low levels of divalent ions that we have come to expect in teleostean fishes. In regard to the high osmotic concentration of body fluids, a value somewhere between the hagfishes and most other marine teleosts, it can ultimately be attributed to the limited excretory capacity for sodium chloride by the mandibular hemibranch.

Glomerular filtration has been considered as a useful preadaptation for life in freshwater and as the result of successful adaptation to a freshwater environment. It is conceivable that paleozoic fishes without the heavy armour of other contemporary fishes developed filtration as a means for controlling the composition of body fluids while living in a marine environment. This alternative view considers the glomerulus as a structure of function and continuous development and not a functionless preadaptation to freshwater. The already present glomerular kidney may have been further refined to increase filtration when such primitive fishes invaded estuaries and streams which were subject to wide fluctuations in salinity. After metamorphosis of leptocephali, the addition of glomerular filtration and gill function permits the juvenile eel to achieve homeostasis of its internal fluid environment even to the point of entering freshwater

streams. These observations on leptocephali rather strongly suggest that fresh consideration is needed regarding the life and ancestry of eels as well as that of glomerular filtration. The degree of functional and anatomical development observed in premetamorphic leptocephali may be quite adequate for life in the open ocean. Unknown factors, not the least of which may be minute changes in the chemical and physical characteristics of seawater, trigger the metamorphosis of the leptocephalus into an organism adaptable to a wide range of marine and freshwater environments.

The third major organ to show delayed maturation is the gut. In *Ariosoma balearicum*, midportions of the intestine sometimes do not have a discernible lumen. Absorption of nutrients from the gut must be from sites in the foregut. The ingestion of planktonic organisms would be limited to those with digestible skeletons. Of the thousands of eel leptocephali examined throughout the world, no one has commented on finding food material present or likely to have been present in the gut tube. Disparate adjectives describe the gut and teeth. The gut is a simple tube with no apparent contents, but the forward projecting teeth are given names such as canines, grasping, predaceous, and many other similar connotations. The large teeth do not permit complete closure of the mouth at the margins of the jaws, but the velum and the anterior cul-de-sac will prevent water from escaping through the teeth during swallowing. They might also function as a strainer to keep things out of the mouth. The muscles of the mouth and pharynx are well developed at the premetamorphic stage and protoplasmic juices flowing from a punctured organism could be absorbed from the epithelium of the esophagus and stomach. The structure of the outer epidermis and the cells of the pharynx and esophagus suggest another source of nutrition. Rather than a diet of protoplasmic juices, the leptocephalus could obtain its nutrition from a lower trophic level, i.e., dissolved organic material and minute particulate matter. Pütter's theory (1909) of dissolved organics was favourably reviewed by Morris (1955) as a possible supplementary food source for larval fishes. Future work on this subject may show that the premetamorphic leptocephalus derives its nutrition from dissolved and particulate organic material present in seawater. Returning to the teeth, they are firmly anchored to the growing dermal bones of the jaws. At the time of metamorphosis these teeth are no longer visible; possibly they are absorbed. There is no mechanical mechanism for release from their attachment to the premaxillae, maxillae and dentaries. Were the teeth to drop out, the loss of calcium phosphate would exceed the total amount already present in developing dermal bone. A loss of phosphate to the metabolic pool of this magnitude seems physiologically unsound.

Lastly, I have a few comments about the relations of congrid eels viewed from the larval stage. The urohyal found as a distinct bone in adult eels is not present as a bone or cartilaginous element of the gill arches in the larvae. This is as it should be since the urohyal of fishes is not of ectodermal origin like the visceral arches, but derives from the mesodermal somites (Romer 1972). It is destined to develop at some later stage after metamorphosis. The larva of *Ariosoma balearicum* has a distinct separation between the two frontals. This observation again confirms that separation of the frontals is the primitive condition. The premaxillae are two separate bones associated with tiny teeth. No lateralis pits or canals are associated with the premaxillae. What I have described as a rostral commissure is a sensory organ that has evidence of canal formation. Anatomically, it may not connect with the orbital lateralis system, but it can be considered as evidence of a previous ethmoidal commissure and, as such, a link in establishing a relation between the elopiform and anguilliform fishes.

From the late H. W. Smith I learned that the study of the human kidney begins with the fishes. In the years that followed, my interest in ichthyology led to my association with Dr C. R Robins. I am happy to acknowledge the guidance and encouragement of Dr Robins in my continued effort to understand the evolution and organization of fishes. I am also indebted to Dr J. C. Staiger and Dr G. L. Voss for many hours of instruction on trawling operations and the collection of oceanic fishes. Directly related to this work, I am especially grateful to Dr D. G. Smith for information I received from his extensive knowledge of eels and eel larvae. In this same regard I have profited from discussions with Dr Catherine H. Robins, Dr D. M. Dean, Dr J. E. Böhlke and Dr N. B. Marshall. Had it not been for the capable assistance given by Margarita Villoch, Barbara J. Reitberg, J. L. Belleme and G. Musil, I hesitate to guess when this work would have been completed. M. Weakley executed the three-dimensional illustrations of the chondrocranium. I thank J. Belleme and Margarita Villoch for cutting hundreds of sections and for photographing nearly as many. Their assistance and suggestions have been of inestimable value.

Support for the early part of this work (1969–72) was provided in part by Designated Part I Funds, Veterans Administration Central Office, Washington, D.C., to myself as principal investigator. More recently (1975–6) grant support was received from the National Science Foundation, NSF BMS 75-08675, W. H. Hulet, M.D., Ph.D. and D. G. Smith, Ph.D., co-principal investigators. I am particularly grateful to Dr S. Wolf, Director, The Marine Biomedical Institute, for his support which permitted the completion of this work. Additional support was received through a grant (NSF-GB-7015) from the National Science Foundation for studies on oceanic fishes, C. Richard Robins, principal investigator. Shiptime support for R/V *Pillsbury*, R/V *Gerda*, R/V *Columbus Iselin* and R/V *James M. Gilliss* has been through NSF-GA-4569, NSF-GD-27252, NSF-GB-28440, NSF-GB-24994 and NSF-BMS-75-08675). Collecting gear used on these cruises was purchased from funds of the National Geographic Society's programme in deep-sea biology, G. L. Voss and F. M. Bayer, principal investigators and Marine Medicine General Budget Account 9-11500-765000 of the Marine Biomedical Institute, University of Texas Medical Branch, Galveston, Texas, U.S.A.

Explanation of abbreviations used on figures

a	artery
a.p.a.	afferent pseudobranchial artery
b.br.	basibranchial cartilage
br.ar.	branchial arches
br.c.	brain case
b.m.	basement membrane
bul.a.	bulbus arteriosus
c.c.	connecting cartilage
cart.	cartilage
c.a.	carotid artery
c.br.	ceratobranchial
c.hy.	ceratohyal
ce	cerebellum
culd.s.	cul-de-sac
dl.a.	dorsolateral aortae
d.a.	dorsal aorta
dt	dentary
e.br.	epibranchial cartilage
epi.t.	epiphysial tectum
e.hy.	epihyal
eso	esophagus
end.c.	endothelial cell
epi.c.	epithelial cell
eff.a.	efferent artery
e.p.	ethmoid plate
e.p.a.	efferent pseudobranchial artery
ect.eth.	ectethmoid cartilage
f.hy.VII	foramen for hym. branch of VII
f.p.	filamentous processes
g.n.X	ganglion of vagus nerve
gl.hy.	glossohyal
gs.g.	Gasserian ganglion
g.b.	gall bladder
h.br.	hypobranchial cartilage
hym	hyomandibular cartilage
hym.VII	hyomandibular branch of VII
in.	incurrent
i.sep.	internasal septum
i.o.m.	inferior oblique eye muscles
i.br.	infrapharyngobranchial cartilage
j.v.	jugular vein
l.s.c.	lateral semicircular canal
m.eth.	mesethmoid cartilage
m.eth.pr.	process for oblique eye muscles
mk	Meckel's cartilage
mln	melanophores
md	medulla
man.join.	mandibular joint
mx	maxillary bone
m.p.	mucopolysaccharide
n	nasal
n.I	olfactory nerve
n.II	optic nerve
n.X	vagus nerve
n.d.	nephric duct
not	notochord
o	orbital
o.l.	olfactory lobe of brain
op.l.	optic lobe
op.c.	opercular cartilage
olf.or.	olfactory organ
o.m.c.	oromandibular cavity
oper	operculum
oph.a.	opthalmic artery
occ.ar.	occipital arch
oto	otolith
olf.n.	olfactory nerve
opt.n.	optic nerve
p.c.a.	posterior cerebral artery
pec	scapulocoracoid cartilage
p.s.c.	posterior semicircular canal
p.f.	pectoral fin
ps	pseudobranch (mandibular hemibranch)
pit.	pituitary
pin	pineal evagination of brain
pil.c.	pillar cell
p.m.	plasma membrane
p.b.	pharyngeal bone
pmx	premaxillary bone
p.orb.	postorbital cartilage
pr.ot.	prootic cartilage
ps.b.	parasphenoid bone
ps.br.	pseudobranchial cartilage
q	quadrate
r	rostrum
rct.p.	prominence for rectus eye muscle
ros.c.	rostral commissure
s.o.b.	supraorbital bar
s.o.m.	superior oblique eye muscles
sac	sacculus
scl.	sclerotic cartilage
sp.cr.	spinal cord
s.r.m.	superior rectus muscle
t	tooth
tr.c.	trabecula communis
v.a.	ventral aorta
vel	velum
ven.	ventricle
u.hy.	urohyal
ur.bl.	urinary bladder

References

Allis, E. P., Jr. 1903 The lateral sensory system in the Muraenidae. *Int. Monatsschr. Anat. Physiol.* **20**, 125–170.

Bauchot, Marie-Louise 1959 Etude des larves leptocéphales du groupe *Leptocephalus lanceolatus* Strömman et identification à la famille des Serrivomeridae. *Dana-Report no.* 48, 1959, 148 pages.

Berry, F. H. 1964 Aspects of the development of the upper jaw bones in teleosts. *Copeia* **2**, 375–384.

Böhlke, J. E. 1949 The systematic position of the apodal fish genus *Bathymyrus*. *Copeia* **3**, 218.

Böhlke, J. E. & Chaplin, C. C. G. 1968 *Fishes of the Bahamas and adjacent tropical waters*, 771 pages. Wynnewood, Pa.: Livingston Publishing Co.

Bolognani-Fantin, A. M. & Bolognani, L. 1964 Contributo alla conoscenza della mucigenesi cutanea di *Anguilla vulgaris*. *F. Monit. Zool. Ital.* **72**, 232–242.

Bone, Q. & Denton, E. J. 1971 The osmotic effects of electron microscope fixatives. *J. Cell. Biol.* **49**, 571–581.

Castle, P. H. J. 1964 Congrid leptocephali in Australasian waters with descriptions of *Conger wilsoni* (Bl. and Schn.) and *Conger verreauxi* Kaup. *Zool. Publ.* Victoria Univ. New Zeal. **37**, 1–45.

Castle, P. H. J. 1969 An index and bibliography of eel larvae. Spec. Pub. No. 7, J. L. B. Smith Instit. of Ichthy., Rhodes U., Grahamstown, South Africa, 121 pages.

Choi, J. K. 1963 The fine structure of the urinary bladder of the toad, *Bufo marinus*. *J. Cell. Biol.* **16**, 53–72.

D'Ancona, U. 1931 Uova, larve e stadi giovanili di teleostei Apodes. *Fauna flora Golfo Napoli* **38**, 94–156.

Dawes, C. J. 1971 *Biological techniques in electron microscopy*, 193 pages. New York: Barnes and Noble, Inc.

Dean, D. M. 1968 The metamorphosis of the ophichthid eel *Myrophis egmontis*. Thesis, University of Miami, Coral Gables, Florida.

Delage, M. Y. 1886 Sur les relations de parenté du congre et du leptocéphale. *C. r. hebd. Séanc Acad. Sci., Paris*, **103**, 698–699.

De La Roche, F. E. 1809 Observations sur des poissons recueillis dans un voyage aux îles Baléares et Pythiuses. *Ann. Mus. Natn. Hist. Nat. Paris* **13**, 313–361.

Dobbs, H. H., III. 1974 Soft tissues of marine teleosts. In *Principles and techniques of electron microscopy*, vol. 2, pp. 3–42. New York: Van Nostrand Reinhold Co.

Edwards, J. G. 1928 Studies on aglomerular and glomerular kidneys. *Am. J. Anat.* **42**, 75–108.

Facciolà, L. 1897 Sunto di alcune ricerche su l'organizzazione e lo sviluppo dei Leptocefalidi. *Atti Soc. Nat. Mat.* ser. 3, **14**, 122–145.

Gabe, M. 1971 Polysaccharides in lower vertebrates. In *Handbuch Der Histochemie*. Band II, Polysaccharide Dritter Teil. 543 pages. Stuttgart: Gustav Fisher Verlag.

Goodrich, E. S. 1930 *Studies on the structure and development of vertebrates*. London: Macmillan. Reprinted by Dover publications, New York, 1958, 2 volumes.

Gosline, W. A. 1971 *Functional morphology and classification of teleostean fishes*, vol. i–ix, 208 pages. Hawaii, Honolulu: University Press.

Greenwood, P. H., Rosen, D. E., Weitzman, S. H. & Myers, G. S. 1966 Phyletic studies of teleostean fishes, with a provisional classification of living forms. *Bull. Am. Mus. Nat. Hist.* art. 4, **131**, 341–455.

Grassi, G. B. & Calandruccio, S. 1892 Le Leptocefalide e la loro trasformazione in murenide. *Atti Accad. Naz. Lincei Rc.*, Ser. 5, **1** (2), 375–379.

Grassi, G. B. & Calandruccio, S. 1897 Descrizione d'un *Leptocephalus brevirostris* in via di trasformarsi in *Anguilla vulgaris*. *Atti. Accad. Naz. Lincei Rc.*, Ser. 5, **6** (1), 239–240.

Harrington, R. W., Jr. 1955 The osteocranium of the American Cyprinid fish, *Notropis bifrenatus*, with an annotated synonymy of teleost skull bones. *Copeia* (4), 267–290.

Hayat, M. A. 1970 *Principles and techniques of electron microscopy: Biological applications*, vol. 1, pp. 1–412. New York: Van Nostrand Reinhold Co.

Holland, N. D. & Jespersen, A. 1973 The fine structure of the fertilization membrane of the feather star *Comanthus japonica* (Echinodermata: Crinoidea). *Tissue & Cell* **5**, 209.

Hulet, W. H., Fischer, J. & Rietberg, B. J. 1972 Electrolyte composition of Anguilliform leptocephali from the Straits of Florida. *Bull. Mar. Sci.* **22**, 432–448.

Jespersen, P. 1942 Indo-Pacific leptocephalids of the genus *Anguilla*. Systematics and biological studies. Dana-Report no. 22, 1942, 128 pages.

Jones, M. P., Holliday, F. G. T. & Dunn, A. E. G. 1966 The ultrastructure of the epidermis of larvae of the herring (*Clupea harengus*) in relation to the rearing salinity. *Mar. Biol. Ass. U.K.* **46**, 235–239.

Kerr, J. G. 1919 *Textbook of embryology*, vol. II *Vertebrata with the exception of Mammalia*, 591 pages. London: Macmillan.

Keys, A. B. 1931 Chloride and water secretion and absorption by the gills of the eel. *Z. Vergleich. Physiol.* **15**, 364–388.

Krogh, A. 1939 *Osmotic regulation in aquatic animals*. Cambridge University Press. Reprinted by Dover Publications, Inc., New York, 1965.

Luppa, H. 1966 Ein Beitrag zur Funktion der Appendices pyloricae der fische. *Morphol. Jhb.* **109**, 315–339.

Manfredi-Romanini, M. G. 1964 Ricerche sulla differenziazione della mucosa gastrica in embrioni ed in avanotti di trota. *Rend. Sci. Inst. Lombardo* B **98**, 48–66.

Morris, R. W. 1955 Some considerations regarding the nutrition of marine fish larvae. *J. Cons. perm. int. Explor. Mer.* **20**, 255–265.

Musil, G. & Belleme, J. 1970 Illumination for photomicrography of unstained specimens. *J. biol. Photogr. Ass.* **38**, 67–69.

Nelson, G. J. 1966 Gill arches of teleostean fishes of the order Anguilliformes. *Pacif. Sci.* **20**, 391–408.

Newstead, J. D. 1967 Fine structure of the respiratory lamellae of teleostean gills. *Z. Zellforsch.* **79**, 396–428.

Norman, J. R. 1926 The development of the chondrocranium of the eel (*Anguilla vulgaris*) with observations on the comparative morphology and development of the chondrocranium in bony fishes. *Phil. Trans. R. Soc. Lond.* B **214**, 369–464.

Nybelin, O. 1961 Über die Frage der Abstammung der rezenten primitiver Teleostier. *Palaontol. Z.* **35**, 114–117.

Orton, G. L. 1963 Notes on larval anatomy of fishes of the order Lyomeri. *Copeia*, 1963 (1), 6–15.

Peyer, B. 1968 *Comparative odontology*. (transl. and ed. R. Zangerl). Chicago: University Press.

Pütter, A. 1909 Die Ernährung der Copepoden. *Arch. Hydrobiol.* **15**, 70–117.

Raffin, J. P. 1967 Histochemie et formation des gaines cordales chez un salmonidé, *Salmo fario* L. *Annls Histochim.* **12**, 293–312.

Rebhun, L. I. 1972 Freeze-substitution and freeze-drying. In *Principles and techniques of electron microscopy*, vol. 2, 3–42. New York: Van Nostrand Reinhold.

Regan, C. T. 1912 The osteology and classification of the teleostean fishes of the order Apodes. *Ann. Mag. Nat. Hist.* Ser. 8, **10**, 377–387.

Robertson, J. D. 1954 The chemical composition of the blood of some aquatic chordates, including members of the Tunicata, Cyclostomata and Osteichthyes. *J. expl. Biol.* **31**, 424–442.

Robins, C. H. 1971 The comparative morphology of the Synaphobranchid eels of the Straits of Florida. *Proc. Acad. nat. Sci. Philad.* **123**, 153–204.

Robins, C. H. & Robins, C. R. 1971 Osteology and relationships of the eel family Macrocephenchelyidae. *Proc. Acad. nat. Sci. Philad.* **123**, 127–150, 7 figs.

Romer, A. S. 1962 *The vertebrate body*. Philadelphia: W. B. Saunders Co.

Romer, A. S. 1972 The vertebrate as a dual animal – somatic and visceral. In *Evolutionary Biology*, vol. 6, pp. 121–156 (ed. T. Dobzhansky, M. Hecht & W. Steere). New York: Appleton Century Crofts.

Satchell, G. H. 1971 *Circulation in fishes*. Pp. 1–131. Cambridge University Press.

Schmidt, J. 1922 The breeding places of the eel. *Phil. Trans. R. Soc. Lond.* B **211**, 179–208.

Smith, D. G. 1969 Xenocongrid eel larvae in the Western North Atlantic. *Bull. Mar. Sci.* **19**, 377–408.

Smith, D. G. 1971 Osteology and relationships of the congrid eels of the Western North Atlantic (Pisces, Anguilliformes). Dissertation, The University of Miami, Coral Gables, Florida.

Smith, H. W. 1930 The absorption and excretion of water and salts by marine teleosts. *Am. J. Physiol.* **93**, 480–505.

Spartà, A. 1938 Contributo alla conoscenza dello svilluppo embrionale e post-embrionale nei Muraenoidi. 4. *Ophisoma balearicum* De La Roche. *Memie R. Com. Talassogr. Ital.*, **252** 1–9.

Spurr, A. R. 1969 A low-viscosity epoxy resin embedding medium for electron microscopy. *J. Ultrastruct. Res.* **26**, 1–31.

Valentine, J. W. & Moores, E. M. 1970 Plate-tectonic regulation of faunal diversity and sea level: a model *Nature, Lond.* **228**, 657–659.

Waddington, C. H. 1956 *Principles of Embryology*. London: Allen & Unwin.

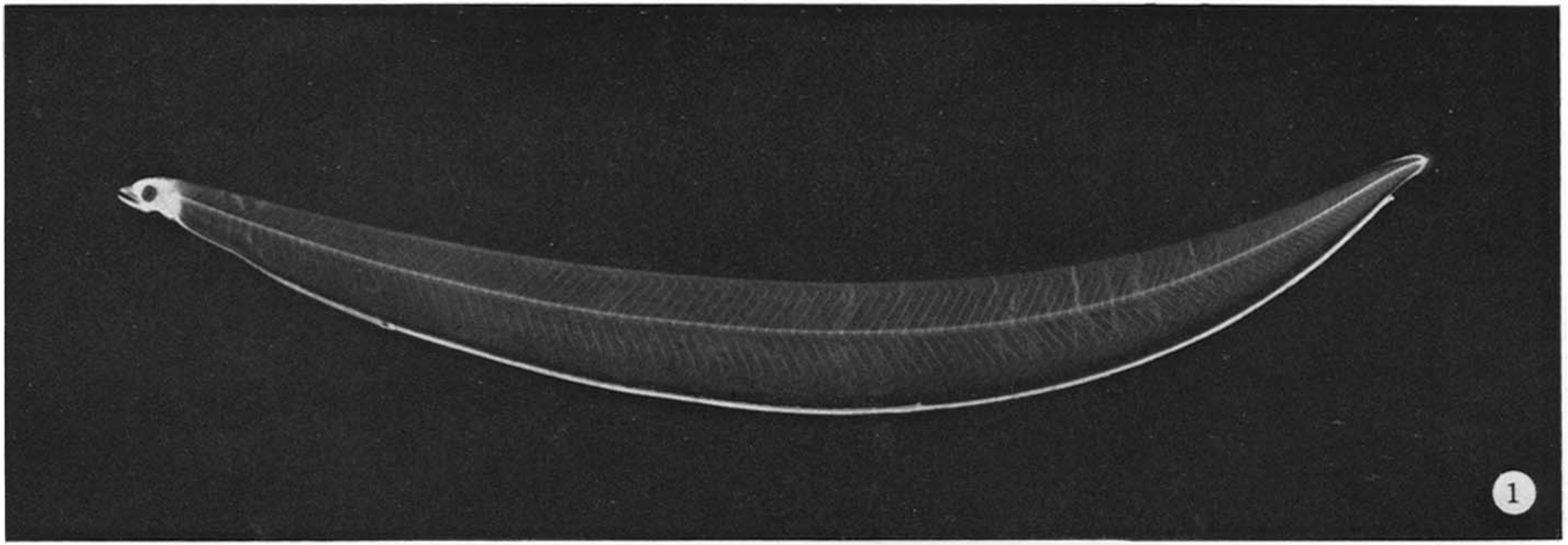

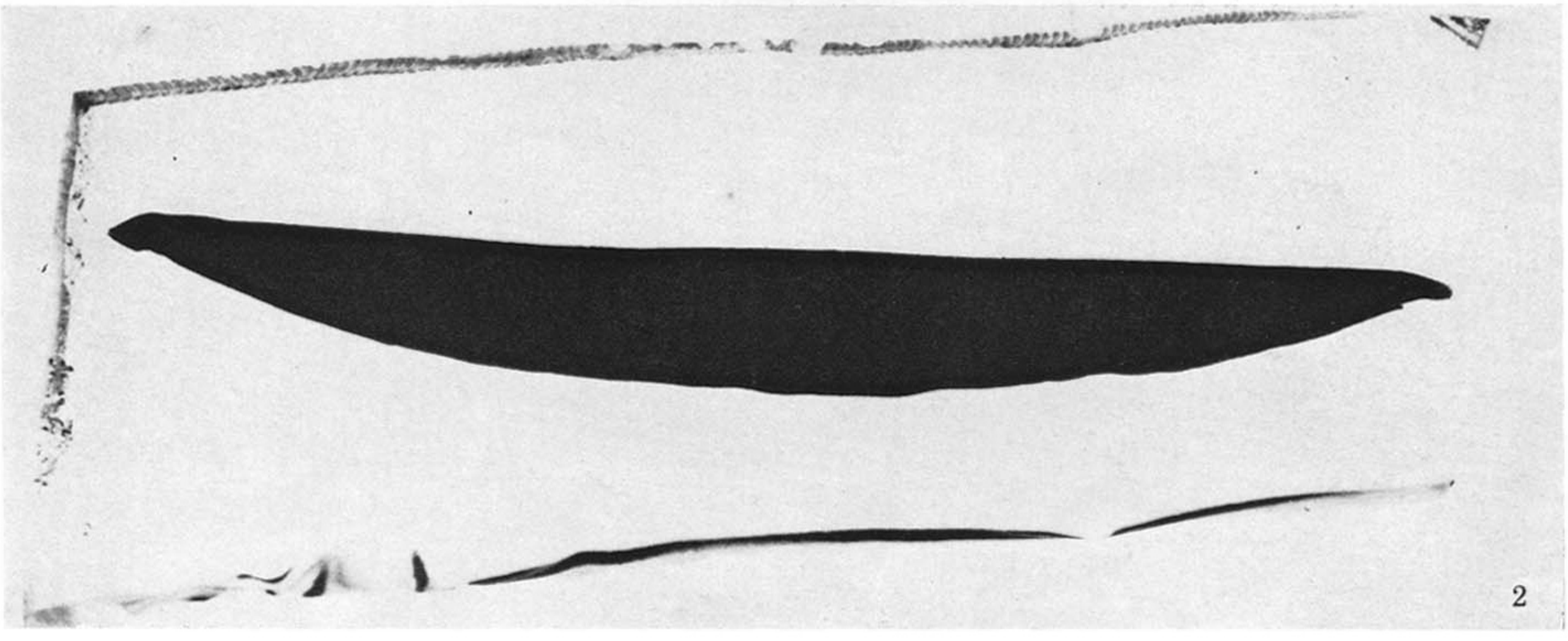

FIGURE 1. Formalin-fixed premetamorphic leptocephalus. All figures are of *Ariosoma balearicum*. (Magn. × 1.35.)

FIGURE 2. Leptocephalus, whole mount. Specimen fixed in glutaraldehyde, post-fixed in osmium tetroxide and embedded in Spurr low-viscosity media. Specimen WM(S)-3, 78 mm s.l.

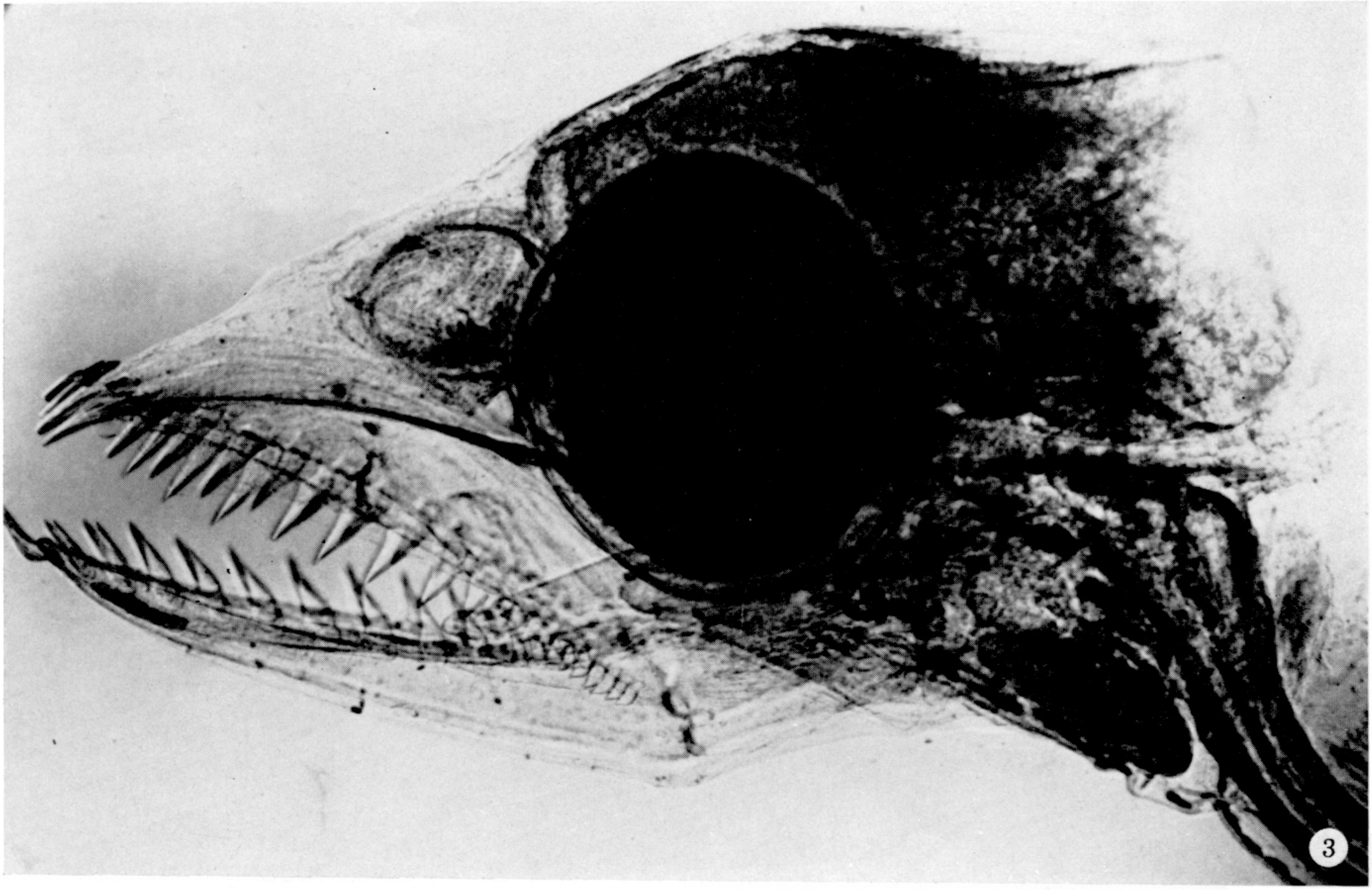

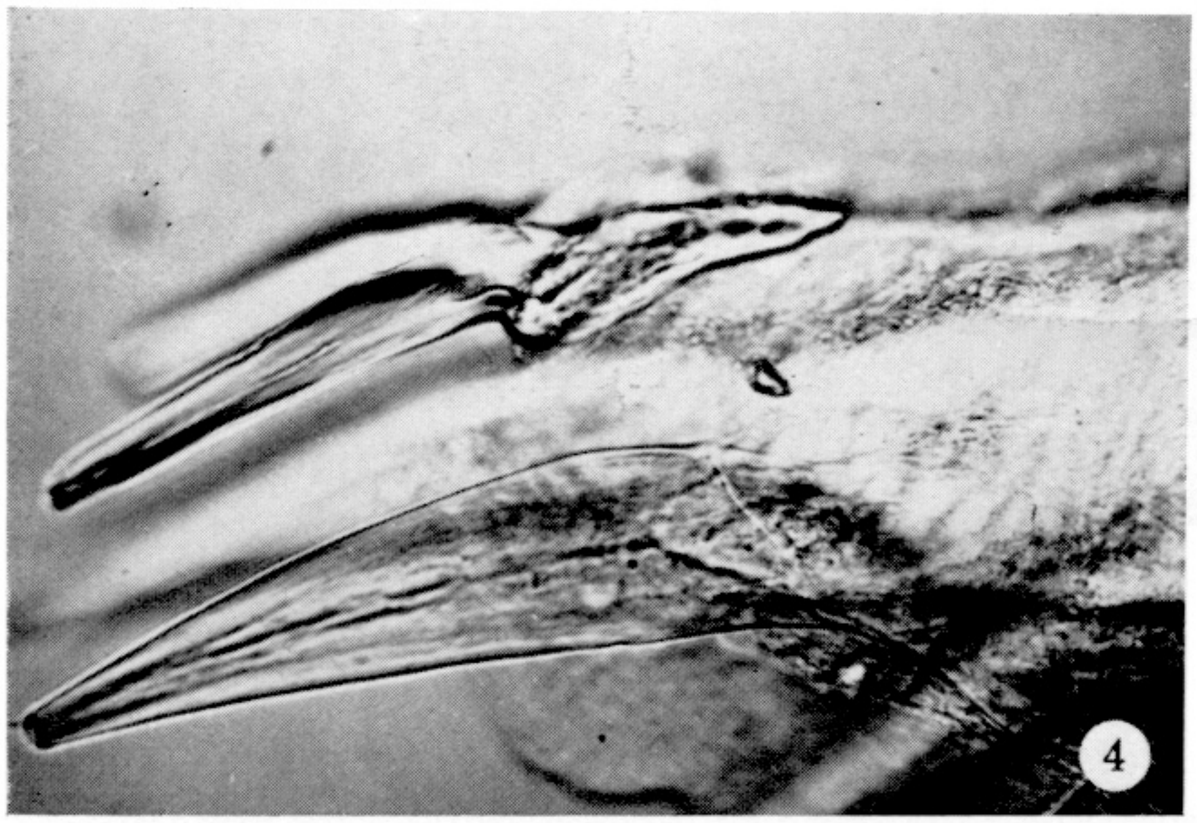

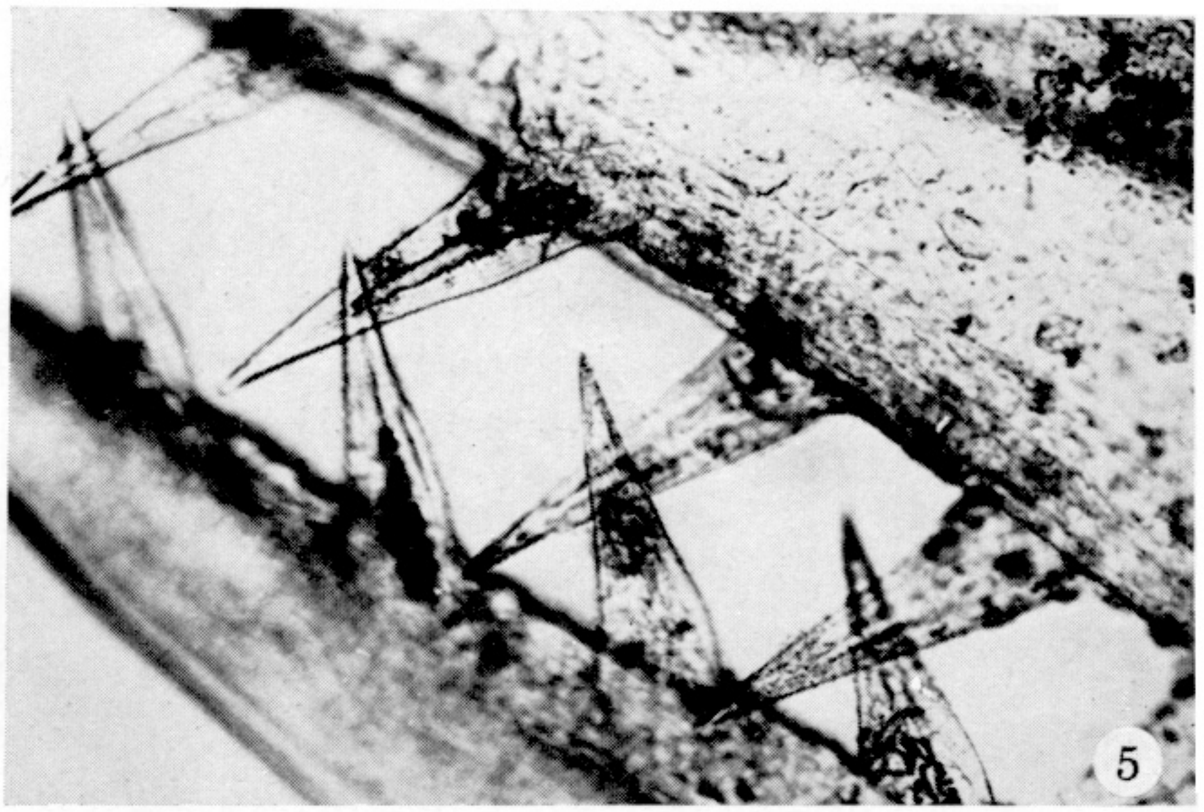

FIGURE 3. Head and anterior body of leptocephalus in glutaraldehyde. The numerous small teeth on the maxilla are well visualized. The esophagus bends sharply downward as it passes over the ventricle. The eye has been blacked out.

FIGURE 4. The left premaxilla and its attached tooth are above the first tooth of the maxilla.

FIGURE 5. Anterior teeth. Note that the teeth are inclined forward.

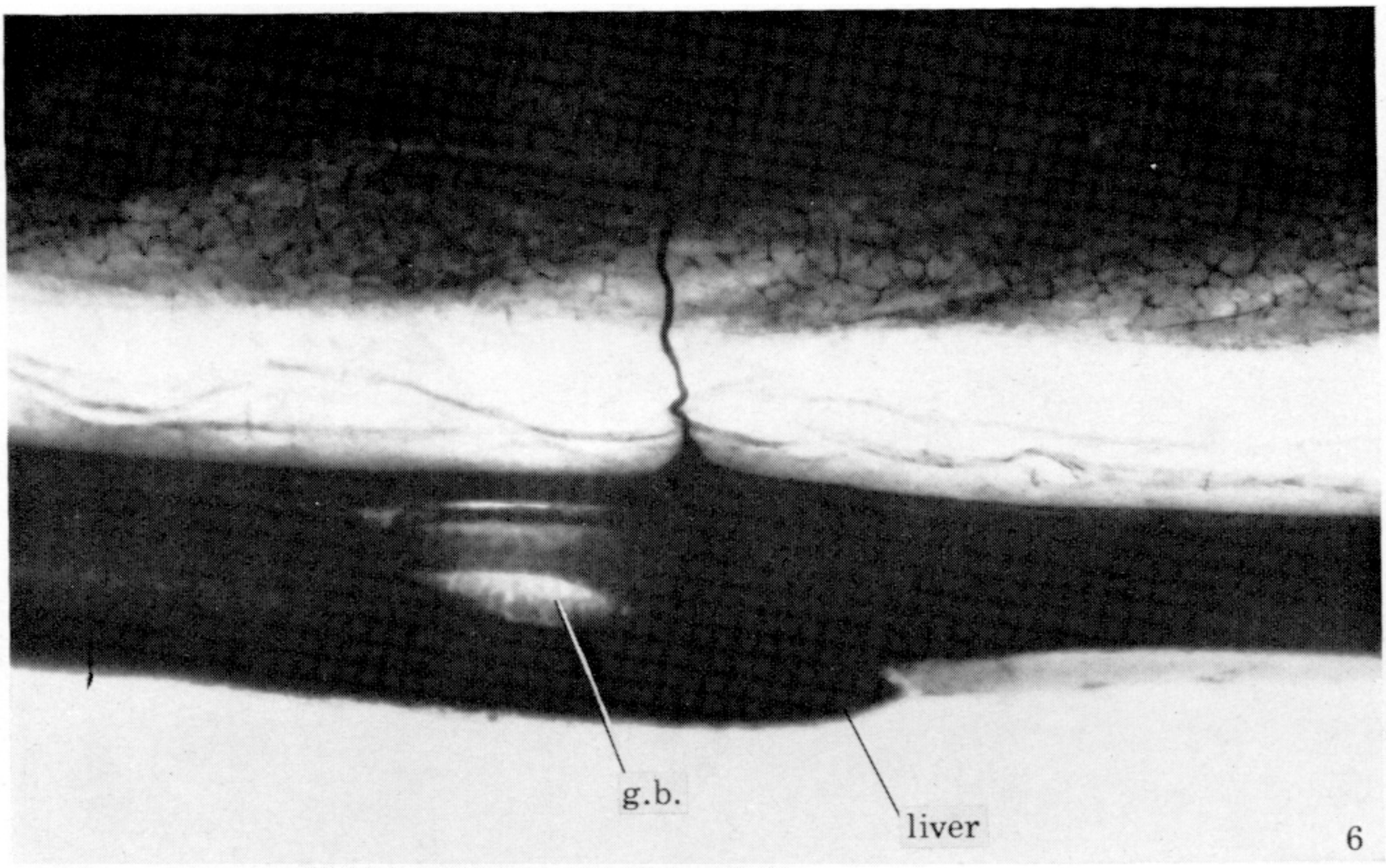

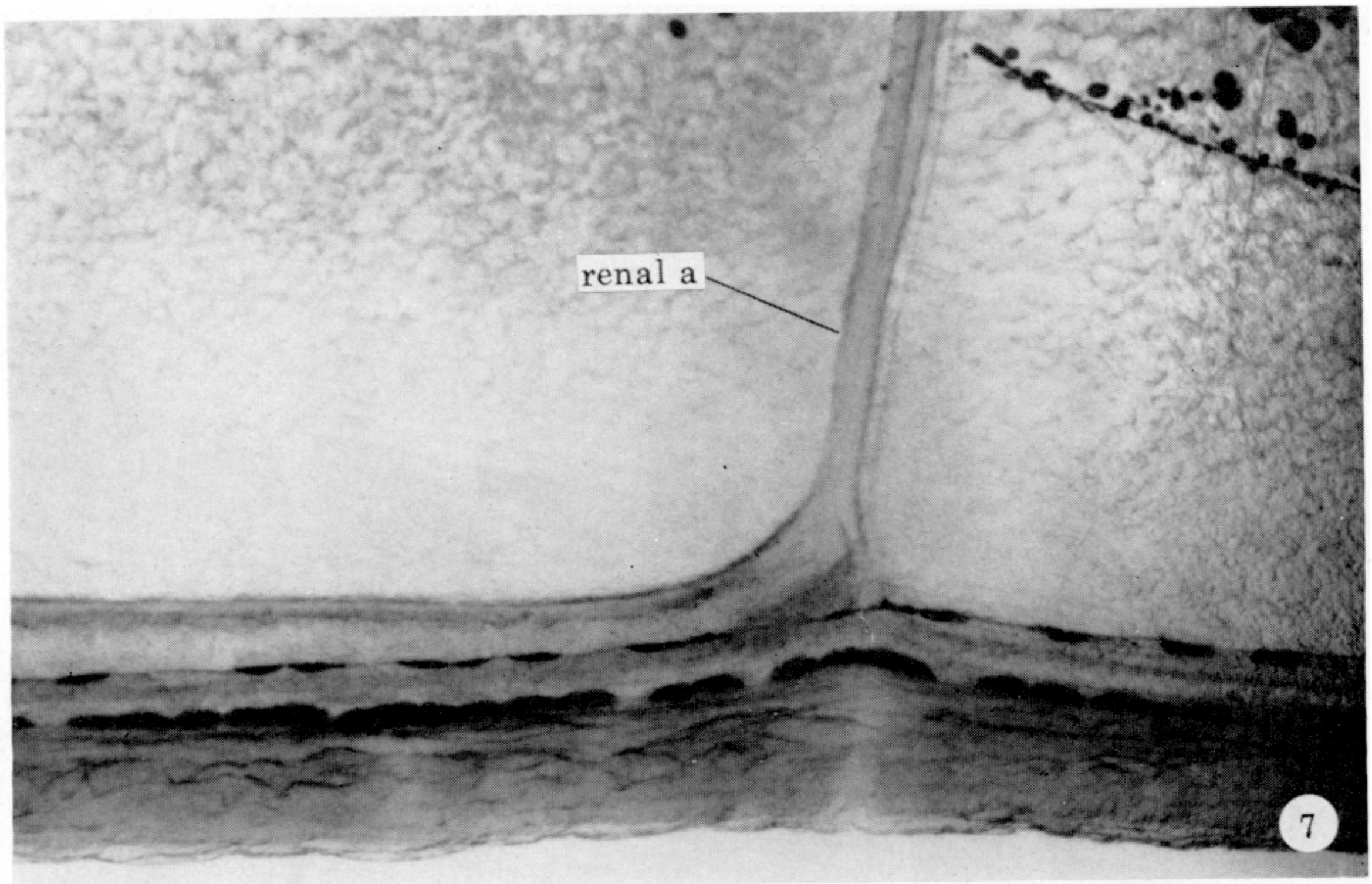

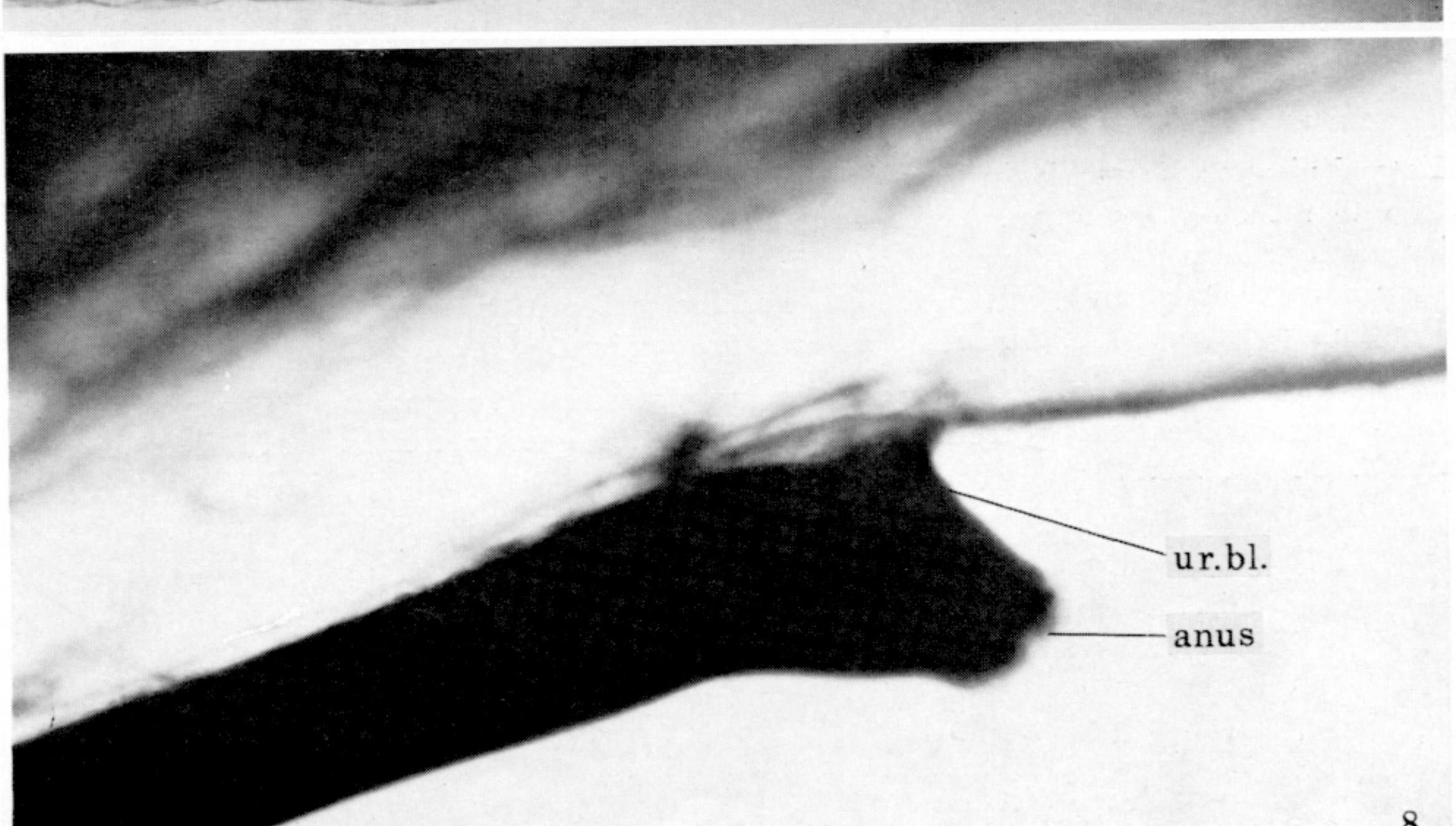

FIGURES 6–8. For description see opposite.

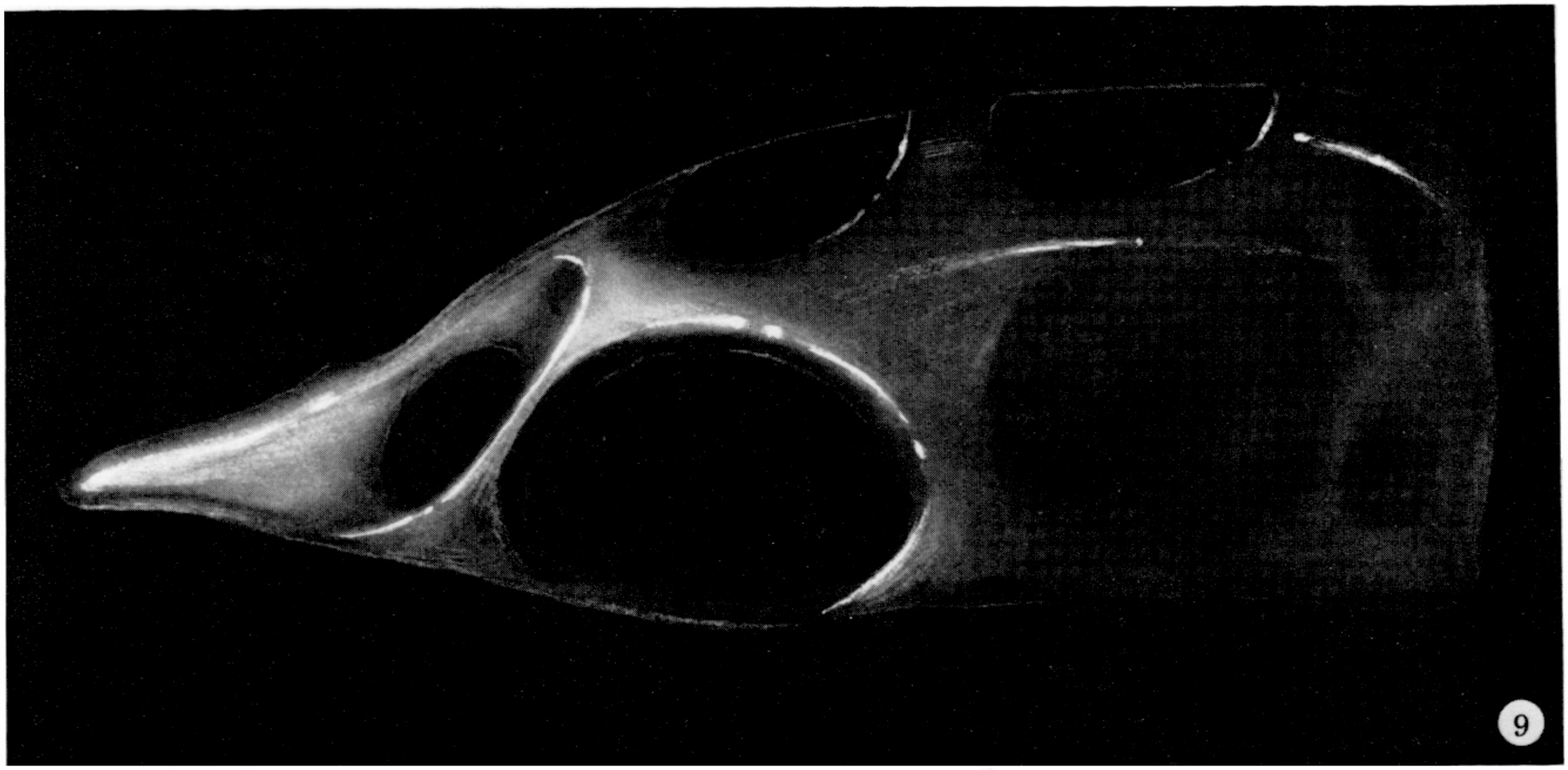

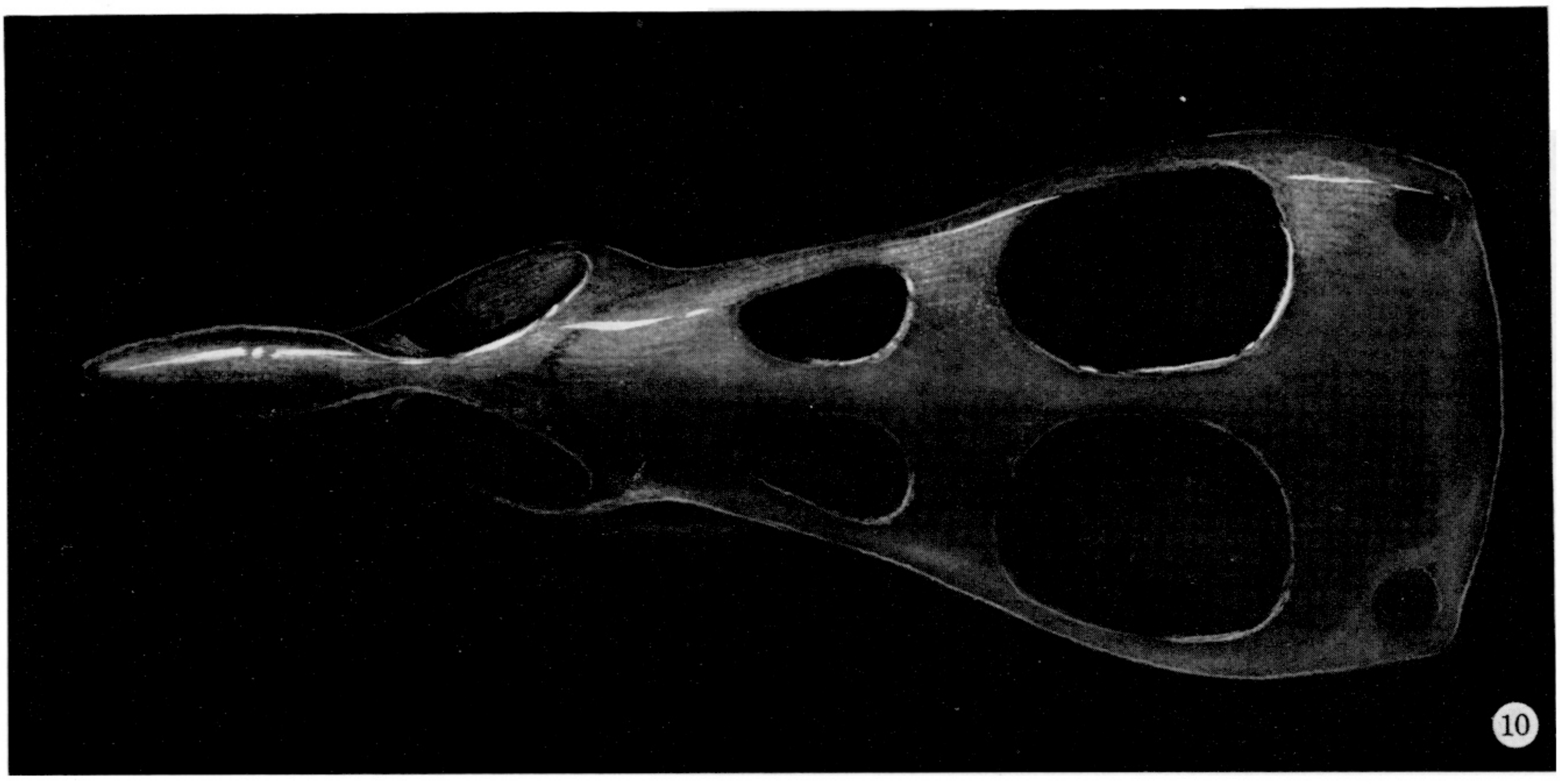

FIGURE 9. Lateral view of the cartilaginous neurocranium. Anteriorly, the ethmoid cartilage gives support and protection to the olfactory organ. Three structures join the anterior cartilaginous neurocranium to the posterior portion: (*a*) a thin midline ribbon of cartilage from the ethmoid to the epiphysial tectum, (*b*) the lateral supraortibal bars, and (*c*) the ventral, midline trabecula communis. Posteriorly, the otic capsule comprises the major portion of the cartilaginous neurocranium. (Magn. × 38.)

FIGURE 10. Viewed from above, the dorsal aspect of the brain receives little protection. The epiphysial tectum and the midline cartilage extending from the ethmoid to the synotic tectum leave four large fontanelles unprotected. (Magn. × 38.)

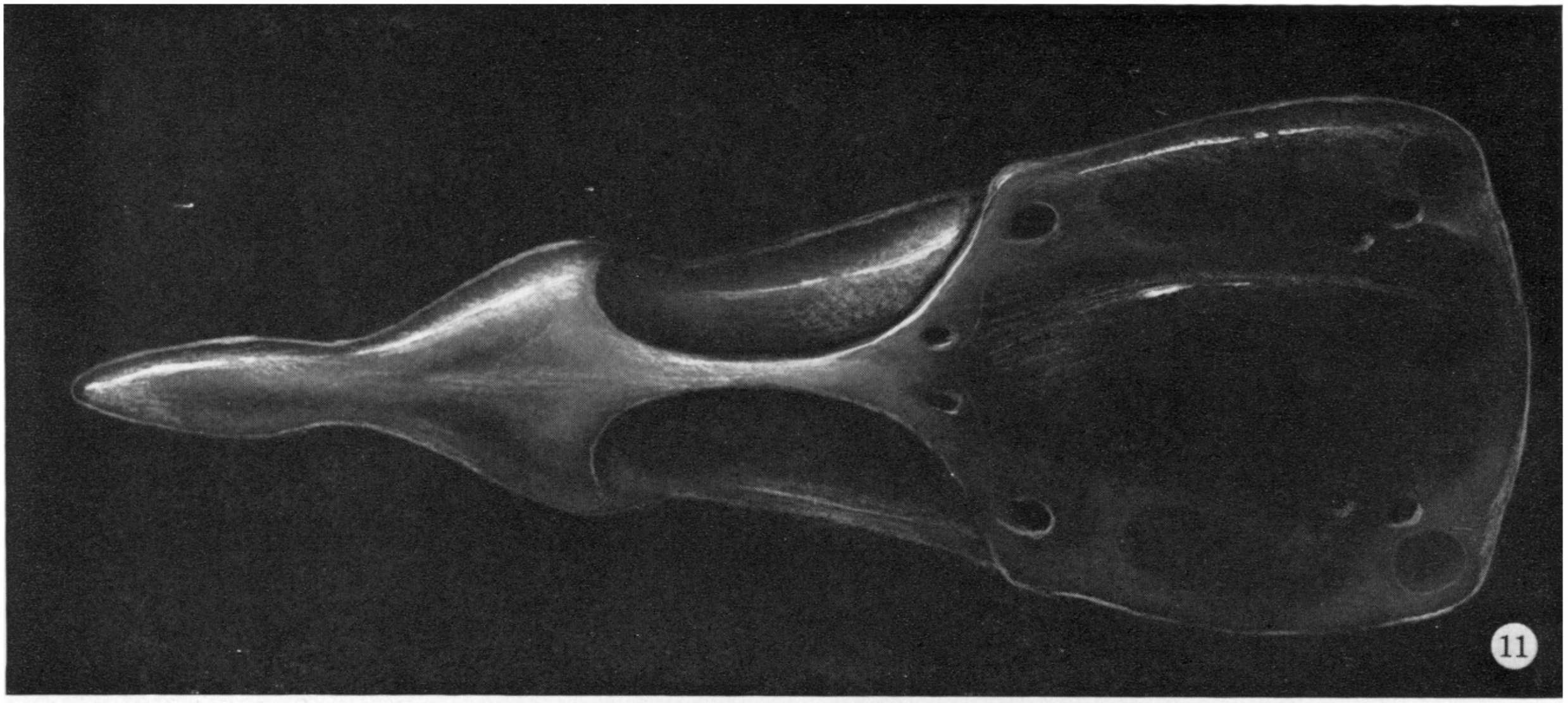

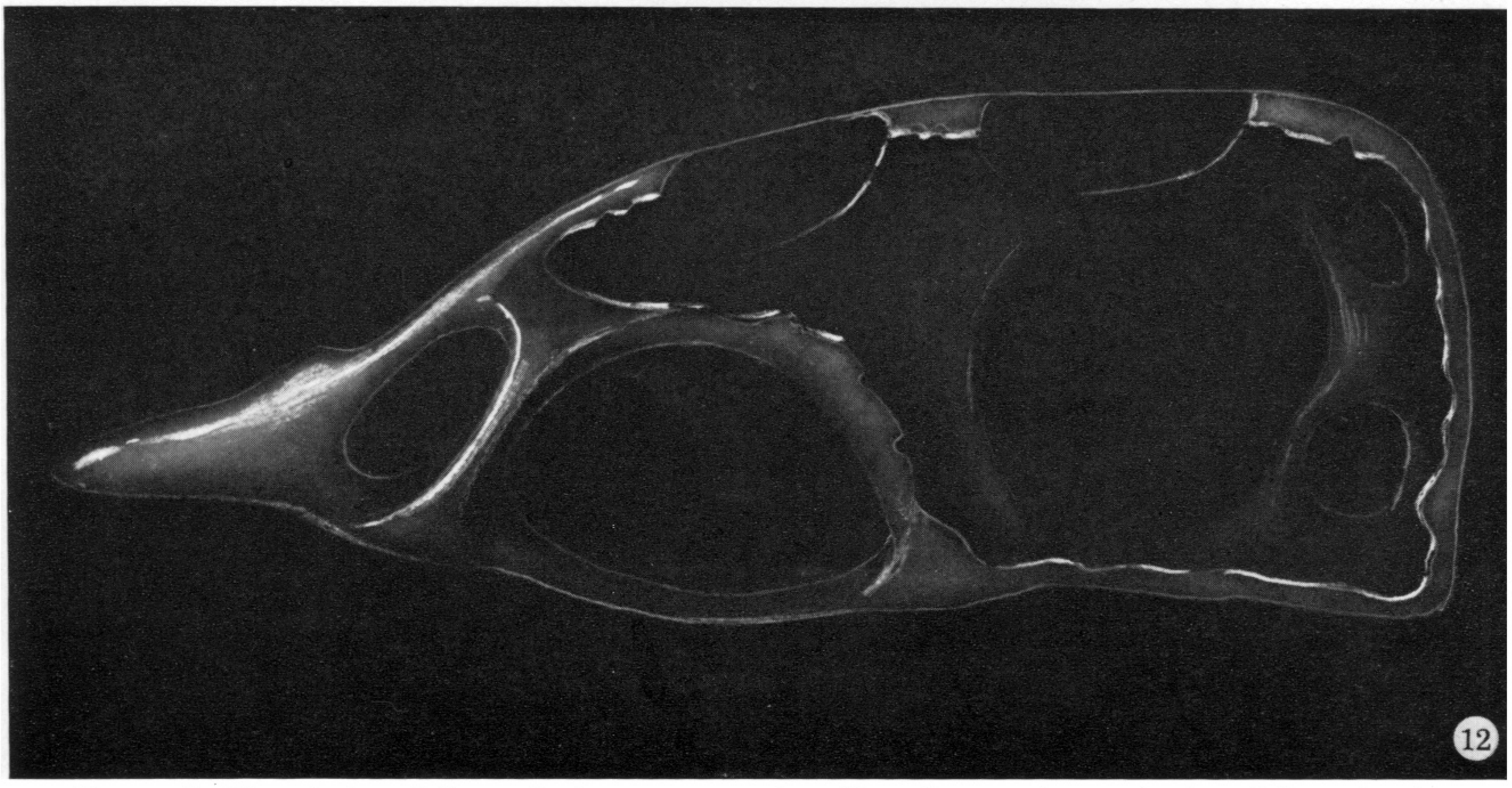

FIGURE 11. Ventral view of the cartilaginous neurocranium. Near the posterior termination of the trabecula communis, two foramina provide entry for the carotid arteries; foramina for the facial nerve (VII) are slightly more posterior and lateral. Posteriorly, the glossopharyngeal (IX) and vagus (X) nerves leave through paired foramina in a groove between the parachordal cartilage and the otic capsule. (Magn. × 38.)

FIGURE 12. Internal view of the auditory region. Posterior to the circular bulge of the cartilaginous otic capsule are additional supports for the posterior and lateral semicircular canals. (Magn. × 38.)

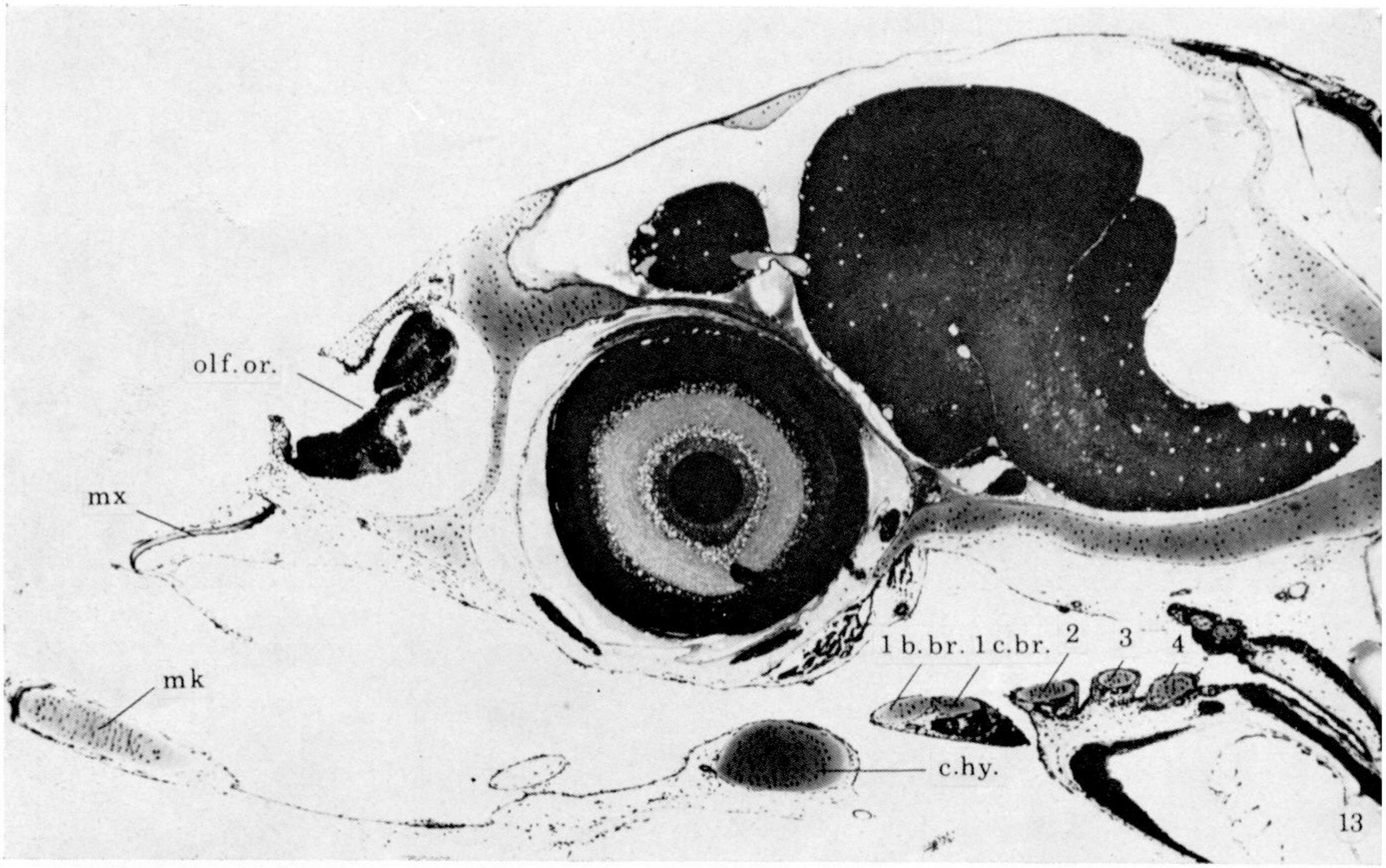

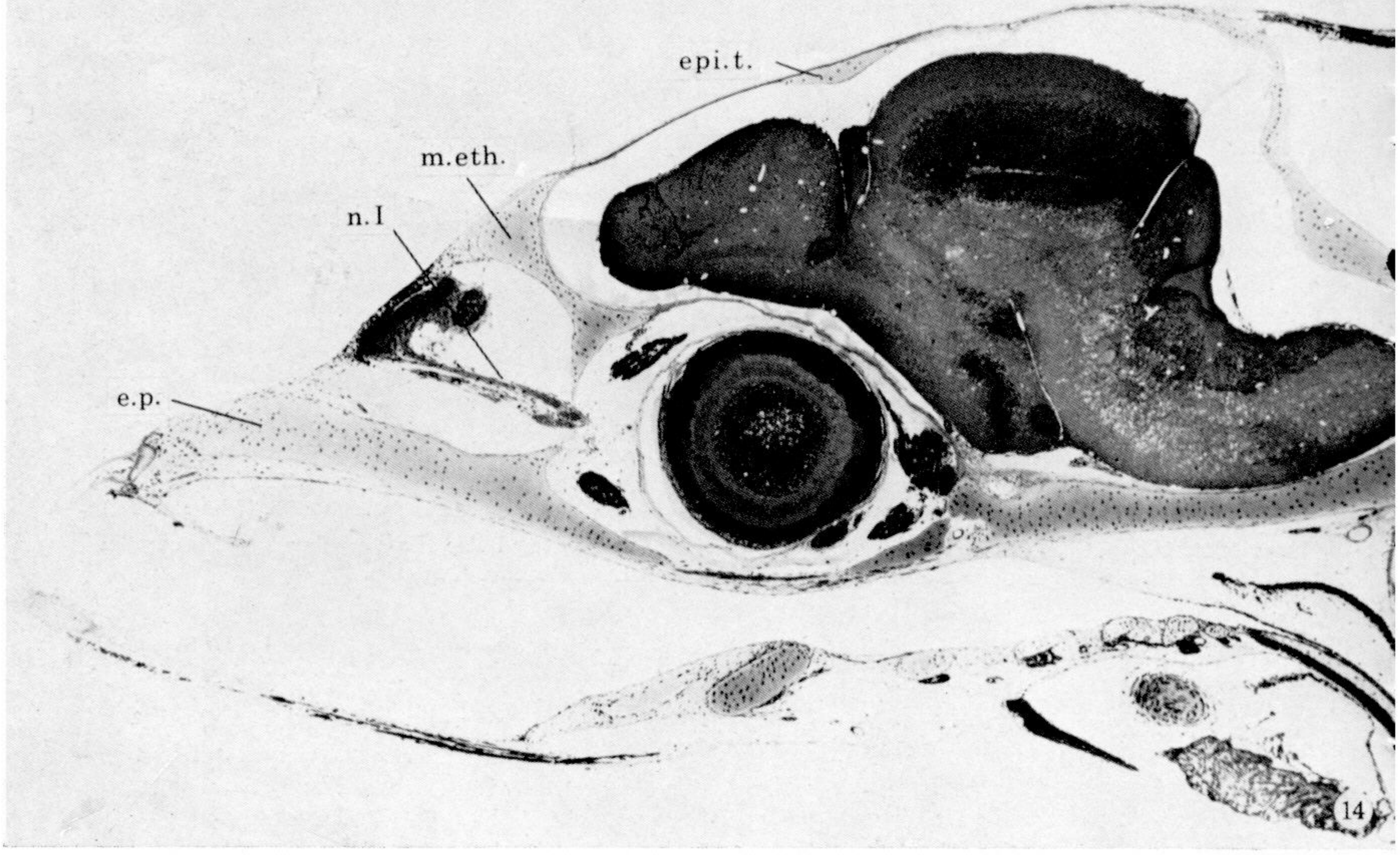

FIGURE 13. Sagittal section of head, left side. Figures 13–22 are from specimen WM(A)-4, 82 mm s.l. (Magn. × 60.)

FIGURE 14. Sagittal section of head, left side, medial to figure 13. (Magn. × 58.)

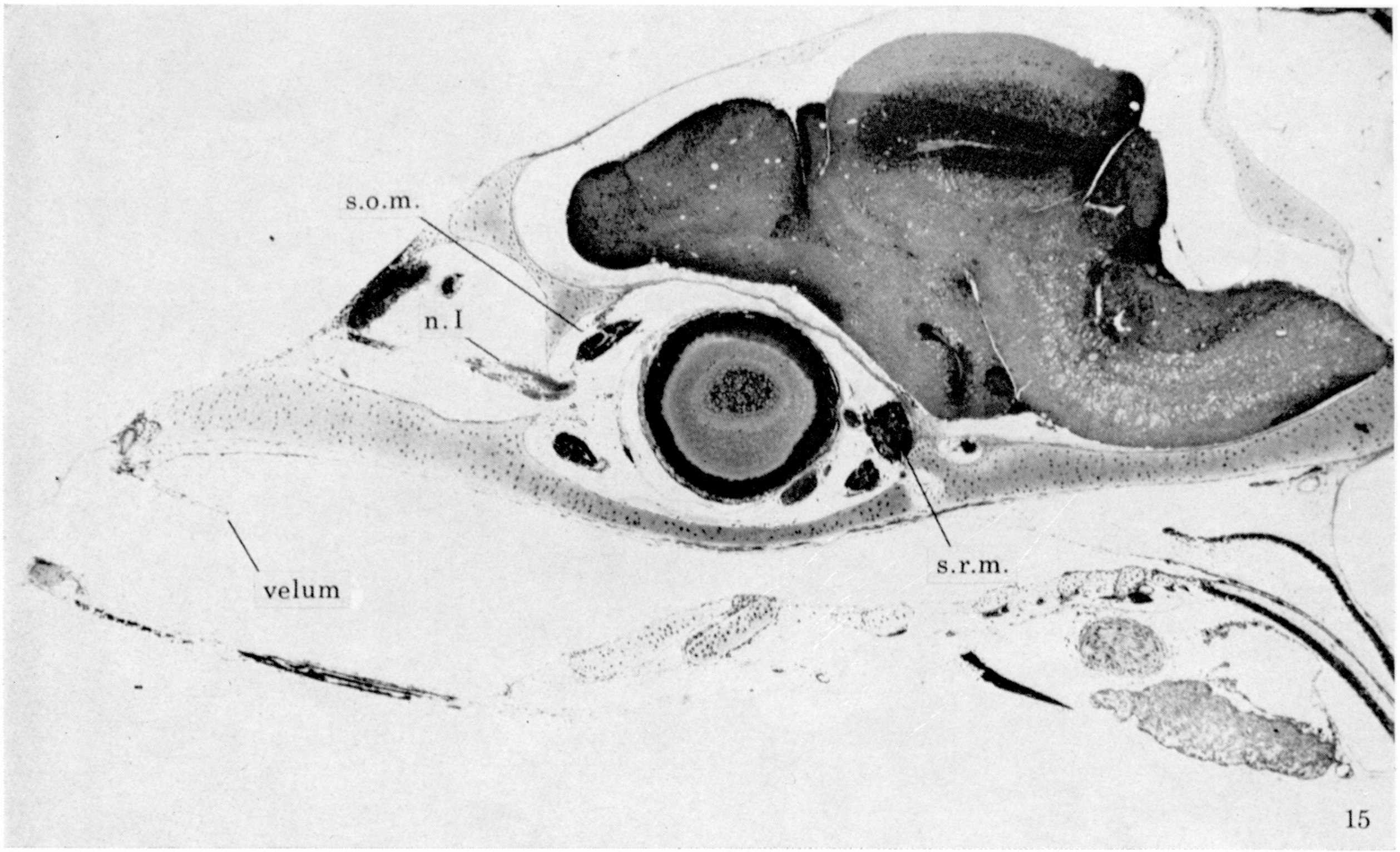

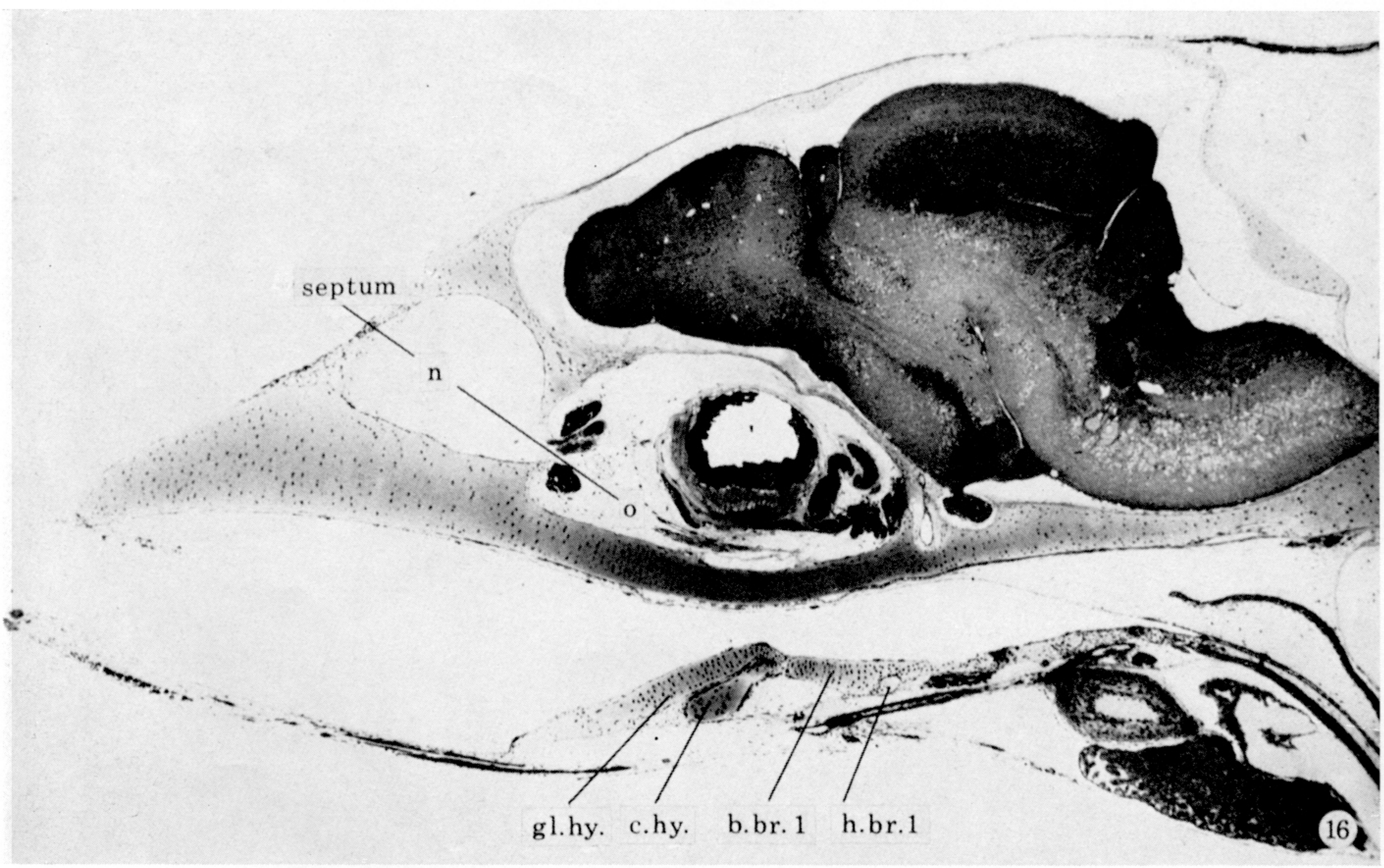

FIGURE 15. Sagittal section of head, left side, medial to figure 14. (Magn. ×57.)

FIGURE 16. Sagittal section of head, left side, medial to figure 15. (Magn. ×57.)

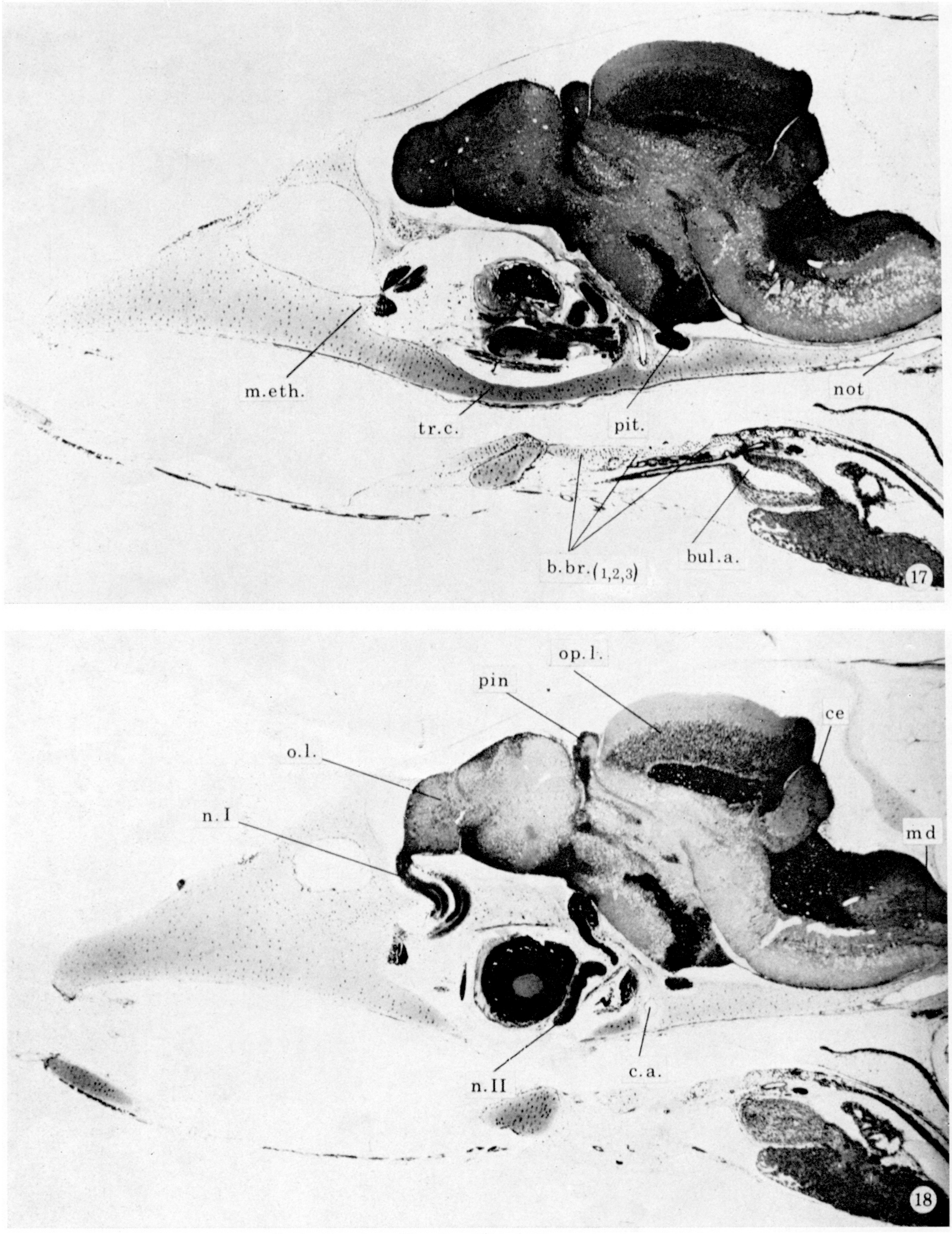

FIGURE 17. Sagittal section of head, midline. (Magn. × 58.)

FIGURE 18. Sagittal section of head slightly to right of midline. (Magn. × 66.)

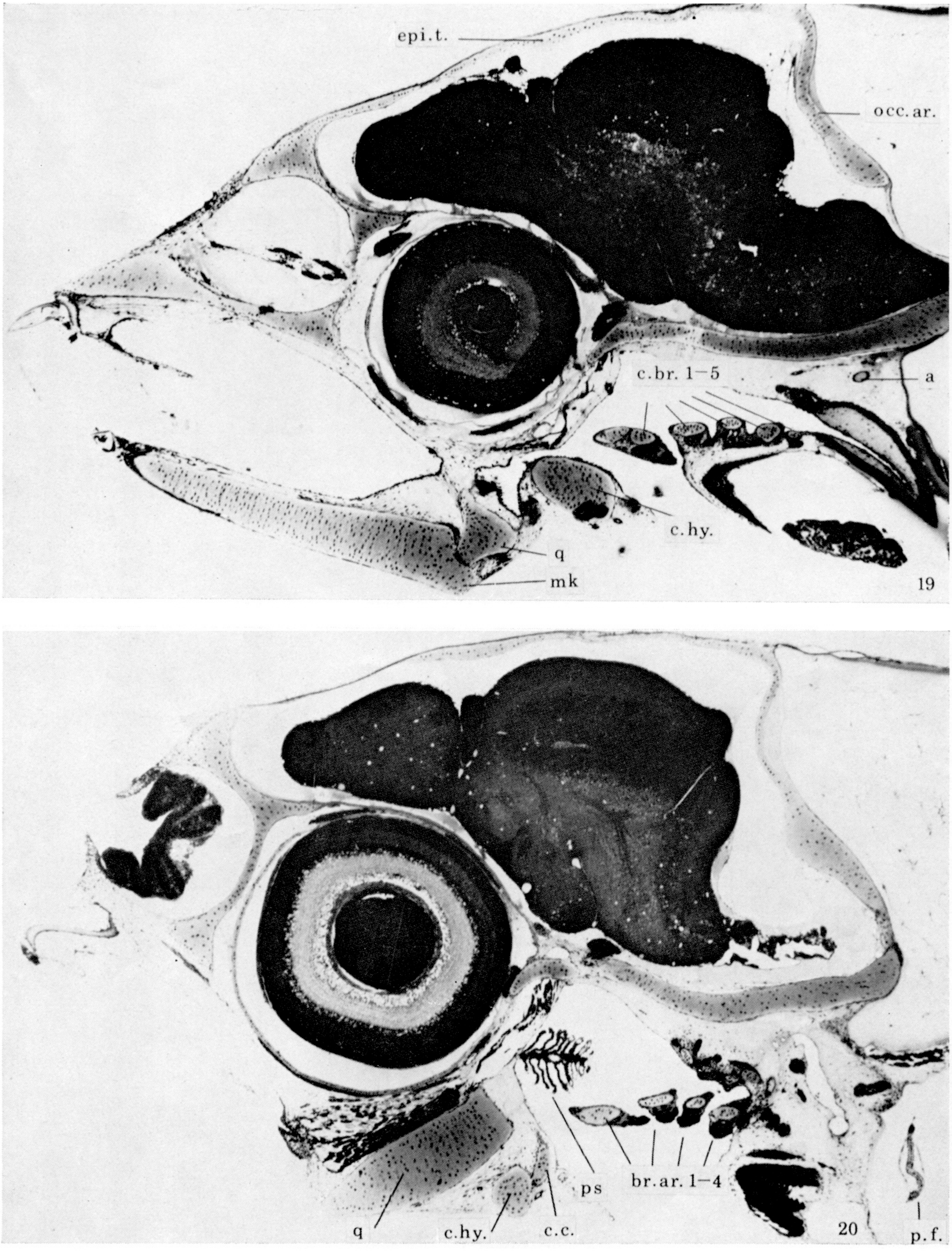

FIGURE 19. Sagittal section of head to the right of figure 18. (Magn. ×58.)

FIGURE 20. Sagittal section of head to the right of figure 19. (Magn. ×63.)

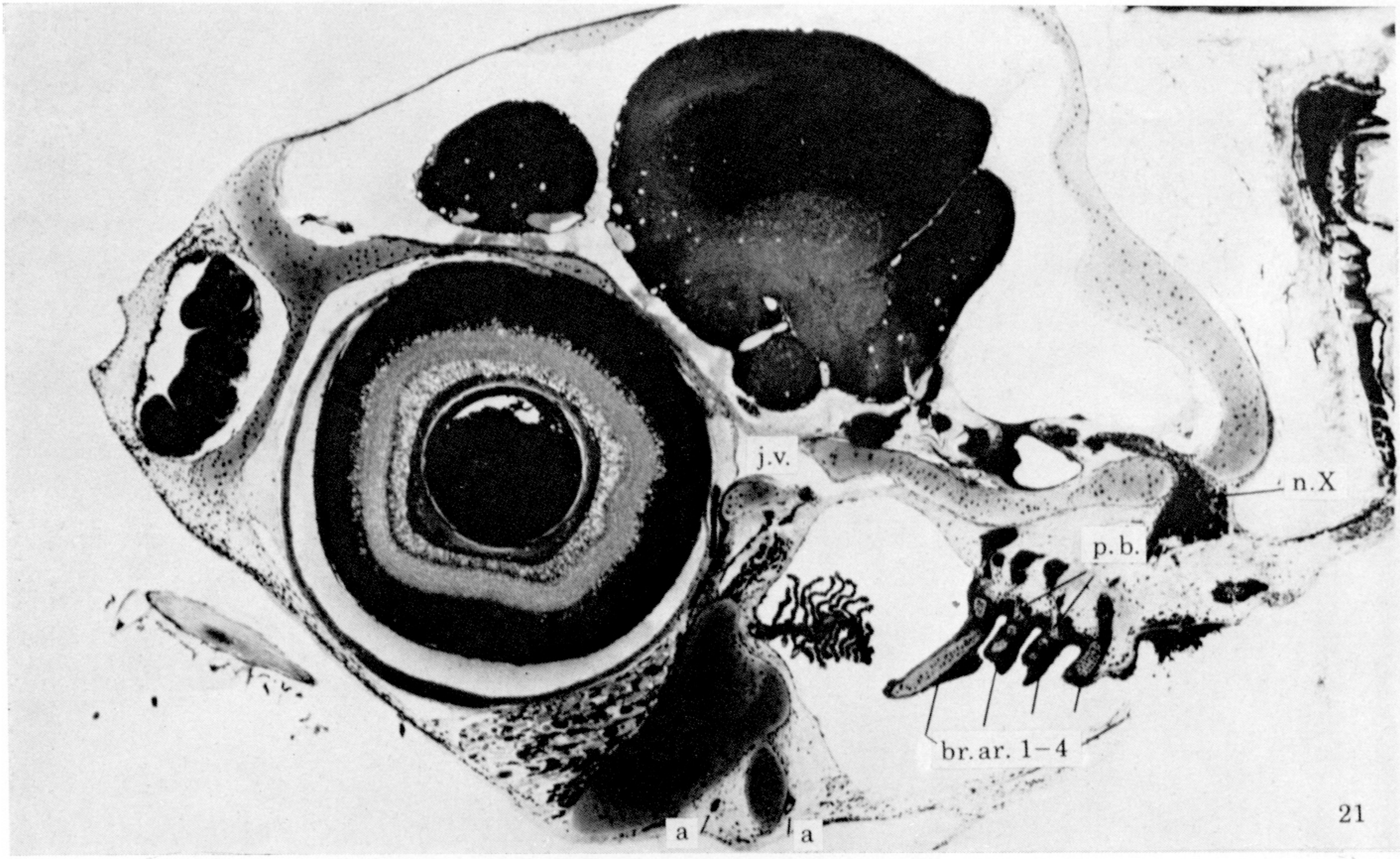

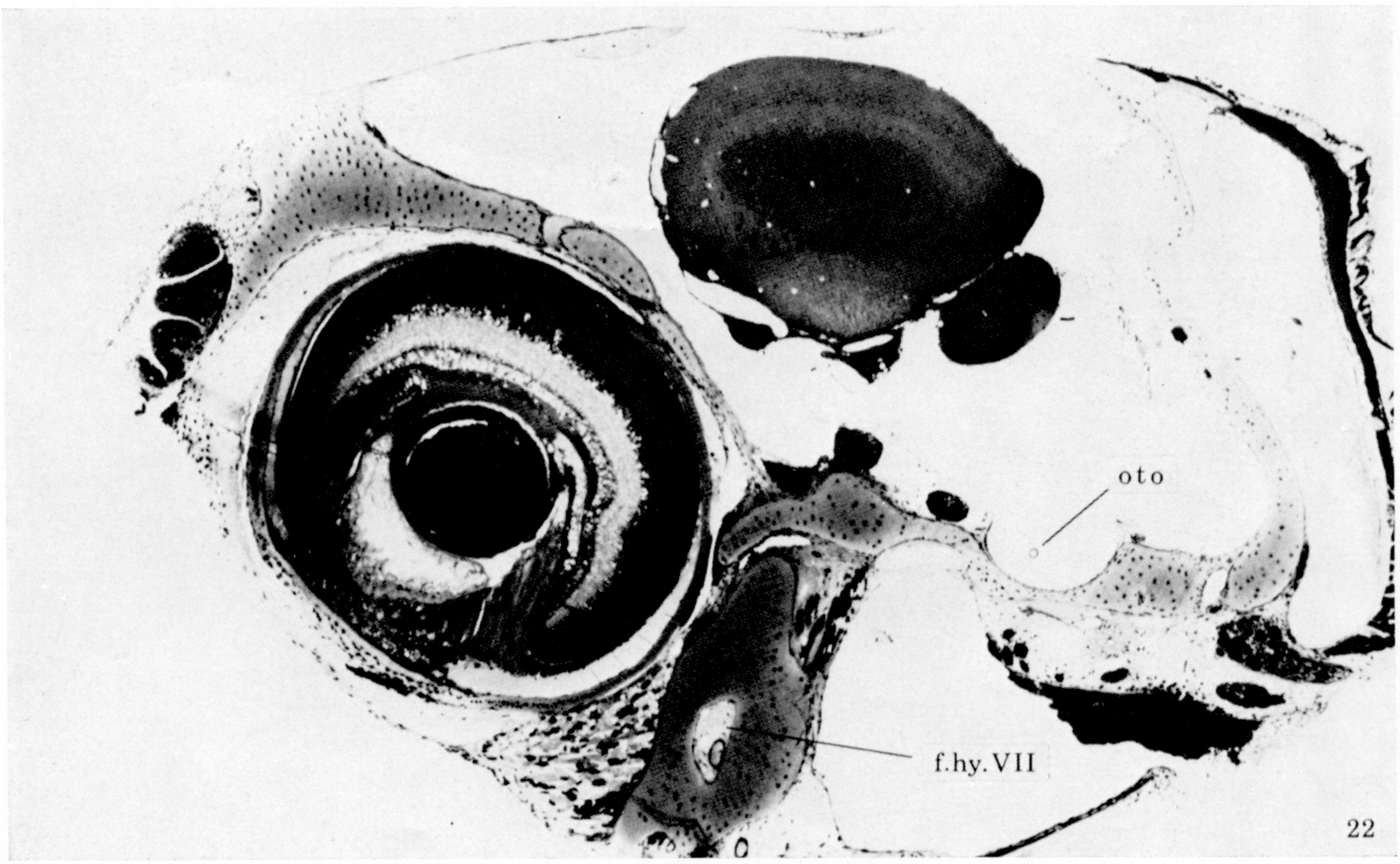

FIGURE 21. Sagittal section of head lateral to figure 20. (Magn. × 63.)

FIGURE 22. Sagittal section of head lateral to figure 21. The mass of tissue in the roof of the pharynx is the thymus. Above is the ganglion of the vagus nerve. (Magn. × 74.)

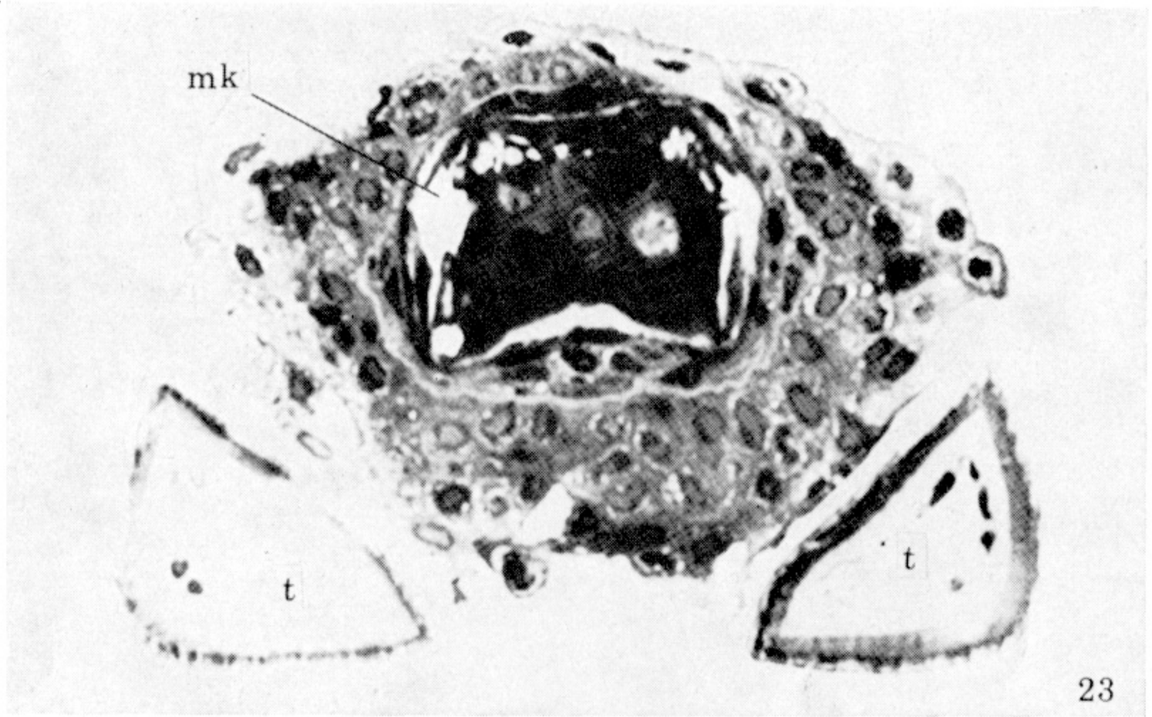

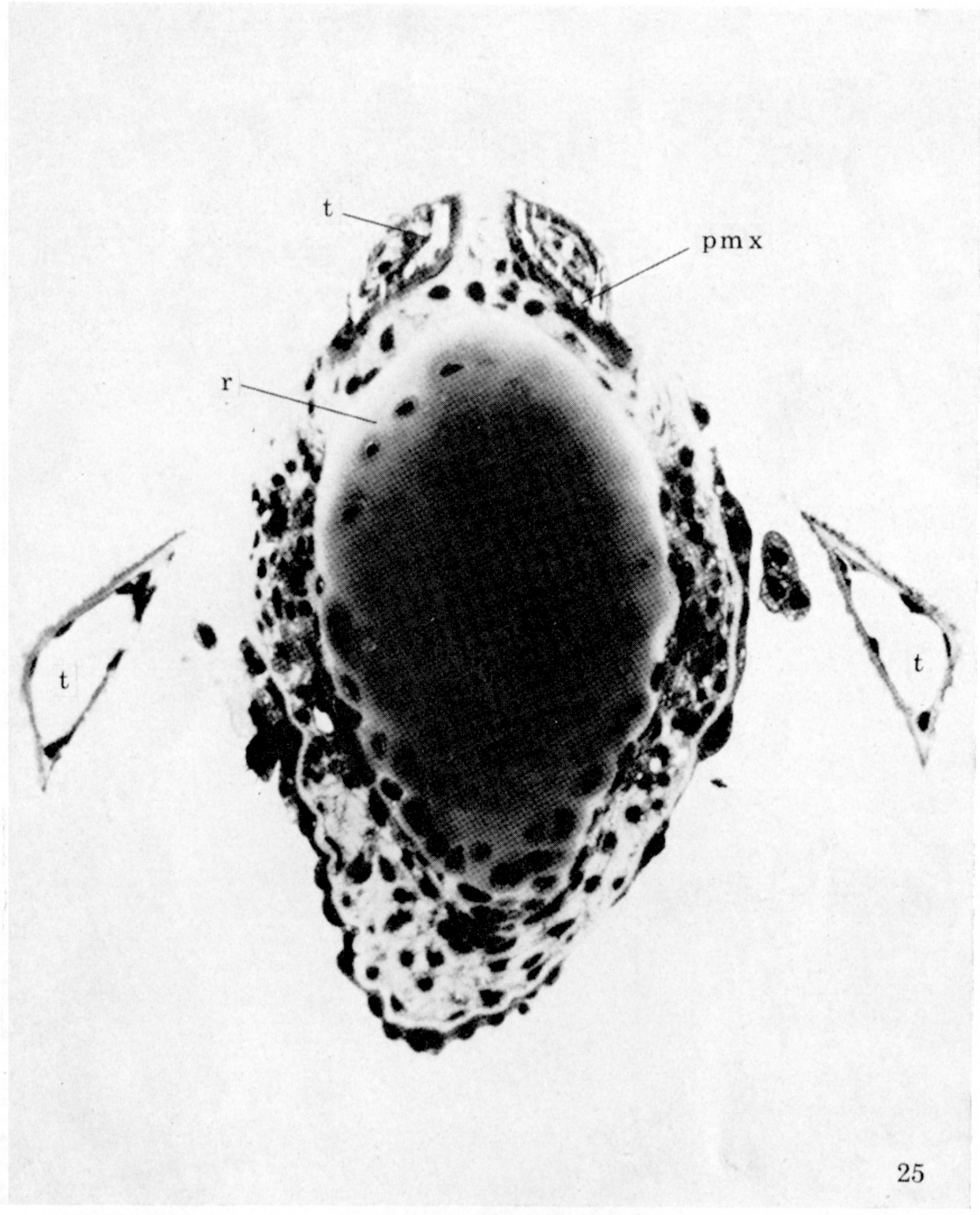

FIGURE 23. Tip of lower jaw showing the fusion of Meckel's cartilage. (Magn. × 640.) Figures 23–60 show the head of the leptocephalus in serial transverse sections (specimen EM507, 104 mm s.l.).

FIGURE 24. Fused Meckel's cartilage with dentaries on the lateral margins. (Magn. × 640.)

FIGURE 25. Tip of upper jaw with each premaxilla bearing a single, small tooth. (Magn. × 525.)

FIGURES 26–29. For description see opposite.

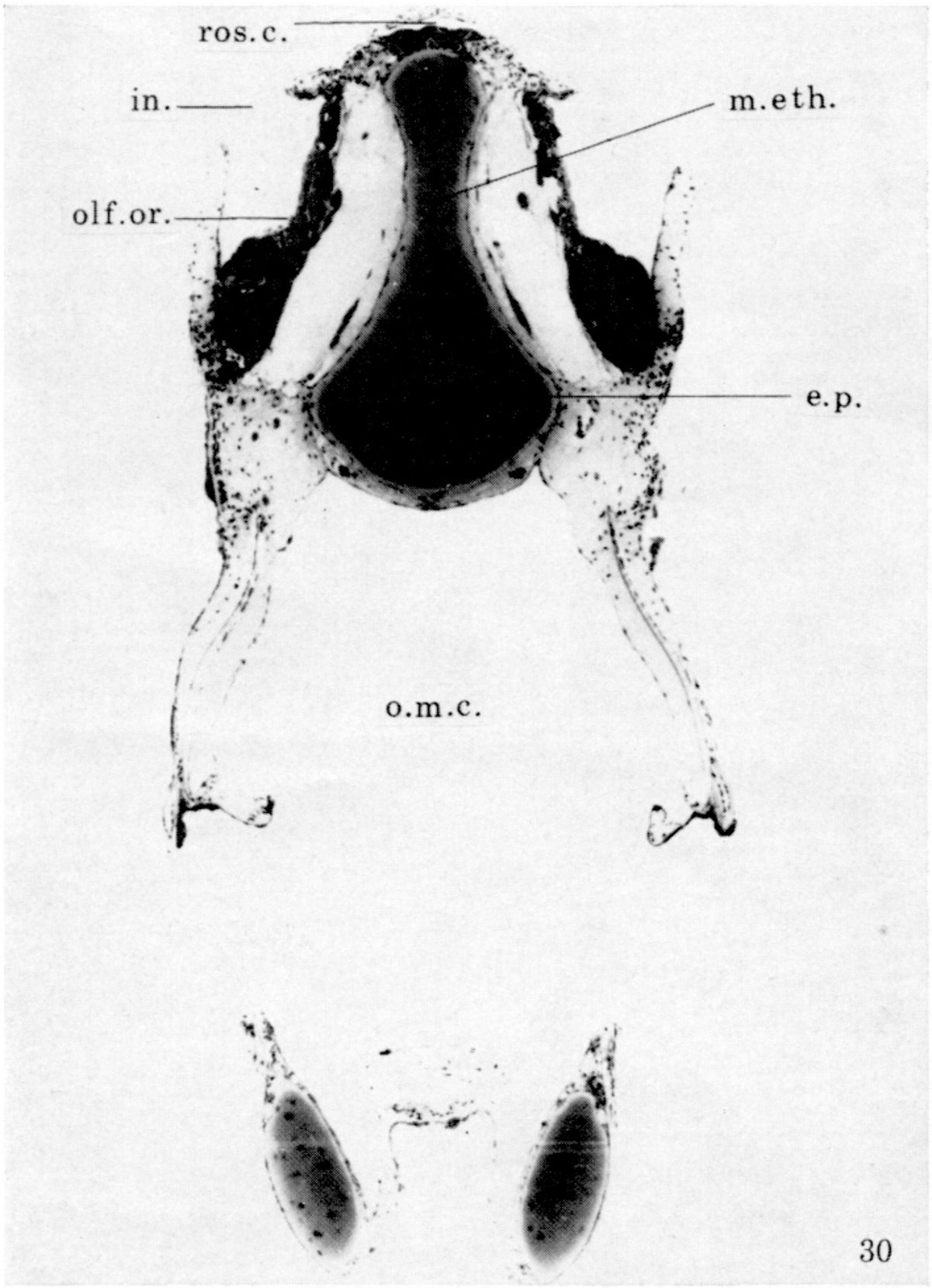

30

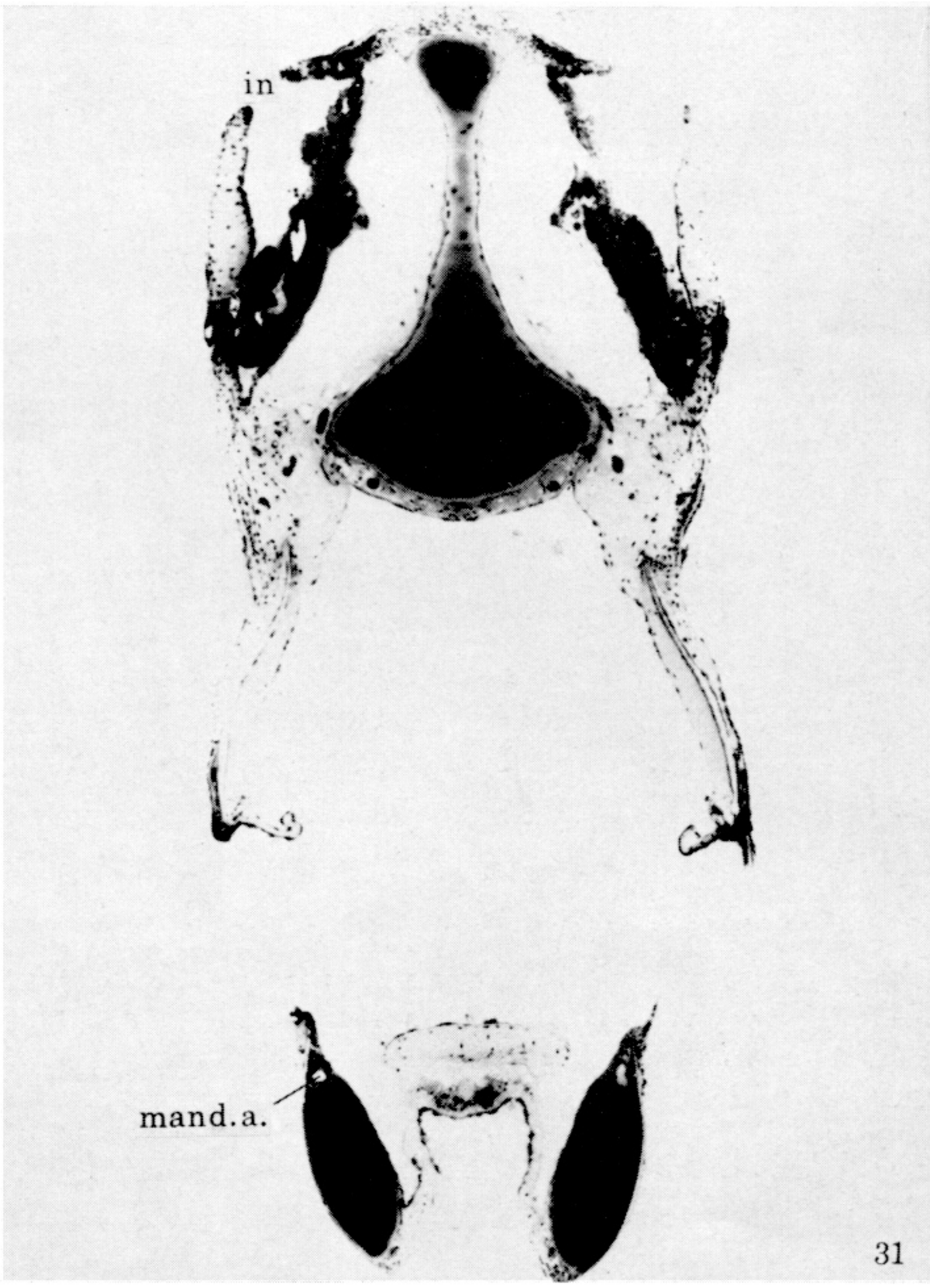

31

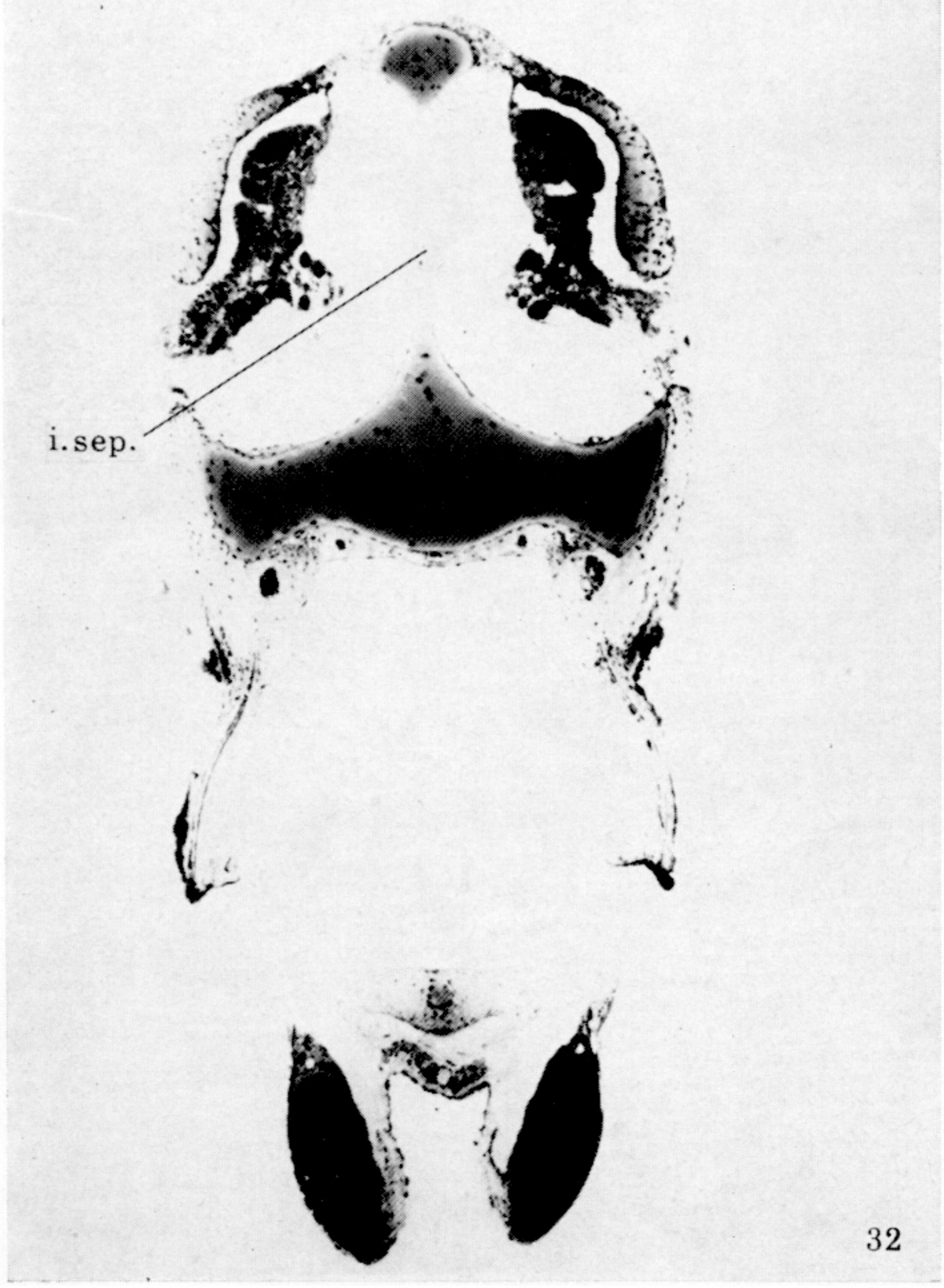

32

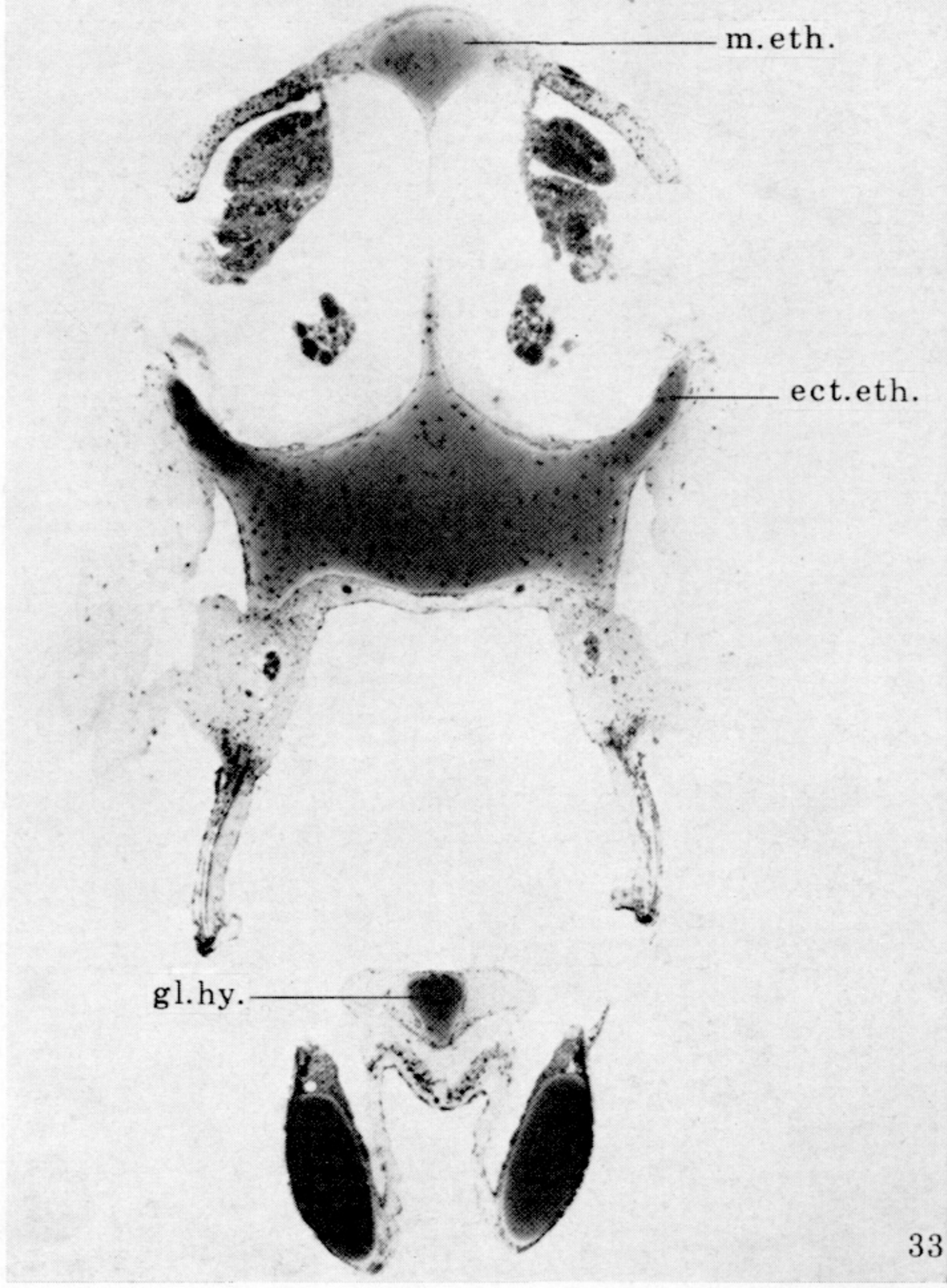

33

FIGURES 30–33. For description see opposite.

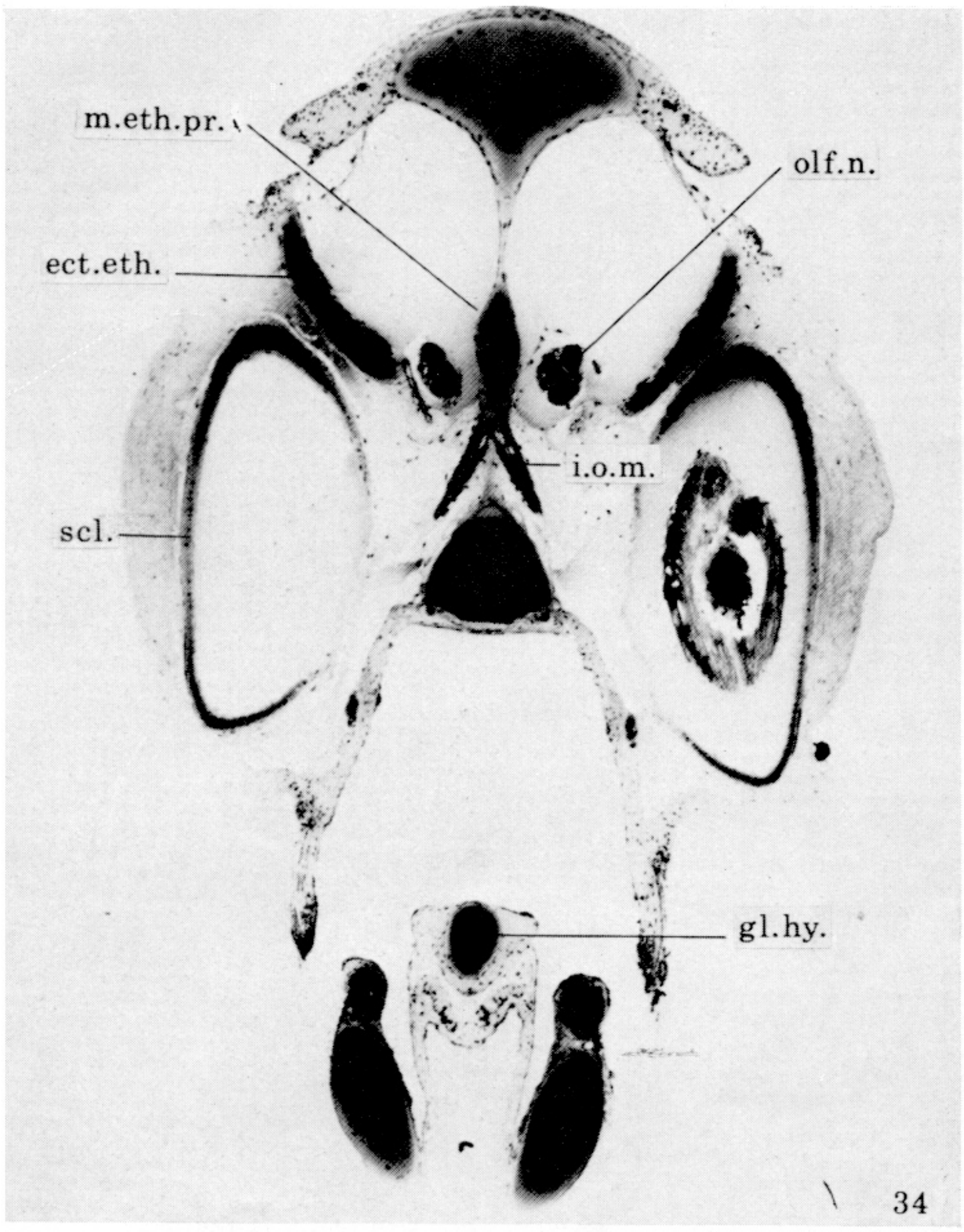

34

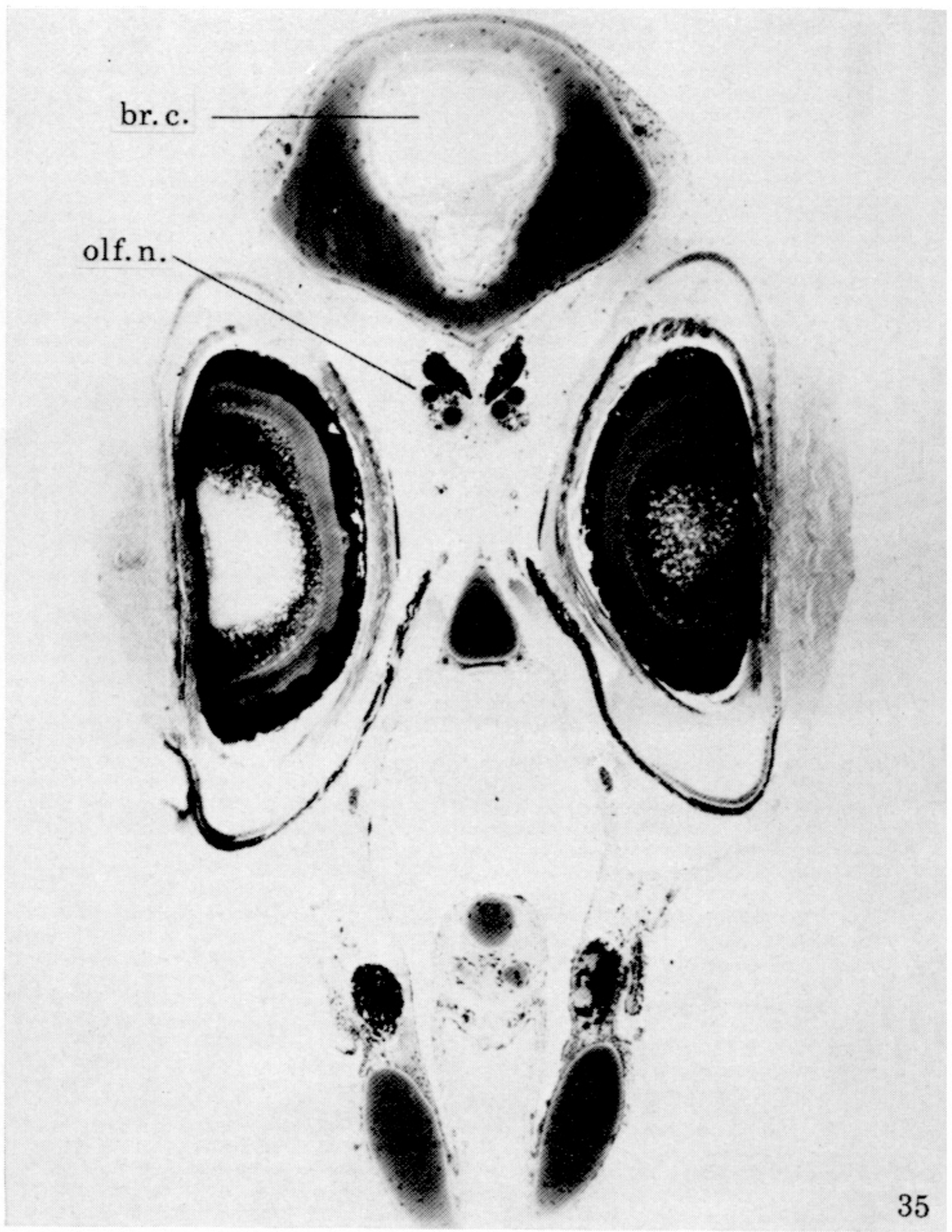

35

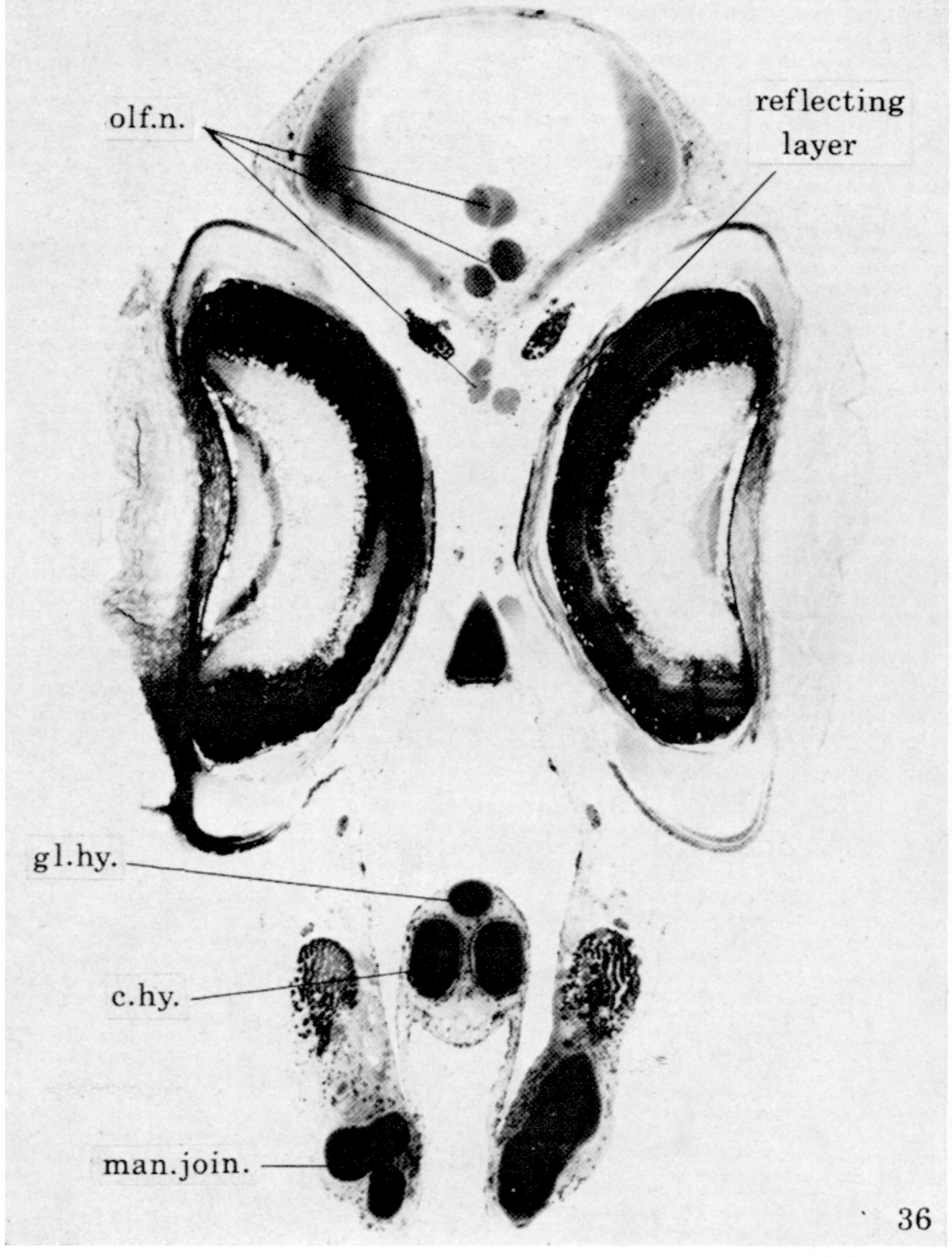

36

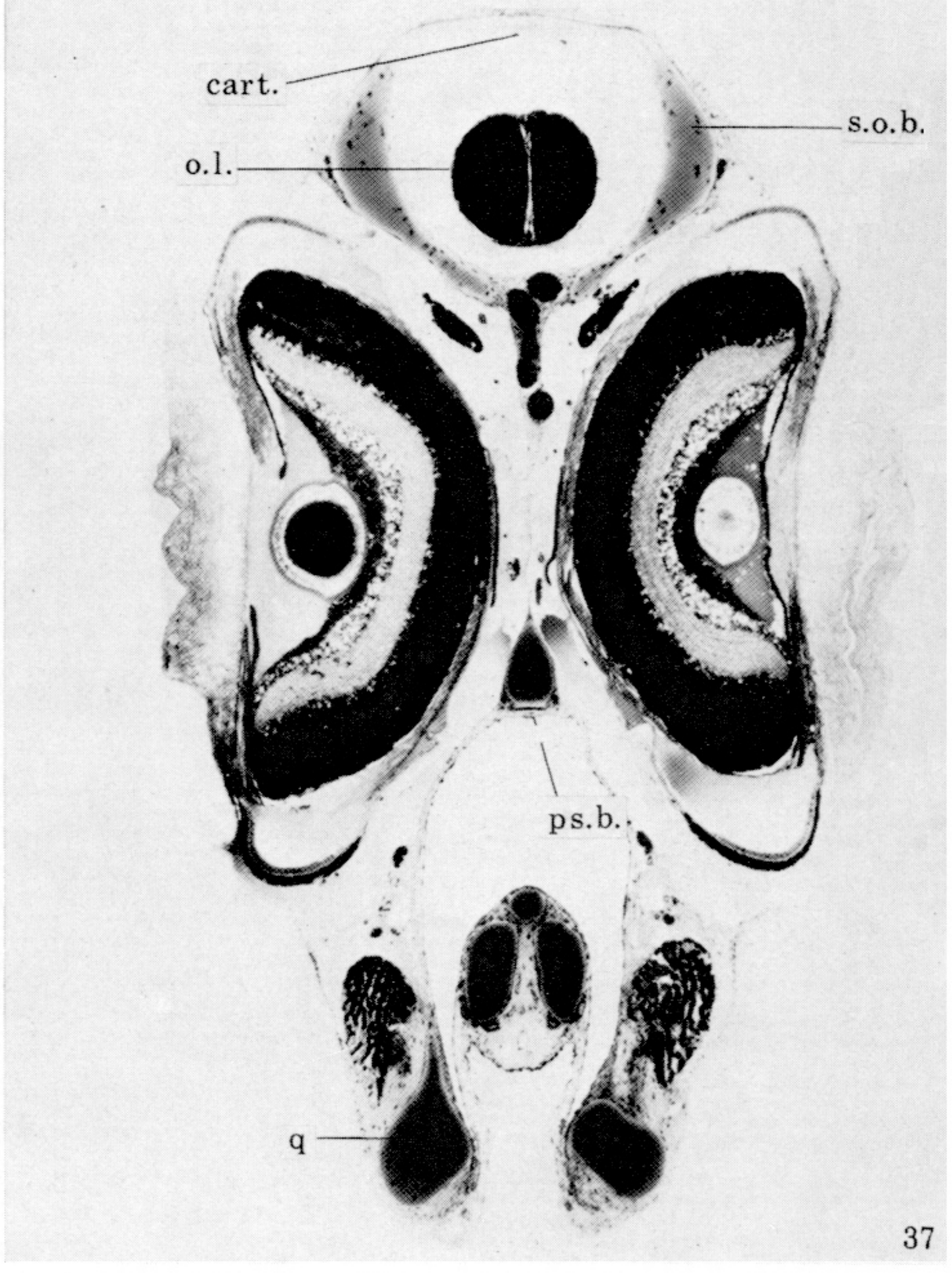

37

FIGURES 34–37. For description see p. 118.

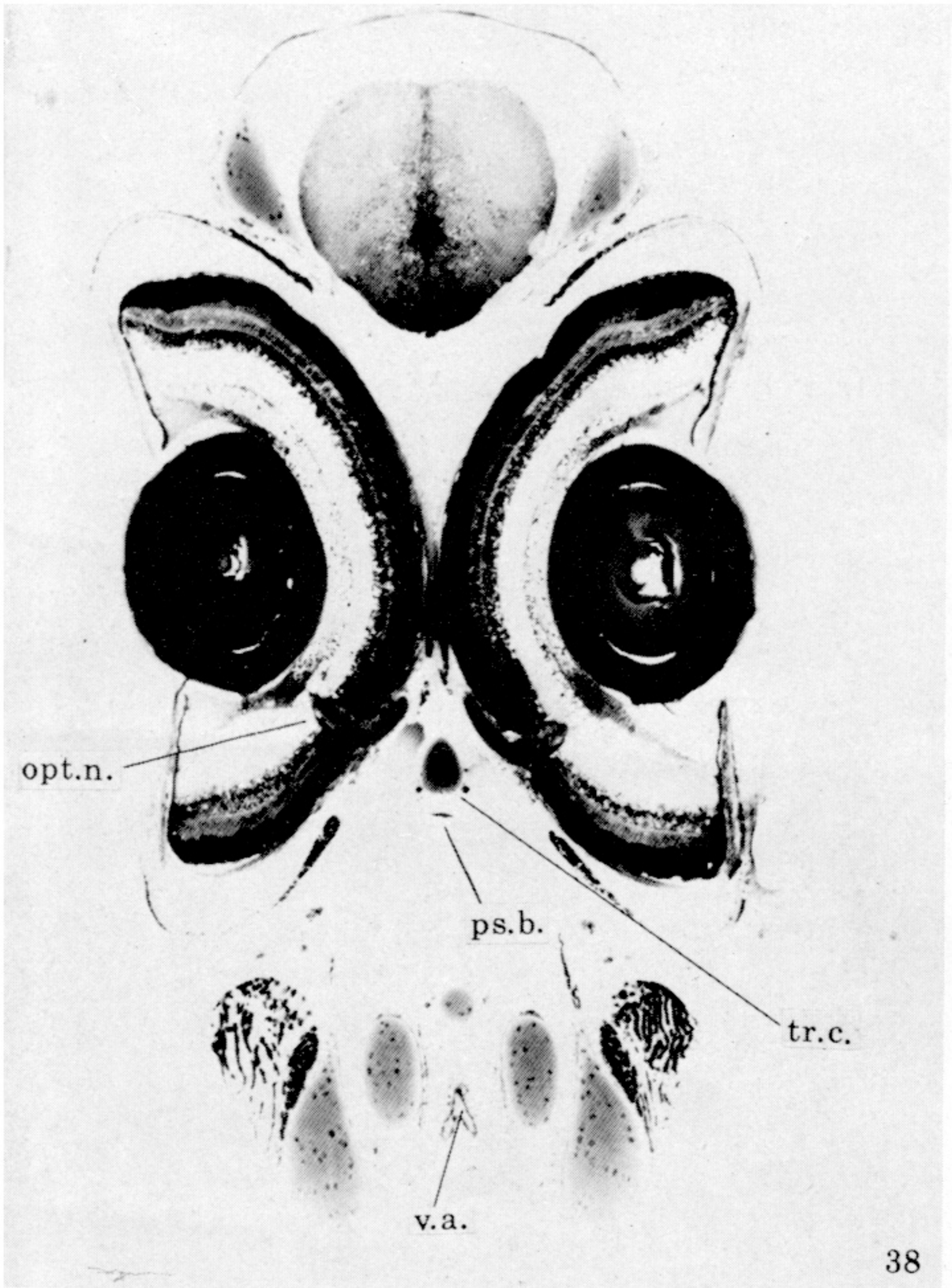

38

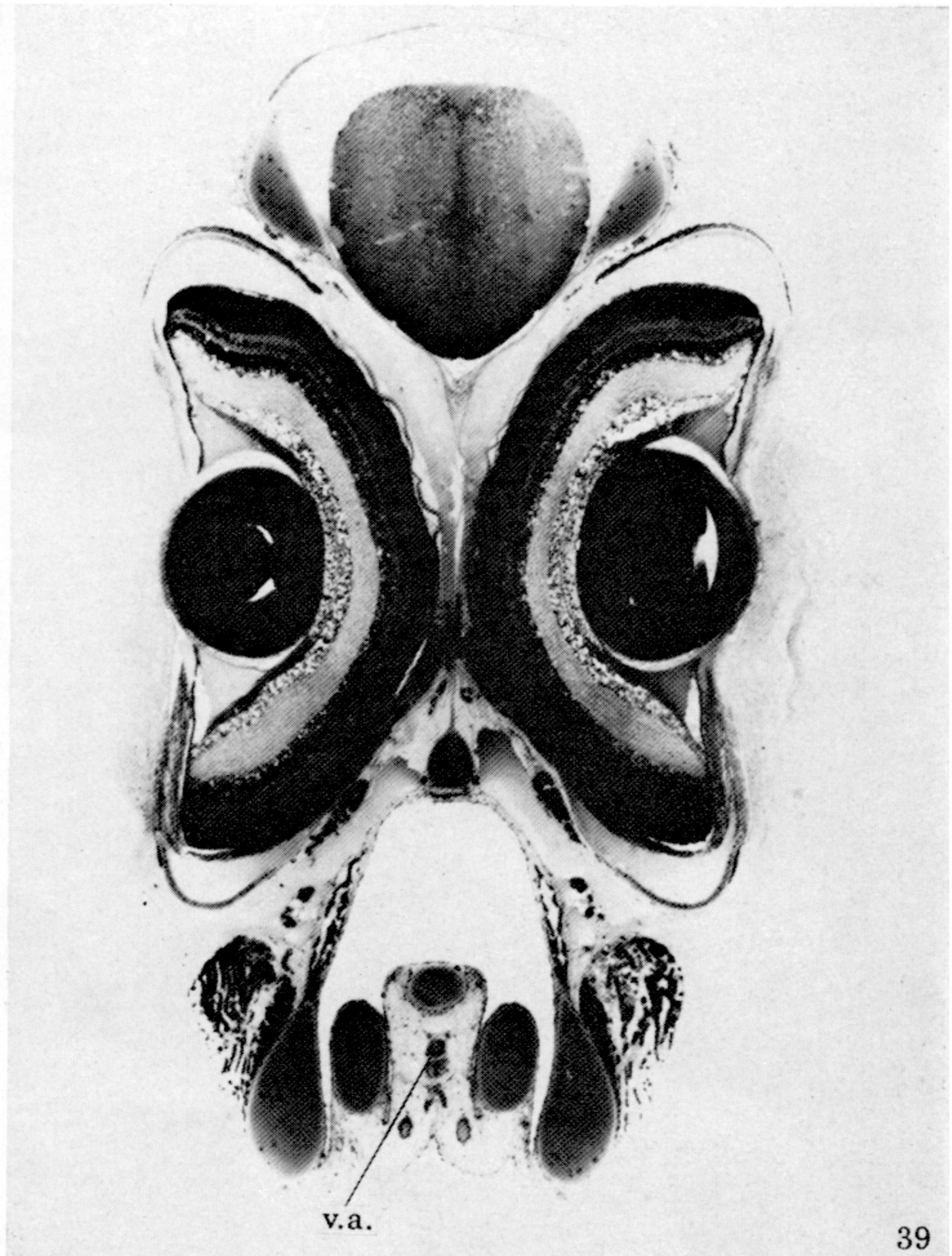

39

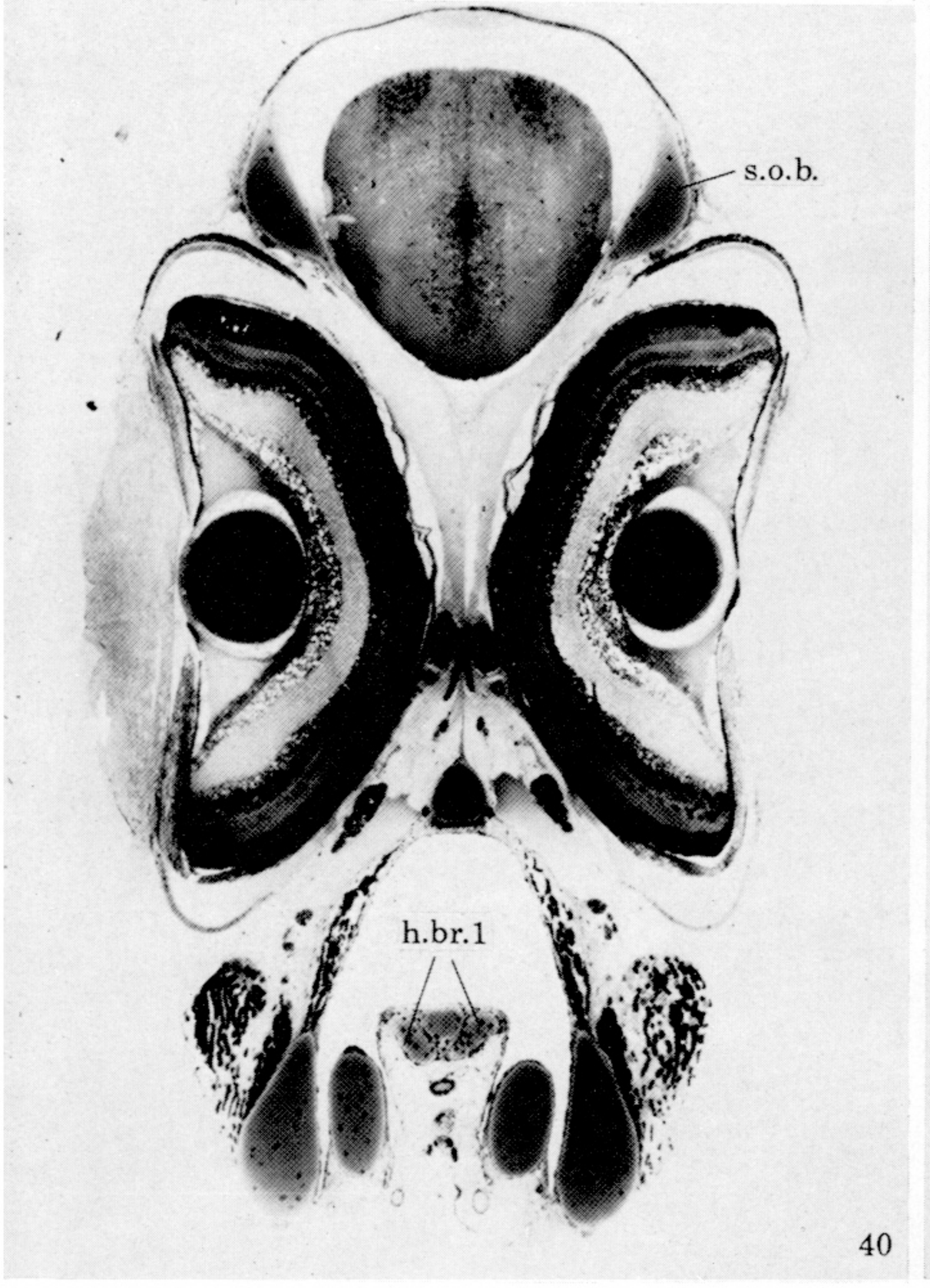

40

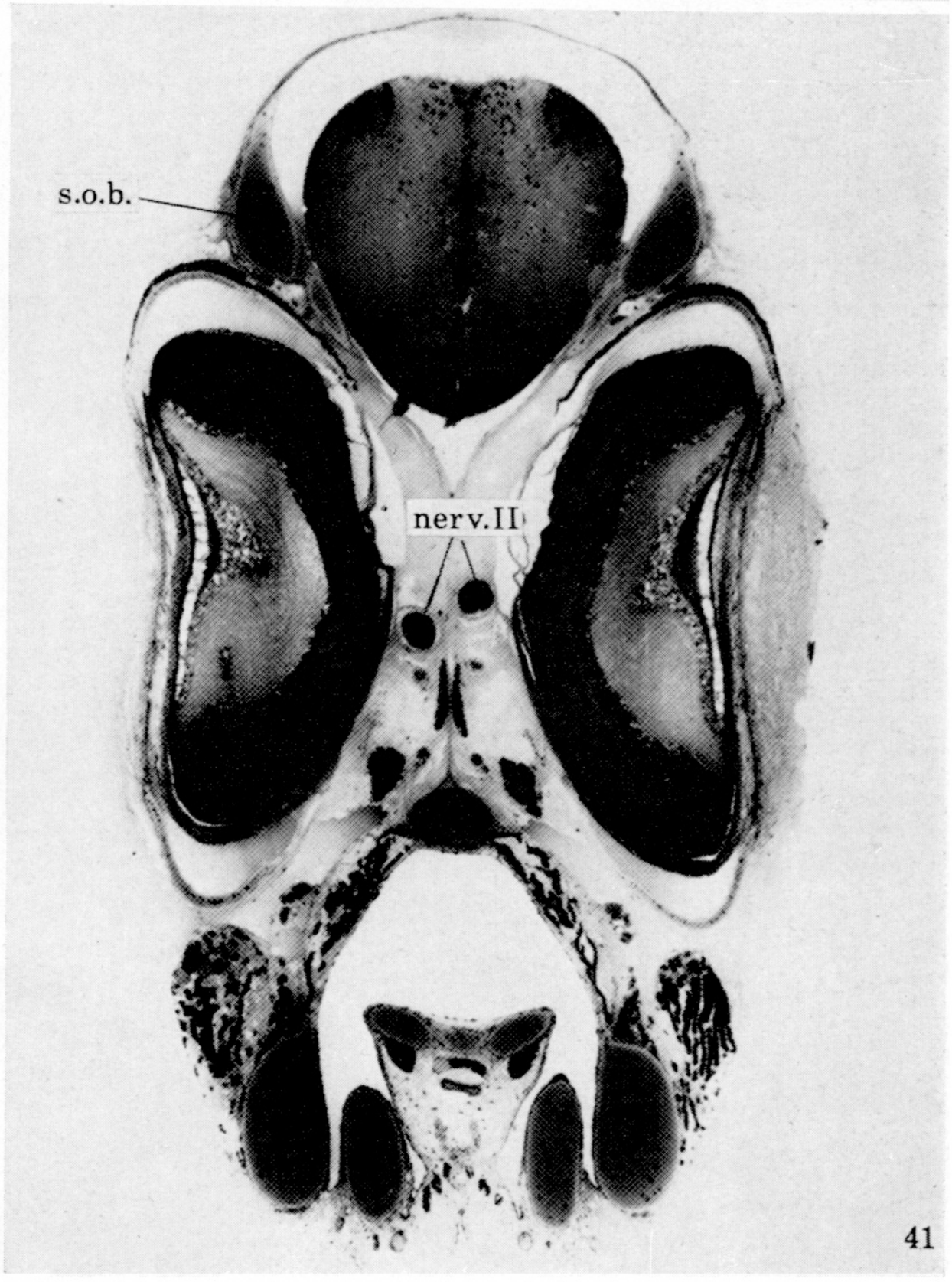

41

FIGURES 38–41. For description see p. 119.

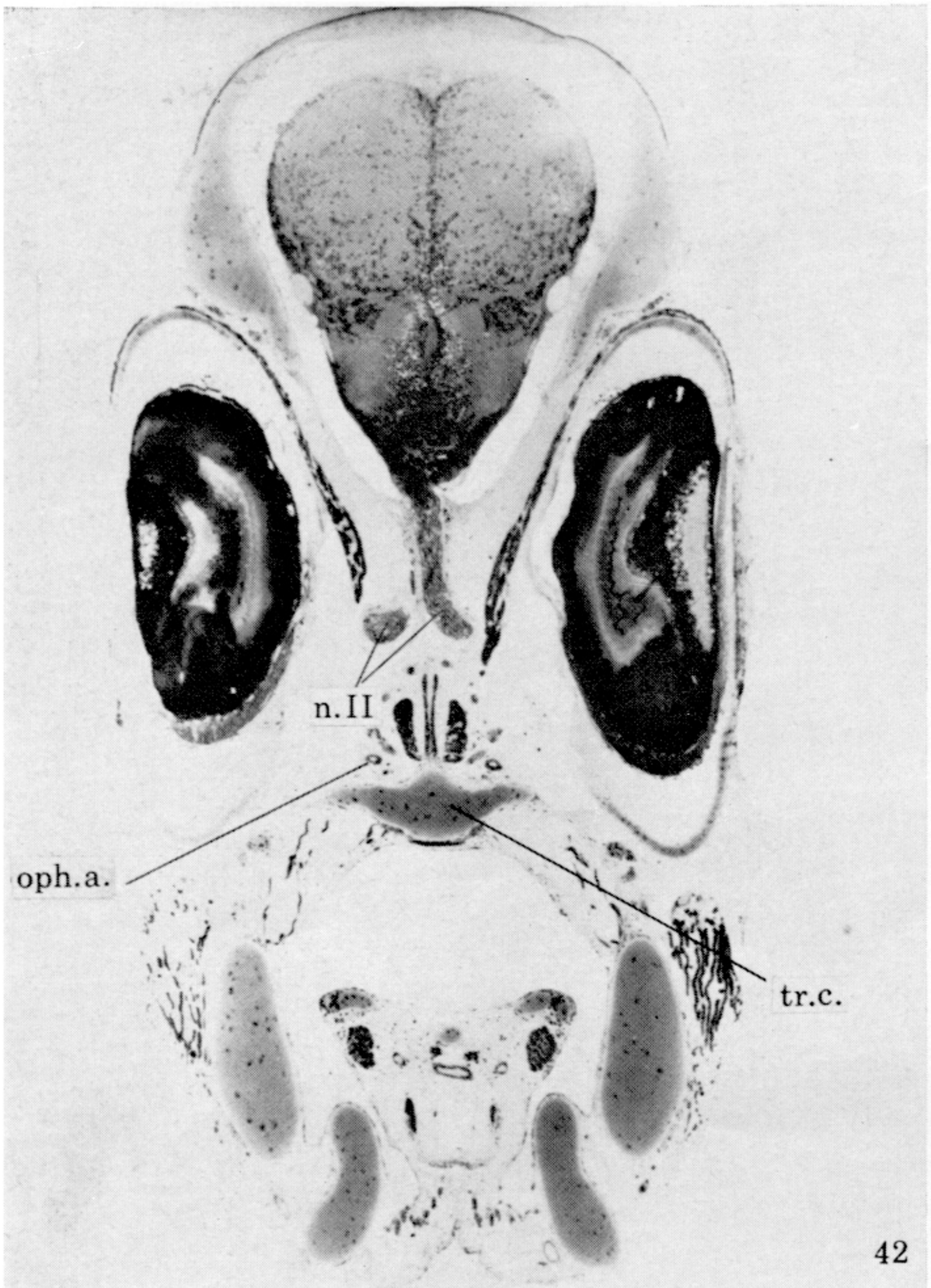

42

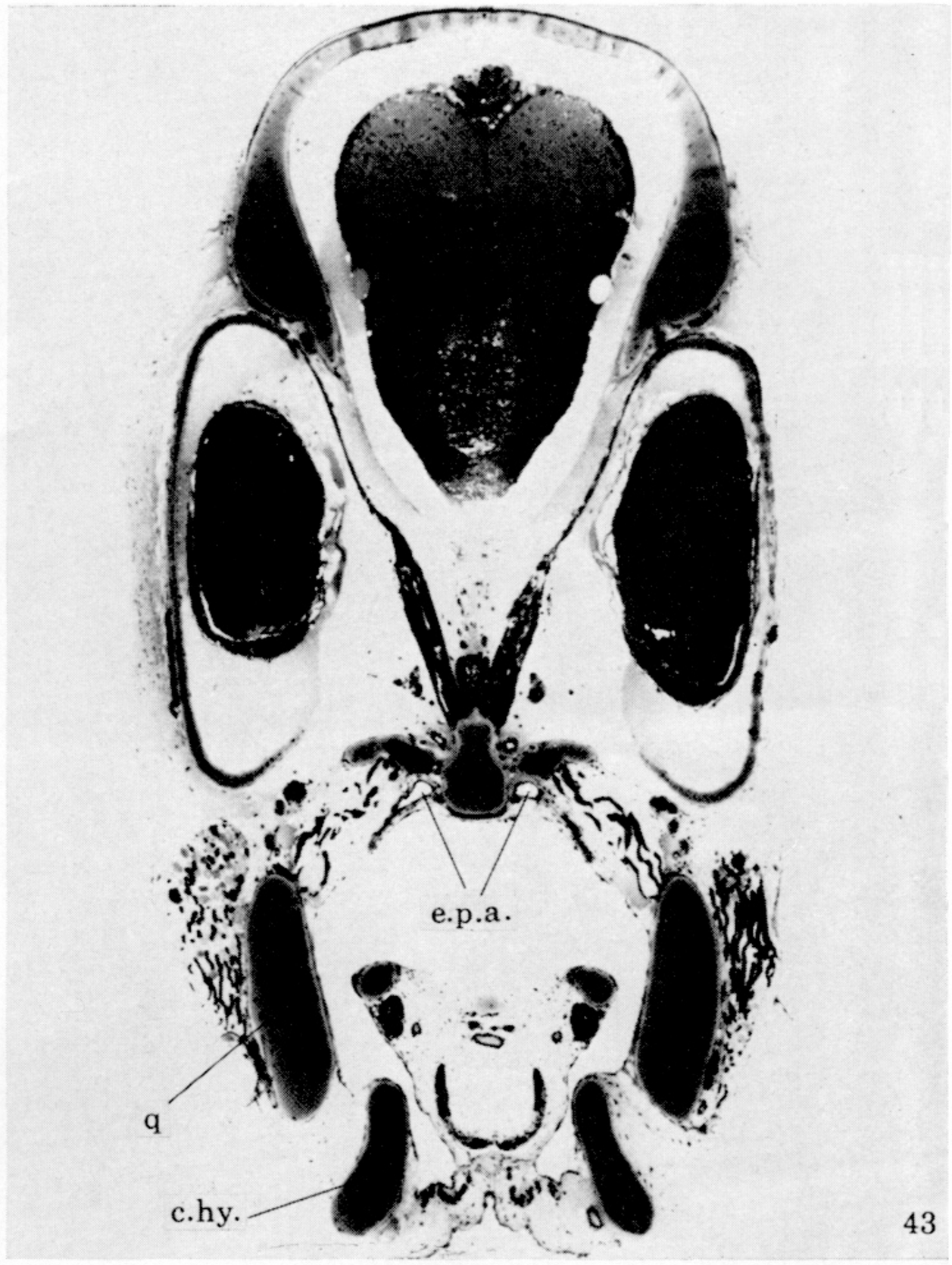

43

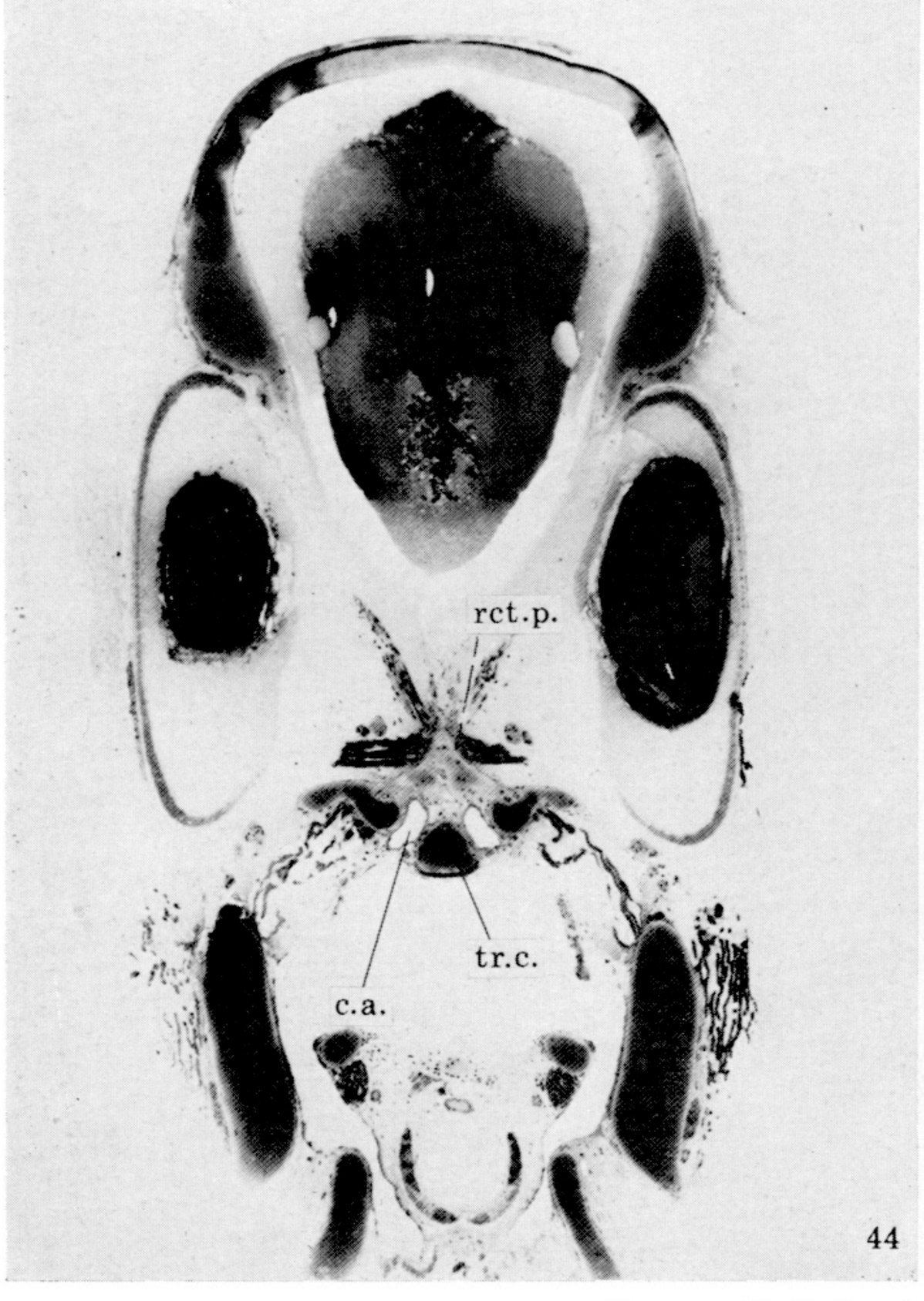

44

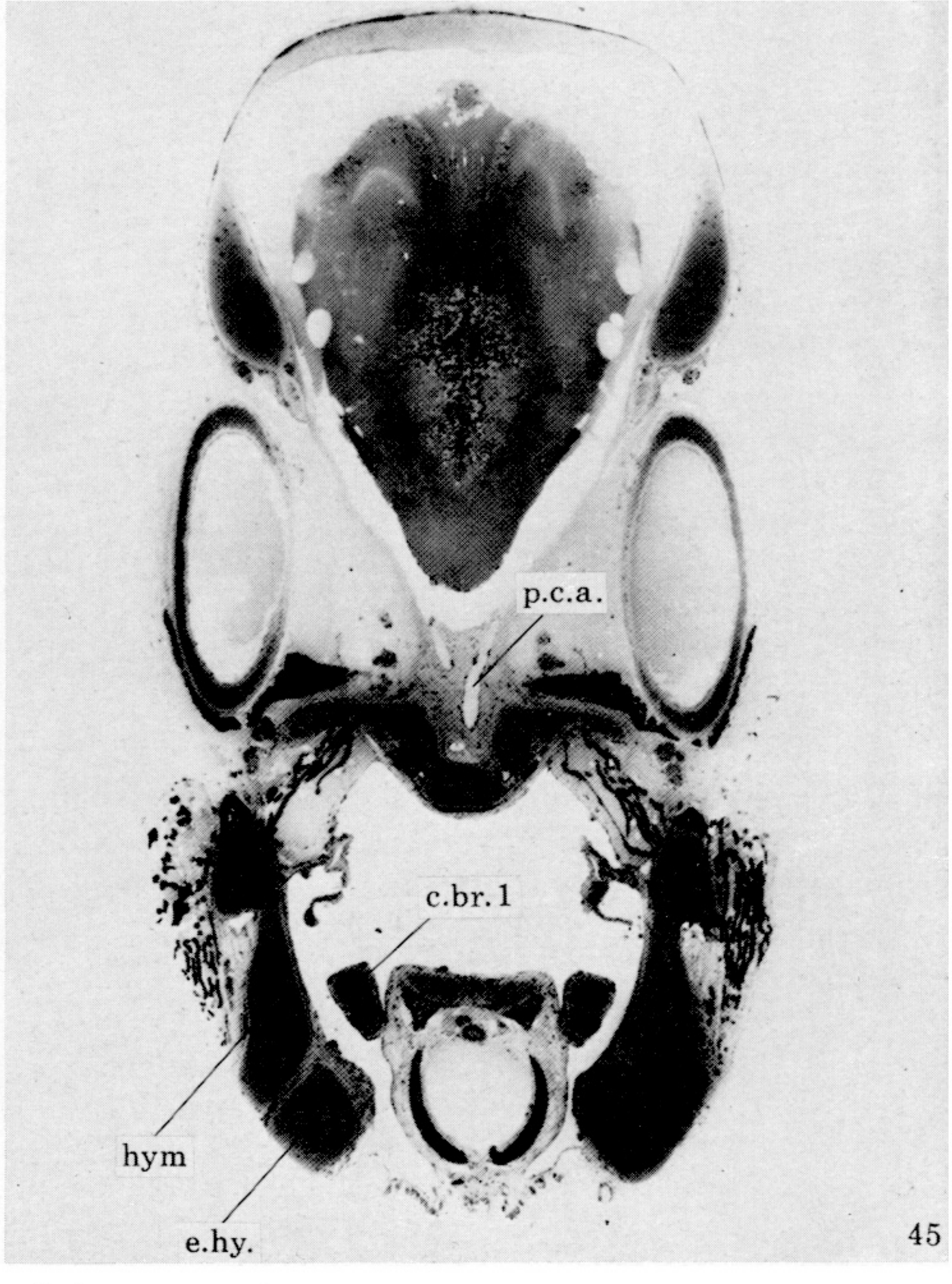

45

FIGURES 42–45. For description see opposite.

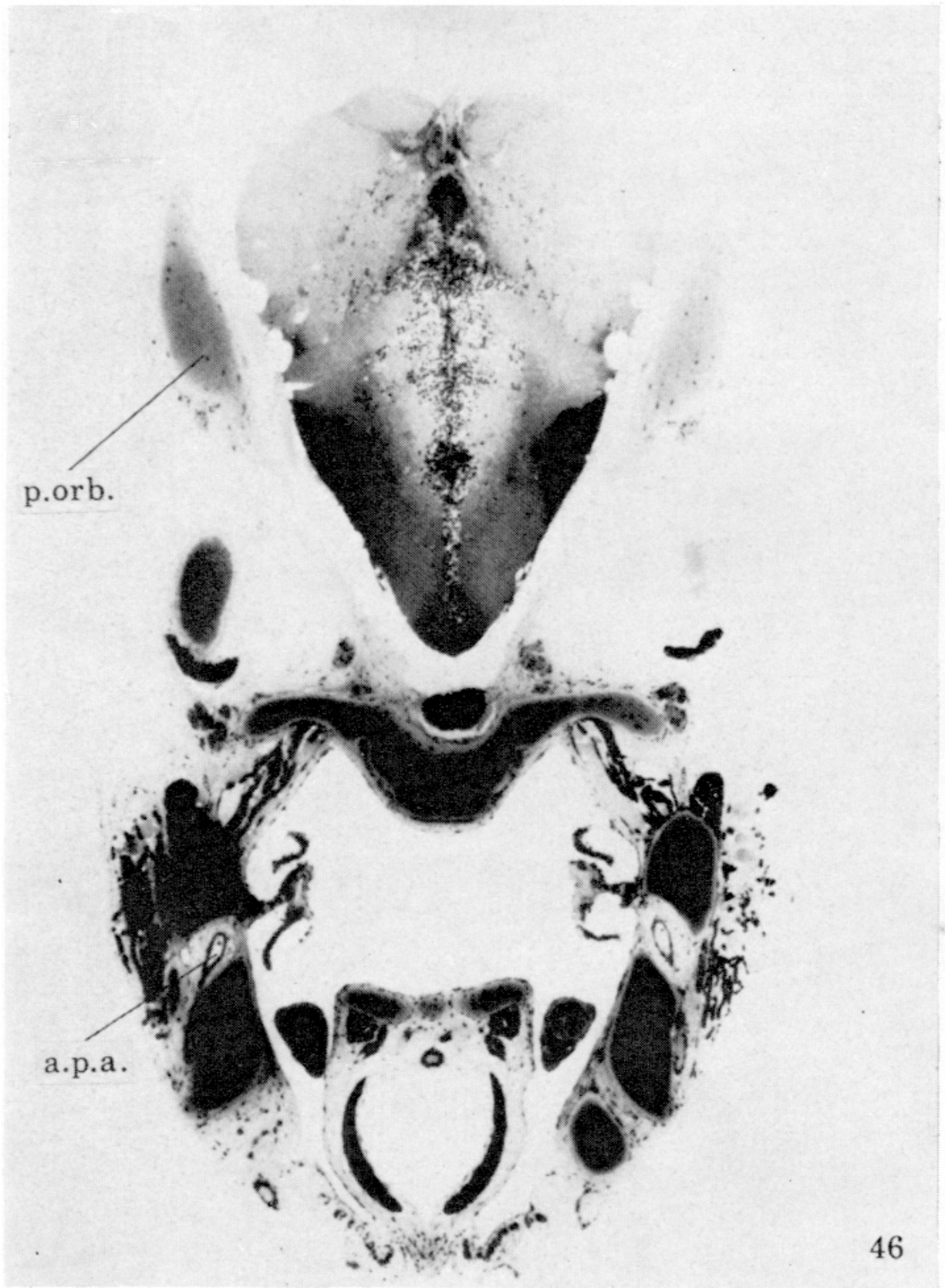

46

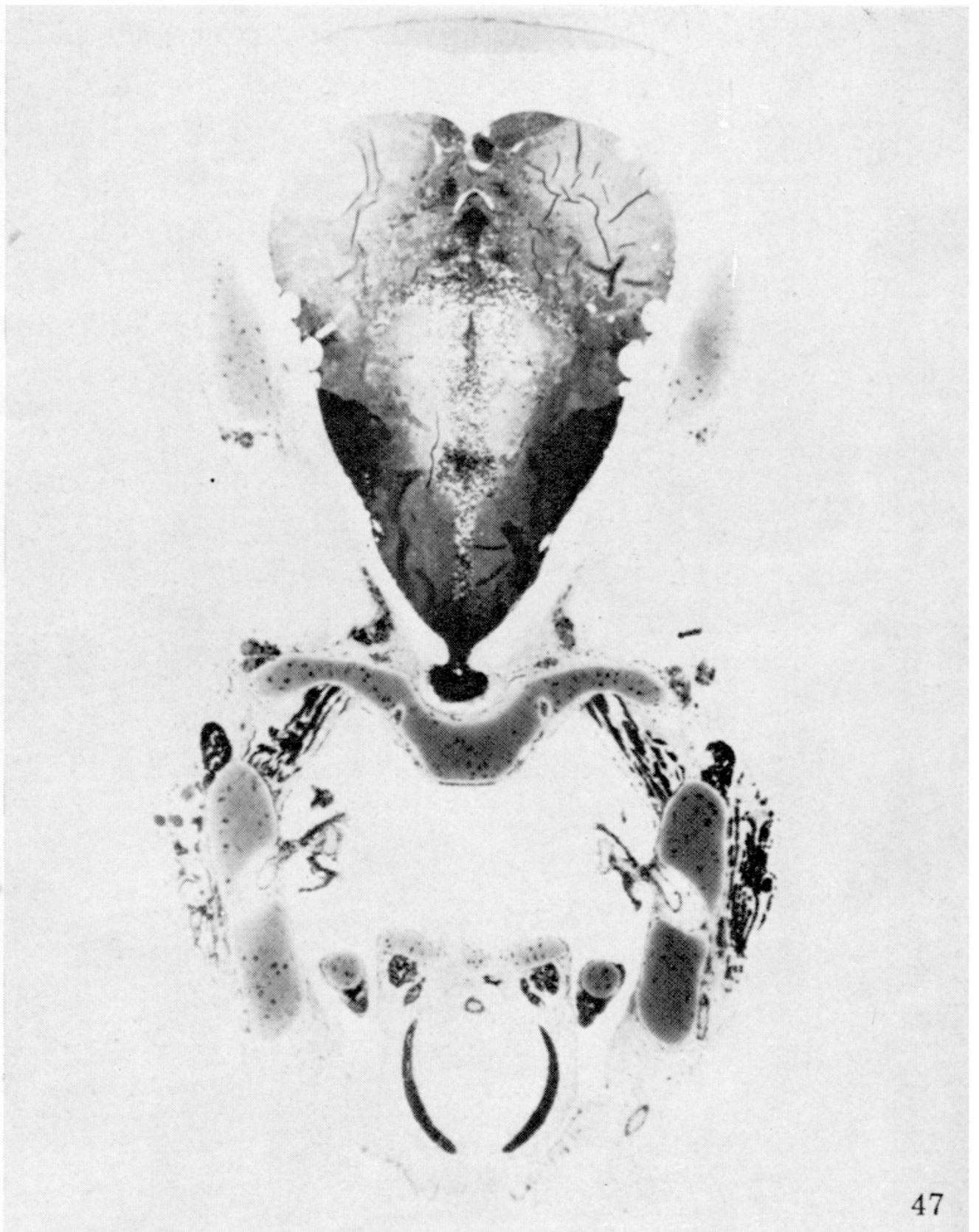

47

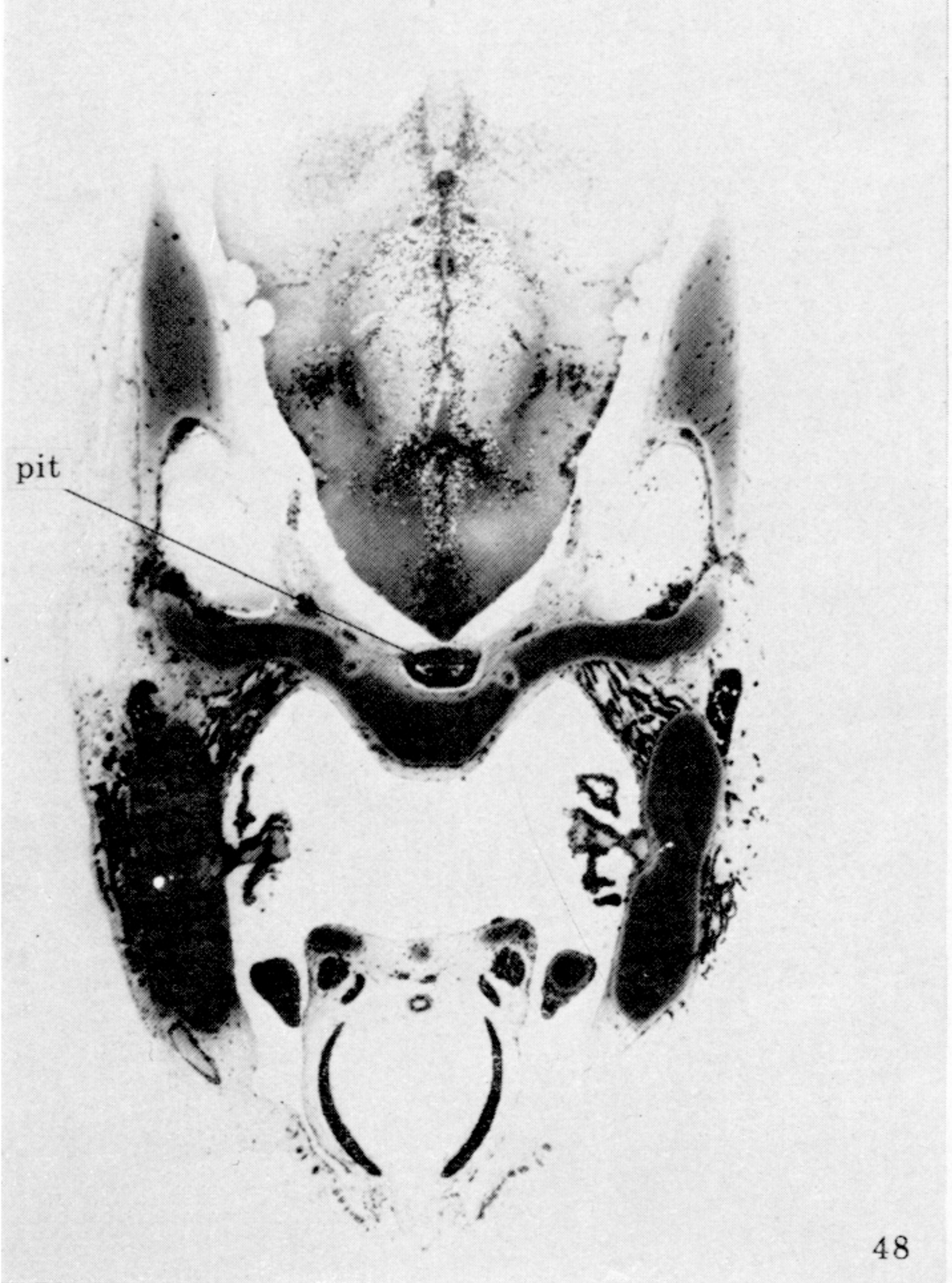

48

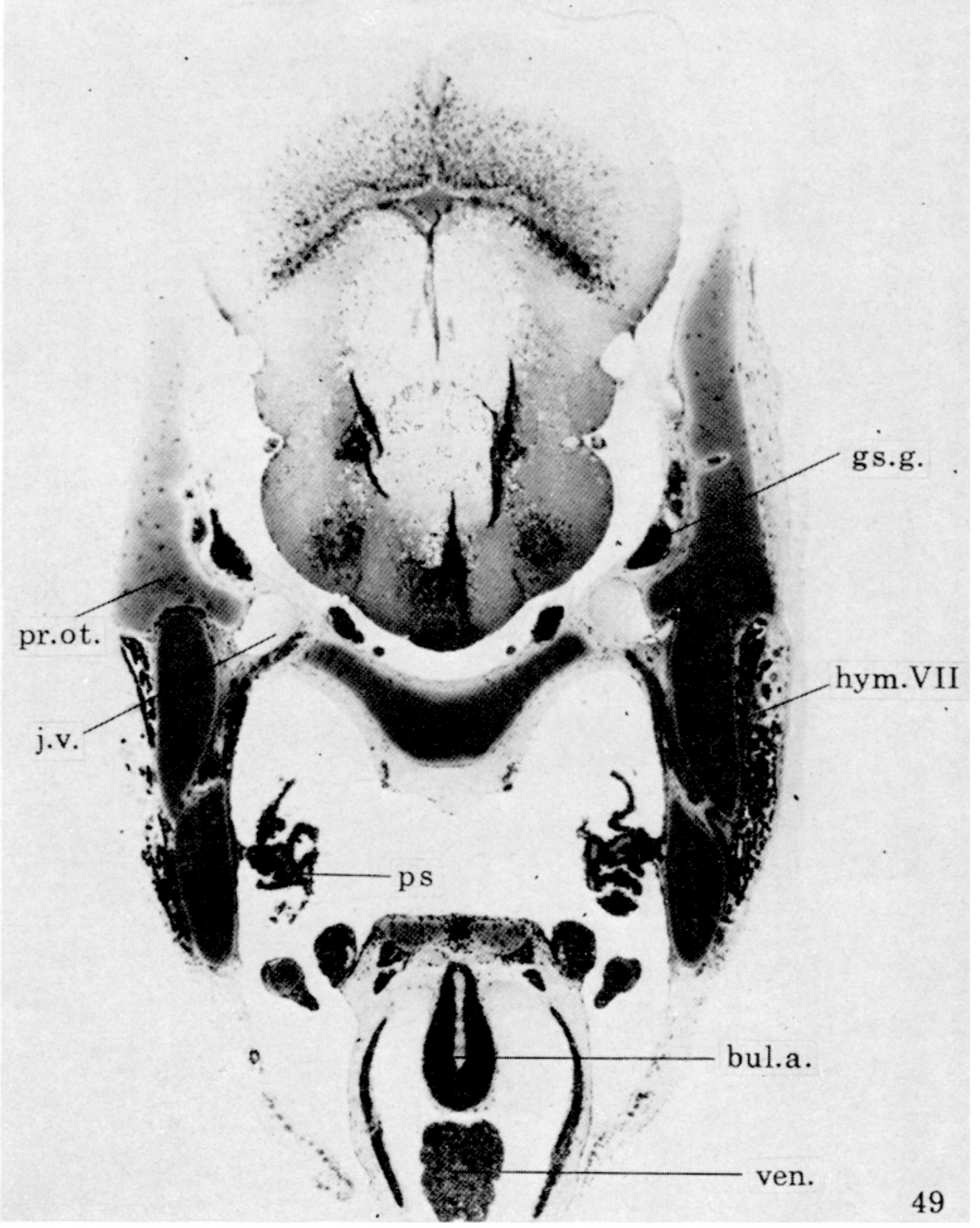

49

FIGURES 46–49. For description see opposite.

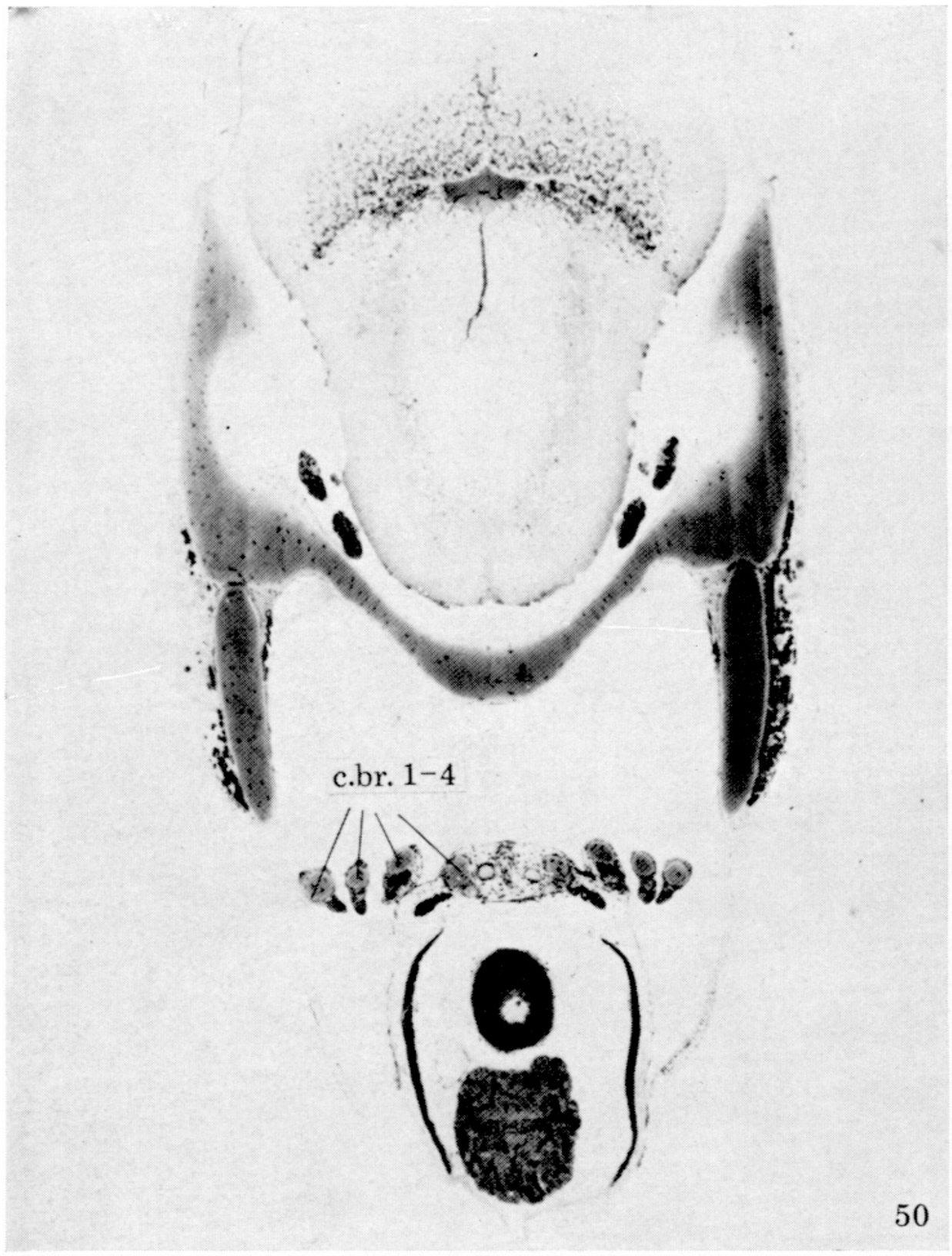

50

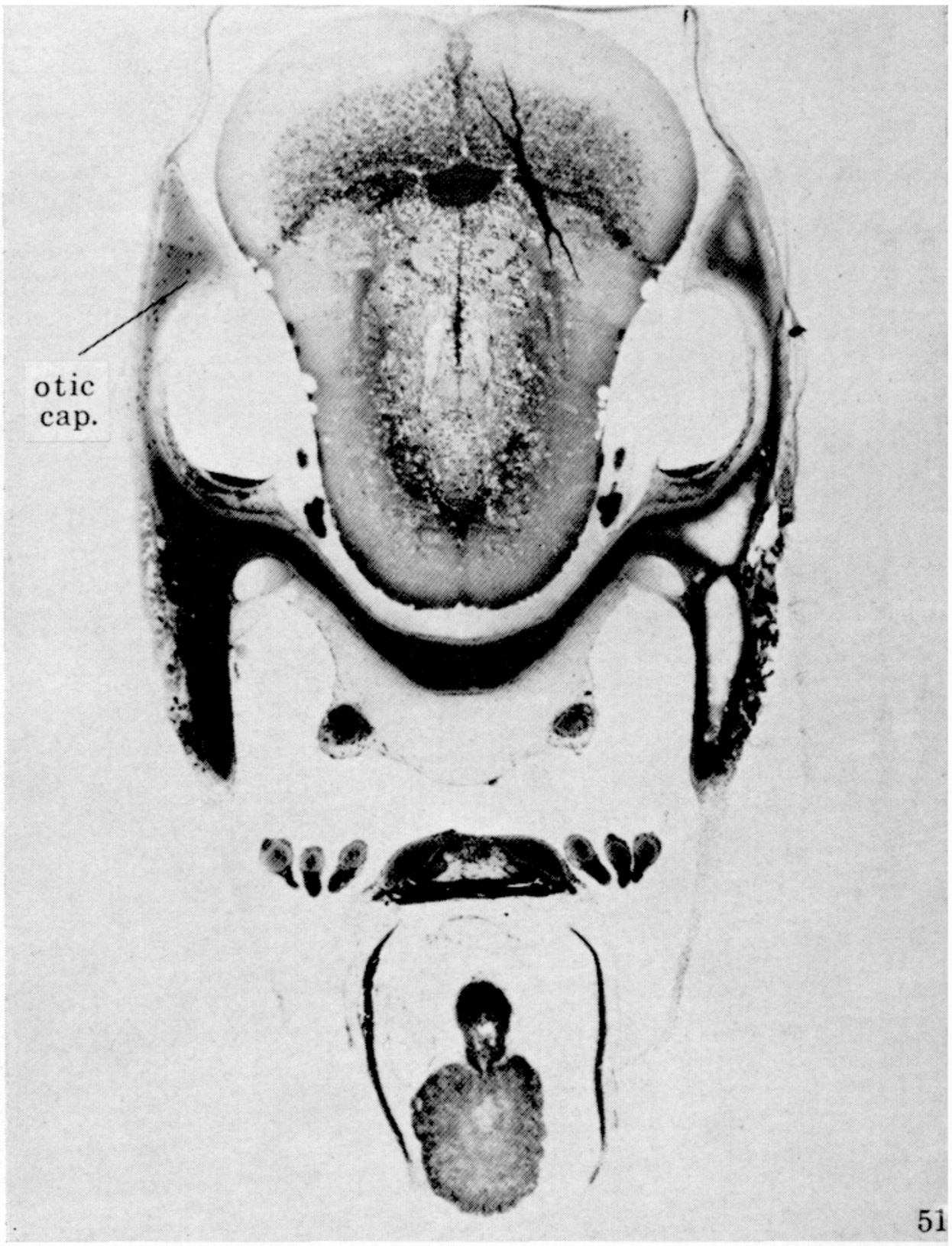

51

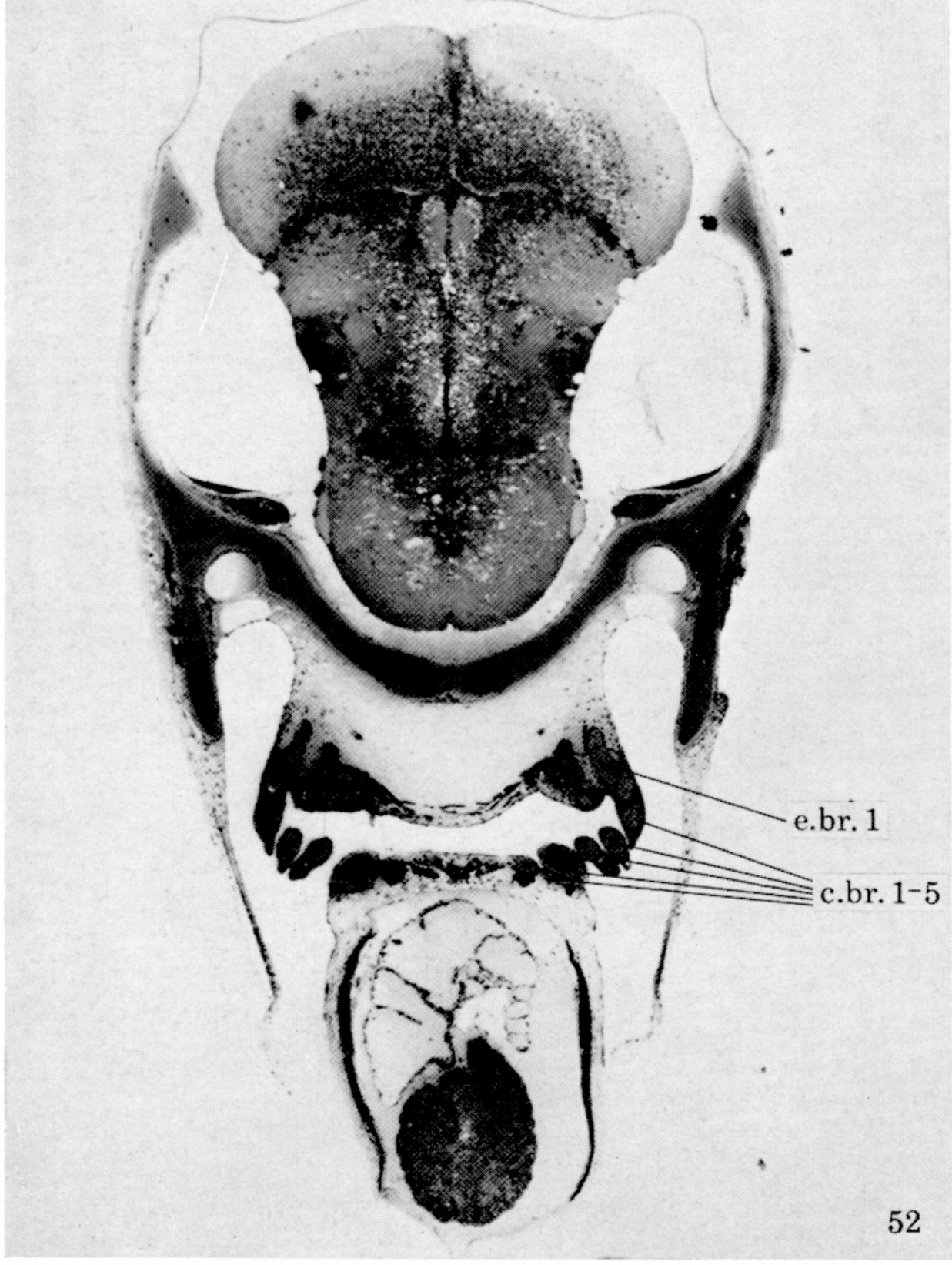

52

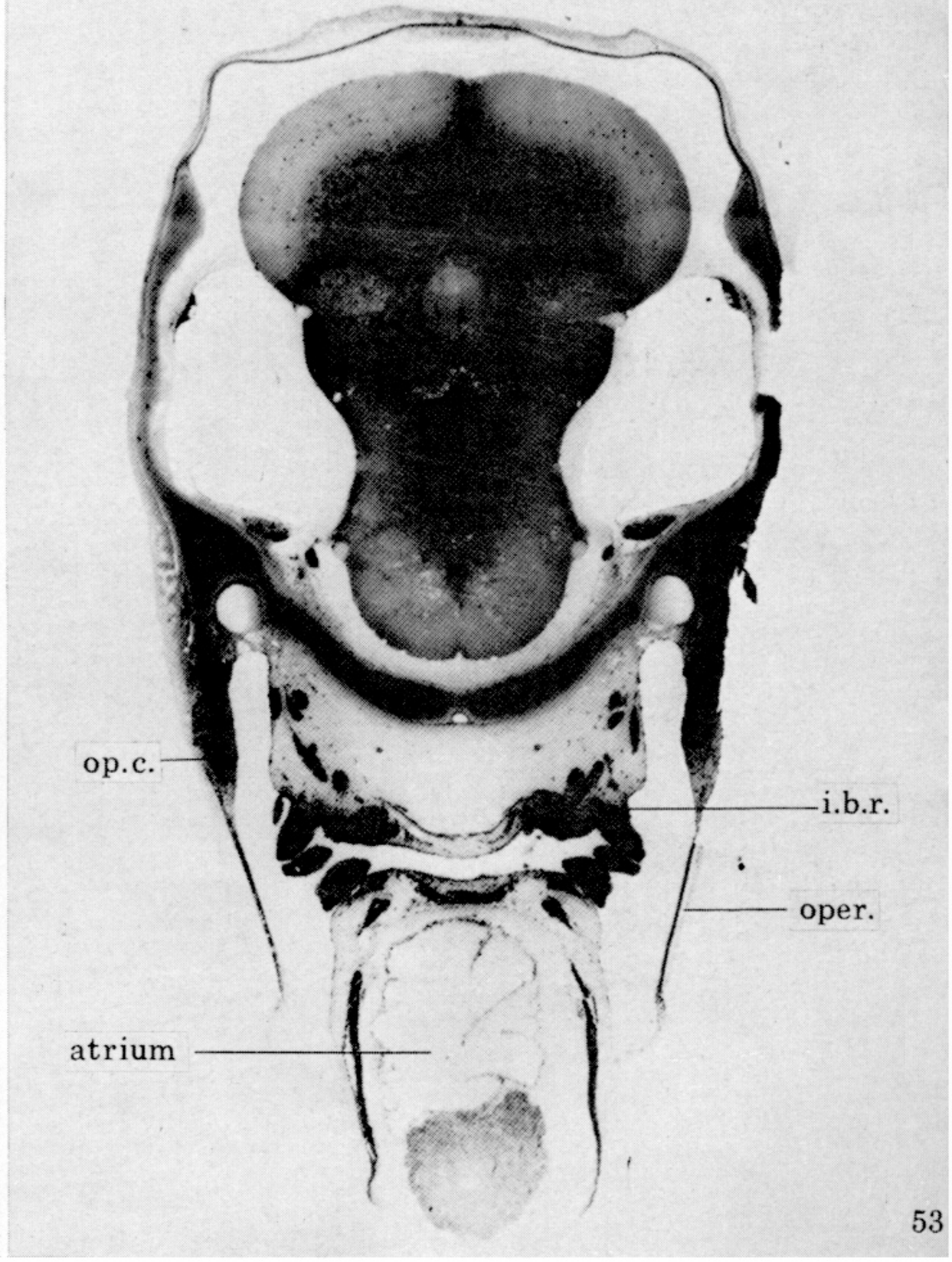

53

FIGURES 50–53. For description see p. 122.

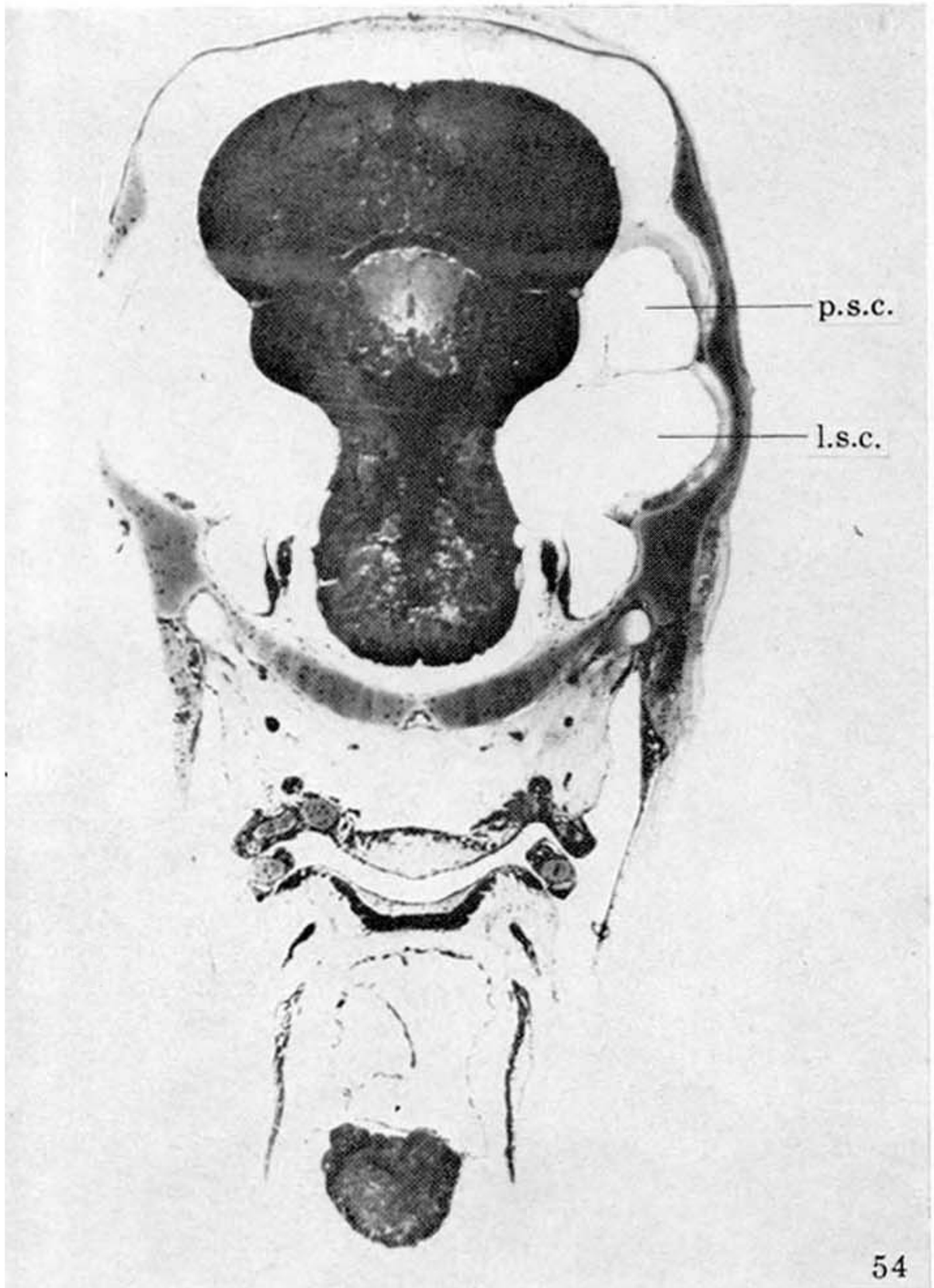

54

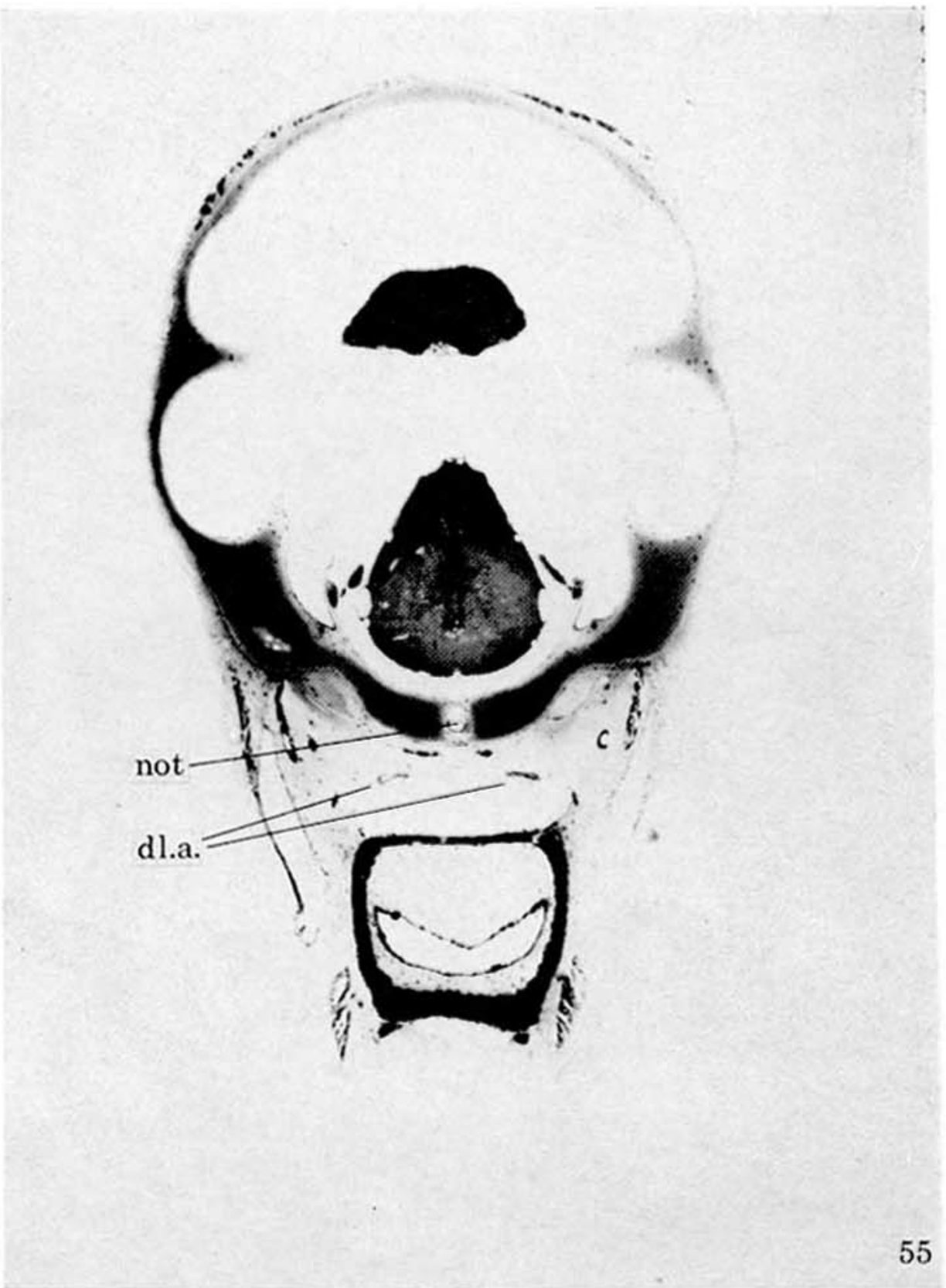

55

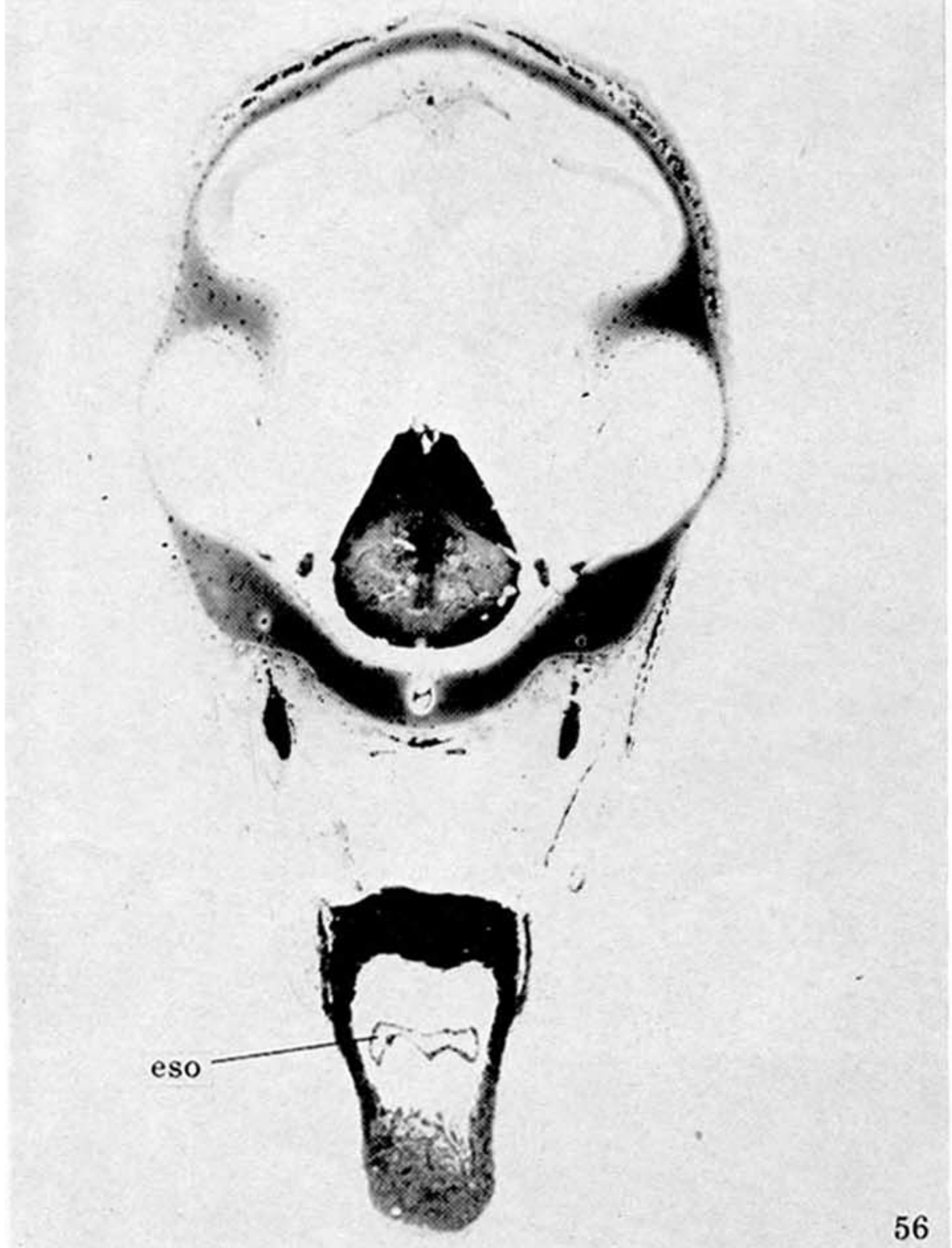

56

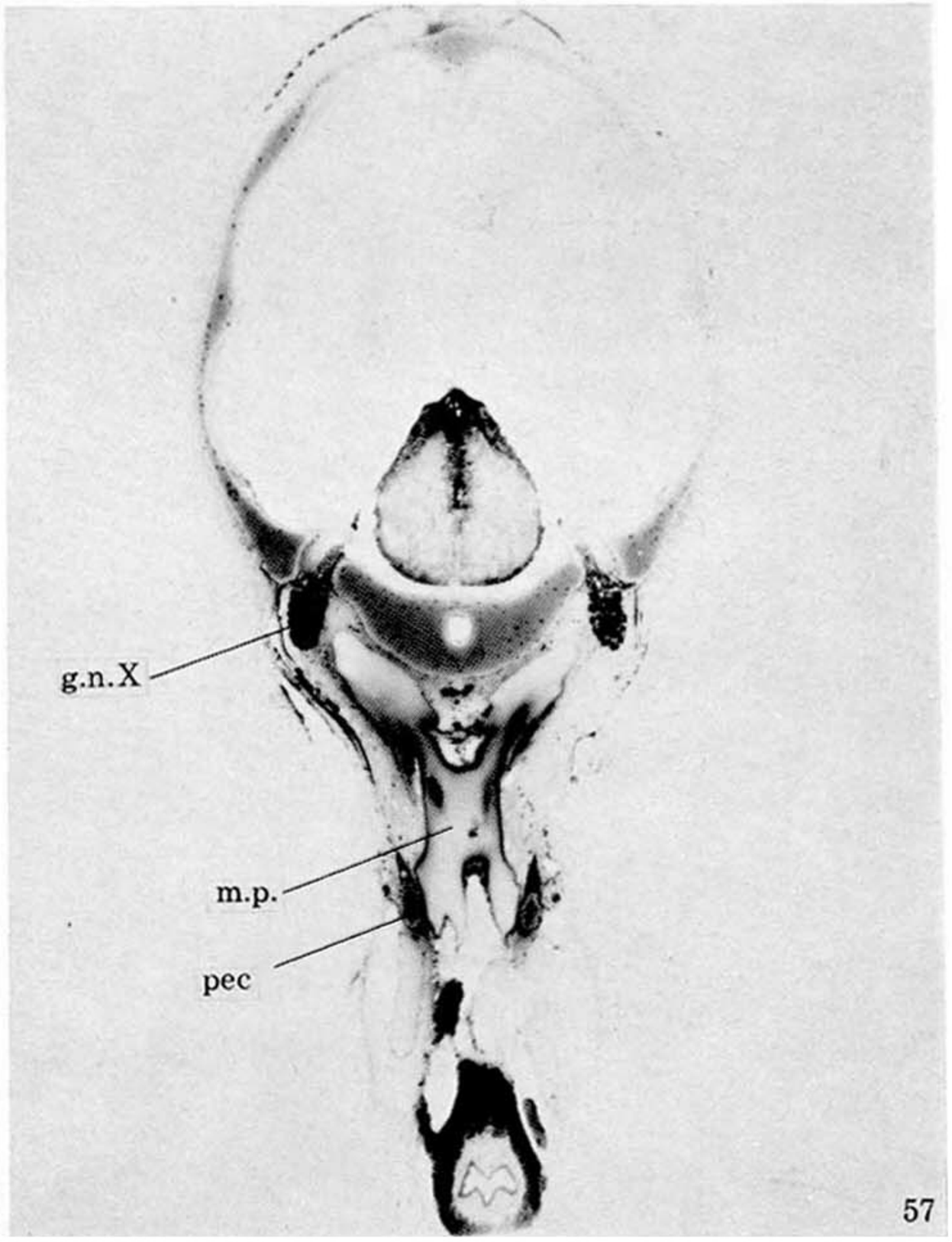

57

FIGURES 54–57. For description see p. 123.

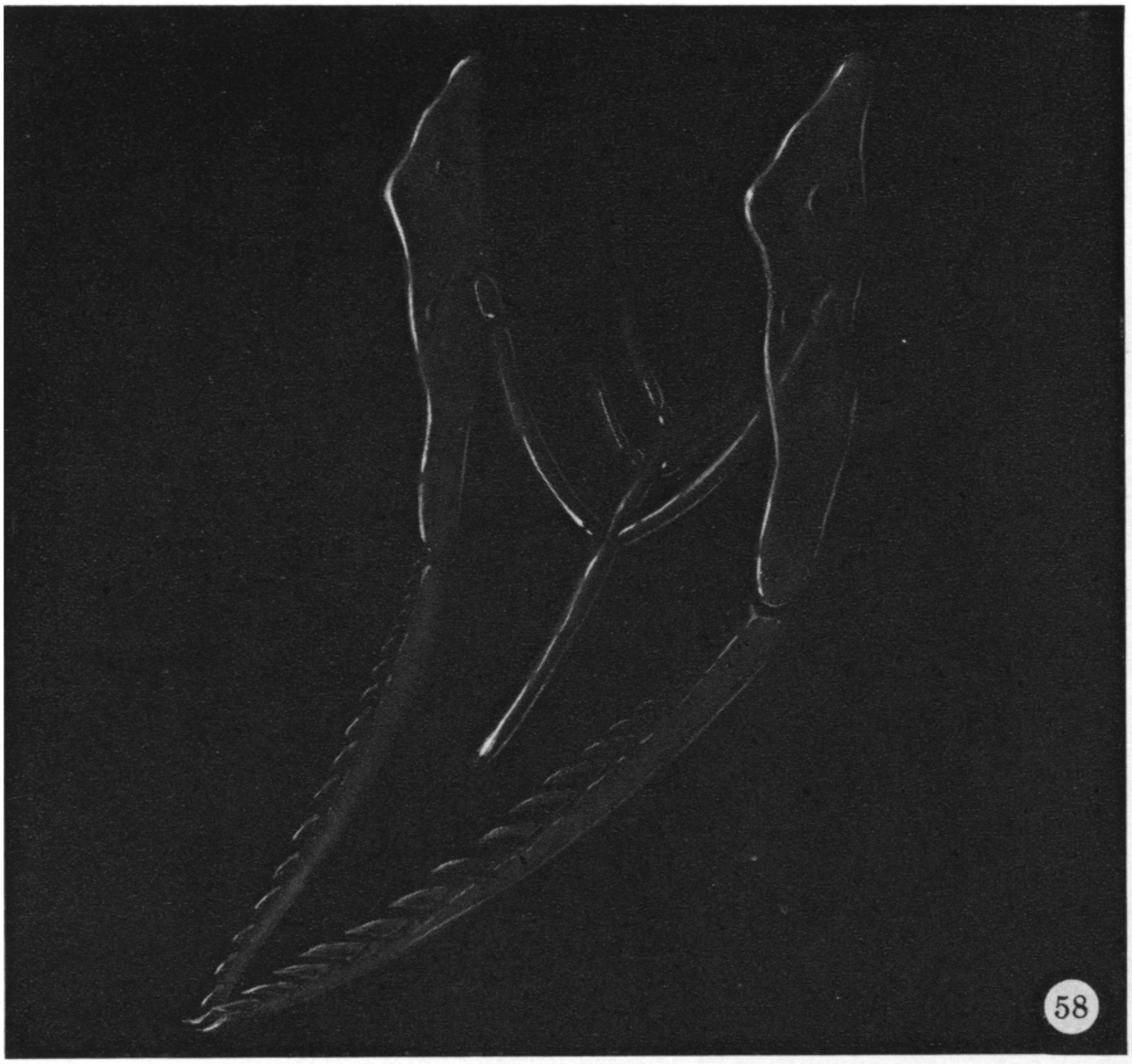

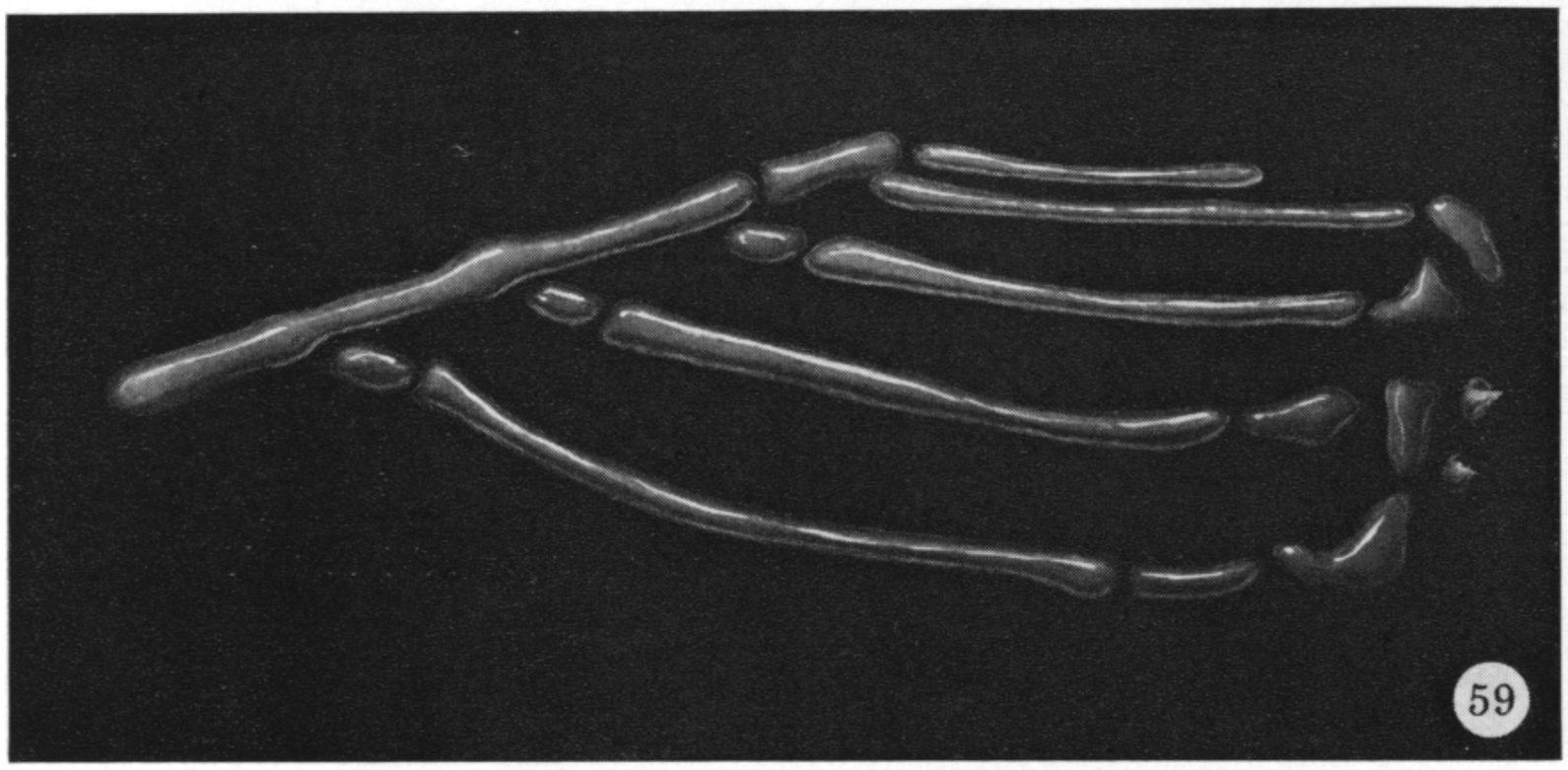

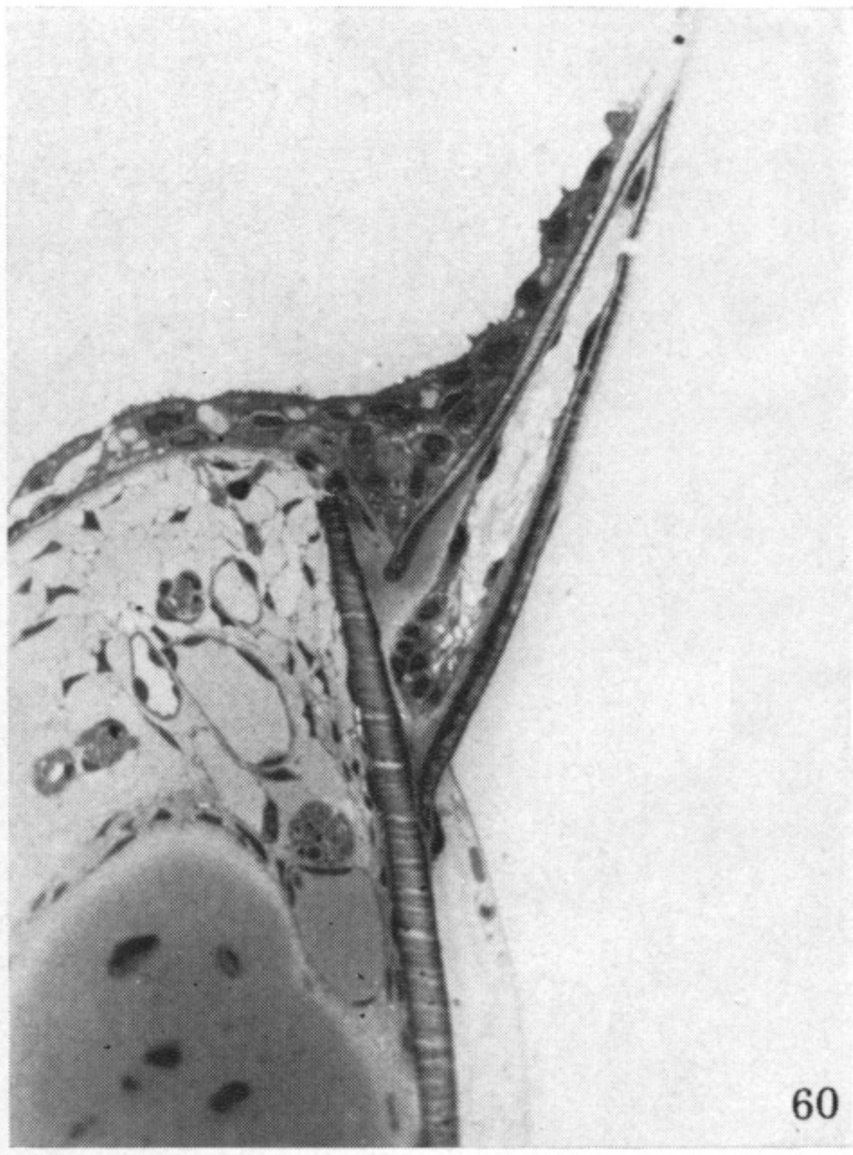

Description of plate 20

Figure 58. Hyoid arch. The ceratohyals arise just posterior to the long glossohyal and attach to the hyomandibular through the intermediary epihyal. The foramina in the hyomandibular branch of the facial (VII) nerve (upper) and the afferent pseudobranchial artery (lower). The first basibranchial is directly behind the glossohyal. (Magn. × 27.)

Figure 59. Cartilages of the gill arches on the left side. A single basibranchial serves for the attachment of the three hypobranchials. Hypobranchials 4 and 5 are absent. Four ceratobranchials attach to four epibranchials positioned dorsally in the pharyngeal chamber. Two infrapharyngobranchials complete the cartilaginous elements. Two minute osseous plates, each with a projecting tooth, represent the upper pharyngeal. (Magn. × 37.)

Figure 60. Tooth attached to the dentary. All teeth are attached to developing dermal bone.

Figure 61. Tip of a tooth. The pulp cavity reaches to the tip of the calcified matrix. No enamel coat is present. (Electron micrograph; magn. × 8300.)

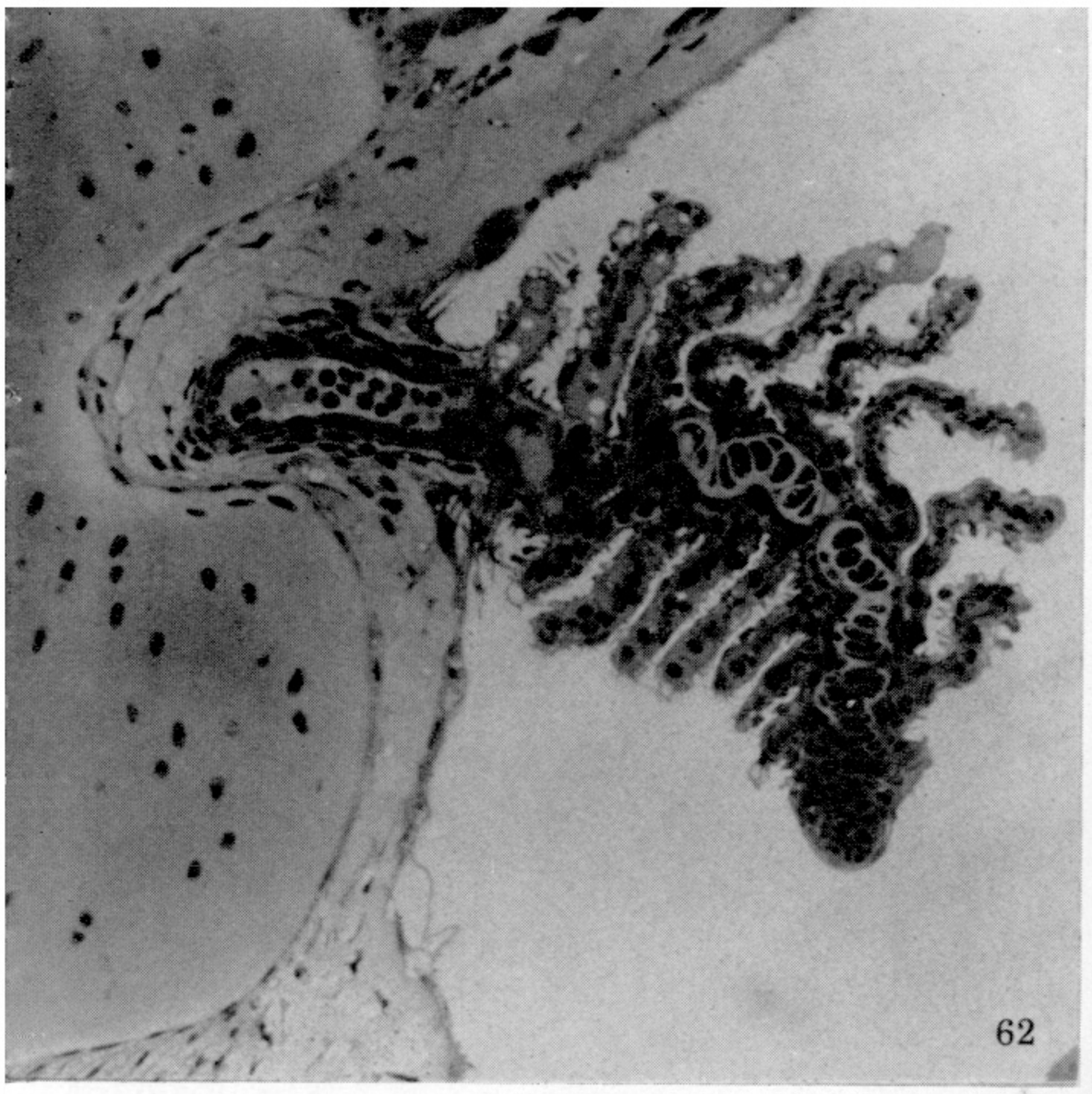

62

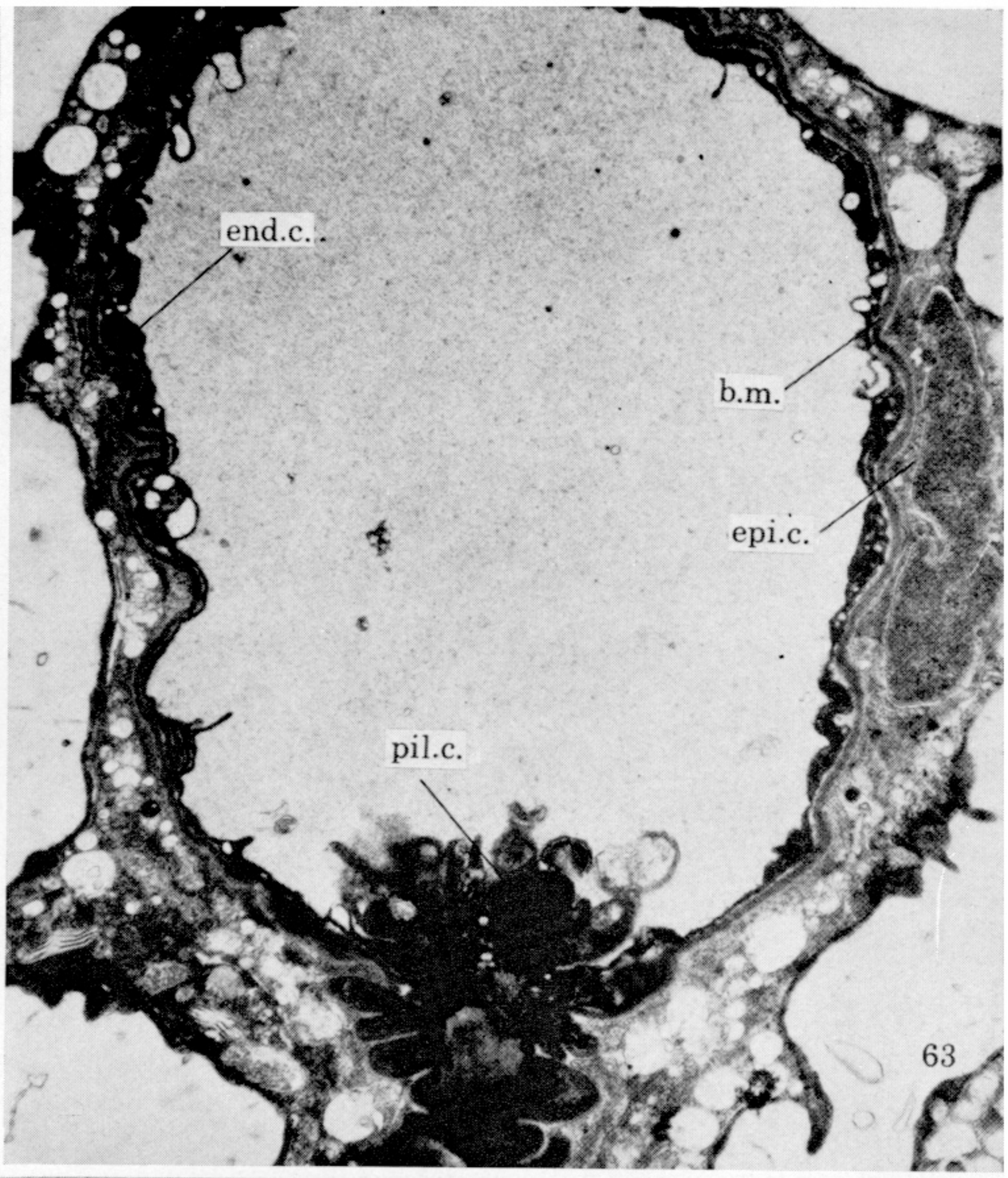

63

64

65

FIGURES 62–65. For description see opposite.

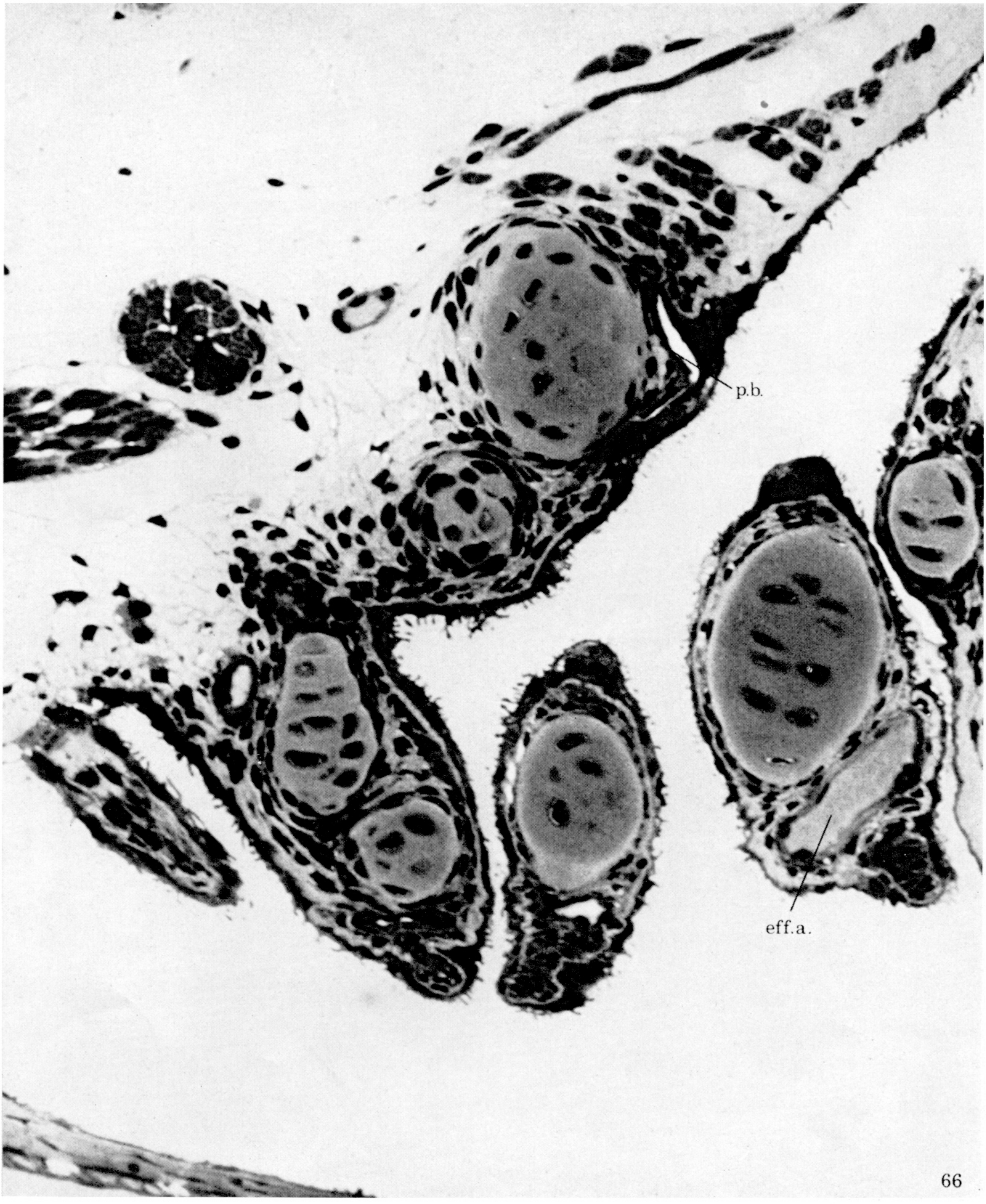

FIGURE 66. The upper pharyngeal bone is beginning to ossify. In the branchial arches, only one vessel (efferent artery) is patent along the course of the ceratobranchial.

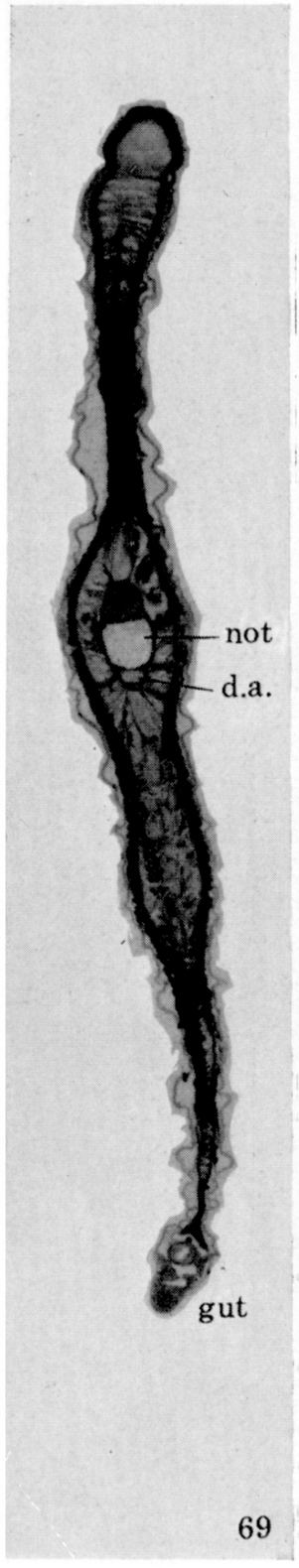

69

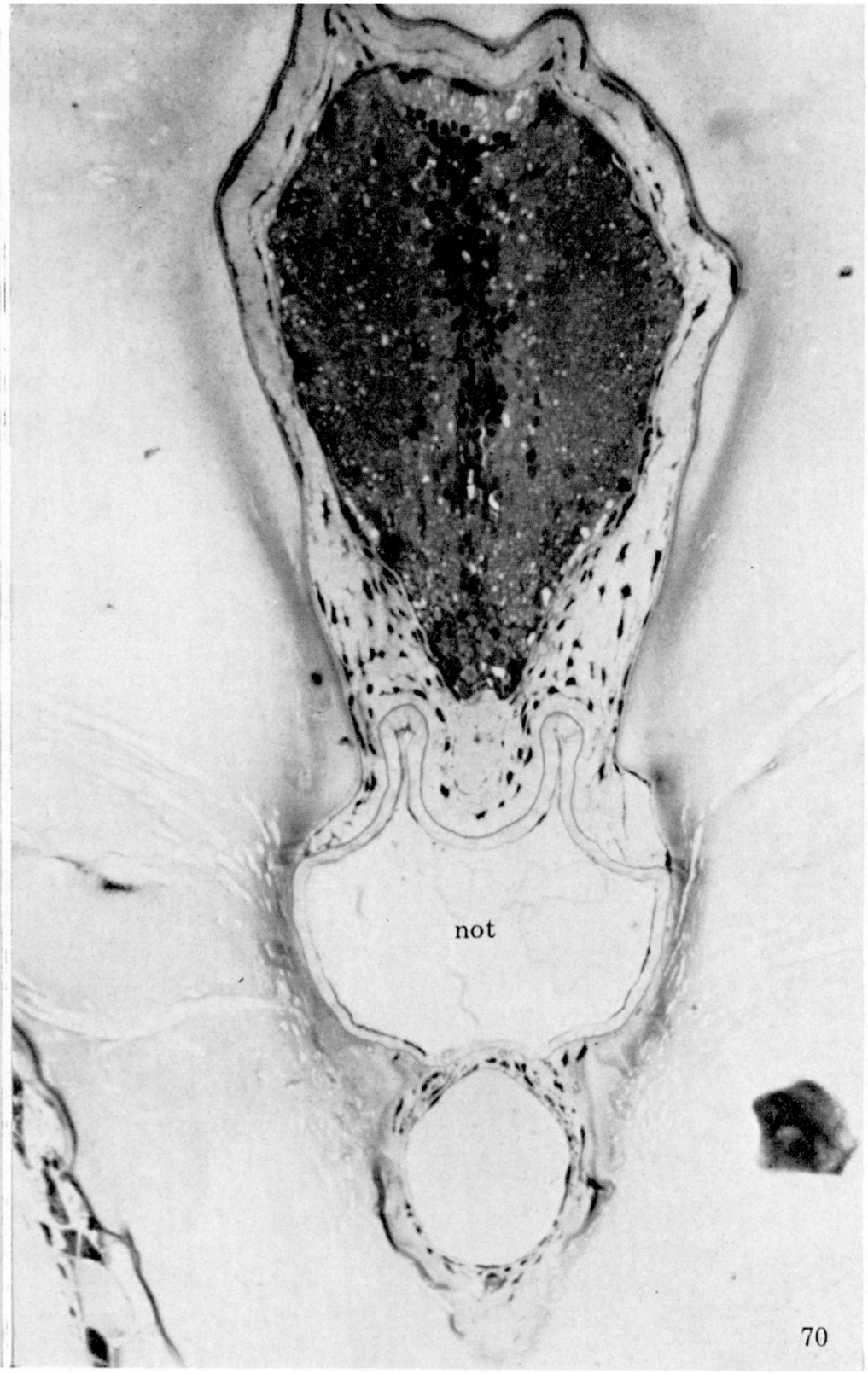

70

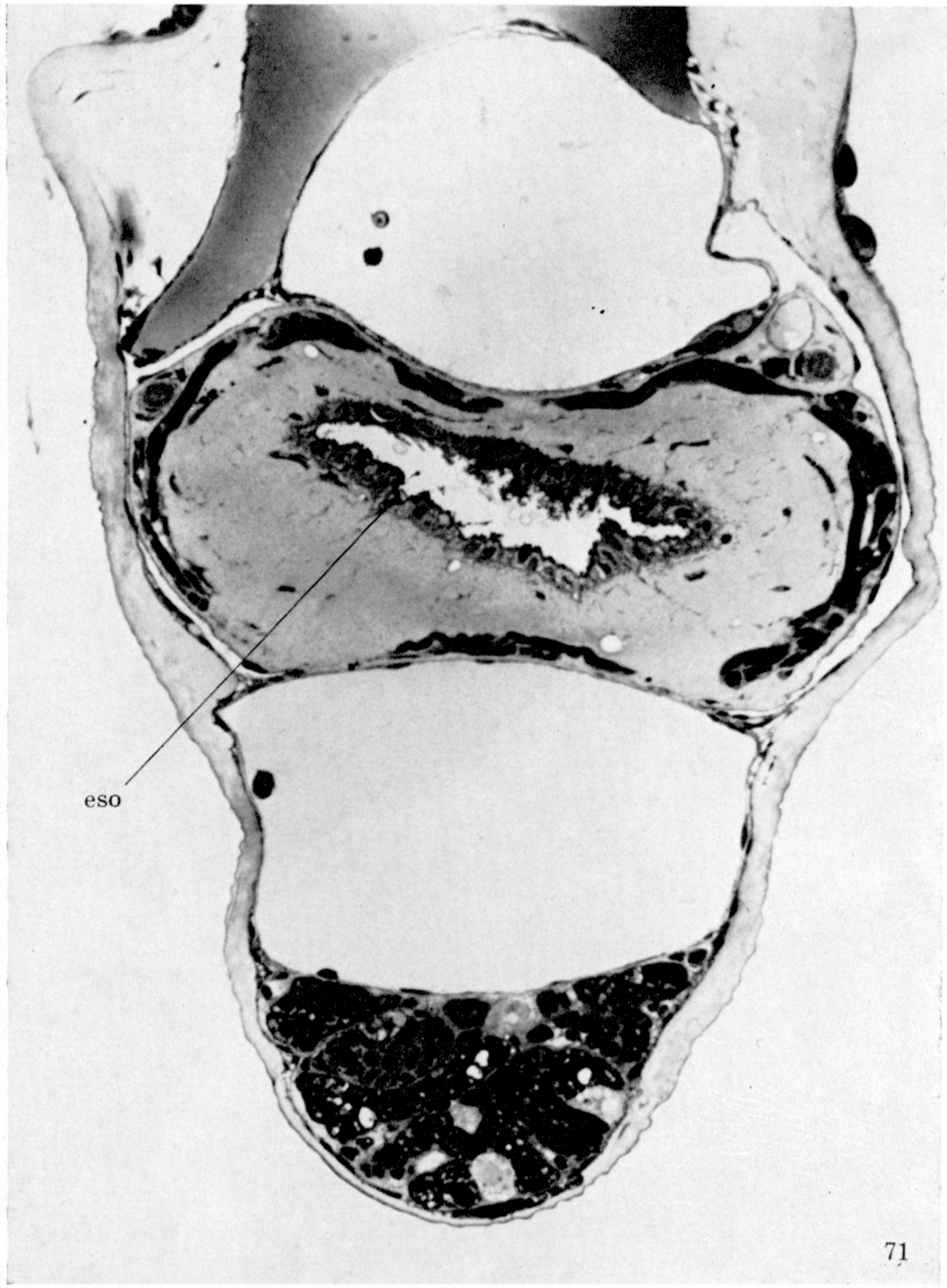

71

FIGURE 69. A cross section through the whole body of a leptocephalus at the level of the esophagus and ventral lobe of the liver. Note the distance between the dorsal aorta and the viscera of the gut. (Magn. × 40.)

FIGURE 70. The notochord is between the spinal cord and dorsal aorta. Acellular mucus material surrounds the three structures.

FIGURE 71. A single post-cardinal vein lies above the esophagus. The large hepatic vein is beneath the esophagus.

FIGURE 72. The skin is extremely fragile and only a few cell layers in thickness. The epithelial cells in contact with seawater are basically flat with numerous ridges. The outer surface of these cells is covered with fine filamentous projections. (Electron micrograph; magn. × 43780.)

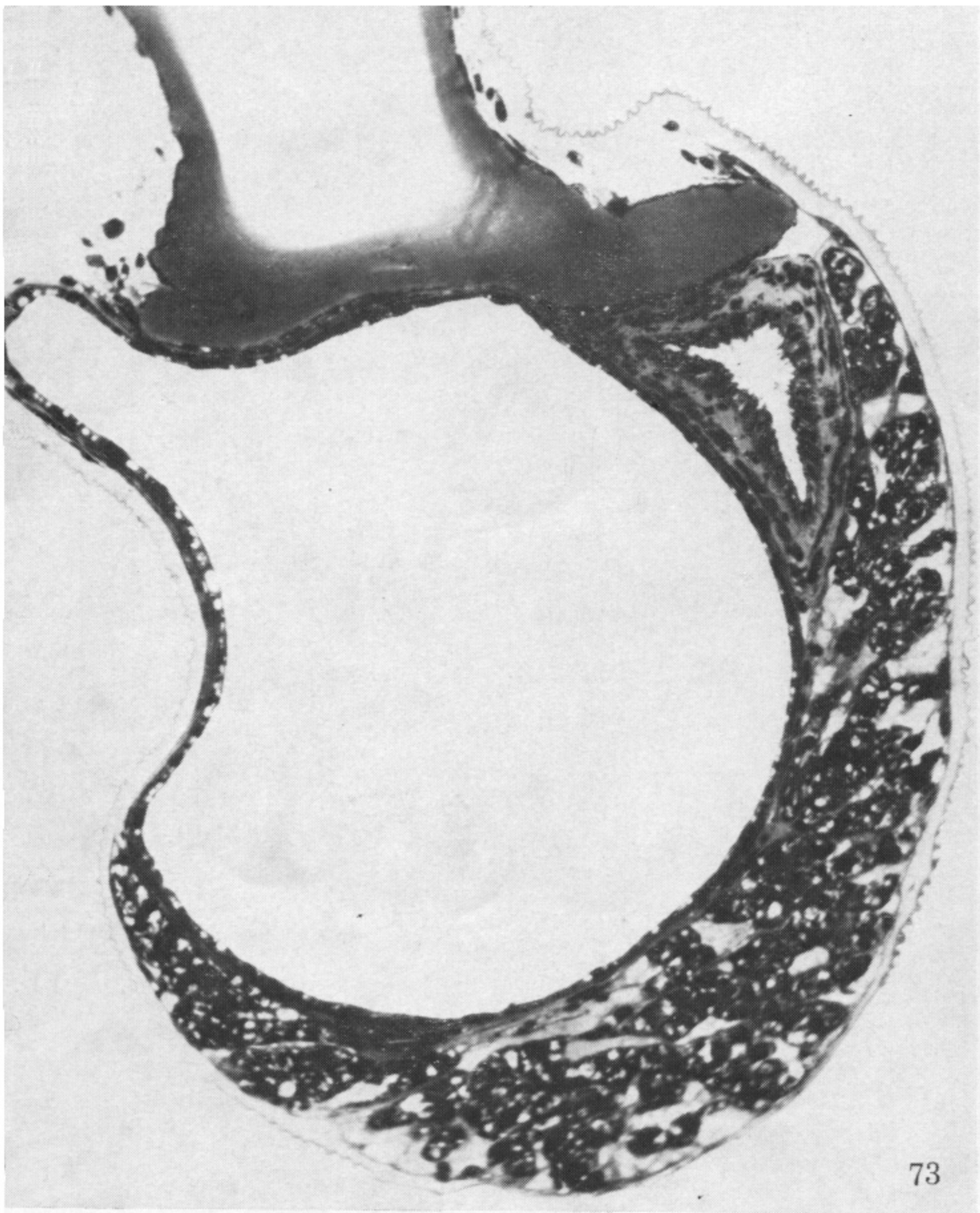

73

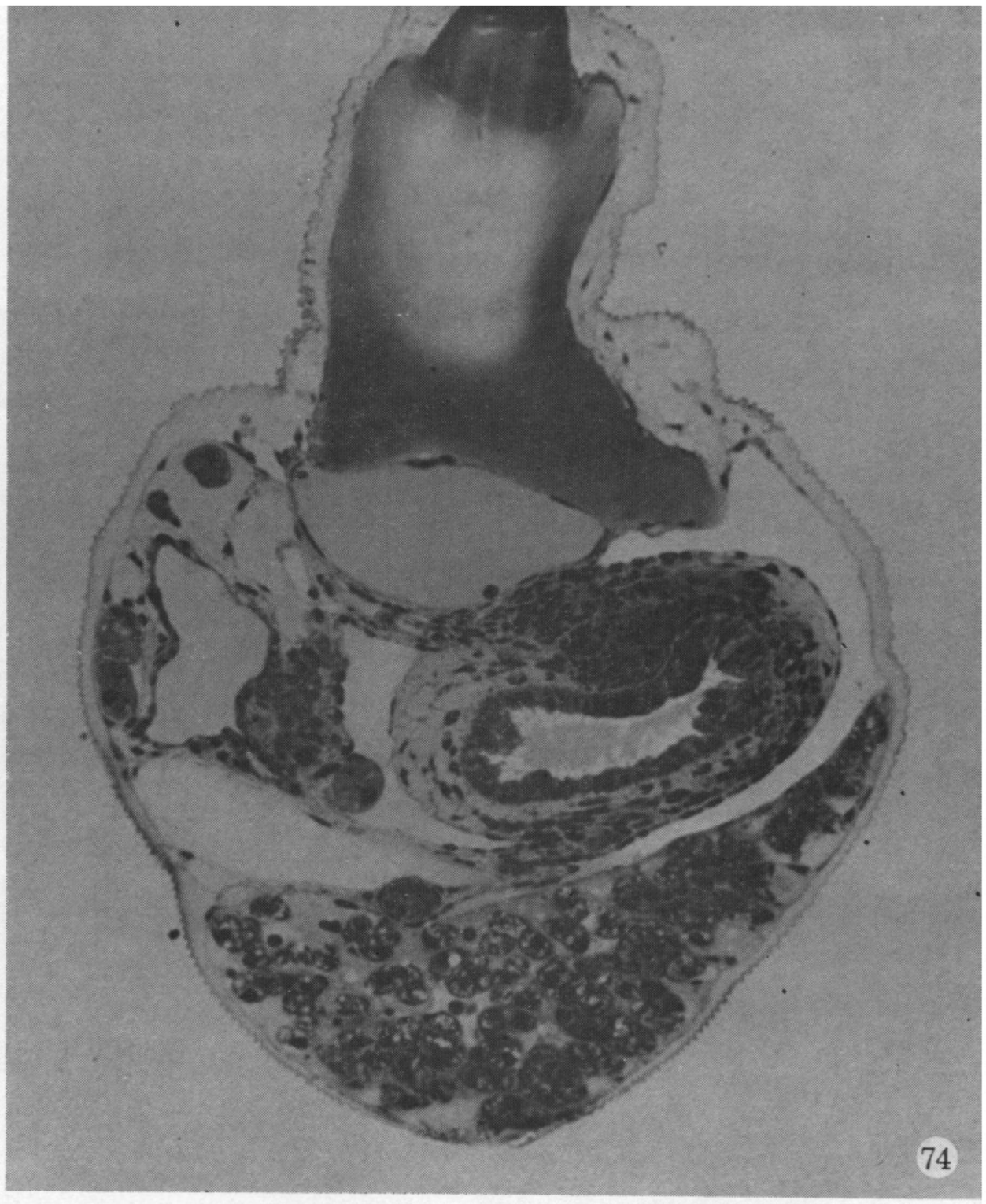

74

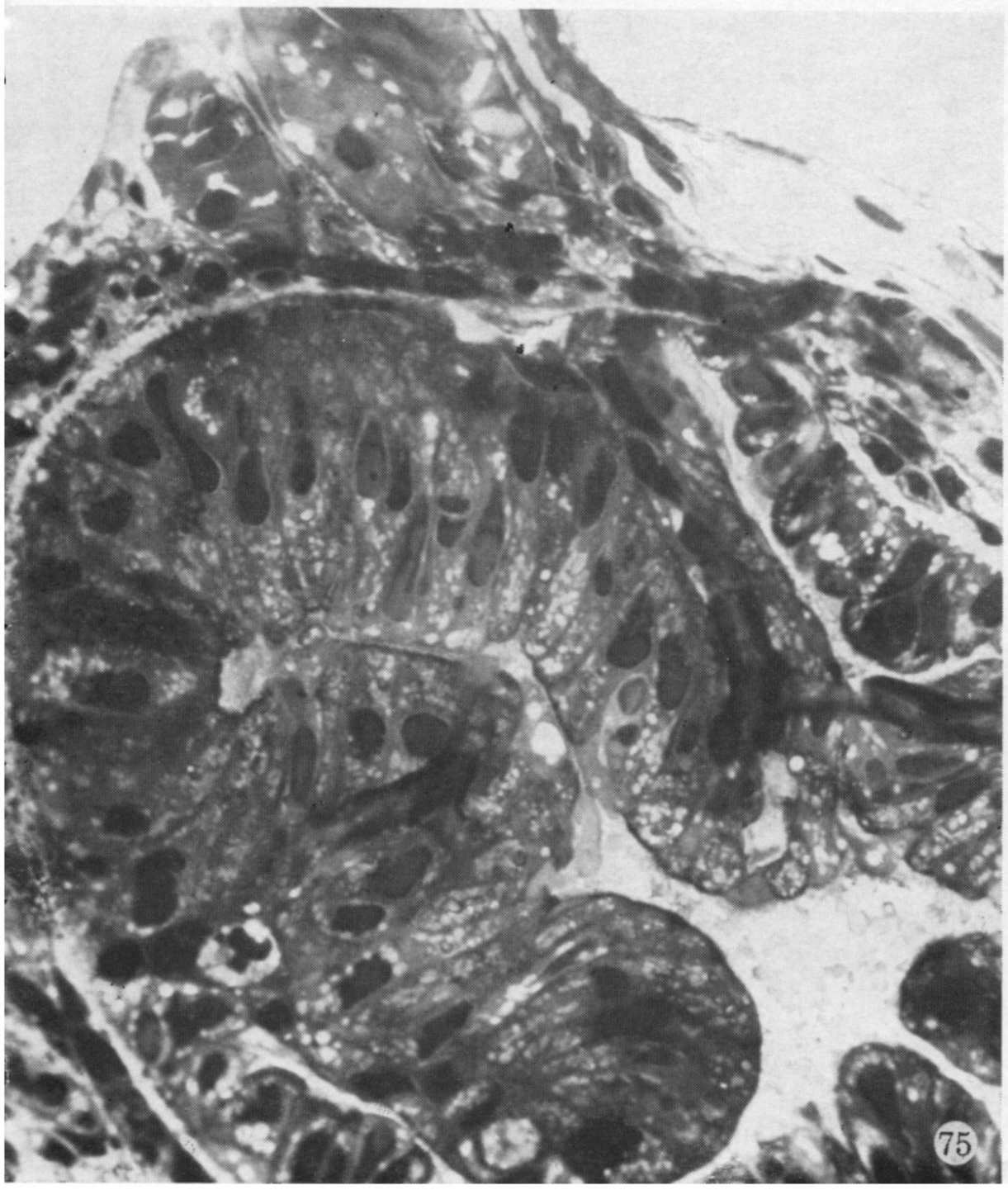

75

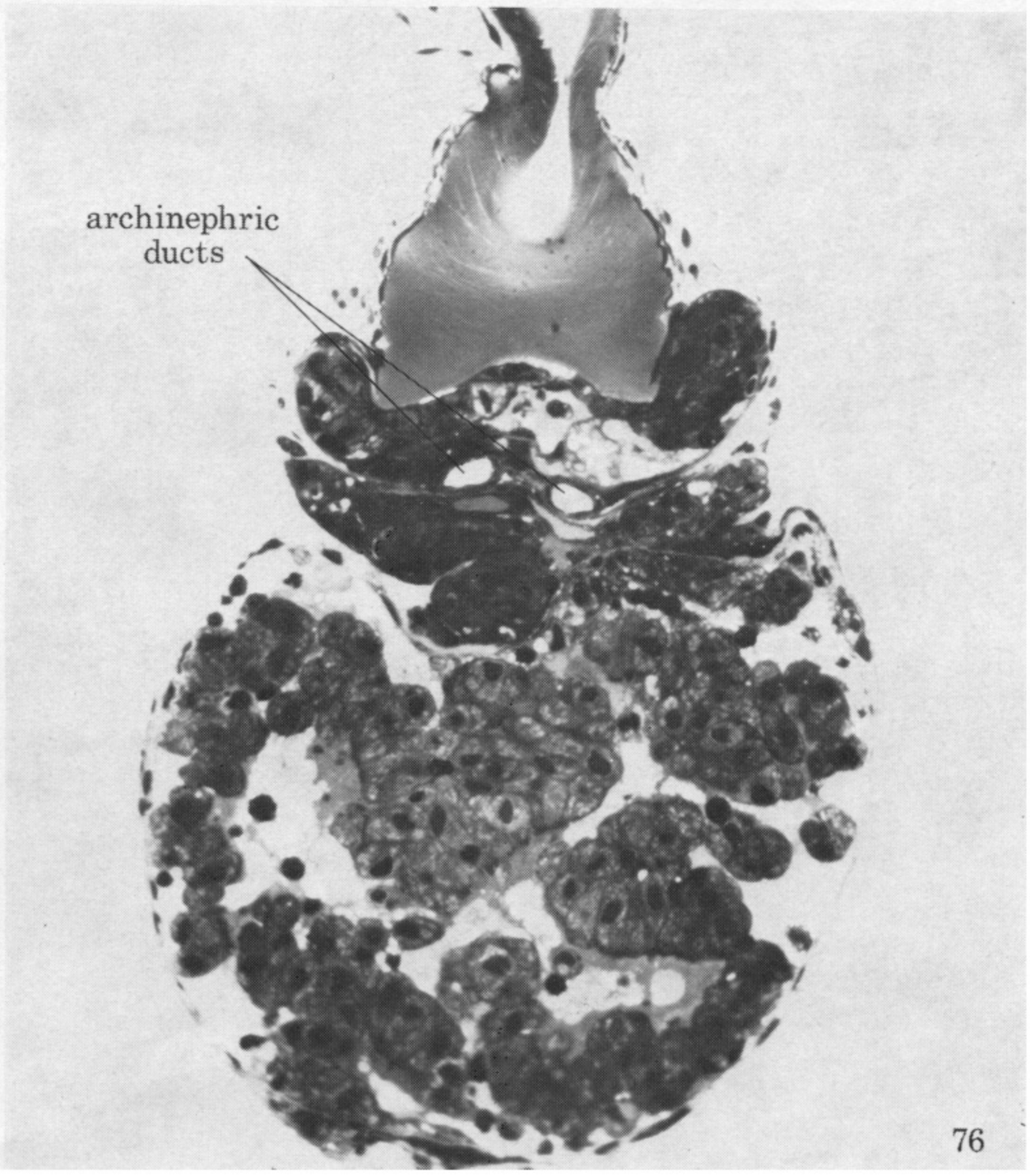

76

FIGURES 73–76. For description see opposite.

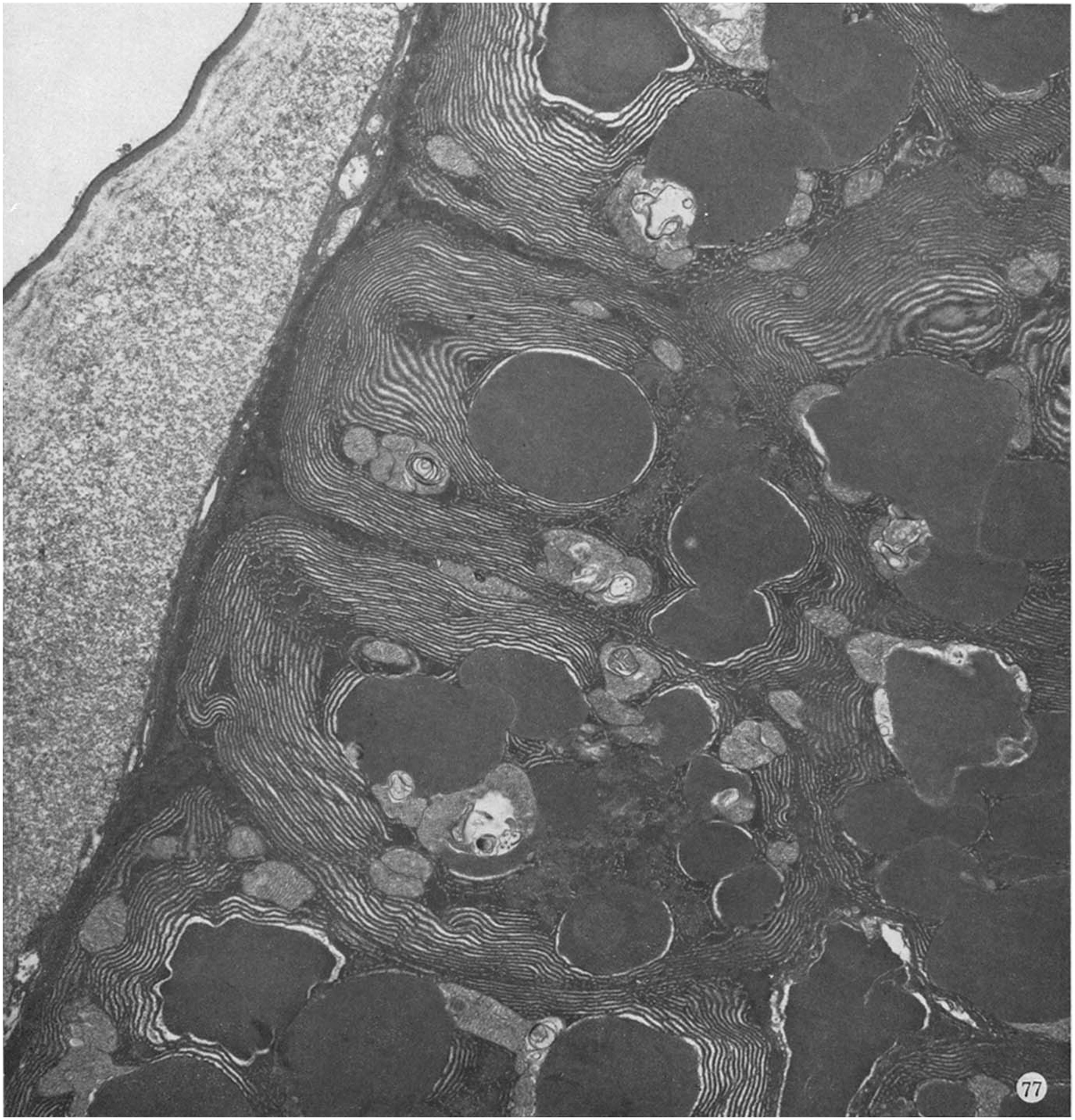

FIGURE 77. Pancreatic acinar cells. The rough endoplasmic reticulum and mitochondria are typical, but the extremely large secretory granules are unusual. (Electron micrograph; magn. ×6700.)

FIGURE 78. The two aglomerular pronephric tubules begin posterior to the hepatogastric region. They are separated from the lumen of the vascular channel by a layer of endothelial cells. As archinephric ducts they drain the aglomerular opisthonephric tubules.

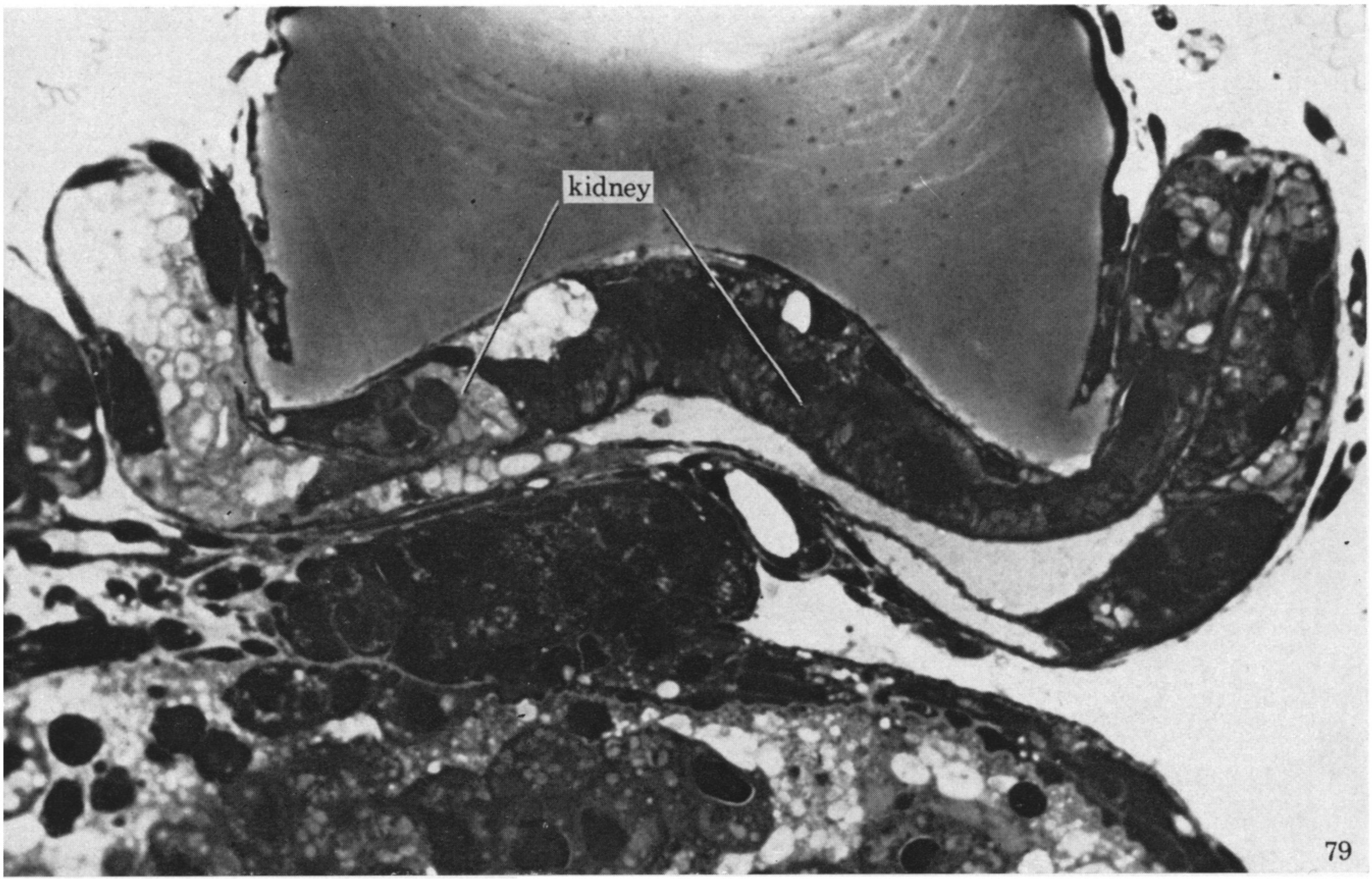

FIGURE 79. The renal parenchyma is a solitary structure and it is not separated into the right and left organs. Renal tubules surround a midline vascular sinus.

FIGURE 80. A renal tubule shown in cross section. The mitochondria are large and are surrounded by cell membranes. (Electron micrograph; magn. × 10980.)

FIGURE 81. Lumen of a renal tubule. The cilia show the familiar '9 + 2' organization of microtubules. (Electron micrograph; magn. × 50400.)

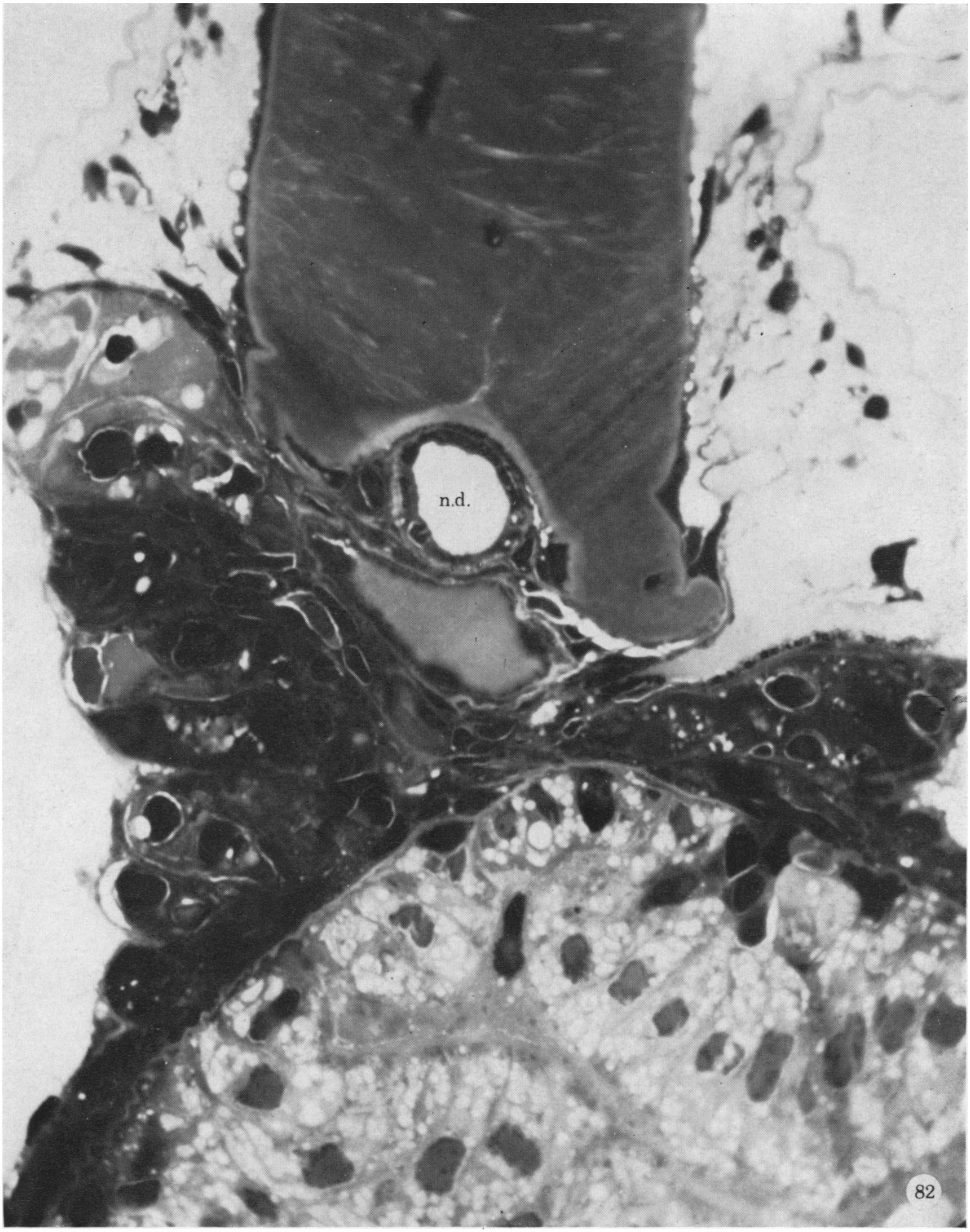

FIGURE 82. A single nephric duct leads from the kidney to the exterior.

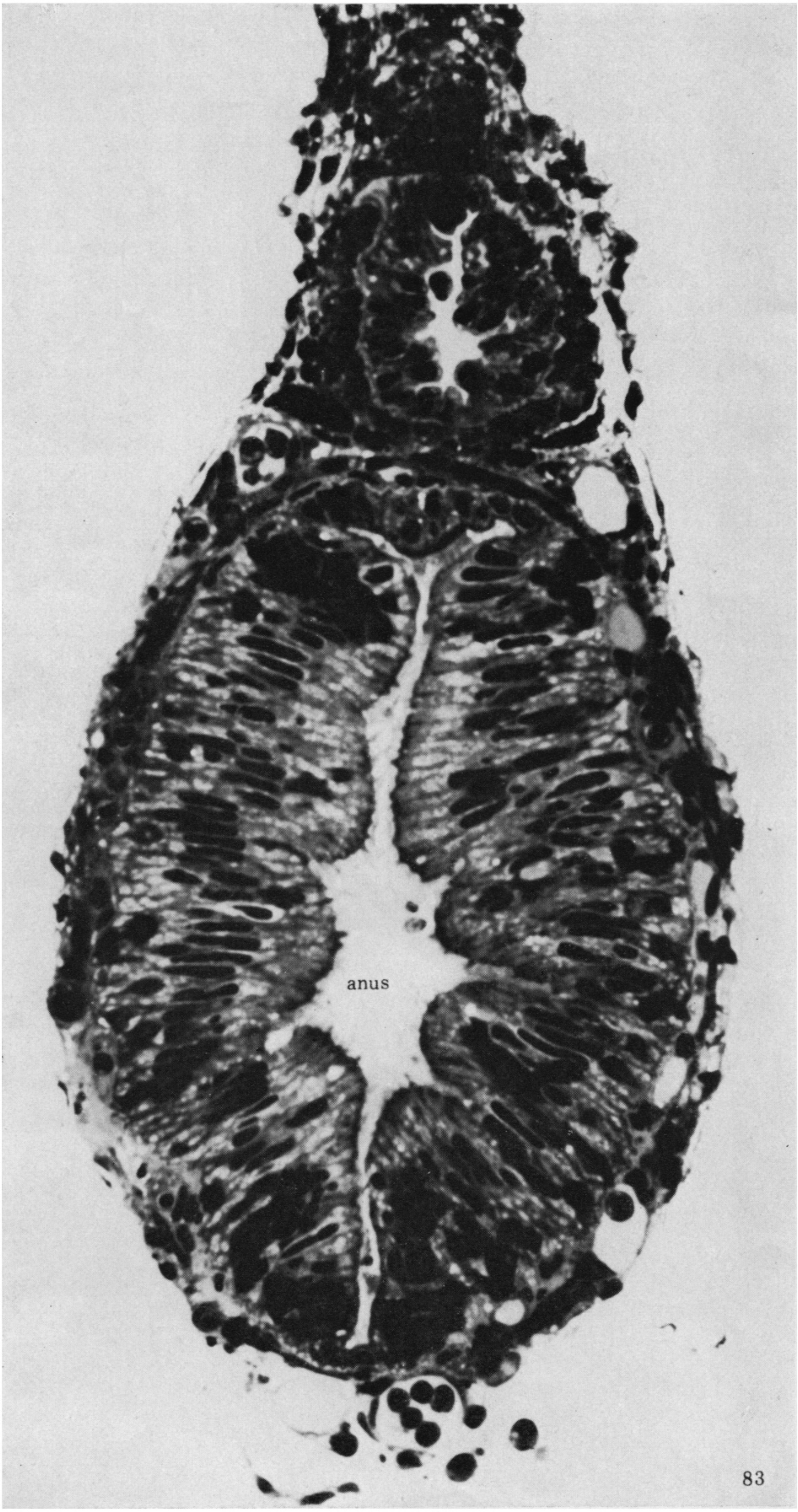

FIGURE 83. Above the anus is the opening of the urinary bladder.